1991

Experimental investigation and computer simulation of nitrous oxide(x) and sulfur oxide(x) absorption in a continuous-flow packed column.

Kam Foon. Chan
University of Windsor

National Library
of Canada

Acquisitions and
Bibliographic Services Branch

395 Wellington Street
Ottawa, Ontario
K1A 0N4

Bibliothèque nationale
du Canada

Direction des acquisitions et
des services bibliographiques

395, rue Wellington
Ottawa (Ontario)
K1A 0N4

Your file Votre référence

Our file Notre référence

NOTICE

The quality of this microform is heavily dependent upon the quality of the original thesis submitted for microfilming. Every effort has been made to ensure the highest quality of reproduction possible.

If pages are missing, contact the university which granted the degree.

Some pages may have indistinct print especially if the original pages were typed with a poor typewriter ribbon or if the university sent us an inferior photocopy.

Reproduction in full or in part of this microform is governed by the Canadian Copyright Act, R.S.C. 1970, c. C-30, and subsequent amendments.

AVIS

La qualité de cette microforme dépend grandement de la qualité de la thèse soumise au microfilmage. Nous avons tout fait pour assurer une qualité supérieure de reproduction.

S'il manque des pages, veuillez communiquer avec l'université qui a conféré le grade.

La qualité d'impression de certaines pages peut laisser à désirer, surtout si les pages originales ont été dactylographiées à l'aide d'un ruban usé ou si l'université nous a fait parvenir une photocopie de qualité inférieure.

La reproduction, même partielle, de cette microforme est soumise à la Loi canadienne sur le droit d'auteur, SRC 1970, c. C-30, et ses amendements subséquents.

Canada

EXPERIMENTAL INVESTIGATION AND COMPUTER SIMULATION OF NO_x AND SO_x ABSORPTION IN A CONTINUOUS–FLOW PACKED COLUMN

by

Kam Foon Chan

A Dissertation
Submitted to the
Faculty of Graduate Studies and Research
through the Department of
Chemical Engineering in Partial Fulfillment
of the Requirements for the Degree
of Doctor of Philosophy at
the University of Windsor

Windsor, Ontario, Canada

1991

ISBN 0-315-78892-5

ABSTRACT

Gas streams containing pure nitrogen oxides (NO_x) or sulphur dioxide (SO_2), at levels simulating typical coal–fired thermal plant emissions (NO_x : 150 ppm – 1640 ppm; SO_2 : 500 ppm – 3000 ppm), were scrubbed with water and sodium chlorite solutions. Experiments were conducted at room temperature and at near atmospheric pressure in a six–inch diameter column packed with 15.8 mm (5/8") stainless steel Pall rings.

Nitrogen oxide removal efficiency up to 14% was obtained with water and 80% with sodium chlorite solutions with wide variation of chlorite concentration. Efficiencies exceeding 90% were obtained for sulphur dioxide removal with water. Essentially 100% removal efficiencies were achieved when sodium chlorite solutions were used for scrubbing. The effects of scrubbing liquid and gas flow rates and inlet NO_x and SO_2 levels on absorption were also examined. Material balances were made for all the experiments performed. The gas phase composition changes determined from measurement at the inlet and outlet of the column with an NO_x/SO_2 analyzer agreed very closely with the liquid phase nitrate and sulphate concentrations determined chemically from analyses of the liquid effluents.

Mathematical models based on the two–film theory and liquid residence time distribution function were derived to facilitate prediction of physical and chemical absorption data for the following processes:

. NO_x or SO_2 absorption by water.

. NO_x or SO_2 absorption by sodium chlorite solutions.

The predicted values agreed closely with experimental data over the range of variables studied. The physical absorption model developed for the NO_x–H_2O or SO_2–H_2O system is not limited to the oxides of nitrogen and sulphur. It can be extended to any other system involving physical absorption.

A reaction mechanism has been proposed for the absorption of mixtures of NO and NO_2 found at typical flue gas levels. It is postulated that N_2O_3 is the major species involved when water scrubbing is employed. However, for absorption with $NaClO_2$ solution, NO is the major diffusing species.

TO MY PARENTS, ANITA, DR. GNYP AND DR. ST. PIERRE

ACKNOWLEDGEMENTS

The author would like to express his sincere thanks to his supervisor, Dr. A. W. Gnyp, for his guidance, valuable advice, encouragement, and critical comments during all phases of this research. Dr. Gnyp spent many weekends on the final review with the author. The technical support provided during the selection of instrumentation by the author's co–supervisor, Dr. C. C. St. Pierre is deeply appreciated. The critical review comments by Dr. St. Pierre and his efforts associated with this project are gratefully acknowledged. Discussions with Professor M. B. Powley concerning absorption theory were very helpful and fruitful.

The author would like to acknowledge Dr. D. Granatstein, his external examiner from Nova Scotia Power, who reviewed the work with such care and made so many helpful suggestions. The work is better for all his input.

Appreciation is also extended to the author's committee member, Dr. D. McKenny, for providing information during the study and allowing use of his equipment for nitrate analysis. Dr. D. McKenny also kindly helped to clarify

the NO_x composition at the inlet of the packed column with his Chemiluminescent NO_x Analyzer. This work also benefited from the comments of Dr. R. A. Stager. The skill and help of Mr. G. Ryan during the installation of the equipment for this work is gratefully acknowledged. The experimental work of senior students associated with this research, Michael Wong and Samuel Hui, is also appreciated.

The financial support from the Natural Sciences and Engineering Research Council of Canada (NSERC) is also gratefully acknowledged. Thanks are also extended to the many early investigators who made such important contributions to the understanding of the processes under investigation.

As always, the author has been assisted and encouraged during the course of this work by his wife, Anita. Without her enthusiasm, her patience, tolerance and love and her belief in his work, this study would never have been completed.

TABLE OF CONTENTS

Page

LIST OF TABLES

LIST OF FIGURES

LIST OF APPENDICES

NOMENCLATURE

a	=	Interfacial area per unit column volume, $m^2.m^{-3}$
$\bar{a}_L$	=	Mean stream interfacial area per unit liquid volume, $m^2.m^{-3}$
$a_{L,i}$	=	Stream interfacial area per unit liquid volume, $m^2.m^{-3}$
a_s	=	Geometric surface area per unit liquid volume of packing particle, $m^2.m^{-3}$
a_t	=	Total surface area of packing per unit column volume, $m^2.m^{-3}$
a_w	=	Wetted surface area of packing per unit column volume, $m^2.m^{-3}$
δa_i	=	Stream interfacial area per unit column volume, $m^2.m^{-3}$
A	=	Absorbing gaseous component, (NO, NO_2, SO_2) ,dimensionless
B	=	Liquid reactant, ($NaOH$, $NaClO_2$), dimensionless

C_A ; C_A^* = Bulk and interfacial concentrations of the absorbing gaseous component A in liquid absorbent respectively, kmole.m^{-3}

$\overline{C}_{A,j-1}$;$\overline{C}_{A,j}$ = Mean concentration of component A in liquid phase leaving $(j-1)^{th}$ and j^{th} stages respectively, kmole.m^{-3}

C_B^o = Initial liquid reactant concentration, kmole.m^{-3}

$\overline{C}_{B,j-1}$;$\overline{C}_{B,j}$ = Mean liquid reactant concentration leaving $(j-1)^{th}$ and j^{th} stages respectively, kmole.m^{-3}

d = Nominal packing diameter, m

d_p = Diameter of a sphere having the same geometric surface area per unit volume of packing particle, m, $d_p = \frac{(1-\epsilon)}{a_s}$

D_{AL};D_{AG} = Liquid phase and gas phase molecular diffusivities of gaseous component A respectively, m^2.s^{-1}

EO = Eotvos number, dimensionless

$$EO = \frac{\rho_L g d^2}{\sigma}$$

$E(t)$ = Residence time distribution function of liquid, s^{-1}

$F_A;F_B$	=	Stoichiometric coefficients, dimensionless
g	=	Acceleration due to gravity, $m.s^{-2}$
G	=	Superficial mass velocity of gas, $kg.m^{-2}.s^{-1}$
$h_t;h_d;h_s$	=	Total, dynamic and static liquid hold–up in a column respectively, $m^3.m^{-3}$
H	=	Henry's law constant for the absorbing component, $atm.m^3.kmole^{-1}$
δh_i	=	Liquid hold–up for a stream i, $m^3.m^{-3}$
$I_{B_1};I_{B_2}$	=	Ionic strength of $NaClO_2$ and NaOH respectively, $kg\text{–}ion.m^{-3}$
k	=	Third order rate constant for reaction NO, $(m^3.kmole^{-1})^2.s^{-1}$
k_2	=	Second order rate constant for reaction of SO_2, $m^3.kmole^{-1}.s^{-1}$
k_3	=	Third order rate constant for reaction NO, $(m^3.kmole^{-1})^2.s^{-1}$
k_c	=	Rate constant, $(m^3.kmole^{-1})^2.s^{-1}$
k_G	=	Gas side mass transfer coefficient, $kmole.m^{-2}.s^{-1}.atm^{-1}$
k_L	=	Liquid side mass transfer coefficient, $m.s^{-1}$

$k_L a$	=	Stochastic rate coefficient, s^{-1}
$k'_{L,i}$	=	Local liquid side mass transfer coefficient, for a stream i, $m.s^{-1}$
k_{L,ClO_2^-}; $k_{L.OH^-}$	=	Liquid side mass transfer coefficients of ClO_2^- and OH^- respectively, $cm.s^{-1}$
k_p	=	Rate constant, defined by Equation 2.33, $atm^{-2}.s^{-1}$
K_{B_1} ; K_{B_2}	=	Salting out parameters for the electrolytes $NaClO_2$ and NaOH respectively, $m^3.kmole^{-1}$
K_a	=	Thermodynamic equilibrium constant, defined by Equation 2.7, $gmole.L^{-1}$
L	=	Superficial liquid mass velocity, $kg.m^{-2}.s^{-1}$
n	=	Number of stages, dimensionless
N_A	=	Rate of absorption of component A, $kmole.m^{-2}.s^{-1}$
P_A	=	Partial pressure of component A in bulk gas, atm
P_A^*	=	Partial pressure of component A at interface, atm

Pe	=	Peclet number, dimensionless, defined by $Pe = \frac{\overline{U}d}{\aleph}$
P_t	=	Total pressure of the system, atm
Q	=	Volumetric flow rate of liquid absorbent in a column, $m^3.s^{-1}$
δq_i	=	Volumetric flow rate for a stream i, $m^3.s^{-1}$
R	=	Gas Constant, $atm.m^3.kmole^{-1}.K^{-1}$
S	=	Column cross sectional area, m^2
S_p	=	Specific surface of a particle, $m^2.m^{-3}$
t_i	=	Stream residence time, s
$\overline{t}$	=	Mean residence time, s
t	=	Contact time, s
T	=	Absolute temperature, K
$\overline{U}$	=	Mean real liquid velocity, $m.s^{-1}$ $\overline{U} = \frac{Q\epsilon h_t}{S}$
v_L	=	Liquid velocity, $m.s^{-1}$ $v_L = \frac{Q}{S}$

$x_a;x_c;x_g$ = Contribution to salting out parameter K, of anions, cations and the gas respectively, $m^3.kg\text{–}ion^{-1}$

$Y_{A,j}$ = Molar fraction of absorbing component A, dimensionless

Y_A^* = Molar fraction of absorbing component A at interface in equilibrium with C_A^*, dimensionless

$\overline{Y}_{A,j}$ = Mean molar fraction of absorbing component A defined by Equation 3.7, dimensionless

Z = Total height of packing, m

ΔZ = Height of a stage, m

Greek Symbols:

φ = Distribution coefficient, dimensionless

ℓ = Scale turbulence, dimensionless

β = Liquid fraction passing through the stagnant region, dimensionless

ζ = Parameter used to account for the various hydrodynamic conditions in a column, $m.s^{-1/2}$, defined by Equation 3.8a

ϵ = Porosity (void fraction), dimensionless

θ = Exposure time, s

λ = Defined by Equation 3.13C,

μ = Dynamic viscosity, $kg.m^{-1}.s^{-1}$

ψ_i	=	Valency of ion, dimensionless
ρ	=	Density, $kg.m^{-3}$
σ	=	Surface tension of liquid, $N.m^{-1}$ or $kg.s^{-2}$
σ_c	=	Critical surface tension of packing material, $N.m^{-1}$ or $kg.s^{-2}$
$\Gamma_1;\Gamma_2$	=	Mean residence time of liquid, defined by Equations 3.5a and 3.5b respectively, s
ϕ	=	Mass transfer enhancement factor, dimensionless
γ	=	Residence Correction factor, dimensionless defined by Equation 5.1
$\aleph$	=	Axial dispersion coefficient, $m^2.s^{-1}$

Subscripts:

A	=	Flue gas component A
$A_1;A_2$	=	Dissolved flue gas component (SO_2 and NO respectively)
B	=	Liquid reactant B
$B_1;B_2$	=	Liquid phase reactant ($NaClO_2$ and NaOH respectively)
i	=	Referring to stream i
j	=	Referring to stage j

L	=	Liquid phase
G	=	Gas phase
Chem	=	Chemical absorption
Phy	=	Physical absorption

CHAPTER 1

INTRODUCTION

The industrial developments of the recent past have created problems related to air and water contamination. As a result, innovative and effective cleaning technologies must be developed to meet the current and future pollution standards. The design of new devices that can satisfy national needs, especially in the area of acid rain abatement, is particularly urgent.

In 1985, a program similar to the Municipal–Industrial Strategy for Abatement (MISA) for waste water pollution control, was launched by the Ministry of the Environment to establish limits for acid gas emissions. Under the Clean Air Program – CAP, Ontario's four major acid gas producers – Inco Limited, Ontario Hydro, Falconbridge Limited and Algoma Steel Corportion must reduce their sulphur dioxide emissions to one third of the 1980 level by 1994 (Environmental Science & Engineering, September, 1990).

The Environmental Protection Act and the Air Pollution Control Regulation 308 are currently under review to reflect these needs (Monthly Report, ECO/LOG Canadian Pollution Legislation, September, 1990). The Ontario Hydro Regulation, (O. Reg. 281/87), as required by the Environmental

Protection Act, has recently been revised to limit its fossil–fueled electric generating stations not to exceed 175 kilotonnes of sulphur dioxide and oxides of nitrogen emissions by 1994 (Environmental Science & Engineering, September 1990). Other source owners are expected to have appropriate air pollution control devices to limit their emissions within the next ten years. According to the Clean Air Program draft regulation (Monthly Report,ECO/LOG Canadian Pollution Legislation, September, 1990), source owners are required to apply for certificates of approval to construct and to operate the facilities. The phase–in period is expected within the next two years assuming a 1991 filing date for the regulation. The permit to operate is subject to review every ten years to ensure proper operation and continuous improvements to air pollution control.

There has been a trend of increasing dependence on coal for energy production which leads to serious NO_x/SO_x emissions. Thermal generating plants represent the major stationary sources of acid rain. The principal gaseous pollutants resulting from coal combustion are summarized in Table 1.1. According to Iya (1986), the primary constituent of NO_x is inactive nitric oxide (NO). Over 90% of SO_x is sulphur dioxide (SO_2). Once emitted from a stack at low concentrations ($<$ 1000 ppm), the nitric oxide will react slowly with oxygen in the air to form the more reactive NO_2, which is a reddish brown, toxic gas. The nitric oxide can also react with nitrogen dioxide to give higher oxides of nitrogen, which can readily undergo a series of reactions involving combination with water vapor in the air to form acid rain. The NO_x is also

Table 1.1 **Analysis of Flue Gas from a Typical Fossil Fuel Fired Power Plant (Egan and Felker, 1986).**

Component	Mole %
N_2	74.55
* CO_2	12.55
H_2O	7.76
O_2	4.86
* SO_2	0.22
* NO_x	0.06
* HCl	0.006
* SO_3	0.005

* potential pollutants

known to be responsible for smog formation in most cities. Damage caused by acid rain and smog is well documented.

Significantly more NO_x and SO_x are produced during coal combustion than from any other fossil fuel, because coal contains about 0.5% to 2% nitrogen and about 0.3% to 10% sulphur while other fuel may contain less fuel–bound nitrogen and sulphur. Portions of the nitrogen and sulphur are converted to NO_x and SO_x during combustion. Pruce (1981) indicated that, on average, between 60% and 80% of all NO_x generated by the combustion of coal is attributable to fuel–bound nitrogen. About 20% to 40% is formed through the thermal fixation reaction. In principle, NO_x formation can be suppressed by:

. Reducing peak flame temperatures and residence times in the combustion zone.
. Reducing nitrogen levels at peak flame temperatures.
. Decreasing oxygen levels at peak flame temperatures of the combustion process.

These three concepts formed the basis for the technique of combustion modification in the late seventies (1979 – 1981) for control of NO_x emissions.

Generally, two approaches have been considered for control of NO_x

discharges from power plant boilers. One involves suppression of NO_x formation in the early stages via combustion modification. The other depends on flue gas treatment processes after the NO_x has formed. Recent commercial demonstrations have shown that boiler modifications can not achieve more than about 50% reduction in NO_x emissions. On the other hand the flue gas treatment processes such as Selective Catalytic Reduction (SCR) provide higher removal efficiencies, ranging from 70% to 95%. The technology for SO_x removal is much better developed than for NO_x. The wet flue gas desulphurization (FGD) technology has been applied commercially to SO_2 emission control for some time. More recent commercial applications involve dry alkaline spray using lime or magnesium oxide to remove SO_2 in the upper furnace or in a flue gas desulphurization reactor. The dry injection technique has removal efficiencies ranging from 25 to 75% while the wet FGD technology has a higher efficiency of about 90% to 95%. Future stringent regulation of NO_x/SO_x emissions will require sophisticated flue gas treatment processes that can be implemented as retrofits to existing plants. The add–on processes can be subdivided into dry and wet methods. The wet methods have several advantages over the dry ones. For instance, they can be:

. Combined with any already present wet flue gas desulphurization process (FGD).

. Operated at normal stack temperatures.

In view of these advantages, a study of wet absorption technology is important for potential industrial applications. Although a major disadvantage of the wet processes is the generation of waste products that create water pollution, previous research indicates some success in developing absorbents that can be regenerated to minimize the amount of wastes produced.

Although the wet flue gas desulphurization (FGD) processes have been well established for the removal of SO_x, few wet processes have been developed for the removal of NO_x or the simultaneous removal of NO_x/SO_x. Considerable efforts have been devoted to the development of more efficient systems capable of handling both NO_x and SO_x. However, such integrated processes are very difficult to develop because of the low solubility of nitric oxide. The search for a promising scrubbing liquid for both NO_x and SO_x continues to be a major objective in this area.

At present, two approaches are considered for the removal of nitric oxide by wet processes. One depends on the gas phase oxidation of NO to the more reactive NO_2 by strong oxidizers such as ozone (O_3) or chlorine dioxide (ClO_2). Ozone is an ideal oxidizing agent since it can oxidize NO to NO_2 during a one second residence time. However, it is very expensive. Although ClO_2 is comparatively cheaper, its use introduces considerable amounts of chlorides into the scrubbing liquor, which cause waste disposal problems. Although NO can

also be oxidized by the oxygen in the flue gas, noncatalytic conversions are very low with the prevailing low NO concentrations. For a flue gas containing 5% oxygen and 750 ppm of NO, a residence time of about 150 minutes is required for the conversion of 90% of the NO to NO_2 at a temperature of 300 ^{o}F.

The other approach is through the liquid phase oxidation of NO as it is being absorbed. Aqueous sodium chlorite ($NaClO_2$), hydrogen peroxide and potassium permanganate solutions (Uchida, Kobayashi and Kageyama, 1983) have been shown to be effective oxidizing solutions in tests with laboratory–type reactors. Hydrogen peroxide is an ideal absorbent, but not cost effective. Although sodium chlorite ($NaClO_2$) is cheaper, it poses some difficulty in terms of waste water treatment.

The lack of promising scrubbing liquids for nitric oxide and potentially less expensive methods for converting NO to NO_2 remain as the main problems to be solved. In addition, the hydrodynamic conditions are also of fundamental importance to the understanding of the absorption processes. Some of the previous research efforts concerning this aspect are summarized in Tables 2.1 and 2.2, in the next chapter. As indicated, most of these studies were confined to either semi–batch processes or the simple removal of NO_x at relatively high NO_x concentration. Comparatively little attention has been given to the continuous flow, simultaneous, low–level removal of NO_x/SO_x.

The objectives of this work were to:

. Establish the removal efficiencies of NO_x and SO_x with respect to liquid and gas flow rates, and liquid absorbent and flue gas concentrations under counter–current flow conditions.
. Derive a model governing the absorption process for the low NO_x or SO_2 concentrations encountered in coal–fired flue gases, on the basis of previous semi–batch studies.
. Collect the necessary data on NO_x/SO_x absorption and perform a complete computer simulation.
. Formulate conclusions regarding:
  – the applicability of the mathematical model.
  – the chemistry of the absorption process.

The system proposed by Sada et al.(1978), using sodium chlorite ($NaClO_2$), was selected for the present study because the:

. Absorption data are well correlated under semi–batch operations.
. Sodium chlorite appears to be very promising for controlling NO_x/SO_x emissions.

The validated models will provide a bridge between the original batch or semi–batch and the more recent flow systems used for the removal of NO_x/SO_x. Also they will be useful for the design of scrubbers for the removal of NO_x/SO_x and for other similar process simulations.

CHAPTER 2

LITERATURE REVIEW

The absorption of NO_x/SO_x into water and aqueous alkaline sclutions is important to many industries (in the production of nitric and sulphuric acids and the current interest in air pollution abatement). A large volume of literature concerning NO_x and SO_x removal is available. Unfortunately, most of these early fundamental and applied studies have used relatively high NO_x concentrations. On the other hand, most of the recent studies, involving low NO_x concentration, have been performed on either batch or semi–batch type reactors which are not readily applicable to flue gas absorption under continuous flow condition. Some of these research efforts are summarized in Tables 2.1 and 2.2. As indicated, most of these studies were confined to either semi–batch processes or the simple removal of NO_x or SO_x. Very little work has been done on individual or combined removal of NO_x and SO_x in packed columns under continuous–flow conditions. The work of Counce and Perona (1979, 1980, 1983), and Myerson and Sandy (1981) represent the rare exceptions. However, their efforts were limited to the individual removal of either NO_x or SO_x.

Although systems for eliminating SO_x have been well established, an

Table 2.1 Recent Absorption Studies on NO_x

Researcher	Scrubbing Liquid	Type of Reactor
Chappell (1973)	Na_2SO_3/NaOH $Mg(OH)_2$ Slurry	Spray Column
Conclusions:	. NO_2 and SO_2 are effectively absorbed by Na_2SO_3 solutions. . The data showed that the sulphite solutions would effectively absorb NO_x only if NO had been oxidized to NO_2 upstream from the scrubber.	
Takeuchi et al. (1977)	$Na_2SO_3/NaHSO_3$	Batch Reactor
Conclusions:	. Rate of NO absorption was very slow. . Suggests a need for a catalyst that will enhance the reaction in the liquid phase to remove No after converting it into NO_2 by a gas phase reaction e.g. O_3, ClO_2.	
Teramoto et al. (1978)	Fe(II)–EDTA Fe(II)–EDTA/Na_2SO_3	Batch Reactor
Conclusions:	. Rate and equilibrium constants for the reaction of NO with	

Table 2.1 Recent Absorption Studies on NO_x (continued)

Researcher	Scrubbing Liquid	Type of Reactor
Teramoto et al. (1978) (continued)	. Fe(II)–EDTA were determined. These values are much higher than the values for the reaction between NO and Fe(II) in the absence of EDTA. . The absorption rates of NO in aqueous solutions of Fe(II)–EDTA were much higher than those for other liquid absorbents investigated. . The absorption rates were explained satisfactorily on the assumption that NO co–ordinates to Fe(II)(EDTA)(SO_3^{2-}) irreversibly.	
Sada et al. (1977)	$KMnO_4$/NaOH	Batch Reactor
Conclusions:	. Kinetic studies of the reaction between NO and $KMnO_4$ in neutral and alkaline solution can be expressed as first–order with respect to NO and first–order with respect to $KMnO_4$. . An increase in the alkaline (NaOH) concentration resulted in an increase in the reaction rate constant. . The derived reaction rate constants were expressed as functions of the NaOH concentration.	

Table 2.1 Recent Absorption Studies on NO_x (continued)

Researcher	Scrubbing Liquid	Type of Reactor
Sada et al. (1978)	$NaClO_2$/NaOH	Semi–batch
Conclusions:	. The reaction was found to be second–order in nitric oxide and first–order in sodium chlorite. . The reaction rate constants decreased exponentially with increasing sodium hydroxide concentrations.	
Sada et al. (1979)	$NaClO_2$/NaOH	Semi–batch
Conclusions:	. The rate of NO_2 absorption was determined by the parallel reactions involving oxidation and hydrolysis and to be second–order with respect to NO_2. . Rate constant for the reaction was evaluated. . The effect of NaOH concentration on the absorption rate became significant when concentrations exceeded 0.6 M.	

Table 2.1 Recent Absorption Studies on NO_x (continued)

Researcher	Scrubbing Liquid	Type of Reactor
Sada et al. (1979) (continued)	. There appeared to be a gradual increase in absorption of NO at the interfacial concentration of NO ranging from $5x10^{-7}$ to $2x10^{-6}$ M with chlorite concentrations lower than 1.M. . Above this transition region, the order of reaction in NO approached 2 as previously derived. Below the transition region, the order of reaction in NO changed from unity to slightly less than one. . The gradual increase of absorption rate in the transition region suggested the presence of some intermediate product with more oxidative power than chlorite ion.	
Counce et al. (1979)	HNO_3(dilute)	Sieve–plate column
Conclusions:	. Removal efficiencies varied between 75% to 90%. . The conversion of NO_x varied directly as a function of the gas flow rate and the partial pressure of NO_2^* (NO_2+$2N_2O_4$).	

Table 2.1 Recent Absorption Studies on NO_x (continued)

Researcher	Scrubbing Liquid	Type of Reactor
Counce et al. (1979) (continued)	. The build–up of HNO_2 in the scrubber liquid resulted in a decrease in scrubbing efficiency. . Destroying HNO_2 in the scrubber liquid before recycling to the column increased the NO_x removal efficiency of the system.	
Counce et al. (1980)	HNO_3(dilute)	Sieve–plate column
Conclusions:	. A mathematical model utilizing kinetic and equilibrium constants from the literature was proposed.	
Counce et al. (1983)	Water	Packed Column
Conclusions:	. Nitrogen oxide removal efficiencies of 55% to 97% were obtained. . A mathematical model based on mass transfer, kinetic and equilibrium data was presented.	

Table 2.1 Recent Absorption Studies on NO_x (continued)

Researcher	Scrubbing Liquid	Type of Reactor
Myerson et al. (1981)	Water	Packed Column (limestone)
Conclusions:	. The oxidation of nitric oxide to nitrogen dioxide was crucial to the attainment of high absorption efficiencies. . The absorption efficiency was found to be a function of gas flow velocity and NO_x partial pressure (at low partial pressures). . The amount of limestone packing in the column was found to affect the absorption efficiency significantly. . The build–up of HNO_2 decreased the absorption efficiency.	
Aoki et al. (1982)	NaOH(46%)	Semi–batch
Conclusions:	. The absorption rate was not dependent on the concentration of hydroxide ion if the pH near the interface was not lower than a critical value (being between 4.01 and 6.86). If the pH became lower, the rate decreased remarkably, presumably, due to the reverse reaction of HNO_2.	

Table 2.1 Recent Absorption Studies on NO_x (continued)

Researcher	Scrubbing Liquid	Type of Reactor
Uchida et al. (1983)	$KMnO_4$/NaOH $Na_2SO_3/FeSO_4$	Semi–batch Bubble Column

Conclusions:

. The rate of NO absorption into $KMnO_4$ solution decreased with time due to the production of MnO_2 which covered the gas–liquid interface and prevented NO transfer. When NaOH was added to the solution, the production of MnO_2 was prevented and the absorption rate did not decrease.

. The absorption rate of NO in $Na_2SO_3/FeSO_4$ showed a maximum at a specific concentration of Na_2SO_3. When its concentration was too high, $Fe(OH)_2$ precipitated and the absorption rate decreased.

Table 2.1 Recent Absorption Studies on NO_x (continued)

Researcher	Scrubbing Liquid	Type of Reactor
Carta et al. (1983)	HNO_3(dilute) /Water	String of spheres (falling film absorber)
Conclusions:	. Considerable enhancement of the absorption rate was achieved with 25 to 30 wt.% nitric acid solutions.	
	. The accumulation of HNO_2 at the interface had an important beneficial effect. Its rate of decomposition determined the rate of absorption of nitric oxide in nitric acid solutions.	

Table 2.2 Recent Absorption Studies on SO_2

Researcher	Scrubbing Liquid	Type of Reactor
Chang et al. (1981)	Water–Bisulphite Water–HCl(dilute) Water–NaCl	Continuous stirred vessel

Conclusions:

. For the sulphur dioxide – water system, the gas absorption mechanism could be modeled by mass transfer with an instantaneous reversible reaction of the type:

$$A \rightleftharpoons 2B$$

. For the sulphur dioxide – hydrogen chloride system, the equilibrium chemical reaction scheme became:

$$A \rightleftharpoons B$$

The enhancement factor was independent of gas phase sulphur dioxide partial pressure.

. For the sulphur dioxide – sodium chloride system, the absorption could be described by the surface renewal theory accompanied by an equilibrium reaction of the type:

$$A \rightleftharpoons B + C$$

Table 2.2 Recent Absorption Studies on SO_2 (continued)

Researcher	Scrubbing Liquid	Type of Reactor
Chang et al. (1981) (continued)	. The presence of a relatively high concentration of sodium chloride dissipated any gradient of electric potential and allowed hydrogen ion to diffuse much faster. . Sodium chloride also increased the value of the effective equilibrium constant through its effect on activity coefficients. These factors were reflected by the increase in the SO_2 absorption rate with the addition of sodium chloride.	
Sada et al. (1982)	$CaSO_3/Mg(OH)_2$	Stirred tank Semi–batch
Conclusions:	. The rate of absorption of NO_2 in the presence of SO_2, into aqueous slurries of $Mg(OH)_2$, was greatly enhanced by sulphite ion formation.	
Fan et al. (1982)	$CaOH–Mg(OH)_2$ $CaOH–Mg(CO_3)_2$ $CaOH–MgSO_4$	Wetted–wall column
Conclusions:	. The addition of magnesium hydroxide, magnesium carbonate or magnesium sulphate significantly improved the absorption rate of low concentration sulphur dioxide into calcium hydroxide solutions.	

Table 2.2 Recent Absorption Studies on SO_2 (continued)

Researcher	Scrubbing Liquid	Type of Reactor
Fan et al. (1982) (continued)	. Magnesium hydroxide provided the highest improvement, which was followed, in order, by magnesium carbonate and magnesium sulphate. . The experimental results suggested a catalytic effect of magnesium hydroxide precipitate on sulphur dioxide absorption into calcium hydroxide solution containing magnesium additives.	
Uchida et al. (1984)	Melamine Slurry	Stirred tank Semi–batch
Conclusions:	. The absorption rates were under complete gas film control when the stirring speed was 242 $min.^{-1}$ or the concentration of SO_2 in the feed gas was 1001 ppm. . The rate increased slightly if the slurry concentration was kept above 5 wt %.	

integrated wet absorption system capable of handling both species has not yet been developed because the solubility of NO_x, in most common absorbents used for SO_x, is much lower than that of SO_x. Various absorbents have been tested and absorption mechanisms proposed recently in the literature. The elimination of NO_x has been considered as a target of these recent investigations simply because a good absorbent for NO is also an ideal scrubbing liquid for SO_x , in general.

This chapter will review the current evidence related to the nature of the reactions and transporting species that are important for the development of predictive models. The review begins with SO_x studies and ends with an examination of NO_x data. Special attention is given to absorption studies conducted with low concentrations corresponding to typical flue gas levels.

2.1 SO_2 Studies

The next three sections are concerned with SO_2 studies. They concentrate on the absorption of SO_2 into water and the mechanisms involved. Studies of SO_2 absorption into organic and inorganic solutions are also discussed.

2.1.1 Absorption of SO_2 into Water

The physical properties of SO_2 in water were provided by Campbell and Maass (1930). Since their work, numerous papers have discussed the properties of SO_2–containing aqueous solutions (Johnstone and Leppler, 1934; Rabe and Harris, 1963; Eriksen, 1969; Douabul and Riley, 1979; Leaist, 1984). Much effort has been made to understand their fundamental nature and transport properties, not only because the absorption of SO_2 into water is a process of considerable importance to the production of sulphuric acid, and the pulp and paper industries, but also because of the recent interest in pollution control.

In spite of the considerable amount of data available for this process at high SO_2 concentrations, information concerning the absorption and transport mechanisms, particularly for low partial pressures of typical flue gas desulphurization (FGD) processes, is rarely found in the earlier works. However, there has been a general belief from these earlier works that SO_2 absorbed at low concentrations is largely hydrolysed and transported as an ionic species. Unfortunately, the concentration limit at which this acid hydrolysis occurs has not been established. A knowledge of this limit is important to predictive model development or similar activities where knowledge of transport species and diffusivities is required. According to Leaist (1984), hydrolysis influences the diffusion coefficient in two important ways. First, for a given concentration

gradient, hydrolysis increases the gradient of chemical potential, the driving force for diffusion. On the other hand, because the transport of the hydrolysis products, H_3O^+ and HSO_3^- , is subject to more frictional resistance than transport of a single molecular species, hydrolysis tends to reduce the effective mobility of the sulphur dioxide component and thereby decreases the rate of absorption. Hence, from the standpoint of applications and of understanding of the transport mechanism, experiments with low partial pressures of sulphur dioxide are desirable. The recent works of Hikita et al. (1978), Roberts and Friedlander (1980), Chang and Rochelle (1981), and Kaji et al. (1985) represent some of the important investigations related to flue gas desulphurization processes.

2.1.1.1 Chemical Reaction Kinetics of SO_2

In discussing the various equilibria involved in solutions of sulphur dioxide in water, it is both usual and convenient to start with the gaseous phase. The following reactions may be postulated to represent the fundamentals involved in the absorption process:

$$SO_{2(g)} \rightleftharpoons SO_{2(l)} \qquad \text{.....(2.1)}$$

$$SO_{2(l)} + H_2O_{(l)} \rightleftharpoons H_2SO_{3(l)} \qquad .....(2.2)$$

$$H_2SO_{3(l)} \rightleftharpoons HSO^-_{3(l)} + H^+_{(l)} \qquad .....(2.3)$$

The ionization may proceed further according to:

$$HSO^-_{3(l)} \rightleftharpoons SO^{2-}_{3\,(l)} + H^+_{(l)} \qquad .....(2.4)$$

Reaction 2.1 represents the equilibrium at the gas–liquid interface while reactions 2.2, 2.3, and 2.4 correspond to the hydrolysis and ionization of the absorbed SO_2.

Numerous studies have been conducted on aqueous solutions of SO_2, including ultraviolet (DeMaine, 1957), infrared (Falk and Giguere, 1958; Jones and McLaren, 1958) and Raman spectroscopy (Jones and McLaren, 1958). These investigations indicated that the predominant ionic sulphur species is the bisulphite ion. No evidence has been found for the existence of H_2SO_3 molecules from the work of Falk and Giguere (1958). On the basis of these data, Falk and Giguere (1958), and Eriksen (1969) suggested that reactions 2.2 and 2.3 are most likely represented by:

$$SO_{2(aq.)} + 2H_2O_{(l)} \underset{k_{-1}}{\overset{k_1}{\rightleftharpoons}} H_3O^+_{(l)} + HSO^-_{3(l)} \qquad .....(2.5)$$

The forward rate constant for the reaction at 20 ^{o}C has been measured by Eigen et al. (1961) to be 3.4×10^6 s^{-1}. According to Morgan and Maass (1931), the second ionization, reaction 2.4, is generally so small in an aqueous solution that it may be safely neglected. Hence, the absorption of SO_2 into water may be regarded as an instantaneous, reversible reaction represented by reaction 2.5. The equilibrium constant, K for this reaction was given by Campbell and Maass (1930). The best value of K based on the work of Huss and Eckert (1977), is 1.4×10^{-2} g–mol.L^{-1}.

This hydrolysis reaction of SO_2 is extremely important to the transport of SO_2 through aqueous solutions. The values of k_1, as summarized by Roberts (1979), are provided in Table 2.3. Very large discrepancies among these values are evident. The range exceeds eight orders of magnitude. The difference observed is probably due to the experimental conditions as the rate of reaction is strongly pH dependent.

Roberts and Friedlander (1980), in their study of the steady state flux of sulphur dioxide through films of water and neutral and alkaline salt solutions,

Table 2.3 Rate Constant for Reaction 2.5 (Roberts, 1979)

k_1 $[s^{-1}]$	Conditions
>250. (estimated)	20. ^{o}C, dilute
1.62	11.2 ^{o}C, dilute
4.09 (extrapolated)	25. ^{o}C, dilute
3.4×10^{6}	20. ^{o}C, I = 0.1 M
3.17×10^{-2}	25. ^{o}C
>0.2	25. ^{o}C
>16.	$\cong$ 0 ^{o}C, dilute

showed that HSO_3^- is responsible for 83% to 95% of the flux. An examination of the data in Table 2.4, obtained by Leaist (1984), shows that the apparent degree of hydrolysis was about 0.86 to 1 for concentrations of $SO_{2(l)}$ below $2.8x10^{-3}$ M.

Roberts and Friedlander (1980) also provided a lower limit for the forward rate constant for the hydrolysis process (reaction 2.5) that was approximately 10^4 larger than the value reported by Wang and Himmelblau (1964). These authors pointed out that this value came closer to substantiating Eigen's (1961) value than other estimates in the literature. They also confirmed that the reaction of $SO_{2(aq)}$ with water is fast, and can be regarded as instantaneous.

Using the Harned conductimetric technique, Leaist (1984) measured the diffusion coefficients of aqueous sulphur dioxide over the concentration range $3x10^{-3}$ to 0.1 M. At concentrations lower than about 0.02 M, an appreciable fraction of the sulphur dioxide component was converted, by hydrolysis, into the more rapidly diffusing bisulphite and hydrogen ions.

The diffusion coefficients of aqueous sulphur dioxide are listed in Table 2.4. As the total concentration of SO_2 increases, the diffusion coefficients of aqueous sulphur dioxide decrease and approach the diffusion coefficient of

Table 2.4 Diffusion Coefficients of Aqueous SO_2 at 25 ^{o}C (Leaist, 1984)

Total Concentration of SO_2 $[mol.L^{-1}]$ $Cx10^3$	Degree of Hydroysis $[-]$ α	Diffusion Coefficient $[m^2.s^{-1}]$ $Dx10^9$
0.0	1.00	2.316
2.8	0.86	2.130
5.4	0.78	2.076
9.5	0.70	2.021
20.5	0.58	1.950
29.7	0.52	1.924
52.1	0.43	1.891
70.3	0.39	1.876
84.4	0.36	1.868
97.2	0.35	1.862

molecular SO_2 which has a value of $1.76x10^{-9}$ $m^2.s^{-1}$ at 25 ^oC (Hikita et al., 1978). It can be inferred from Table 2.4 that acid hydrolysis of absorbed SO_2 seems less likely to occur when total SO_2 concentrations are above $9.72x10^{-2}$ M, as the degree of hydrolysis above this value is less than 0.35. Therefore above this concentration, molecular SO_2 may be regarded as the main diffusing species and the use of the molecular diffusion coefficient of SO_2 would be appropriate for higher SO_2 concentrations.

2.1.1.2 Modeling of SO_2 Absorption in Terms of Fundamental Theories

Hikita et al. (1978), using the penetration model as a basis, formulated SO_2 absorption according to reaction 2.5. Their differential equations could not be solved analytically and no attempt was made to solve them numerically. However, with a modification of the diffusivity ratios, they obtained an approximate expression for the rate of absorption of SO_2 provided that the two reaction products, HO_3^+ and HSO_3^-, had equal diffusivities and equal bulk concentrations. The equal diffusivities assumption seems very unlikely. However, these authors confirmed their derived model by conducting absorption experiments in a wetted–wall column. Their studies were conducted at atmospheric pressure for temperatures of 15^o, 25^o, 35^o, and 45^oC. The gas

phase was pure sulphur dioxide saturated with water vapor at the temperature of the experiment. The absorbent was water. The measured values of the absorption rate were in good agreement with their model.

Some of the physical properties used in their calculations are reported in Table 2.5. An examination of the diffusivity data in Table 2.5, shows that these authors considered aqueous SO_2 to diffuse as a molecular species. The data in Table 2.5 imply that the bulk concentration of sulphur dioxide was 1.04 M, a concentration that is about ten times higher than that at which hydrolysis occurs. Hence, the absorbed SO_2 was prevalent in its molecular form. Therefore, their choice of transporting species and use of the molecular diffusivity of SO_2 were appropriate.

Kaji, Hishinuma, and Kuroda (1985) used the expression given by Hikita et al.(1978) to calculate the liquid–film mass transfer coefficient of SO_2 in distilled water droplets. Water droplets of a constant diameter of 2.2 mm were formed from a hypodermic needle approximately every two seconds and allowed to fall through distances ranging from 23 to 113 cm which corresponded to contact times of 0.155 to 0.431 seconds respectively. The effect of contact time on SO_2 absorption is an important parameter to be clarified for a sound spray scrubber design. The experiments were performed at the controlled temperature of 20^{o}C with SO_2 concentrations of 620, 1126 and 1968 ppm. Kaji et al. (1985)

Table 2.5 **Physical Properties for the Sulphur Dioxide – Water System at 15^{o}, 25^{o}, 35^{o}, and $45^{o}C$ (Hikita et al., 1978)**

Temperature $[^{o}C]$	A_i $[g\text{–}mol.L^{-1}]$	$D_A x10^{9}$ $[m^{2}.s^{-1}]$	$Kx10^{2}$ $[g\text{–}mol.L^{-1}]$
15	1.64	1.34	2.19
25	1.16	1.76	1.70
35	0.831	2.25	1.31
45	0.595	2.81	0.991

reported their experimental results on the liquid–film mass transfer coefficients to fall in the range of 55 to 75 kmole.m^{-2}.hr^{-1} for the absorption of SO_2 by water droplets. They also concluded that the liquid–film mass transfer coefficients were independent of the SO_2 concentration in the gas phase. When their results are compared with values predicted by the Handles and Baron expression (1959), a fairly significant discrepancy is observed for shorter contact times. However, a better agreement is found for contact times exceeding 0.4 seconds. These authors suggested that the discrepancy evident for shorter contact times may be due to the internal circulation created by liquid flow through the hypodermic needle during the formation period.

Reaction 2.5 was also studied by Chang and Rochelle (1981) for SO_2 partial pressures ranging from 0.0002 to 0.98 bar. This range covers the typical concentrations found in stack gases containing from 1000 to 4000 ppm SO_2. Experiments were carried out on the absorption of sulphur dioxide from both pure SO_2 and SO_2/N_2 mixtures into pure water in a continuous stirred tank. The absorption data were interpreted in terms of the surface renewal model which had been previously solved numerically, by these authors.

It is interesting to note that the model derived by Hikita et al.(1978), on the basis of the penetration theory, and the model obtained by Chang and Rochelle (1981), based on surface renewal theory, provided the same expression

for the absorption of sulphur dioxide into water. This similarity can be attributed to the fact that when sulphur dioxide is absorbed into pure water, there are no other ionic species, except the two reaction products, present in the liquid phase. Therefore, electrical neutrality requires that the concentration and effective diffusivity of HO_3^+ must always equal those of HSO_3^-. As a result, the rates of absorption derived on the basis of different theories are equivalent when the diffusivities of all diffusing species are equal. However, the two models differ when the diffusivity ratios deviate from unity.

2.1.2 Absorption of SO_2 into Organic Solutions

The absorption of SO_2 into organic or inorganic solutions has several advantages over water. These solutions have higher absorption capacities and potentials to absorb nitric oxide. As a result, such systems can be integrated into a single unit capable of removing both acidic gases simultaneously. However, the inorganic absorption processes are limited by their normally irreversible nature. Consequently a flue gas desulphurization process using a lime or limestone slurry creates a difficulty in terms of disposing of the end products ($CaSO_4$ and/or $CaSO_3$). Recent studies with amine solutions indicated that the spent liquor could be regenerated. Current findings in this area will be reviewed and discussed later.

Mohamed and Klinzing (1984) employed a gas–liquid chromatographic method to search for a multipurpose solvent for absorbing NO, NO_2 and SO_2. Unfortunately, none of the organic solvents that were tested absorbed NO. Conversely, these authors observed that SO_2 was absorbed by all the tested solvents while NO_2 was absorbed only by methanol. As a result, they concluded methanol could be used as a multipurpose solvent for these acidic gases provided that NO was first converted to NO_2.

Chappell (1973), in a screening program for liquid absorbents, first reported that concentrated amine solutions are very effective for absorbing NO and SO_2. Taking the suggestion from Chappell (1973), Uchida, Miyazaki, and Masumoto (1984) used melamine slurries to absorb simulated stack flue gases. Their absorption studies were carried out in a stirred tank reactor which operated batchwise with respect to melamine. Relative effects of varying the concentrations of melamine slurry and concentrations of SO_2 were examined. The absorption mechanism as well as the kinetic reactions w[illegible]t clarified. The rate of absorption was interpreted in terms of the film model assuming an instantaneous, irreversible, reaction at the experimental conditions. The results showed that the predicted absorption rates differed from the experimental values by as much as 20%. Minor effects of slurry concentration on the SO_2 absorption rate were reported.

According to these authors, SO_2 reacts with aqueous melamine slurry to

form hydrated melamine sulphite, which precipitates according to the following reactions:

$$SO_{2(l)} + H_2O_{(l)} \longrightarrow H_2SO_{3(l)} \qquad \text{.....(2.6)}$$

$$C_3H_6N_{6(s)} + H_2O_{(l)} \longrightarrow C_3H_6N_{6(aq)} \qquad \text{.....(2.7)}$$

$$2C_3H_6N_{6(aq)} + H_2SO_{3(l)} + 4H_2O_{(l)} \longrightarrow (C_3H_6N_6)_2.H_2SO_3.4H_2O_{(l)}$$

.....(2.8)

In the regeneration process, melamine sulphite is thermally decomposed at 100^{o} to 200 ^{o}C to yield melamine, $SO_{2(g)}$ and water vapor as illustrated by:

$$(C_3H_6N_6)_2.H_2SO_3.4H_2O_{(l)} \longrightarrow 2C_3H_6N_{6(s)} + SO_{2(g)} + 5H_2O_{(g)}$$

.....(2.9)

However, if SO_3 is present in the flue gas, hydrated melamine sulphate is precipitated according to:

$$SO_{2(g)} + \tfrac{1}{2}\,O_{2(g)} \xrightarrow{\text{slow}} SO_{3(g)} \qquad \text{.....(2.10)}$$

$$SO_{3(g)} + H_2O_{(l)} \longrightarrow H_2SO_{4(l)} \quad .....(2.11)$$

$$2C_3H_6N_{6(aq)} + H_2SO_{4(l)} + 2H_2O_{(l)} \longrightarrow (C_3H_6N_6)_2.H_2SO_4.2H_2O_{(l)} \quad .....(2.12)$$

Unlike melamine sulphite, the precipitated sulphate can not be regenerated thermally. Therefore, methods of preventing the oxidation of the $SO_{2(g)}$ are essential.

In this proposed reaction scheme, the formation of $H_2SO_{3(l)}$, according to reaction 2.6, is questionable at the typical flue gas concentrations. Previous reviews indicated that under such input levels, the absorbed $SO_{2(l)}$ will hydrolyse significantly to produce 80% to 90% of the HSO_3^- species rather than $H_2SO_{3(l)}$. Hence, for reactions 2.6 to 2.11 to correctly represent the absorption kinetics, they should occur at rates that are comparable to the hydrolysis reaction of the absorbed $SO_{2(l)}$. Otherwise the $H_2SO_{3(l)}$ needed for the formation of melamine sulphite will not be available for reaction 2.8.

Using a gas–liquid chromatographic technique, Ho and Klinzing (1986) carried out tests on several amine solutions on a trial and error basis. Of the four solutions tested, only one solvent, triethylenetetramine (TETA) was found

to absorb both SO_2 and NO. Henry's law constants for these gases in the tested solvents were determined. A comparison of the Henry's law constants listed in Table 2.6 showed that SO_2 is roughly about twenty times more soluble than NO in TETA. However, no information on the absorption mechanisms or kinetic reactions was given. The design of gas–liquid contacting systems for gas absorption with chemical reaction requires thorough knowledge of the mass transfer mechanisms as well as the kinetic reactions involved. Therefore, further investigations into the mass transfer and kinetic reactions are neccessary, before reliable operations can be constructed.

Basu and Dutta (1987) studied SO_2 absorption in dimethylaniline (DMA) solutions using a short falling film apparatus. The relative effects of gas and liquid concentrations, contact times and temperatures on the rate of absorption were examined. Equilibrium constants and the rate equations for the forward and reverse reactions were established. The absorption data were interpreted using the penetration theory, assuming simultaneous pseudo–first–order reactions.

In this system, sulphur dioxide reacts reversibly with dimethyaniline to form an addition compound (Riesenfeld and Kohl, 1974), according to:

$$C_6H_5N(CH_3)_2 + SO_{2(l)} \underset{k_{-1}}{\overset{k_1}{\rightleftharpoons}} C_6H_5N(CH_3)_2{\cdot}SO_2 \qquad \text{.....(2.13)}$$

Table 2.6 **Henry's Law Constants for SO_2 and NO in Triethylenetetramine (TETA) Solution (Ho and Klinzing, 1986)**

Temperature [^oC]	H_{SO_2} x10^{-6} [Pa]	H_{NO} x10^{-6} [Pa]
20	0.6967	17.10
25	0.7906	18.28
70	2.02	30.13
80	2.56	32.93
90	3.02	36.41
100	3.61	41.24

where

$k_1 = 2.524 \times 10^7 \exp(-35.55/RT)$, $L.mol^{-1}.s^{-1}$

(second order forward rate constant)

$k_{-1} = 1.187 \times 10^{10} \exp(-54.69/RT)$, s^{-1}

(first order reverse rate constant)

R = gas constant, $kJ.mol^{-1}.K^{-1}$

T = temperature, K

These authors also noted that the enhancement of absorption rate in dilute solutions of amine obtained in their study was rather low in comparison with that in a lime slurry. In other words, the system was not as effective as a lime system. However, the lime system is a non–regenerative process which represents a major disadvantage as indicated earlier.

2.1.3 Absorption of SO_2 into Inorganic Solutions

Johnstone and Singh (1937) carried out an absorption study on SO_2 in a grid packed tower using a dilute sodium hydroxide solution. The liquid side

mass transfer coefficient was correlated analogously to the Chilton–Colburn heat transfer type equation. No attempt was made to interpret the absorption data in terms of a mechanistic model.

Using a radioactive tracer technique, Wang and Himmelblau (1964) performed a kinetic study of sulphur dioxide in aqueous solutions of sodium bisulphite. Forward and reverse rate values were reported for the $SO_2 - H_2O$ system for the first time. However, these rate values were later shown, by Roberts (1979), to be much lower than the results of Eigen et al. (1961) which are believed to be more reliable.

Bjerle, Bengstsson and Farnkvist (1972) studied the absorption of SO_2 in $CaCO_3$ slurry in a laminar jet absorber. Tests were made with SO_2 concentrations varying from 0.01 to 1 volume per cent. Relative effects of temperature were examined. The overall gas phase mass transfer coefficient and enhancement factor for the system were determined experimentally. The absorption rate of SO_2 in $CaCO_3$ slurry was found to be only slightly higher than in water. Consequently, this system was not promising from the standpoint of practical application. Moreover, no information on the kinetic and absorption mechanisms of this system was developed.

On the basis of two film theory, McMichael, Fan and Wen (1976)

developed a model for SO_2 absorption into limestone and limestone – magnesium oxide slurries. Scrubbing data were collected from a pilot–plant scale spray column and a small, laboratory–scale, turbulent contacting absorber (TCA). Absorption was assumed to be gas film controlled under the experimental conditions (pH > 4.7). They argued that the interfacial partial pressure of SO_2, maintaining equilibrium with the liquid at the interface was negligible when compared to the much higher partial pressure of SO_2 in the flue gas, and thus can be ignored in their model. A ratio of the gas to liquid film mass transfer resistances was defined to interpret the gas phase diffusion mechanism. These authors observed that as the partial pressure of SO_2 in the flue gas decreased, the SO_2 transfer became more gas film controlled.

As indicated by the work of Bjerle et al. (1972), the rates of absorption of SO_2 in limestone and limestone slurries were too low for practical application. As a result Rochelle and King (1977) extended the investigation of the system with alkali additives. The effects of alkali additives on mass transfer were quantified and reported. An absorption model was derived on the basis of the penetration theory. Several assumptions were made in their derivation. Firstly, instantaneous, bimolecular reaction of dissolved alkalinity with SO_2 was assumed. Secondly, total alkalinity was defined to account for the complex chemistry and was taken to be constant. Thirdly, effective solubility was defined to account for the possible contribution from dissolved and dissociated

SO_2 and was assumed to be constant. However, these assumptions of constant total alkalinity and effective solubility were later deemed, by Roberts (1979), to be inappropriate. In fact, Rochelle and King (1977) were aware of the limitations of their assumption of effective solubility. Consequently, they estimated the possible change in this effective solubility over the height of the scrubber to vary by a factor of two. Yet, this factor was far too low, as indicated by Roberts (1979), who suggested that a factor of ten would be more reasonable. Despite these limitations, Rochelle and King (1977) successfully interpreted their results with the derived model. As a final note to these studies, it should be mentioned that for the first time an effective liquid–side mass transfer coefficient was estimated and used in a model to account for the various sulphur species resulting from hydrolysis.

A similar limestone based slurry was used by Sada et al. (1982). In their SO_2 absorption study, experiments were performed with a stirred tank reactor which was operated batchwise with respect to the liquid phase and continuously with respect to the gas phase. The absorption process was formulated on the basis of chemical absorption theory. The chemical reactions between dissolved SO_2 and suspended slurry were assumed to occur within the liquid film and also on the solid surface of the slurry. In other words, the dissolved gas was assumed to react instantaneously with the dissolved solid reactant as well as the solid surface suspended between the reaction plane and the liquid film. The

formulated differential equations were solved to yield an exact expression for the enhancement factor which was used to interpret their observed results. Dilute SO_2 was used in these experiments. The dissolved SO_2 could undergo hydrolysis under the experimental conditions. Unlike that of Rochelle and King (1977), this model did not account for this phenomenon.

Laohavichitra et al. (1982) conducted their SO_2 absorption experiments in a wetted wall column. Tests were made with calcium hydroxide solutions supplemented with various magnesium additives. The concentrations of SO_2 in the feed stream varied from 1000 ppm to 5000 ppm. These concentrations cover the range normally occurring in the flue gases emitted from power plants and smelters. The effects of different magnesium additives on the SO_2 absorption rate were clarified. It was found that the addition of $Mg(OH)_2$ significantly enhanced the absorption rate of the system. The increase in the SO_2 absorption rate with $Mg(OH)_2$ as an additive was probably due to the high alkaline nature of the solution. This conclusion agreed with the findings of McMichael and co–workers (1976), and Rochelle and King (1977).

Recently, studies on magnesia (MgO) slurries have shown that this flue gas desulphurization system could eliminate scrubber sludge problems. The chemical reactions involved in this process are given as:

$$MgO_{(s)} + H_2O_{(l)} \longrightarrow Mg(OH)_{2(aq)} \qquad \text{.....(2.14)}$$

$$Mg(OH)_{2(aq)} + SO_{2(l)} \longrightarrow MgSO_{3(aq)} + H_2O_{(l)} \quad \text{.....(2.15)}$$

According to reaction 2.14, the magnesia is hydrated in the slurry and then reacts with the dissolved SO_2 to form magnesium sulphite. This magnesium sulphite can be dried and thermally decomposed at higher temperature to regenerate MgO for recycling. The more concentrated SO_2 resulting from the decomposition process could be used for sulphuric acid or sulphur production. To make this process more useful, studies have been carried out recently on dry scrubbing by Egan and Felker (1986). Experiments were performed by these authors on a bench scale spray dryer with simulated flue gas. The relative effects of magnesia slurry concentrations, inlet flue gas temperatures, dryer temperatures, gas flows and slurry flow rates on SO_2 removal efficiency were examined. It was found that more than 90% SO_2 removal could be achieved with an excess magnesia input. A ratio of $Mg(OH)_2$ to SO_2 exceeding 1.4 would safeguard the performance. Definitely, there are certain advantages to operating such a system. Firstly, a dry product instead of a slurry is produced in the process thereby reducing the waste handling problem. Secondly, since no crystallizer is necessary, as with a wet slurry, equipment costs are reduced. Thirdly, the costs of maintenance, energy and pumping requirements are reduced. On the other hand, such a process might suffer from higher particulate emission levels and limits to SO_2 removal. It was also indicated by these authors that ways to prevent partial oxidation to sulphate are important

because this sulphate product can not be readily decomposed to MgO for recycling. Furthermore, the contaminants in the magnesia would accumulate during recycling and pose signiiicant problems for this process. Further research in this area is necessary.

2.2 NO_x Studies

The absorption of NO_x is probably the most complex process of all known absorption operations. Not only do absorption and desorption phenomena occur simultaneously but also various complex reactions occur in this system. For instance, in the $NO_x - HNO_x - H_2O$ system producing nitric acid, reversible, parallel, and consecutive reactions are observed during absorption and desorption processes. All of these reactions proceed in the gas phase as well as in the liquid phase. The complete absorption mechanism is not well understood nor documented. This is particularly true for the flue gas absorption process dealing with low NO_x levels. Desorption may be safely neglected for low NO_x absorption provided that nitrous acid in the scrubber liquid does not exceed 18 % by weight. Similar reactions in the gas and liquid phases should be expected as in the nitric acid production process.

In the following sections, the literature dealing with NO_x absorption will

be critically reviewed to help establish the most probable reaction mechanism for absorption at low NO_x levels. Reactions of NO_x and oxyacids in the gas phase and dilute aqueous solutions (e.g. H_2O, and $NaClO_2$) are discussed. The nature of dissolved NO_x molecules is presented and the predominant diffusing species are identified. The best values of Henry's law constant, diffusivity, equilibrium and kinetic constants are selected from the available data. It is important to know the magnitudes of these constants, particularly for the interpretation of kinetic processes and modeling activities.

2.2.1 Reactions of NO_x

The absorption of NO_x involves a number of chemical reactions, both in the gas and liquid phases. In the sections that follow, these reactions are critically examined and identified for the low concentrations (< 0.1% or 1000 ppm) pertaining to flue gases.

2.2.1.1 Gas Phase Reactions of NO_x

Table 2.7 lists the gas phase reactions of NO_x that have been identified in the manufacture of nitric acid and in the previous investigations on NO_2

Table 2.7 Gas Phase Reactions of NO_x

$2NO_{(g)} + O_{2(g)} \longrightarrow 2NO_{2(g)}$	.....(2.16)
$NO_{(g)} + O_{3(g)} \longrightarrow NO_{2(g)} + O_{2(g)}$	.....(2.17)
$2NO_{2(g)} \rightleftharpoons N_2O_{4(g)}$	.....(2.18)
$NO_{(g)} + NO_{2(g)} \rightleftharpoons N_2O_{3(g)}$	.....(2.19)
$NO_{(g)} + NO_{2(g)} + H_2O_{(g)} \rightleftharpoons 2HNO_{2(g)}$	.....(2.20)
$3NO_{2(g)} + H_2O_{(g)} \rightleftharpoons 2HNO_{3(g)} + NO_{(g)}$	.....(2.21)
$2NO_{2(g)} + H_2O_{(g)} \longrightarrow HNO_{3(g)} + HNO_{2(g)}$	.....(2.22)
$3NO_{2(g)} \rightleftharpoons N_2O_{5(g)} + NO_{(g)}$	.....(2.23)
$3HNO_{2(g)} \rightleftharpoons HNO_{3(g)} + 2NO_{(g)} + H_2O_{(g)}$	.....(2.24)
$NO_{2(g)} + HNO_{2(g)} \rightleftharpoons HNO_{3(g)} + NO_{(g)}$	.....(2.25)
$N_2O_{4(g)} + H_2O_{(g)} \rightleftharpoons HNO_{2(g)} + HNO_{3(g)}$	.....(2.26)
$N_2O_{3(g)} + H_2O_{(g)} \rightleftharpoons 2HNO_{2(g)}$	.....(2.27)
$N_2O_{5(g)} + H_2O_{(g)} \rightleftharpoons 2HNO_{3(g)}$	.....(2.28)

absorption mechanisms. Most of these reactions were derived from NO_2 studies at relatively higher concentrations than those found in flue gases.

All of these earlier studies were conducted at concentrations which were rarely lower than 2000 ppm (0.2% or $8.2x10^{-5}$ M) of NO_2. Therefore, care must be taken when interpreting absorption studies since some of these listed reactions are more prevalent and critical than others under specific conditions. In other words, the relative importance of these reactions in the case of absorption is dependent primarily on the initial NO_x compositions, and concentrations and kinetic rate constants.

Of the twelve reactions listed in Table 2.7, the first six are relatively important to absorption of NO_x gas. These reactions are discussed separately in the following sections.

2.2.1.1.1 Oxidation of NO with O_2

The oxidation of NO is an important step in the manufacture of nitric acid and in the removal of NO_x from flue gases. The gas phase oxidation of NO with molecular oxygen is given by:

$$2NO_{(g)} + O_{2(g)} \longrightarrow 2NO_{2(g)} \qquad .....(2.16)$$

According to Hasche and Patric (1925), Kassel (1930), and Treacy and Daniels (1955), the reaction follows third–order kinetics with the rate equation given by:

$$-\frac{dC_{NO}}{dt} = k_C C_{NO}^2 C_{O_2} \qquad .....(2.29)$$

where

k_C = rate constant, $(kmole.m^{-3})^{-2}.\ s^{-1}$

C_i = concentration, $(kmole.m^{-3})$, i = NO, O_2

Early studies by Hasche and Patric (1925), Kassel (1930), and Treacy and Daniels (1955), made important contributions to the understanding of the reaction. Later investigations by Tipper and Williams (1955), Ashmore et al. (1962), Morrison et al. (1966), Greig and Hall (1967), and Hisatune and Zafonte (1969), added more details to the reaction and precision to the rate constant. There is a strong consensus in the literature that the reaction is exothermic and follows third–order kinetics when partial pressures of NO are greater than 0.2 mmHg and the temperature is below 350 ^{o}C.

About fifteen values for k_C have been reported. Good summaries of these

rate values are given by Counce (1980) and Schuck and Stephens (1980). From a statistical treatment of these rate constants, Schuck and Stephens (1980) recommended a value of (7.5 $\pm$ 1.) x 10^3 $L^2.mole^{-2}.s^{-1}$ for k_C at 25 ^oC. The rate constant can also be predicted from the Arrhenius equation involving the use of activation energy according to:

$$k_C = A_o \exp\left(-\frac{E}{RT}\right) \qquad .....(2.30)$$

where

A_o = Arrhenius constant, 4.0645 x 10^2 $L^2.mole^{-2}.s^{-1}$

R = gas constant, 1.9843 $cal.K^{-1}.mole^{-1}$

E = activation energy, -1.7 $kcal.gmole^{-1}$

T = absolute temperature, K

The activation energy, as determined by different investigators, is given in Table 2.8. Oxidation of nitric oxide at low concentrations (< 1000 ppm) with molecular oxygen is relatively slow and thereby becomes the rate controlling step as experienced in most NO_x flue gas treatment processes or low NO concentration absorption studies. Strong gas phase oxidizing agents such as O_3 are necessary when the concentration of nitric oxide is less than 50 ppm. However, this rate limiting step becomes unimportant at high NO concentrations because this oxidation reaction proceeds readily to yield NO_2,

Table 2.8 Activation Energy for Reaction 2.16

$$2NO_{(g)} + O_{2(g)} \longrightarrow 2NO_{2(g)} \qquad (2.16)$$

Temperature [^{o}C]	Activation Energy [kcal.gmole^{-1}]	Reference [–]
0 – 60	-1.55 ± 0.2	Ashmore et al.(1962)
20 – 70	–1.75	Greig and Hall (1967)
30 – 90	–1.70	Hisatune and Zafonte (1969)
205	–1.0	Treacy and Daniels (1955)

a higher oxide of nitrogen, which has a solubility in water that is about six times higher than NO.

As indicated in the study of Galbally and Ray (1978), at concentrations of 100 ppm or greater, the half life for the oxidation of NO to NO_2 by atmospheric oxygen is one hour or less, whereas at low concentrations ($\cong$ 0.01 ppm) the half life for the oxidation is of the order of 10^4 hour. This variation in the oxidation rate by molecular oxygen explains why NO, at low concentration, becomes critical to the removal of NO_x from flue gases and perhaps explains why in some of the laboratory studies at high concentration of NO, NO_2 is detected or absorbed rather than NO. Therefore, this reaction is relatively important in cases of high concentration studies. A knowledge of the rate constant, dilution rate, and concentration of NO in the flue gas will permit the estimation of the NO conversion according to Equation 2.29.

2.2.1.1.2 The $NO_2 - N_2O_4$ Equilibrium Reaction

Verhoek and Daniels (1931) studied this equilibrium. Their investigations showed that the dissociation of nitrogen tetroxide proceeds according to:

$$N_2O_{4(g)} \rightleftharpoons 2NO_{2(g)} \qquad .....(2.18)$$

Dissociation constants were measured at 25, 35 and 45^{o}C. The equations which best described their research are summarized in Table 2.9. Equilibrium constants predicted from the Verhoek and Daniels expression (1931) are about 10% higher than that of Joshi et al. (1985) . Later studies by Vosper (1976) provided more details about this reaction. A value of 6.86 atm^{-1} for the equilibrium constant at 25 ^{o}C has been recommended by Schwartz and White (1981).

2.2.1.1.3 The $NO - NO_2 - N_2O_3$ Equilibrium Reaction

In addition to the gas phase dimerization of NO_2 to yield N_2O_4, an equilibrium reaction also occurs with NO and NO_2. Several investigators (Verhoek and Daniels, 1931; Beattie and Bell, 1957; Beattie, 1963) have indicated that the following reaction occurs in the gas phase:

$$NO_{(g)} + NO_{2(g)} \rightleftharpoons N_2O_{3(g)} \qquad .....(2.19)$$

Table 2.9 **Expressions for Calculating Equilibrium Constants for Reaction 2.18**

$$2NO_{2(g)} \rightleftharpoons N_2O_{4(g)} \qquad .....(2.18)$$

Counce (1980)

Definition: $$K_{-1} = \frac{P^2_{NO_2}}{P_{N_2O_4}}$$

Expression:

$$\log_{10} K_{-1} = \frac{2692}{T} + 1.75\log_{10}T + 4.83\times10^{-3}T - 7.144\times10^{-6}T^2 + 3.062$$

Unit : atm

Remark: N_2O_4 decomposition for the temperature range : 282 – 404 K

Verhoek and Daniels (1931)

Definition: $$K_{-1} = \frac{P^2_{NO_2}}{P_{N_2O_4}}$$

Table 2.9 **Expressions for Calculating Equilibrium Constants for Reaction 2.18 (continued)**

$$2NO_{2(g)} \rightleftharpoons N_2O_{4(g)} \qquad .....(2.18)$$

Expression:

$$\log_{10} K_{-1} = 9.8698 - \frac{3\,1\,9\,9\,8}{T}$$

Unit : atm

Remark: N_2O_4 decomposition for the temperature range : 298 – 318 K

Hoftyzer and Kwanten (1972)

Definition:
$$K = \frac{P_{N_2O_4}}{P^2_{NO_2}}$$

Expression:

$$K = 7.07 \times 10^{-10} \exp\left(\frac{6\,8\,6\,6}{T}\right)$$

Unit : atm^{-1}

Remark: On the basis of Verhoek and Daniels data (1931) and JANAF (1985)

Table 2.9 **Expressions for Calculating Equilibrium Constants for Reaction 2.18 (continued)**

$$2NO_{2(g)} \rightleftharpoons N_2O_{4(g)} \qquad .....(2.18)$$

Joshi et al. (1985)

Definition: $$K = \frac{P_{N_2O_4}}{P^2_{NO_2}}$$

Expressions:

$$\log_{10} K = \frac{2993}{T} - 9.226$$

Unit : atm^{-1}

$$\log_{10} K = \frac{2993}{T} - 11.232$$

Unit : $[kN.m^{-2}]^{-1}$

The equilibrium constant for this reaction, according to Beattie and Bell (1957) and Beattie (1963), is given by:

$$\log_{10} K = \frac{2072}{T} - 7.234 \qquad .....(2.31)$$

where K is in atm^{-1} or in SI units, $[kN.m^{-2}]^{-1}$

$$\log_{10} K = \frac{2072}{T} - 9.240 \qquad .....(2.32)$$

Other values for this reaction, available in the literature, have been listed in Table 2.10.

This equilibrium has been re–examined in 1976 by Vosper (1976) who utilized spectrophotometric measurements of NO_2 at visible wavelengths. A later review by Schwartz and White (1981) recommended a value of 0.535 atm^{-1} at 25 ^{o}C for this reaction.

2.2.1.1.4 The $NO - NO_2 - H_2O - HNO_2$ Equilibrium Reaction

The vapor phase equilibrium reaction,

$$NO_{(g)} + NO_{2(g)} + H_2O_{(g)} \rightleftharpoons 2HNO_{2(g)} \qquad .....(2.20)$$

Table 2.10 Equilibrium Constants for Reaction 2.19

$$NO_{(g)} + NO_{2(g)} \rightleftharpoons N_2O_{3(g)} \qquad .....(2.19)$$

Temperature	Value of K_e Obtained by Various Investigators	
[K]	Verhoek and Daniels (1931)	Beattie and Bell (1957)
278	–	0.595
288	–	1.082
298	2.105	1.916
308	3.673	3.097
318	6.880	5.193

Definition: $$K_e = \frac{P_{NO} P_{NO_2}}{P_{N_2O_3}} \quad \text{atm}$$

for reverse of reaction 2.18

was examined by Wayne and Yost (1951), Ashmore and Tyler (1961) and Waldorf and Babb (1963). Their studies showed that the reaction proceeds rapidly to form nitrous acid vapor even for rather low concentrations of the reactants. The reaction is catalyzed, apparently, by water vapor and the equilibrium is established instantaneously.

Considerable variations among the values of K are observed when compared to the values calculated from the compiled thermodynamic data (NBS, 1968; JANAF, 1985). However, there is a good consensus in the literature on the earlier values. A later review by Schwartz and White (1981) recommended a value of 1.69 atm^{-1} ($1.67x10^{-2}$ $[kN.m^{-2}]^{-1}$) for K at 25 ^{o}C, which essentially confirmed the values reported earlier.

Other equilibrium values were summarized by Counce (1980). Values of K_e can also be predicted by the Hoftyzer and Kwanten equation (1972) which is based on the reported data of Wayne and Yost (1951), Ashmore and Tyler (1961), and Waldorf and Babb (1963). This expression takes the form:

$$K_e = 0.187x10^{-6}\exp\left(\frac{4723}{T}\right) \qquad .....(2.33)$$

where

K_e = equilibrium constant for reaction 2.20, atm^{-1}

T = absolute temperature, K

The forward rate constant was later measured by Graham and Tyler (1972) and by Kaiser and Wu (1977). However, very poor agreement among the reported values was observed. Reaction 2.20 has been re-examined recently by Vosper (1976) and by Chan et al.(1976). Their data confirmed the older investigations (Wayne and Yost, 1951; Ashmore and Tyler, 1961; Waldorf and Babb, 1963).

2.2.1.1.5 The $NO_2 - H_2O - HNO_3 - NO$ Equilibrium Reaction

The equilibrium reaction:

$$3NO_{2(g)} + H_2O_{(g)} \rightleftharpoons 2HNO_{3(g)} + NO_{(g)} \qquad .....(2.21)$$

has been studied by a number of investigators (Chambers and Sherwood, 1937; Forsysthe and Giauque, 1942). The studies were carried out at much higher NO_2 concentrations (exceeding 2000 ppm) than the levels normally found in flue gases (< 1000 ppm). Values of the equilibrium constant from these earlier works are summarized in Table 2.11. As shown, there is good agreement among the reported values. However, a later value which is recommended by Schwartz

Table 2.11 Equilibrium Constants for Reaction 2.21

$$3NO_{2(g)} + H_2O_{(g)} \rightleftharpoons 2HNO_{3(g)} + NO_{(g)} \qquad ....(2.21)$$

Value of K_e [atm^{-1}] at 25 °C Obtained by Various Investigators		
Chambers and Sherwood (1937)	Forsythe and Giauque (1942)	Schwartz and White (1981)
1.7×10^{-2}	1.05×10^{-2}	5.3×10^{-3}

Definition:

$$K_e = \frac{P^2_{HNO_3} P_{NO}}{P^3_{NO_2} P_{H_2O}}$$

Unit : atm^{-1}

and White (1981) differs from the old values by a factor of two. Schwartz and White (1981) indicated that the factor of two difference is due probably to the errors remaining in the free energies which were adopted for computational purposes.

Smith (1947) studied the reverse reaction photometrically at low concentrations of NO (over a range varying from 1300 ppm to 5.26×10^4 ppm). He observed that lowering the concentrations of nitric oxide and nitric acid favored the reaction to proceed towards completion.

Goyer (1963), in his studies of the gas phase reaction of nitrogen dioxide (800 to 84000 ppm) with water vapor (0.5%), found that in the presence of NO, the equilibrium shifted towards NO_2. He concluded that the addition of NO to a HNO_3 mist laden gas would significantly suppress the nitric acid formation through a shift in the equilibrium of the gas phase reaction as represented by reaction 2.21.

It has been inferred from the works of Smith (1947) and Goyer (1963) that for absorption into water of low level (<< 1000 ppm) NO_x flue gas, nitric acid gas is not likely to be formed via reaction 2.21. Therefore, at low concentrations of NO_x, absorption will form oxyacids, most likely, according to:

$$2NO_{2(g)} + H_2O_{(g)} \rightleftharpoons HNO_{2(g)} + HNO_{3(g)} \qquad \text{.....(2.22)}$$

with the equilibrium constant for reaction 2.22 equal to 9.36×10^{-4} $[kN.m^{-2}]^{-1}$ or 9.484×10^{-2} $[atm]^{-1}$ as recommended by Schwartz and White (1981).

This inference was confirmed in later studies by England and Corcoran (1974) who evaluated the third–order rate constant to be $(5.50 \pm 0.29) \times 10^{4}$ $L^{2}.mole^{-2}.s^{-1}$ at 25 ^{o}C. The initial rate of disappearance of nitrogen dioxide was first order with respect to water and second order with respect to nitrogen dioxide. The concentration of nitrogen dioxide used was less than 5 ppm in the presence of nitric oxide at 520 ppm. Their results are described best by reaction 2.22 rather than reaction 2.21. Their work provides direct experimental evidence that supports reaction 2.22 for low NO_x level absorption common to flue gas removal processes. Early evidence was also available from the Caudle and Denbigh (1953) studies to provide additional support for reaction 2.22.

England and Corcoran (1974) also indicated that reaction 2.21 occurs spontaneously at ambient conditions provided that the concentrations of nitrogen dioxide or water vapor are not too low. Otherwise, the gas–phase reaction proceeds to a very limited extent. Increasing temperatures hindered the reaction.

There has been considerable confusion about the control mechanism associated with NO_2 absorption. Some researchers (Peter et al., 1955) believed

that the rate of absorption was controlled by the gas phase reaction. Others (Chamber and Sherwood, 1937) suggested that control existed in the gas film, yet some argued (Caudle et al., 1953; Wendel and Pigford, 1958; Carberry, 1959) that the rate of absorption was controlled by chemical reaction in the liquid. However, all of these conflicts are resolved if the studies are divided into high concentration (> 0.1% or 1000 ppm NO_2) and low concentration studies (< 0.1% NO_2).

As suggested by England and Corcoran (1974), at high concentrations of NO_2, the rate of absorption is controlled by diffusion of gases through the gas film. The important gas phase diffusants are nitric acid vapor, NO_2 and N_2O_4. As the concentration of NO_2 decreases, the gas phase reaction becomes slow and occurs to a lesser extent. The liquid phase reaction becomes important.

The rate of absorption will be controlled, presumably, by the reaction of NO_2 or N_2O_4 with the solution as is the case in the absorption of oxides of nitrogen from flue gases (concentration range from 100 to 1000 ppm). Thus to increase the rate of absorption of NO_2 at low concentration, addition of chemicals to the water absorbent is necessary to speed up the chemical reaction. However, chemical additives become ineffective if the NO_2 concentration exceeds 0.1 % simply because the gas film is in control.

2.2.2 Henry's Law Solubility of Oxides and Oxyacids of Nitrogen in Water

A comparison of physical solubilities or Henry's law coefficients of nitrogen oxides and oxyacids in water provides a good indication of the roles of the individual NO_x and HNO_x species in aqueous absorption processes. In the following sections, the available information concerning Henry's law coefficients of NO_x and HNO_x in water is examined.

According to Henry's law, the solubility of a solute gas in a liquid is proportional to the partial pressure of that gas in equilibrium with the liquid provided that the dissolved gas does not react in the solution phase. Thus the amounts of gaseous NO_x and/or HNO_x that will dissolve according to Henry's law can be represented by the relationship:

$$C_i = P_i H_i \qquad .....(2.34)$$

where

C_i = liquid phase saturation concentration of solute gas i, $kmole.m^{-3}$

P_i = partial pressure of solute gas i in the gas phase, atm

H_i = Henry's law coefficient or physical solubility of gas i, kmole.m^{-3}.atm^{-1}

The Henry's law coefficient may be readily determined from Equation 2.34 by direct measurement of the gas phase partial pressure and aqueous concentration of the solute. In the measurement, it is understood that the non–reactive partitioning criterion of a solute between the gaseous and solution phase is satisfied. However, all higher oxides of NO_x and HNO_x are highly reactive, with nitric oxide as an exception. Therefore, in cases of highly reactive oxides of nitrogen and gaseous acids, Henry's law coefficients must be inferred indirectly on the basis of thermodynamic cycles as suggested by Schwartz and White (1981) or, in favorable cases, from kinetic studies.

A recommended set of Henry's law coefficients, based on the Schwartz and White (1981) review, is given in Table 2.12, as well as the values reported from previous studies as summarized by Counce (1980). It is evident that there is a substantial difference between the recommended and the adopted values for HNO_3.

2.2.2.1 Nitric Oxide (NO)

The non–reactive nature of NO in water ensures that the Henry's law

Table 2.12 Henry's Law Coefficients for Nitrogen Oxides and Oxyacids at 25 ^{o}C

Gas Species i	H_i [kmole.m^{-3}.atm^{-1}] Recommended by Schwartz and White (1981)	H_i [kmole.m^{-3}.atm^{-1}] Summarized by Counce (1980)
NO	1.93×10^{-3}	1.93×10^{-3}
NO_2	$(1.2 \pm 0.4) \times 10^{-2}$	4.1×10^{-2}
N_2O_3	0.6 ± 0.2	0.39
N_2O_4	1.4 ± 0.7	1.30
HNO_2	49.0	32.79
HNO_3	$2.1 \times 10^{5} \pm 14\%$	1.22×10^{12}

coefficient can be determined directly. Of the various constants for the oxides of nitrogen, the Henry's law constant for nitric oxide in water is the only well established value that is consistent with the reported values. As is generally the case, the solubility of nitric oxide decreases with increasing temperature according to:

$$\log_{10} H_{NO} = \frac{-1463.32}{T} + 2.178 \qquad .....(2.35)$$

where

H_{NO} = Henry's law coefficient of nitric oxide in water, $kmole.m^{-3}.(kN.m^{-2})^{-1}$

The dependence of Henry's law coefficient of NO on ionic strength and pH has been examined by Armor (1974). He reported that the Henry's law coefficient decreased with increasing ionic strength. This decrement amounts to about 8% for an ionic strength of 0.1 M and is insignificant for concentrations in flue gases. This is particularly true for flue gas absorption in water.

For aqueous electrolyte solutions, the solubility of nitric oxide can be

evaluated from:

$$\log \frac{H_i^*}{H_{i,w}} = -\sum K_s I \qquad .....(2.36)$$

where

H_i^* = Henry's law coefficient of solute gas i in electrolyte solution, $kmole.m^{-3}.(kN.m^{-2})^{-1}$

$H_{i,w}$ = Henry's law coefficient of solute gas i in water, $kmole.m^{-3}.(kN.m^{-2})^{-1}$

K_s = salting out parameter, defined by,

$$K_s = i^+ + i^- + i_g$$

where i^+, and i^- are the contributions due to the cations and anions of the electrolyte and i_g is the contribution of the solute gas i, ($i_g = 0.037$ $[m^3.kgion^{-1}$ for NO]).

I = Ionic strength, $(kg.ion).m^{-3}$

Armor (1974) also showed that the solubility of NO in aqueous solutions is independent of pH over the range 2 to 13. This behavior eliminates significant complex formation or reaction of NO within this pH range.

2.2.2.2 Nitrogen Dioxide (NO_2)

Unfortunately, the high reactivity of NO_2 in water has precluded the direct determination of its Henry's law coefficient. Any attempt at direct measurement will result in serious error. Therefore, indirect inference or kinetic studies provide more reliable estimates of the coefficient.

The Henry's law coefficient of NO_2 in water has been determined kinetically from absorption studies by Andrew and Hanson (1961) and Komiyama and Inoue (1980). The value reported by Andrew and Hanson (1961) was adopted by Counce (1980) as shown in Table 2.12 (H_{NO_2} = 0.04 kmole.m^{-3}.atm^{-1} at 25^{o}C, whereas a value of 0.024 kmole.m^{-3}.atm^{-1} was obtained by Komiyama and Inoue (1980) at 15^{o}C. By taking into account the possible contribution from dissolved N_2O_4 and a temperature effect, the Komiyama and Inoue (1980) value was corrected to 1.8x10^{-2} kmole.m^{-3}.atm^{-1} at 25 ^{o}C by Schwartz and White (1981). This value is in reasonable agreement with the value obtained indirectly by the same authors on the basis of thermodynamic cycles.

As pointed out by several authors (Joshi et al., 1985; Schwartz and White, 1981), the large differences observed in these values probably reflected

the different values of diffusivity and reaction rate used for the calculation of H_{NO_2}.

As a preliminary estimate of H_{NO_2}, Graedel et al. (1975) proposed the following relation on the basis of the physical properties of the molecules:

$$\frac{H_{NO_2}}{H_{NO}} = \frac{H_{CO_2}}{H_{CO}} \qquad .....(2.37)$$

2.2.2.3 Dinitrogen Trioxide (N_2O_3)

As with NO_2, the high reactivity of N_2O_3 in water has prevented reliable direct determination of its Henry's law coefficient. It has been found that, under normal conditions of low concentrations in solutions as expected with flue gas absorption by water, N_2O_3 is largely hydrolyzed to form nitrous acid. As a result, the Henry's law coefficient for N_2O_3 can only be determined indirectly. The value of $H_{N_2O_3}$ obtained by Schwartz and White (1981), based on thermodynamic cycles, is 0.6 ± 0.2 kmole.m^{-3}. atm^{-1}. This recommended values is about twice that adopted by Counce (1980) in Table 2.12.

2.2.2.4 Dinitrogen Tetroxide (N_2O_4)

Similarly to NO_2 and N_2O_3 , N_2O_4 is highly reactive in water. This reactivity precluded direct measurement of its Henry's law coefficient. Several kinetic studies (Abel and Schmid, 1928; Gratzel et al., 1969; Kramers et al., 1961) were designed to measure this quantity indirectly. The studies of Kramers et al. (1961) led to a value of 1.31 ± 0.08 kmole.m^{-3}.atm^{-1} at 25 ^{o}C. This value is roughly a factor of two higher than the value ($H_{N_2O_4} = 1 \pm 0.4$ kmole.m^{-3}.atm^{-1}) reported by Abel and Schmid (1928) and Gratzel et al. (1969). A basis of thermodynamic cycles was used by Schwartz and White (1981) to evaluate $H_{N_2O_4}$. The recommended value of $H_{N_2O_4}$ is 1.4 ± 0.7 kmole.m^{-3}.atm^{-1} at 25 ^{o}C which is in good agreement with the value obtained by Kramers et al. (1961).

2.2.2.5 Oxyacids (HNO_x)

The oxyacids are extremely reactive in water thereby prohibiting the direct measurement of their Henry's law coefficients. Under normal conditions of low concentrations in solutions, both HNO_2 and HNO_3 are, virtually, completely dissociated. For instance, the fractional dissociation of HNO_3 solution is 97% (1 M at 25 ^{o}C) and is increased at lower concentrations.

Consequently, aqueous nitric acid is, essentially, completely dissociated under all conditions of flue gas absorption by water. Similarly to HNO_3, nitrous acid is also completely dissociated (94%) provided that the pH of the water is greater than 5.6. Thus, the extent to which nitrous acid is dissociated depends on the pH of the solution.

Schwartz and White (1981) have evaluated the Henry's law coefficients of nitrous and nitric acids and recommended values of 49.0 $kmole.m^{-3}.atm^{-1}$ and (2.1×10^5) $\pm$ 14% $kmole.m^{-3}.atm^{-1}$ for H_{HNO_2} and H_{HNO_3} respectively at 25 ^{o}C.

Abel and Neusser (1929) obtained a value of 33.0 $kmole.m^{-3}.atm^{-1}$ at 25 ^{o}C for H_{HNO_2} which is in reasonable agreement with the recommended value.

2.2.3 Liquid Phase Reactions of NO_x

Various liquid and gas phase reactions involving gaseous NO_x and HNO_x species with water are listed in Table 2.13. These reactions have been identified in the manufacture of nitric acid and previous studies on NO_2. All of these reactions are equally likely to participate in the absorption process. However,

Table 2.13 Liquid Phase Reactions of NO_x and HNO_x with Water

$NO_{(g)} \rightleftharpoons NO_{(l)}$	.....(2.38)
$NO_{2(g)} \rightleftharpoons NO_{2(l)}$	.....(2.39)
$N_2O_{3(g)} \rightleftharpoons N_2O_{3(l)}$	.....(2.40)
$NO_{(l)} + NO_{2(l)} \rightleftharpoons N_2O_{3(l)}$	.....(2.41)
$N_2O_{4(g)} \rightleftharpoons N_2O_{4(l)}$	.....(2.42)
$2NO_{2(l)} \rightleftharpoons N_2O_{4(l)}$	.....(2.43)
$2NO_{2(l)} + H_2O_{(l)} \longrightarrow HNO3_{(l)} + HNO_{2(l)}$	.....(2.44)
$N_2O_{3(l)} + H_2O_{(l)} \longrightarrow 2HNO_{2(l)}$	.....(2.45)
$N_2O_{4(l)} + H_2O_{(l)} \longrightarrow HNO_{3(l)} + HNO_{2(l)}$	.....(2.46)
$3HNO_{2(l)} \rightleftharpoons HNO_{3(l)} + 2NO_{(g)} + H_2O_{(l)}$	.....(2.47)
$HNO_{2(l)} + HNO_{3(l)} \longrightarrow 2NO_{2(g)} + H_2O_{(l)}$	.....(2.48)
$3NO_{2(g)} + H_2O_{(g)} \longrightarrow 2HNO_{3(g)} + NO_{(g)}$	.....(2.21)
$\frac{3}{2} N_2O_{4(g)} + H_2O_{(g)} \longrightarrow 2HNO_{3(g)} + NO_{(g)}$	.....(2.49)

for specific operating conditions, such as low levels of NO_2 (< 800 ppm) and the presence of NO, some of these reactions may be eliminated. In the discussion that follows, the available information concerning NO_x absorption by water is examined. From the collected evidence, a more reasonable series of reactions should be derived for low level NO_x absorption.

2.2.3.1 NO_x Absorption into Water

Wendel and Pigford (1958) absorbed nitrogen dioxide into water in a short wetted–wall column (< 7 "). Under their experimental conditions, nitrogen tetroxide was the predominant species which dissolved and reacted with water rapidly. The nitrogen tetroxide which formed by dimerization of NO_2 represented approximately 0.06 to 0.2 mole fraction of the gas phase. The rate of absorption was linearly proportional to the nitrogen tetroxide and was in good agreement with previous studies by Denbigh and co–workers (1953, 1947) and Peter et al. (1955). They concluded that the rate of absorption was controlled by the hydrolysis of nitrogen tetroxide rather than by gas phase diffusion. The reactions that best described their work involved:

$$2NO_{2(g)} \rightleftharpoons N_2O_{4(g)} \qquad .....(2.18)$$

$$N_2O_{4(g)} \rightleftharpoons N_2O_{4(l)} \qquad .....(2.42)$$

$$N_2O_{4(l)} + H_2O_{(l)} \longrightarrow HNO_{2(l)} + HNO_{3(l)} \qquad .....(2.46)$$

Reaction 2.46 is, essentially, irreversible provided that the $HNO_{3(l)}$ concentration is less than 0.1 weight per cent. Prior research (Denbigh and Prince, 1947) has shown that the reverse reaction is of importance only when HNO_3 concentrations are greater than 20 % by weight. Wendel and Pigford (1958) also observed that a fog or mist occurred when the total nitrogen tetroxide concentration exceeded about 25 mole %, but occasionally formed at levels as low as 5 mole %. The presence of the fog or mist indicated the possibility of reactions 2.21 and 2.49 according to:

$$3NO_{2(g)} + H_2O_{(g)} \longrightarrow 2HNO_{3(g)} + NO_{(g)} \qquad .....(2.21)$$

$$\frac{3}{2} N_2O_{4(g)} + H_2O_{(g)} \longrightarrow 2HNO_{3(g)} + NO_{(g)} \qquad .....(2.49)$$

Although neither the occurrence of a mist nor the presence of nitric oxide in the exit gas stream from an absorber should be used as conclusive evidence of a vapor phase reaction between nitrogen dioxide and water, it is nevertheless, a good indication of these reactions occurring at high NO_2 concentration as consistently observed by some investigators (Chamber and Sherwood, 1937; Peter et al., 1955; Dekker et al., 1959).

The rate constant for the hydrolysis of nitrogen tetroxide according to reaction 2.46 ($k = 290\ s^{-1}$) and the equilibrium constant for reaction 2.42 ($K_e = 9.55\ x10^{-4}$ gmole.cm^{-3}.atm^{-1}) were determined at 25 ^{o}C. The solubility of dissolved but unreactive nitrogen tetroxide in equilibrium with gaseous nitrogen tetroxide was found to be determined by $H_{N_2O_4} = 58$ gmole $N_2O_4^{-1}$.gmole solution.atm.

Dekker, Snoeck and Kramers (1959) worked with short wetted–wall columns (< 7"). The absorption rate of NO_2 into water was measured for various inlet concentrations of NO_2 (3 – 15 %). When total NO_2 concentrations exceeded about 9% , the appearance of a mist led them to believe that a vapor phase reaction between NO_2 and/or N_2O_4 and water occurred near the gas–liquid interface. As a result, these authors concluded that both gas and liquid phase reactions are possible. They indicated that gas phase resistance controlled the rate of absorption at high NO_2 concentrations. As NO_2 concentration in the gas phase decreased, the main resistance to mass transfer shifted towards the liquid phase. Moreover, under their experimental conditions and because of the slow decomposition rate of HNO_2 , reaction 2.47 was assumed to be negligible:

$$3HNO_{2(l)} \longrightarrow HNO_{3(l)} + 2NO_{(g)} + H_2O_{(l)} \qquad .....(2.47)$$

They also concluded that N_2O_4 rather than NO_2 was the major transporting

species in the absorption process.

The effect of NO on the kinetics involved in the aqueous absorption of mixtures containing NO, NO_2 and N_2O_4 was first reported by Caudle and Denbigh (1953). Later studies by Peters and Koval (1959; 1960) suggested that nitric oxide significantly influences the rate of reaction of nitrogen dioxide with water. The influence of NO on nitric acid production and on the kinetics and mechanisms involved in the absorption of NO_2 into water was further examined by Koval and Peters (1960) in a long wetted–wall column (30"). They observed that:

- When NO was added with NO_2 in the inlet gas stream, the HNO_2 production increased while the nitric acid production decreased.
- At very high NO concentrations, total acid production decreased and almost all acid production was HNO_2.

At high concentrations of NO, these authors were unable to explain the observed results on the basis of the mechanisms proposed by Wendel and Pigford (1958). Thus, they inferred that some mechanism other than direct reaction between N_2O_4 or NO_2 and water must be involved. They proposed the following reaction schemes:

$$NO_{(g)} + NO_{2(g)} \rightleftharpoons N_2O_{3(g)} \qquad .....(2.19)$$

$$N_2O_{3(g)} \rightleftharpoons N_2O_{3(l)} \qquad .....(2.40)$$

$$N_2O_{3(l)} + H_2O_{(l)} \longrightarrow 2HNO_{2(l)} \qquad .....(2.45)$$

in addition to the reactions:

$$2NO_{2(g)} \rightleftharpoons N_2O_{4(g)} \qquad .....(2.18)$$

$$N_2O_{4(g)} \rightleftharpoons N_2O_{4(l)} \qquad .....(2.42)$$

$$N_2O_{4(l)} + H_2O_{(l)} \rightleftharpoons HNO_{2(l)} + HNO_{3(l)} \qquad .....(2.46)$$

These mechanisms appear to fit their experimental data and to agree well with all prior observations.

Andrew and Hanson (1961) studied the absorption of NO_2 into water in a sieve plate tower. A number of reactions was proposed. They indicated that the relative importance of the reactions was dependent primarily on the NO_2 concentration. At high gas concentration, ($[NO_2] > 11200$ ppm or $5x10^{-7}$ $mole.cm^{-3}$), the following reaction determined the overall absorption:

$$N_2O_{4(l)} + H_2O_{(l)} \longrightarrow HNO_{3(l)} + HNO_{2(l)} \qquad .....(2.46)$$

The same reaction had been used by Wendel and Pigford (1958) and by Dekker et al. (1959) to interpret their results.

At low gas concentration, ($[NO_2] < 1120$ ppm or $5.x10^{-8}$ mole.cm^{-3}), the predominant reaction was:

$$N_2O_{3(l)} + H_2O_{(l)} \longrightarrow 2HNO_{2(l)} \qquad .....(2.45)$$

The increasing importance of this reaction relative to reaction 2.46 in the presence of NO was noted by Caudle and Denbigh (1953) and by Koval and Peters (1960).

Andrew and Hanson (1961) also argued that the gas phase reactions:

$$NO_{2(g)} + NO_{(g)} + H_2O_{(g)} \longrightarrow 2HNO_{2(g)} \qquad .....(2.20)$$

$$3/2N_2O_{4(g)} + H_2O_{(g)} \longrightarrow 2HNO_{3(g)} + NO_{(g)} \qquad .....(2.49)$$

are not important at any gas concentrations since they are kinetically limited at low concentrations and limited by exhaustion of the available water vapor at

high concentrations. This argument conflicted with some of the previous observations (Chambers and Sherwood, 1937; Peter et al., 1955; Dekker et al., 1959).

These authors also estimated the gas and liquid phase equilibrium compositions. As indicated in Table 2.14, at high NO_2 concentration, the major gas transporting species were identified as NO, NO_2 and N_2O_4 , while in the liquid phase N_2O_3, N_2O_4 and HNO_2 were found to be important in the transfer process. At low gas concentrations, the predominant gas phase diffusion species were NO, NO_2 and HNO_2 with NO_2 and HNO_2 being identified as important species in the liquid phase. Komiyama and Inoue (1980) later confirmed NO_2 as the major transporting species at low concentrations.

Previous absorption studies on NO_2 into water involved the use of relatively high gas concentrations which were normally higher than several per cent. From these earlier studies, there is a good consensus that N_2O_4 is the predominant transporting species and that the rate of absorption is of second order dependence on NO_2 (or first order on N_2O_4) concentration. However, deviations were noticed by Andrew and Hanson (1961) and Sada et al. (1979) at low concentrations. To clarify the observed discrepancy, Komiyama and Inoue (1980) absorbed NO_2 and a mixture NO and NO_2 into water with emphasis on the low concentration range (5 to 800 ppm). They proposed the following reaction scheme:

Table 2.14 Equilibrium Concentrations in Gas and Liquid Phases (Andrew and Hanson, 1961)

Species	Concentrated Gas $[NO_2] > 5x10^{-7}$ [mole.cm^{-3}]		Dilute Gas $[NO_2] < 5x10^{-8}$ [mole.cm^{-3}]	
	Gas Phase [mole.cm^{-3}]x10^6	Liquid Phase [mole.cm^{-3}]x10^6	Gas Phase [mole.cm^{-3}]x10^6	Liquid Phase [mole.cm^{-3}]x10^6
NO	9.0	0.45	$1x10^{-2}$	$5x10^{-4}$
NO_2	3.9	3.90	$1x10^{-2}$	$1x10^{-2}$
N_2O_3	0.3	1100.00	$9x10^{-6}$	$3.5x10^{-3}$
N_2O_4	2.6	195.00	$1.7x10^{-5}$	$1.3x10^{-3}$
HNO_2	1.3	1100.00	$2.3x10^{-3}$	2.0

$$NO_{(l)} + NO_{2(l)} \longrightarrow N_2O_{3(l)} \qquad .....(2.41)$$

$$2NO_{2(l)} \rightleftharpoons N_2O_{4(l)} \qquad .....(2.43)$$

$$N_2O_{3(l)} + H_2O_{(l)} \longrightarrow 2HNO_{2(l)} \qquad .....(2.45)$$

$$N_2O_{4(l)} + H_2O_{(l)} \longrightarrow HNO_{3(l)} + HNO_{2(l)} \qquad .....(2.46)$$

These authors indicated that, at low gas concentrations,the concentrations of NO_2 and NO become significant relative to N_2O_4 and N_2O_3. Therefore, any model based on N_2O_4 as the predominant transporting species should fail at low concentrations. Indeed, the second order dependence on NO_2 concentration was demonstrated to be true provided that NO_2 concentrations exceeded about 800 ppm. With decreasing concentrations, NO_2 becomes the major transporting species and the dependence on NO_2 concentration is reduced to the 3/2 order. The rate of absorption was expressed by:

$$N_{NO_2} = \left(\frac{4}{3} kK_e D_{NO_2} \varphi^3_{NO_2} [NO_2]^3_g \right)^{\frac{1}{2}} \qquad .....(2.50)$$

for concentration of NO_2 ranging from 250 to 800 ppm.

Where

N_{NO_2} = rate of absorption, mole.m^{-2}.s^{-1}

k = rate constant for reaction 2.46, (554 s^{-1})

K_e = equilibrium constant for reaction 2.43,
(75.72 m^3.$mole^{-1}$)

D_{NO_2} = diffusion coefficient, ($2.0x10^{-9}$ m^2.s^{-1})

φ_{NO_2} = distribution coefficient of NO_2 between gas and liquid, dimensionless (a value of 0.2934 was recommended by Schwartz and White (1981) and 0.556 was used by Komiyama and Inoue (1980).

$[NO_2]_g$ = gas phase molar concentration of NO_2, mole.m^{-3}

For low concentrations of NO_2 mixtures (< 250 ppm), the rate was given by:

$$N_{NO_2} = k_L \varphi_{NO_2} [NO_2]_g \qquad .....(2.51)$$

where

k_L = liquid side mass transfer coefficient, m.s^{-1}
($2.5x10^{-5}$ m.s^{-1})

For the absorption of NO and NO_2 mixtures at low concentrations, reactions 2.41 and 2.45 dominate over reaction 2.43. The reaction scheme follows:

$$NO_{(l)} + NO_{2(l)} \rightleftharpoons N_2O_{3(l)} \qquad .....(2.41)$$

$$N_2O_{3(l)} + H_2O_{(l)} \longrightarrow 2HNO_{2(l)} \qquad .....(2.45)$$

The rate of absorption of either NO or NO_2 , based on equal interfacial concentrations of NO and NO_2 , was given by Komiyama and Inoue (1980) as:

$$N_{NO} = N_{NO_2} = \left(\frac{2}{3}\, kK_e D_{NO_2}\right)^{\frac{1}{2}} \left(\varphi_{NO_2}\varphi_{NO}[NO_2]_g[NO]_g\right)^{\frac{3}{4}} \qquad .....(2.52)$$

where

k = rate constant in reaction 2.45, s^{-1}
$(5.917 \pm 1.48)\times10^5\ s^{-1}$

K_e = equilibrium constant in reaction 2.41,
$m^3.mole^{-1}$ [$16.49 \pm 5.5\ m^3.mole^{-1}$
recommended by Schwartz and White (1981);
$22.84\ m^3\ mole^{-1}$ adopted by Komiyama and
Inoue (1980)]

D_i = diffusion coefficient of species i, $m^2.s^{-1}$

$D_{NO} = 2.50x10^{-9}$ $m^2.s^{-1}$ at 25 °C

$D_{NO_2} = 2.0x10^{-9}$ $m^2.s^{-1}$ at 25 °C

φ_i = distribution coefficient of i between gas and liquid, dimensionless; i = NO = 0.0472;

i = NO_2 = 0.2934

The major gas phase transporting species are NO and NO_2. They were identified previously by Andrew and Hanson (1961). In this reaction scheme N_2O_3 acts as a reactive intermediate and is the dominant reactant. The principal liquid phase diffusing species is HNO_2 rather than NO_2 in this mixture of NO and NO_2 being absorbed.

Lee and Schwartz (1981) studied the reaction kinetics of nitrogen dioxide with liquid water at low partial pressures corresponding to flue gas concentrations of NO_2, which range from 1 ppm to 800 ppm. Their results were interpreted on the basis of the following reaction mechanism:

$$NO_{2(g)} \rightleftharpoons NO_{2(l)} \qquad .....(2.39)$$

$$2NO_{2(l)} \rightleftharpoons N_2O_{4(l)} \qquad .....(2.43)$$

$$N_2O_{4(l)} + H_2O_{(l)} \longrightarrow HNO_{3(l)} + HNO_{2(l)} \qquad .....(2.46)$$

with the overall mixed phase reaction represented by,

$$2NO_{2(g)} + H_2O_{(l)} \longrightarrow HNO_{3(l)} + HNO_{2(l)} \qquad .....(2.44)$$

A 3/2 order dependence on NO_2 concentration was observed, as previously reported by Komiyama and Inoue (1980). The assumption of NO_2 as the principal diffusing species was verified approximately at the higher end of the studied concentrations and essentially confirmed for concentrations of NO_2 less than 110 ppm.

For the concentration range investigated, the following gas phase reaction between NO_2 and water vapor was found to be unimportant:

$$2NO_{2(g)} + H_2O_{(g)} \longrightarrow HNO_{3(g)} + HNO_{2(g)} \qquad .....(2.22)$$

Three limiting reaction regimes were clarified for the examined concentration range. The reaction regime relevant to the flue gas concentrations of NO_2 was found to be convective mass transfer limited (liquid phase controlled). The rate of absorption given by Lee and Schwartz (1981) was similar to that reported by Komiyama and Inoue (1980) at low concentrations, in the form:

$$N_{NO_2} = \frac{1}{2} k_L a H_{NO_2} P_{NO_2} \qquad .....(2.53)$$

for $8.5 \times 10^{-6} < P_{NO_2} < 1.1 \times 10^{-4}$ atm

where

N_{NO_2} = rate of absorption of NO_2, $mole.L^{-1}.s^{-1}$

k_L = liquid side mass transfer coefficient, $m.s^{-1}$

a = interfacial area per unit volume, $m^2.m^{-3}$

$k_L a$ = stochastic rate coefficient for convective mixing [$k_L a = 0.59\ s^{-1}$ as given by Lee and Schwartz (1981)]

H_{NO_2} = Henry's law coefficient, $mole.L^{-1}.atm^{-1}$

$(7.0 \pm 0.5) \times 10^{-3}$ $mole.L^{-1}.atm^{-1}$

P_{NO_2} = partial pressure of NO_2, atm

To establish a correct reaction regime, the following test criterion was given by Joshi et al. (1985):

$$k_L a << k_{NO_2} H_{NO_2} P_{NO_2} \qquad .....(2.54)$$

where

ℓ = scale of turbulence, dimensionless

packed tower = 0.1

plate column = 0.8

$k_L a$ = rate coefficient for physical mass transfer, s^{-1}

packed column = 0.03 s^{-1}

plate column = 0.05 s^{-1}

k_{NO_2} = reaction rate constant, $(mole.L^{-1})^{-1}.s^{-1}$

[$1.0x10^8$ $(mole.L^{-1})^{-1}.s^{-1}$ given by Lee and Schwartz (1981)]

H_{NO_2} = Henry's law coefficient, $mole.L^{-1}.atm^{-1}$

($1.2x10^{-2}$ $mole.L^{-1}.atm^{-1}$)

P_{NO_2} = partial pressure of NO_2, atm

When the condition specified by Equation 2.54 is satisfied, the absorption is physical mass transfer controlled. Under this condition, all of the reaction occurs in the bulk liquid phase and the rate of absorption is expressed by Equation 2.53. However, if the reverse condition is true, the overall absorption is kinetically controlled by the bulk liquid phase reaction between NO_2 and water. As a result another form of rate of absorption should be considered.

Carta and co–workers (1983, 1986) observed that using water as a liquid absorbent tends to be very inefficient because of the very low solubility and reactivity of NO in water. These authors suggested that this difficulty could be resolved with aqueous nitric acid solution as an absorbent. Recent studies by Carta (1986) indicated that an optimal NO_x removal can be achieved with 15 to 25 % nitric acid solutions. The degree of NO oxidation corresponding to this acid strength was about 50 to 80%. The chemistry involved is given by:

$$2NO_{(g)} + H_2O_{(l)} + HNO_{3(l)} \rightleftharpoons 3HNO_{2(l)} \qquad .....(2.47)$$

The mixed phase reaction shows that NO is absorbed and oxidized by aqueous nitric acid to form nitrous acid.

Newman and Carta (1988) absorbed a mixture of NO and NO_2 into aqueous NaOH solutions over a relatively high concentration range. The concentration of NO was varied from 4000 ppm to 50000 ppm, whereas for NO_2 a range of 2000 ppm to 15000 ppm was used. Under these condition, the authors found that both HNO_2 and N_2O_3 were formed in the bulk gas and within the gas diffusion film. These two species were important in the absorption process and were involved according to:

. In the gas phase,

$$2NO_{(g)} + O_{2(g)} \longrightarrow 2NO_{2(g)} \quad .....(2.16)$$

$$NO_{(g)} + O_{3(g)} \longrightarrow NO_{2(g)} + O_{2(g)} \quad .....(2.17)$$

$$2NO_{2(g)} \rightleftharpoons N_2O_{4(g)} \quad .....(2.18)$$

$$NO_{(g)} + NO_{2(g)} \rightleftharpoons N_2O_{3(g)} \quad .....(2.19)$$

$$NO_{(g)} + NO_{2(g)} + H_2O_{(g)} \rightleftharpoons 2HNO_{2(g)} \quad .....(2.20)$$

$$3NO_{2(g)} + H_2O_{(g)} \rightleftharpoons 2HNO_{3(g)} + NO_{(g)} \quad .....(2.21)$$

. In the liquid phase,

$$2NO_{2(l)} + H_2O_{(l)} \rightleftharpoons HNO_{3(l)} + HNO_{2(l)} \quad .....(2.44)$$

$$N_2O_{3(l)} + H_2O_{(l)} \rightleftharpoons 2HNO_{2(l)} \quad .....(2.45)$$

$$N_2O_{4(l)} + H_2O_{(l)} \rightleftharpoons HNO_{3(l)} + HNO_{2(l)} \quad .....(2.46)$$

Reactions 2.16, 2.17, and 2.44 were neglected in their model on the basis that:

. The initial low concentration of NO prohibited any further oxidation at room temperature.
. Previous studies indicated that at partial pressures of NO_2 exceeding 2000 ppm, N_2O_4 is the major transporting species in the absorption process.

However, with the relatively high concentrations of NO used in their experiments, NO would readily oxidize to give NO_2 via reactions 2.16 and 2.17. Furthermore, the neglect of reaction 2.44 is questionable for the range of NO_2 studied. Although N_2O_4 is the major transporting species, NO_2 will surely participate in the absorption process as indicated from the earlier work of Wendel and Pigford (1958) and Koval and Peter (1960). Hence, the mechanism adopted by Newman and Carta (1988) is incomplete and their assumptions that neglect these reactions are questionable.

2.3. Conclusions

To summarize this review, reaction mechanisms are proposed according

to the concentrations and relative compositions of the involved gases. It must be emphasized, at this stage that the reactions for absorption are selected on the basis of their ability to explain most of the previously observed phenomena.

2.3.1 Absorption of NO_2 at High Gas Concentrations ($[NO_2]_g > 2000$ ppm)

At high NO_2 concentrations, a large proportion of the NO_2 molecules join as pairs and appear in the gas mixture as the bulkier N_2O_4 molecules. Most of the earlier studies fall into this concentration range with N_2O_4 as the major transporting species. The rate of absorption is second order in NO_2 concentration and controlled by the gas phase resistance. The reactions are:

$$2NO_{2(g)} \rightleftharpoons N_2O_{4(g)} \qquad .....(2.18)$$

$$N_2O_{4(g)} \rightleftharpoons N_2O_{4(l)} \qquad .....(2.42)$$

$$N_2O_{4(l)} + H_2O_{(l)} \rightleftharpoons HNO_{3(l)} + HNO_{2(l)} \qquad .....(2.46)$$

There is still a controversy about the gas phase reaction:

$$3NO_{2(g)} + H_2O_{(g)} \rightleftharpoons 2HNO_{3(g)} + NO_{(g)} \qquad .....(2.21)$$

However, the presence of this gas phase reaction had no effect on the absorption rate as indicated by Wendel and Pigford (1958).

2.3.2 Absorption of NO_2 at Medium Gas Concentrations (800 ppm < $[NO_2]_g$ < 2000 ppm)

Reactions similar to those proposed for high gas concentration absorption are valid. However, the controlling mechanism shifts to the liquid phase. There is no gas phase reaction observed.

2.3.3 Absorption of NO_2 at Low Gas Concentrations (100 ppm < $[NO_2]_g$ < 800 ppm)

At low concentrations, most of the nitrogen oxides remain as NO_2 , which becomes the major transporting species. The dependence on NO_2 concentration changes to the 3/2 order for NO_2 concentrations varying between 250 and 800 ppm. At concentrations lower than 250 ppm, first order dependence is observed. Reactions occur in the liquid phase according to:

$$NO_{2(g)} \rightleftharpoons NO_{2(l)} \qquad .....(2.39)$$

$$2NO_{2(l)} + H_2O_{(l)} \rightleftharpoons HNO_{3(l)} + HNO_{2(l)} \qquad .....(2.44)$$

2.3.4 Absorption of Mixtures of NO and NO_2 at High Gas Concentrations ($[NO]_g > 1000$ ppm; $[NO_2]_g > 2000$ ppm)

In the presence of NO, an enhancement of NO_2 absorption occurs due to the formation of N_2O_3 and HNO_2 . Reactions occur in the bulk gas phase and within the gas film near the gas–liquid interface according to:

$$2NO_{(g)} + O_{2(g)} \longrightarrow 2NO_{2(g)} \qquad .....(2.16)$$

$$NO_{(g)} + NO_{2(g)} \rightleftharpoons N_2O_{3(g)} \qquad .....(2.19)$$

$$N_2O_{3(g)} + H_2O_{(g)} \rightleftharpoons 2HNO_{2(g)} \qquad .....(2.27)$$

The HNO_2 formed in the gas phase according to the proposed reaction scheme is highly soluble in water. In addition to the previously mentioned scheme, the

following reactions are also expected to occur:

$$2NO_{2(g)} \rightleftharpoons N_2O_{4(g)} \qquad .....(2.18)$$

$$N_2O_{4(g)} \rightleftharpoons N_2O_{4(l)} \qquad .....(2.42)$$

$$N_2O_{4(l)} + H_2O_{(l)} \rightleftharpoons HNO_{3(l)} + HNO_{2(l)} \qquad .....(2.46)$$

The principal diffusing species have been identified as N_2O_3, N_2O_4 and HNO_2.

2.3.5 Absorption of Mixtures of NO and NO_2 at Low Gas Concentrations ($[NO]_g < 800$ ppm; $[NO_2]_g < 250$ ppm)

It is evident from the present review that the most likely mechanisms associated with the absorption of mixtures corresponding to flue gas concentrations will involve:

$$2NO_{(g)} + O_{2(g)} \longrightarrow 2NO_{2(g)} \qquad .....(2.16)$$

$$NO_{(g)} + O_{3(g)} \longrightarrow NO_{2(g)} + O_{2(g)} \qquad .....(2.17)$$

$$NO_{(g)} \rightleftharpoons NO_{(l)} \qquad .....(2.37)$$

$$NO_{2(g)} \rightleftharpoons NO_{2(l)} \qquad .....(2.39)$$

$$NO_{(l)} + NO_{2(l)} \rightleftharpoons N_2O_{3(l)} \qquad .....(2.41)$$

$$N_2O_{3(l)} + H_2O_{(l)} \longrightarrow 2HNO_{2(l)} \qquad .....(2.45)$$

where N_2O_3 is considered as a reactive intermediate and the major transporting species. The rate of absorption will depend on the concentrations both of NO and NO_2.

The reaction between NO and O_2 is essentially irreversible at room temperature. The rate is very low for the range of concentrations encountered in flue gas absorption. Therefore, its contribution is relatively insignificant and can be neglected in most pollution studies unless relatively high concentrations of NO are considered or extremely large reactor volumes are used.

Although the reaction between NO and O_3 is fast, the rate of reaction depends very much on O_3 concentration and the emitted NO gas temperature. The indoor and outdoor ozone concentrations at three office buildings were recently measured by Charles and Helen (1989). Depending on the ventilation

rate, the indoor ozone concentration is estimated to be 20 to 80 percent of that outdoors. The maximum outdoor ozone concentration is found to be 150 ppb. The brownish plume observed at the stack outlet can probably be attributed to NO_2 formation according to reaction 2.17. This reaction may safely be neglected unless sufficient time is given under the experimental condition. The reaction is limited by the indoor ozone concentration.

CHAPTER 3

THEORY

From Tables 2.1 and 2.2, it is evident that a significant number of studies on NO_x and SO_2 absorption have been carried out, predominantly, in batch or semi–batch type reactors. However, little work has been reported on packed column absorption under continuous–flow conditions.

It would be valuable to have a new absorption scheme that would relate the continuous–flow, packed system to the studies conducted on batch and semi–batch units. If this was possible, the performance of a pilot plant could be predicted from the results obtained from a laboratory model. Ultimately, pilot plant data could be extrapolated to commercial units directly. Such a capability would not only provide savings during the scale–up process but would also facilitate evaluation of better liquid absorbents for both NO_x and SO_2. It was this objective that motivated a previous study (Chan, 1983) to search for a valid means of bridging the gap between available and needed data.

A scheme similar to that used previously by Baldi and Sicardi (1975, 1976) was adopted for this investigation. Assuming the equivalence of a batch

reactor to a stage in a packed column, new models have been derived for predicting the outlet concentrations of NO_x or SO_2 in the liquid effluent from a packed column. As suggested by Baldi and Sicardi (1975, 1976), trickle flow conditions are assumed to prevail in the column. To illustrate the steps involved in this methodology, a brief review of the derivation is given in the present chapter.

3.1 Nature of Trickle Flow (Baldi and Sicardi, 1975, 1976)

The nature of trickling flow is so complicated that it is very difficult to model or describe it well from a physical point of view. However, Baldi and Sicardi (1975, 1976) suggested a simplified physical picture. According to them, there are a number of random rivulets which flow separately for a certain height of packing to form new rivulets or "die" into a film or a pocket, from which other rivulets are again formed. The rivulets are likely to be responsible for the main liquid flow rate. A small fraction of the liquid flows as films with different velocities. The zones with lower liquid velocities can represent the "dead" zones which can be active or inactive to mass transfer. During physical absorption, these "dead" zones most probably will be saturated by the absorbing gas and hence ineffective to mass transfer. However, when the absorption is accompanied by chemical reaction, these zones will still be effective.

3.2 Theoretical Development

The mass transfer model is derived on the basis of counter–current flow with flue gas, component A, (NO_x or SO_2) fed to the bottom of the column.

The problem to be considered is that of a gaseous component "A" moving up a column and dissolving into the liquid phase according to Equation 3.1:

$$A_G \rightleftharpoons A_L \qquad .....(3.1)$$

Subsequently irreversible reaction with component B occurs as illustrated by Equation 3.2:

$$F_A A_L + F_B B_L \longrightarrow \text{Product} \qquad .....(3.2)$$

where

F_A, F_B = stoichiometric coefficients, dimensionless

A_L, B_L = solute gas and non–volatile solute dissolved in liquid phase respectively, dimensionless

Baldi and Sicardi (1975, 1976) assumed that the whole column is divided into a series of stages of equal height, ΔZ, such that:

$$\Delta Z = \frac{Z}{n} \qquad .....(3.3)$$

where

Z = height of packing, m

n = number of stages, dimensionless

They further assumed that the liquid flow pattern in each of these stages will approximate trickle flow conditions. The criterion for trickle flow is given by Michell and Furzer (1972) and can be justified if the Peclet number, Pe, falls in the range:

$$0.2 < Pe < 1.2 \qquad .....(3.4)$$

where

$Pe = \frac{\bar{U}d}{\aleph}$, dimensionless

$\bar{U}$ = mean real liquid velocity, $m.s^{-1}$

d = nominal packing diameter, m

$\aleph$ = axial dispersion coefficient, $m^2.s^{-1}$

The trickle flow condition corresponds to liquid flow rates ranging from $1.5x10^{-4}$ to $1.5x10^{-3}$ $m^3.s^{-1}$ in a one–foot diameter packed column (Michell and Furzer, 1972). The true upper Peclet limit for trickle flow is probably 2 (De Wall and Van Memeren, 1965).

According to the trickle flow assumption, each of the liquid streams will take a different path as they flow down the column and remain segregated within a stage. At the end of each stage, these rivulets are assumed to be perfectly mixed to give a uniform liquid solution and a new, segregated path is resumed for the next stage. Therefore, according to this physical picture, each liquid stream, i, will remain in a stage, j, for a different time interval, $t_{j,i}$, defined by (Baldi and Sicardi, 1975, 1976):

$$t_{j,i} = \frac{S\Delta Z \delta h_i}{\delta q_i} \qquad .....(3.5)$$

where

S = column cross sectional area, m^2

δh_i = liquid holdup for stream i per unit column volume, $m^3.m^{-3}$

δq_i = volumetric liquid flow rate of stream i, $m^3.s^{-1}$

If δq_i is the flow rate of stream i, then ($S\Delta Z\delta h_i$) represents the volume occupied by this stream. The distribution of these times for the liquid stream leaving the column may be defined by:

$$\sum_{i=0}^{\infty} \frac{\delta q_i}{Q} = \int_0^{\infty} E(t)dt = 1 \qquad .....(3.6)$$

where

Q = total volumetric liquid flow rate, $m^3.s^{-1}$

and the mean liquid residence time in stage j is expressed by:

$$\bar{t}_j = \int_0^{\infty} t_{j,i} E(t)dt \cong \sum_{i=0}^{\infty} (t_{j,i} E_i \Delta t) \qquad .....(3.7)$$

where E(t) is the residence time distribution function of the liquid in each stage as suggested by Van Swaaij et al. (1969). It takes the form:

$$E(t) = \frac{\beta}{\Gamma_2} e^{\frac{-t}{\Gamma_2}} + \frac{(1 - \beta)}{\Gamma_1} e^{\frac{-t}{\Gamma_1}} \qquad .....(3.8)$$

where

β = liquid fraction passing through the stagnant region, dimensionless

Γ_1, Γ_2 = mean residence times of the liquid for the two parallel mixed cells in a stage, defined from dynamic, h_d, and static, h_s, liquid holdups, and liquid velocity, v_L according to:

$$\Gamma_1 = \frac{\Delta Z h_d}{(1 - \beta) v_L} \qquad \text{.....(3.8a)}$$

$$\Gamma_2 = \frac{\Delta Z h_s}{\beta v_L} \qquad \text{.....(3.8b)}$$

where

h_d = dynamic liquid hold–up per unit column volume, $m^3.m^{-3}$

h_s = static liquid hold–up per unit column volume, $m^3.m^{-3}$

v_L = liquid velocity, $m.s^{-1}$

The expression for E(t), suggested by Van Swaaij et al. (1969), is a two–parameter model (β and n) in which these authors consider the column to be made up of a series of stages of height ΔZ. In each stage, two parallel mixed cells are formed with mean residence times Γ_1 and Γ_2. These cells are assumed to be fed by a fraction $(1-\beta)$ and β of the total liquid flow rate respectively.

It is not possible to measure $t_{j,i}$ directly by experiment or to calculate $t_{j,i}$ from Equation 3.5 as defined by Baldi and Sicardi (1975, 1976). However, if we assume a very large number of streams a mean residence time, $\bar{t}_j$, can be evaluated according to:

$$\bar{t}_j = \frac{S\Delta Z \sum_{i=0}^{\infty} (\delta h_i)}{\sum_{i=0}^{\infty} (\delta q_i)} \qquad .....(3.9)$$

Recognizing that:

$$\sum_{i=0}^{\infty} (\delta h_i) = h_t \qquad .....(3.10)$$

and

$$\sum_{i=0}^{\infty} (\delta q_i) = Q \qquad \text{.....(3.11)}$$

represent the total liquid hold–up and the total liquid flow rate respectively, we have the mean residence time expressed by Equation 3.12 in terms of the measurable quantities h_t and v_L in the form:

$$\bar{t}_j = \frac{S\Delta Z h_t}{Q} = \frac{\Delta Z h_t}{\frac{Q}{S}} = \frac{\Delta Z h_t}{v_L} \qquad \text{.....(3.12)}$$

The value of h_t can be determined from the relationship:

$$h_t = h_d + h_s \qquad \text{.....(3.13)}$$

where

h_d = dynamic or operating hold–up corresponding to the liquid which flows rapidly over the packing surface, $m^3.m^{-3}$

h_s = static hold–up corresponding to the stagnant liquid pockets in the column, $m^3.m^{-3}$

Further discussions on the determination of h_d and h_s are provided in Appendix D.

Baldi and Sicardi (1975, 1976) further assumed that each stream has an interfacial area $\{S\Delta Z\delta a_i\}$ in each stage, and defined the interfacial area per unit liquid volume as:

$$a_{L,i} = \frac{S\Delta Z\delta a_i}{S\Delta Z\delta h_i} \qquad .....(3.14)$$

where

$a_{L,i}$ = stream interfacial area per unit liquid volume, $m^2.m^{-3}$

δa_i = stream interfacial area per unit column volume, $m^2.m^{-3}$

The actual stream interfacial area, $a_{L,i}$, between two phases is not known.

However, for a very high number of streams, the stream interfacial area, $a_{L,i}$, will most likely approach a mean value, $\bar{a}_L$, given by:

$$\bar{a}_L = \frac{S\Delta Z \sum_{i=0}^{\infty} (\delta a_i)}{S\Delta Z \sum_{i=0}^{\infty} (\delta h_i)} \qquad .....(3.15)$$

Recognizing that:

$$\sum_{i=0}^{\infty} (\delta a_i) = a \qquad .....(3.16)$$

and

$$\sum_{i=0}^{\infty} (\delta h_i) = h_t \qquad .....(3.10)$$

are the total interfacial area per unit column volume and the total liquid hold–up respectively, it follows that:

$$\bar{a}_L = \frac{a}{h_t} \qquad .....(3.17)$$

By taking the wet surface of the packing, a_w, to be identical to the gas-liquid interface, a, it is possible to write:

$$\bar{a}_L = \frac{a_w}{h_t} \qquad .....(3.18)$$

The determination of a_w is discussed in Appendix D.

Baldi and Sicardi (1975, 1976) in their original derivation further assumed that in each stage j there exists a uniform mole fraction, $\overline{Y}_{A,j}$, of A in the gas phase given by:

$$\overline{Y}_{A,j} = \frac{1}{2}\left(Y_{A,j} + Y_{A,j+1} \right) \qquad .....(3.19)$$

where

$\overline{Y}_{A,j}$ = a mean value, between the mole fraction in the inlet, $Y_{A,j+1}$, and in the outlet, $Y_{A,j}$, in the gas flow as shown in Figure 3.1, dimensionless

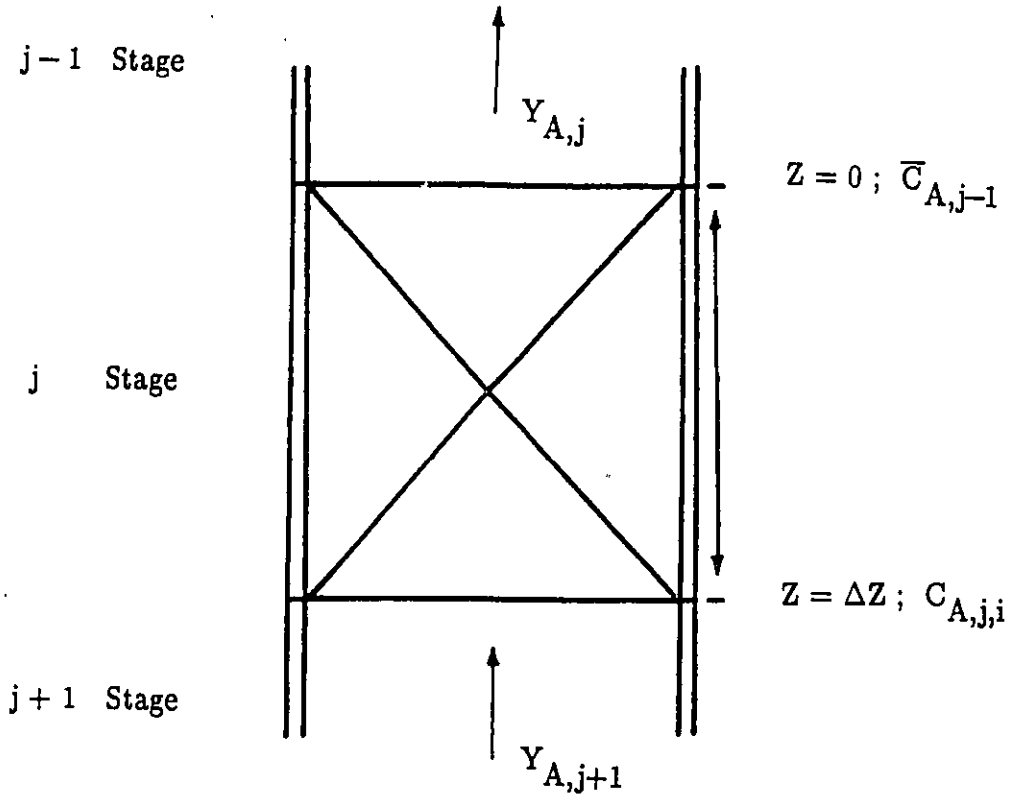

Figure 3.1 A Schematic Diagram of a Stage

Since the absorption of gaseous component A in the column will depend on its solubility and reaction in the liquid absorbent, the treatment of the problem becomes more specific to the system chosen and depends on whether strictly physical absorption or chemical reaction is involved. Therefore, the theoretical developments will be considered separately in the following sections.

3.2.1 Physical Absorption Model

Physical absorption may result in the NO_x–water or SO_2–water system when the dissolved gas species A does not react or reacts slowly with water.

According to the two–film theory, the local flux for physical absorption of component A in each liquid stream i, in any stage j, is expressed by:

$$(N_{A,j,i})_{phy} = k_G P_t(\overline{Y}_{A,j} - Y^*_{A,j}) = k'_{L,j,i}(C^*_{A,j,i} - C_{A,j,i}) \qquad .....(3.20)$$

where

$Y^{*}_{A,j}$ = mole fraction of solute gas A at the interface in equilibrium with $C^{*}_{A,j,i}$, dimensionless

$k'_{L,j,i}$ = local liquid phase mass transfer coefficient of stream i, considered constant along the stream path in the stage and is defined by:

$$k'_{L,j,i} = \frac{\zeta}{\sqrt{t_{j,i}}} \qquad m.s^{-1} \qquad \text{....(3.20a)}$$

where

ζ = an adjustable parameter accounting for various hydrodynamic conditions of the liquid streams, $[m^2.s^{-1}]^{\frac{1}{2}}$

$C^{*}_{A,j,i}$ = interfacial concentration of solute gas A in stream i, in stage j, $kmole.m^{-3}$

A mass balance on the solute gas A in the same stage gives:

$$(N_{A,j,i})_{phy} = \lim_{\Delta Z \to 0} \left(\frac{\delta q_i \Delta C_{A,j,i}}{S \delta a_i \Delta Z} \right) = \frac{\delta q_i dC_{A,j,i}}{S \delta a_i dZ} \qquad \text{....(3.21)}$$

Obviously, Equations 3.20 and 3.21 represent the same absorption flux. Therefore, it is possible to write:

$$k_G P_t (\overline{Y}_{A,j} - Y^*_{A,j}) = k'_{L,j,i} (C^*_{A,j,i} - C_{A,j,i})$$

$$= \frac{\delta q_i dC_{A,j,i}}{S \delta a_i dZ} = \frac{\Delta Z dC_{A,j,i}}{a_{L,i} t_{j,i} dZ} \qquad \text{.....(3.22)}$$

by applying Equations 3.5 and 3.14.

For dilute, non–reactive systems, the gas–liquid equilibrium can be expressed by Henry's law:

$$C^*_{A,j,i} = \frac{P_t Y^*_{A,j}}{H} \qquad \text{.....(3.23)}$$

where

$C^{*}_{A.j,i}$ = the interfacial concentration, assumed constant in the stage, kmole.m^{-3}.

Solution for $C^{*}_{A,j,i}$ from Equations 3.20 by substitution from Equations 3.20a, and 3.23, with rearrangement, leads to a value of $C^{*}_{A,j,i}$, in the form:

$$C^{*}_{A,j,i} = \frac{1}{\zeta + Hk_G\sqrt{t_{j,i}}} \{k_G\sqrt{t_{j,i}}\, P_t Y_{A,j} + \zeta C_{A,j,i}\} \qquad .....(3.24)$$

Further simplification by substitution of , ζ, from Equation 3.20a into Equation 3.24 provides:

$$C^{*}_{A,j,i} = \frac{\sqrt{t_{j,i}}}{(\zeta + Hk_G\sqrt{t_{j,i}})} \{k_G P_t Y_{A,j} + k'_{L,j,i} C_{A,j,i}\} \qquad .....(3.25)$$

Multiplication of the right hand side of Equation 3.25 by $\left(\sum_{i}^{\infty} \frac{q_i}{Q}\sqrt{t_{j,i}}\right)$ in the numerator and denominator, and assumption of very high number of streams, leads to:

$$C^{*}_{A,j,i} = \frac{\int_0^{\infty} t_{j,i}E(t)dt \{k_G P_t \overline{Y}_{A,j} + k'_{L,j,i} C_{A,j,i}\}}{(\zeta \int_0^{\infty}\sqrt{t_{j,i}}E(t)dt + Hk_G \int_0^{\infty} t_{j,i} E(t)dt)} \qquad .....(3.26)$$

Since $\int_0^{\infty} t_{j,i}E(t)dt = \bar{t}_j$ according to Equation 3.7, it follows that:

$$C^{*}_{A,j,i} = \frac{\bar{t}_j(k_G P_t \overline{Y}_{A,j} + k'_{L,j} C_{A,j,i})}{(\zeta \int_0^{\infty}\sqrt{t}_{j,i}E(t) + Hk_G\bar{t}_j)} \qquad .....(3.27)$$

From Equation 3.8, it follows that:

$$\int_0^{\infty} \sqrt{t_{j,i}} E(t)dt = \int_0^{\infty} \sqrt{t_{j,i}} \{ \frac{\beta}{\Gamma_2} e^{\frac{-t}{\Gamma_2}} + \frac{(1-\beta)}{\Gamma_1} e^{\frac{-t}{\Gamma_1}} \} dt$$

.....(3.28)

By applying the principles of the Gamma function (Fogiel, 1986), Equation 3.28 can be integrated to give:

$$\int_0^{\infty} \sqrt{t_{j,i}} E(t)dt = \frac{\beta}{2} \sqrt{\pi \Gamma_2} + \frac{(1-\beta)}{2} \sqrt{\pi \Gamma_1}$$

.....(3.29)

Substitution of Equation 3.29 into Equation 3.27, yields:

$$C^*_{A,j,i} = \frac{\bar{t}_j (k_G P_t Y_{A,j} + k'_{L,j,i} C_{A,j,i})}{\zeta [\frac{\beta}{2} \sqrt{\pi \Gamma_2} + \frac{(1-\beta)}{2} \sqrt{\pi \Gamma_1}] + H k_G \bar{t}_j}$$

.....(3.30)

By multiplying the numerator and denominator of the right hand side of Equation 3.25 by $\left(\sum_{i}^{\infty} \frac{q_i}{Q}\right)$ and assuming a very large number of streams, it becomes possible to write:

$$C^{*}_{A,j,i} = \frac{\int_0^{\infty} \sqrt{t_{j,i}}\ E(t)dt\ \{k_G P_t Y_{A,j} + k'_{L,j,i} C_{A,j,i}\}}{(\zeta \int_0^{\infty} E(t)dt + Hk_G \int_0^{\infty} \sqrt{t_{j,i}}\ E(t)dt)}$$

.....(3.31)

By applying Equations 3.6 and 3.28, Equation 3.31 can be rewritten in the form:

$$C^{*}_{A,j,i} = \frac{(\frac{\beta}{2}\sqrt{\pi\Gamma_2} + \frac{(1-\beta)}{2}\sqrt{\pi\Gamma_1})(k_G P_t Y_{A,j} + k'_{L,j,i} C_{A,j,i})}{\zeta + (\frac{\beta}{2}\sqrt{\pi\Gamma_2} + \frac{(1-\beta)}{2}\sqrt{\pi\Gamma_1})Hk_G}$$

.....(3.32)

A comparison of Equations 3.30 and 3.32 provides us an expression for

determining the mean liquid residence time in stage j according to:

$$\overline{t}_j = \left[\frac{\beta}{2}\sqrt{\pi\Gamma_2} + \frac{(1-\beta)}{2}\sqrt{\pi\Gamma_1} \right]^2$$

.....(3.33)

By substituting Equations 3.8a, 3.8b and 3.12 into Equation 3.33, we obtain an expression for determining the liquid fraction, β , passing through the stagnant region according to:

$$\left(\frac{4h_t}{\pi}\right)^{\frac{1}{2}} = (h_s\beta)^{\frac{1}{2}} + [(1-\beta)h_d]^{\frac{1}{2}}$$

.....(3.34)

Assuming that each stage is a perfect mixer so that the concentration of the dissolved component A in stream i will approach a mean value, $\overline{C}_{A,j-1}$, on leaving that stage, integration of Equation 3.22 for the j^{th} stage between, $\overline{C}_{A,j-1}$, the concentration of the component A in the liquid phase at Z = 0. and $C_{A,j,i}$, the concentration at Z = ΔZ in the i^{th} stream at the end of the stage,

leads to:

$$\zeta a_{L,i}\sqrt{t_{j,i}} \int_{Z=0}^{Z=\Delta Z} \frac{dZ}{\Delta Z} = \int_{\overline{C}_{A,j-1}}^{C_{A,j,i}} \frac{dC_{A,j,\,i}}{(C^{*}_{A,j,\,i} - C_{A,j,i})}$$

.....(3.35)

Taking $a_{L,i} = a_L$, the stream interfacial area per unit liquid volume to be equal for all streams, and treating ΔZ to be constant for the stage, Equation 3.35 becomes:

$$\zeta a_L \sqrt{t_{j,i}} = \int_{\overline{C}_{A,j-1}}^{C_{A,j,i}} \frac{dC_{A,j,\,i}}{(C^{*}_{A,j,\,i} - C_{A,j,i})}$$

.....(3.36)

Substitution of Equation 3.25 into Equation 3.36 with subsequent integration, provides the relationship obtained by Sicardi and Baldi (1976), for a gas phase

controlled process, in the form:

$$\frac{\zeta a_L t_i H k_G}{\zeta + H k_G \sqrt{t_i}} = \ln \left[\frac{P_t Y_{A,j} - H \bar{C}_{A,j-1}}{P_t Y_{A,j} - H C_{A,j,i}} \right] \qquad \text{.....(3.37)}$$

However, substitution of Equations 3.30 and 3.33 into Equation 3.35, leads to:

$$\zeta a_L \sqrt{t_{j,i}} = \int_{\bar{C}_{A,j-1}}^{C_{A,j,i}} \frac{dC_{A,j,i}}{\frac{\bar{t}_j (k_G P_t Y_{A,j} + k'_{L,j,i} C_{A,j,i})}{\zeta \sqrt{\bar{t}_j} + H k_G \bar{t}_j} - C_{A,j,i}} \qquad \text{.....(3.38)}$$

After letting

$$\lambda = \zeta \sqrt{\bar{t}_j} + H k_G \bar{t}_j \qquad \text{.....(3.39)}$$

and subsequently integrating for the j^{th} stage, between, $\overline{C}_{A,j-1}$, the mean concentration of component A in the liquid phase at Z = 0 and $C_{A,j,i}$, the concentration at $Z = \Delta Z$ in the i^{th} stream, it is possible to write:

$$\frac{\zeta a_L \sqrt{\bar{t}_{j,i}}(\bar{t}_j k_{L,j,i} - \lambda)}{\lambda} = \ell n \left[\frac{\bar{t}_j k_G P_t Y_{A,j} + C_{A,j,i}(\bar{t}_j k'_{L,j,i} - \lambda)}{\bar{t}_j k_G P_t Y_{A,j} + \overline{C}_{A,j-1}(\bar{t}_j k'_{L,j,i} - \lambda)}\right]$$

.....(3.40)

If we multiply the numerator and denominator of the left hand side of Equation 3.40 by the cube of the distribution function, $\{\int_0^\infty E(t)dt\}^3$, and apply Equations 3.6, 3.29 and 3.33, we derive the expression:

$$\frac{\zeta \bar{a}_L \sqrt{\bar{t}_j} \quad (I - \lambda)}{\lambda} = \ell n \left[\frac{\bar{t}_j P_t Y_{A,j} + C_{A,j,i}(k'_{L,j,i} - \lambda)}{\bar{t}_j P_t Y_{A,j} + \overline{C}_{A,j-1}(k'_{L,j,i} - \lambda)}\right]$$

.....(3.41)

where

$$I = \int_0^{\infty} k'_{L,i}\, E(t)dt \;=\; \zeta\sqrt{\pi}\,\left[\frac{\beta}{\sqrt{\Gamma_2}} + \frac{(1\;-\;\beta)}{\sqrt{\Gamma_1}}\right]$$

.....(3.42)

Solving for $C_{A,j,i}$ from Equation 3.41 and multiplying its value by $\left(\sum_i^{\infty} \frac{q_i}{Q}\right)$, and by assuming a very large number of streams, the mean concentration, $\overline{C}_{A,j}$, in the liquid leaving the j^{th} stage is given by:

$$\overline{C}_{A,j} \;=\; C_{A,j,i} \sum_i^{\infty} \frac{q_i}{Q} \qquad \text{.....(3.43)}$$

which is equivalent to:

$$\overline{C}_{A,j} \;=\; \int_0^{\infty} C_{A,j,i}\, E(t)dt \qquad \text{.....(3.44)}$$

Upon integration, we have:

$$\overline{C}_{A,j} = \frac{1}{\lambda - I\overline{t}_j}\left[\overline{t}_j k_G P_t \overline{Y}_{A,j} - \left\{\overline{t}_j k_G P_t \overline{Y}_{A,j} - (\lambda - I\overline{t}_j)\overline{C}_{A,j-1}\right\} \exp\left(\frac{-\zeta \bar{a}_L \sqrt{\overline{t}_j}(\lambda - I\overline{t}_j)}{\lambda}\right)\right] \quad \ldots.(3.45)$$

where

$$\frac{\sum_{i=0}^{\infty} a_{L,i}}{\sum_{i=0}^{\infty} i} = \bar{a}_L = \frac{a_w}{h_t} \quad \ldots..(3.18)$$

$\bar{a}_L$ = mean stream interfacial area per unit liquid volume, $m^2.m^{-3}$

a_w = wetted surface area of packing per unit column volume, $m^2.m^{-3}$

h_t = total liquid holdup per unit column volume, $m^3.m^{-3}$

$$\sum_{i=0}^{\infty} \left(\frac{\delta q_i}{Q} t_{j,i}\right) = \int_0^{\infty} t_{j,i} E(t)dt = \bar{t}_j = \frac{\Delta Z h_t}{v_L} \qquad \text{....(3.12)}$$

$\bar{t}_j$ = mean residence time, s

v_L = liquid velocity, $m.s^{-1}$

$$\lambda = \zeta \sqrt{\bar{t}_j} + Hk_G \bar{t}_j \qquad \text{.....(3.39)}$$

$$I = \int_0^{\infty} k'_{L,i} E(t)dt = \zeta \sqrt{\pi} \left[\frac{\beta}{\sqrt{\Gamma_2}} + \frac{(1-\beta)}{\sqrt{\Gamma_1}}\right] \qquad \text{.....(3.42)}$$

and k_G is the gas–side mass transfer coefficient.

3.2.2 Chemical Absorption Model

In the $NO_x - (NaClO_2 + NaOH)$ or $SO_2 - (NaClO_2 + NaOH)$ systems,

the dissolved gaseous component A reacts irreversibly with species B. Such a process can be described by:

$$F_A A_L + F_B B_L \longrightarrow \text{Product} \qquad \text{.....(3.2)}$$

where

B = a non–volatile solute which has been dissolved in the liquid phase prior to its introduction into the packed column, dimensionless

F_A; F_B = stoichiometric coefficients, dimensionless

If we assume that the reaction is sufficiently fast, the local chemical absorption rate of component A in each liquid stream i, in stage j can be expressed by:

$$k_G P_t(\overline{Y}_{A,j} - Y^*_{A,j}) = \phi k'_{L,j,i} C^*_{A,j,i} = -\frac{\Delta Z}{a_{L,i} t_{j,i}} \frac{F_A dC_{B,j,i}}{F_B dZ}$$

....(3.46)

where

ϕ = mass transfer enhancement factor, dimensionless

Depending on the absorption conditions, different models may arise at this point. However, we will discuss only the chemical absorption models concerned with:

. independent removal of NO_x
. independent removal of SO_x

with aqueous mixed sodium chlorite and sodium hydroxide solutions.

3.2.2.1 NO – ($NaClO_2$ + NaOH) System

The reaction between nitric oxide and chlorite ion in alkaline solution is considered to be:

$$4NO_{(l)} + 3ClO_{2(l)}^{-} + 4OH^{-}_{(l)} \longrightarrow 4NO_{3(l)}^{-} + 3Cl^{-}_{(l)} + 2H_2O_{(l)} \quad \text{....(3.47)}$$

Sada et al. (1978, 1979) who confirmed that the system operates under the fast reaction regime, expressed the local absorption flux in terms of the film model by:

$$N_{A_2} = \sqrt{\frac{2}{3} k_3 C_{B_1} C^{*3}_{A_2} D_{A_2 L}} \qquad .....(3.48)$$

where

k_3 = the third order rate constant with a value of 2.1×10^{12} $[m^3.kmole^{-1}]^2.s^{-1}$ at 25 ^oC

$D_{A_2 L}$ = liquid phase diffusivity of nitric oxide, $m^2.s^{-1}$

The symbols A_2 and B_1 refer to nitric oxide (NO) and sodium chlorite ($NaClO_2$) respectively.

Since Equations 3.47 and 3.48 express the same flux of absorption in any stage j, it follows that:

$$\sqrt{\frac{2}{3}\, k_3 C_{B_1} C_{A_2}^{*3} D_{A_2} L} = \phi k'_{L,i} C^*_{A_2} = -\frac{\Delta Z}{a_{L,i}\, t_{j,i}} \frac{F_{A_2}\, dC_{B_1,j,i}}{F_{B_1}\, dZ}$$

.....(3.49)

Integration of Equation 3.49 for the j^{th} stage will lead to the solution of $C_{B_1 j,i}$. Multiplication of $C_{B_1 j,i}$, by $\left(\sum_i^{\infty} \frac{q_i}{Q}\right)$ will give the expression for $\overline{C}_{B_1 j}$, the mean concentration in the liquid stream leaving the j^{th} stage in the form:

$$\overline{C}_{B_1 j} = \left[\sqrt{C_{B_1 j-1}} - \frac{\overline{a}_L \overline{t} F_{B_1} \sqrt{\frac{2}{3} k_3 C_{A_2}^{*3} D_{A_2} L}}{2 F_{A_2}}\right]^2$$

.....(3.50)

3.2.2.2 $SO_2 - (NaClO_2 + NaOH)$ System

When sulphur dioxide is absorbed into aqueous alkaline

chlorite solution, the following reactions are assumed to occur:

$$SO_{2(g)} \rightleftharpoons SO_{2(l)} \qquad \text{.....(3.51)}$$

$$SO_{2(l)} + OH^-_{(l)} \rightleftharpoons HSO^-_{3(l)} \qquad \text{.....(3.52)}$$

$$HSO^-_{3(l)} + OH^-_{(l)} \rightleftharpoons SO^{-2}_{3(l)} + H_2O_{(l)} \qquad \text{.....(3.53)}$$

$$2SO^{-2}_{3(l)} + ClO^-_{2(l)} \rightleftharpoons 2SO^{-2}_{4(l)} + Cl^-_{(l)} \qquad \text{.....(3.54)}$$

Sada et al. (1978) confirmed that this process occurs in the fast reaction regime when sodium chlorite concentrations are less than 0.15 M and partial pressure of SO_2 in the system varies between 0.0012 and 0.011 atmospheres. As a result, it can be argued that gas film controlling resistance prevails. According to Danckwerts (1970), the local rate of SO_2 absorption in any stream i, can be expressed by:

$$N_{A_1} = \sqrt{k_2 C_{B_1 j,i} C^*_{A_1} D_{A_1} L} \qquad \text{.....(3.55)}$$

where

k_2 = rate constant, being equal to 3.64×10^8 $m^3.kmole^{-1}.s^{-1}$ (Wang and Himmelblau, 1964)

D_{A_1L} = liquid phase diffusivity of SO_2, 1.90×10^{-9} $m^2.s^{-1}$

The subscripts A_1 and B_1 refer to SO_2 and $NaClO_2$ respectively.

It can be readily shown that:

$$\overline{\sqrt{k_2 C_{B_1 j,i} C^{*2}_{A_1} D_{A_1 L}}} = \phi k'_{L,j,i} C^*_{A_1} = -\left(\frac{\Delta Z}{a_{L,i} t_i}\right) \frac{F_{A_1} dC_{B_1 j,i}}{F_{B_1} dZ} \qquad .....(3.56)$$

Integration of Equation 3.56, will finally lead to the mean concentration, $\overline{C}_{B_1 j}$,

expressed by:

$$\overline{C}_{B_1 j} = \left[\sqrt{\overline{C}_{B_1 j-1}} - \frac{\overline{a}_L \overline{t} F_{B_1} C^*_{A_1} \sqrt{\overline{k_2 D_{A_1}} L}}{2 F_{A_1}} \right]^2 \qquad \text{.....(3.57)}$$

which permits the chlorite determination.

CHAPTER 4
EXPERIMENTAL PROGRAM
(APPARATUS AND PROCEDURE)

4.1 Experimental Program

Two sets of experiments were performed under similar flow conditions with tap water and aqueous mixed sodium chlorite and sodium hydroxide as liquid absorbents. The effects of solute gas concentrations, liquid absorbent concentrations, pH, gas and liquid flow rates on absorption efficiency were investigated.

Table 4.1 summarizes the parameters under investigation. It also provides the ranges of the experimental conditions and the goals for each set of experiments.

4.2 Description of Apparatus

Absorption studies were carried out in a 15.2 cm I.D.

Table 4.1 Summary of Experimental Program

Set One

Liquid Absorbent: **Water**

Type of Experiments	Operating Conditions				Objectives
	Concentration		Flow Rate		
	Solute Gas	Liquid Absorbent	Air	Liquid	
	[ppm]	[M]	[liter.min^{-1}]		
a. Removal of NO_x	500	–	50–100	1.5–10	Clarify the effects on removal efficiency of: .Gas solute concentration .Gas and liquid flow rates
b. Removal of SO_x	1000	–	50–100	1.5–10	
	2000	–	50–100	1.5–10	
	3000	–	50–100	1.5–10	

Table 4.1 Summary of Experimental Program (continued)

Set Two

Liquid Absorbent: **Alkaline Sodium Chlorite**

Type of Experiments	Operating Conditions				Objectives
	Concentration		Flow Rate		
	Solute Gas	Liquid Absorbent	Air	Liquid	
	[ppm]	[M]	[liter.min^{-1}]		
a. Removal of NO_x	550	0.05	50	1.5–16	Clarify
	550	0.12	50	1.5–16	the effects on removal efficiency of:
	550	0.24	50	1.5–16	.Liquid absorbent concentrations
	200–900	0.24	50–100	4.4	.Liquid flow rates .Gas solute concentrations
	200–900	0.11	50–100	4.4	.Gas flow rates
b. Removal of SO_x	2000	0.05	50–100	1.5–10	

(6 inch) packed column which was designed and used in earlier odour control studies by Chen (1978), who showed that wall effects were negligible for a column of this size. Onda et al. (1959) in their liquid–side mass transfer coefficients studies showed that the end effects decrease as the size of column and packing material increase. For a packed column with an inside diameter of 6 cm (2.4 inch), packed to a height of 30 cm (1 foot), the end effects for 6, 8 and 10 mm Raschig rings were equivalent to a packing height of 3.6, 3.5 and 3.1 cm respectively. It is evident from the works of Onda et al. (1959) that the end effects are well within 10% of the present packed height (33 inch, 15.8 mm Pall ring) for a larger column size and packing material which was used in this investigation. The flow sheet for the experimental equipment is provided in Figure 4.1. The main elements of the system consisted of:

. Feed system
. Absorption column
. Effluent system
. Sampling system

Detailed descriptions of each part of the overall system are given in subsequent sections.

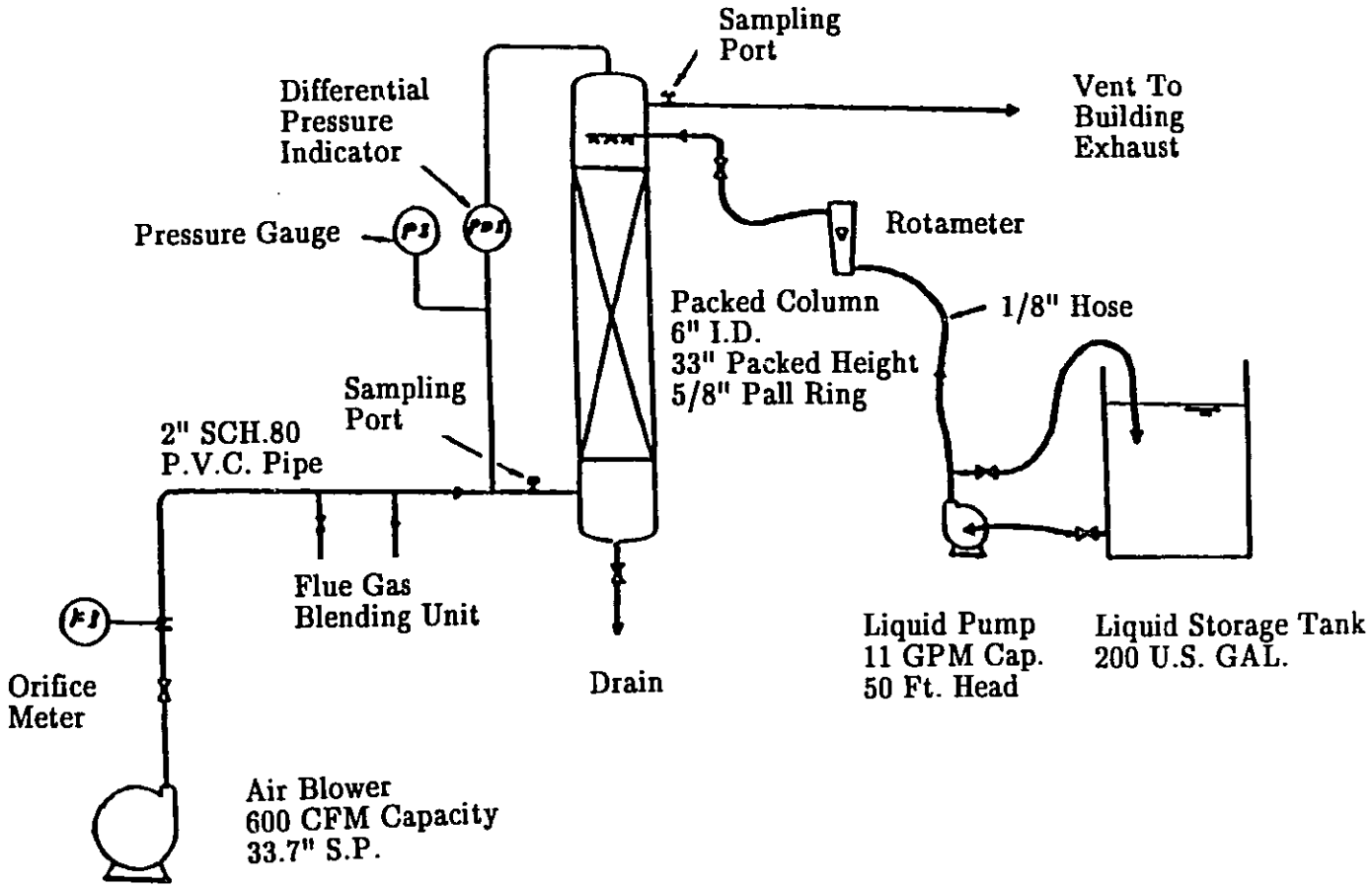

Figure 4.1 Schematic Diagram of Experimental Apparatus

4.2.1 Feed System

The feed system supplied air as diluent, scrubbing solution and a simulated flue gas from three separate units.

4.2.1.1 Air Supply Unit

Compressed air (up to 90 psig) was supplied from the high pressure line in the laboratory. The flow rate of ion air was regulated by a gate valve and was metered by an orifice me n accuracy within $\pm$ 5%. The desired air flow rates were set by adjusting the pressure drop across the orifice meter. Temperature and pressure readings were taken up–stream and down–stream of the orifice meter during each run. This meter was calibrated to reflect the actual flow conditions. The calibration curve for the air flow measurement unit is given in Appendix A.

4.2.1.2 Simulated Flue Gas Supply Unit

Stock gases consisting of 99.0% nitric oxide and 99.98% sulphur dioxide in nitrogen were obtained commercially from the Matheson Company.

Desired test gas concentrations were achieved by diluting a pure stock gas from the pressurized gas cylinder with compressed air, which was introduced down–stream of the gas proportioner. This gas proportioner had two rotameters and two needle valves for metering and controlling the flow of each of the two stock gases independently. The NO_x or SO_2 test gas was then fed to the bottom of the column through a main air line constructed of 2–inch, Schedule 80, PVC pipe.

Individual calibration data for the gas proportioner were obtained from the supplier (Scott Specialty Gases) and further checked with a dry gas meter in the laboratory. Good agreements were observed with the supplier's data to an accuracy within $\pm$ 5%. The pertinent calibration data are shown graphically in Appendix A.

4.2.1.3 Scrubbing Liquor Supply Unit

Two 200–U.S. gallon plastic tanks were used to store the made–up alkaline chlorite liquor. This solution was delivered to the absorption column through a half inch flexible plastic hose by means of a stainless steel, flexible impeller pump with a capacity of 16.5 gpm at 60 feet of head. The liquor flow rate was measured with a calibrated rotameter and was regulated by adjusting

the re–circulation to the storage tank. A calibration curve for the liquid rotameter is provided in Appendix A.

4.2.2 Absorption Column

The experimental column was six inches (0.152 m) in diameter (I.D.). It was a Pyrex Quick Fit unit which was packed randomly with 5/8 inch (0.016 m) stainless steel Pall rings to a height of 33 inches (0.838 m).

The packing was supported on a Teflon plate whose cross–section was drilled with holes to provide 70% void space. Water or alkaline sodium chlorite solution was irrigated over the top of the packed bed through a ring sprayer. The liquid distributor was located one diameter, six inches (0.152 m), above the packing zone. A re–distributor plate was mounted in between the distributor and the packing zone to ensure the liquid absorbent was introduced as evenly as possible across the top of the packing to avoid upper end effects and channelling.

A mesh pad demister was installed at the top of the column to remove water droplets which might interfere with the sampling system associated with the effluent NO_x and SO_2 measurements. Figure 4.2 provides construction details of the column.

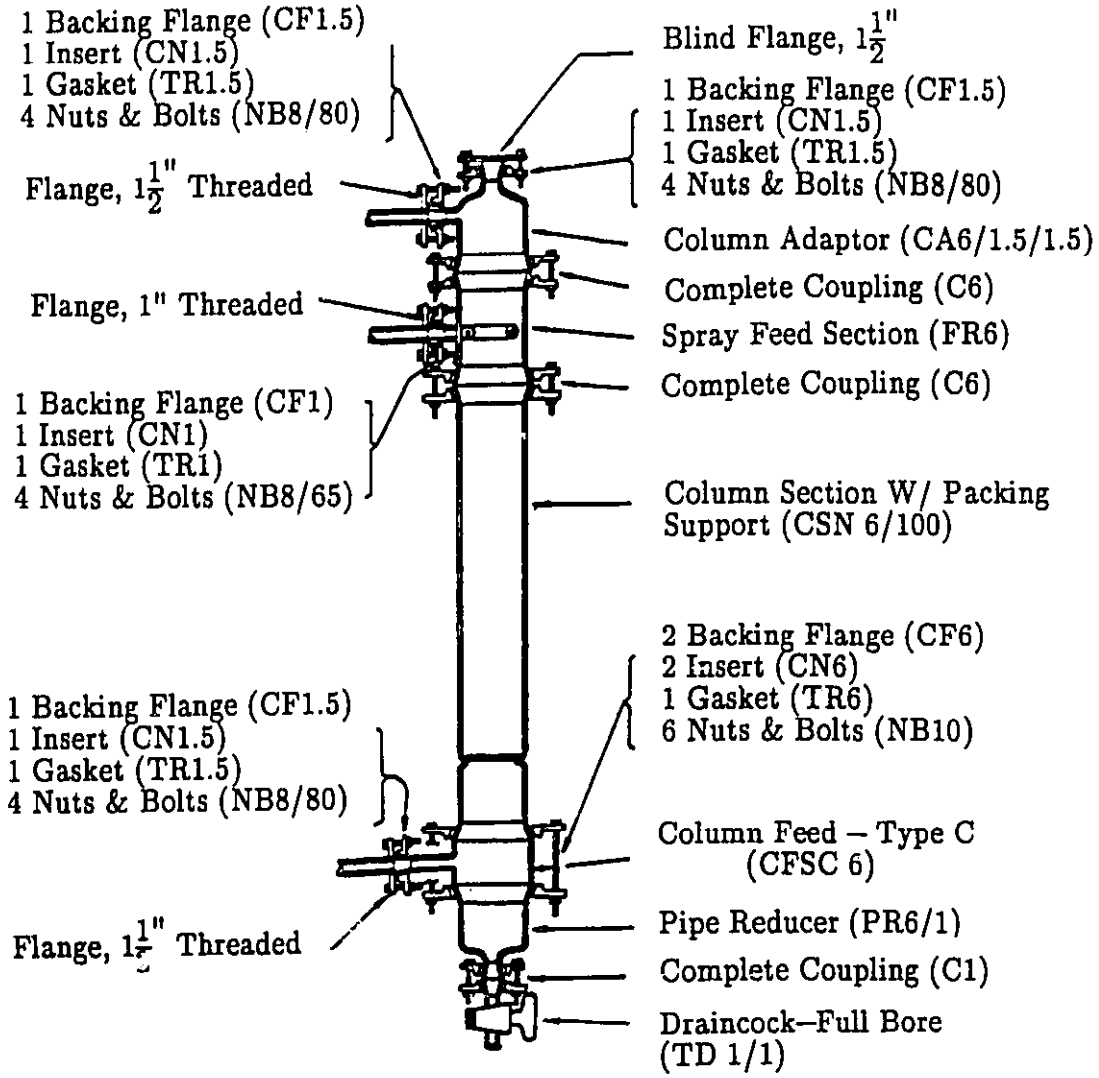

NOTE: ( ) – Q.V.F. CATALOG NO.

Figure 4.2 Column Details

4.2.3 Effluent System

The entire absorption column was located inside a flume–hood. Effluent gas was vented through a half–inch plastic pipe to the flume–hood whereas the spent liquid absorbent was discharged to the sewer system through a half–inch flexible plastic garden hose.

4.2.4 Sampling System

A bypass section allowed the inlet and outlet concentrations of NO_x and SO_2 to be measured continuously by means of a gas analyzer (Model NS–300, SO_2/NO_x Analyzer), based on Faristor technology. This NS–300 analyzer provides a bimodular capability that facilitates independent measurements of NO_x and SO_2 at inlet and outlet locations.

Values obtained from the gas phase measurements with the NS–300 analyzer were compared with liquid phase determinations of nitrate and sulphate species based on the cadmium reduction and modified barium turbidimetric methods respectively.

The liquid phase analyses involved spectrophotometric measurements at

wavelengths of 500 nm and 450 nm for nitrate and sulphate respectively with a Model PYE UNICAM PU 8600 UV/VIS spectrophotometer, manufactured by Philips of England. Appendix A provides the rotameter calibration data generated by the manufacturer of the NO_x/SO_2 Analyzer.

4.3 Experimental Details

4.3.1 Procedure

The procedure for making a run involved:

- Analyzer calibration
- Liquid absorbent preparation
- System operation
- Liquid analysis

These procedures are described in the subsequent sections. A list of the chemicals that were used during this investigation is provided in Appendix B.

4.3.1.1 Analyzer Calibration

The gas analyzer was turned on at least half an hour prior to gas sample measurement to stabilize it before calibration with the span gases obtained from the Matheson Company. Three certified standards of NO and SO_2 were used. Their concentrations were chosen to cover the simulated flue gas inlet levels. Calibration was performed in accordance with the instruction manual provided with the instrument (Model NS–300, SO_2/Nitrogen Oxide analyzer).

4.3.1.2 Liquid Absorbent Preparation

The scrubbing liquor was prepared from sodium chlorite powder (80% by weight). The sodium chlorite concentrations varied between 0.05 M and 0.5 M. They were determined by titration according to the procedure given in Appendix C. Each prepared liquid solution was left overnight and conditioned at room temperature (22 ^{O}C – 24^{O}C) before use.

4.3.1.3 System Operation

In making a run, the investigator was required to:

. Turn on the gas analyzer and switch it to the inlet gas sampling mode.

. Turn on the pump and adjust the liquid absorbent flow rate.

. Turn on the compressed air line and adjust the air flow rate.

. Turn on the appropriate stock gas and control the flow rate until the analyzer indicated approximately the desired concentration level.

. Set the proper simulated flue gas level by adjusting the gas proportioner needle valve.

. Allow for the establishment of steady state conditions as indicated by constancy of the exit NO_x or SO_2 level recorded by the analyzer.

. Record the following:

    . the initial and final analyzer readings at the inlet and outlet locations.

    . the initial and final pHs and temperatures of the liquid absorbent.

    . Room temperature and pressure drop across the orifice meter.

    . Liquid rotameter reading.

. Perform a chemical analysis on the inlet and outlet streams of the liquid absorbent according to the procedure outlined in Appendix C (C.2).

4.3.2 Analytical Methods

4.3.2.1 Determination of Sodium Chlorite Concentration

The concentration of sodium chlorite in the scrubbing solution was determined with standard sodium thiosulphate solution. The preparation of this standard solution and titration procedure were available in most analytical chemistry texts. For a quick review, a summary of this procedure is provided in Appendix C.1.

4.3.2.2 Determination of Nitrate and Sulphate in Liquid Effluent

4.3.2.2.1 Nitrate Determination

In the absorption of NO_x by water and alkaline sodium chlorite solutions, nitrate represents the major product and the most completely oxidized state in the liquid effluent. Nitrite might also exist in the case of water scrubbing, and its presence is taken into account by the cadmium reduction method. Preliminary testings with and without hydrogen peroxide (30% by weight) addition indicated no difference in measurements with the cadmium reduction method. The collected samples were examined for total nitrate resulting from the scrubbing process.

A relatively simple procedure for nitrate and nitrite determinations was given by Wetters and Uglum (1970). However, this method involved very high levels of nitrate and nitrite in liquid effluents. The lowest detection limit of nitrate was 90. $\mu g.mL^{-1}$ and 20. $\mu g.mL^{-1}$ for nitrite in a 1–cm cell. These limits are roughly equivalent to $5x10^4$ and $1x10^4$ ppm NO_x as NO_2 dissolved in liquid absorbent respectively.

Although the use of a 10–cm cell would improve the detection limit to 9 $\mu g.mL^{-1}$ for nitrate and 2 $\mu g.mL^{-1}$ for nitrite, these concentrations limits are again far beyond those that would result from the typical flue gas levels found in stack gases. As a result the application of this procedure to the present study was highly questionable.

A more sensitive cadmium reduction method, employing chromotropic acid indicator, appeared more promising (Levaggi et al., 1976; Hach Chemical, 1975). In this procedure, the formed nitrites are first converted to nitrates. The total nitrates are then reduced to nitrites, diazotized and coupled to form a red dye that is analysed spectrophotometrically at a wavelength of 500 nm. All of these steps can be achieved with a commercially available, ready–made, reagent which is supplied by Hach Chemical Company (1975).

The major disadvantage of this method is that it determines both nitrates and nitrites in a liquid sample and provides no differentiation between the two. Detailed descriptions of this method were available in the literature (Wetters and Uglum, 1970; Levaggi et al., 1976; Hach Chemical, 1975). An evaluation of this method and a modified testing procedure are provided in Appendix C.

4.3.2.2.2 Sulphate Determination

In the absorption of SO_2 by water, both sulphite and sulphate are equally likely to be produced in the liquid effluent. However, when the scrubbing liquor is switched from water to sodium chlorite, only sulphate will be formed. Sulphite is readily oxidized to sulphate in neutral or alkaline solutions (Hach Chemical, 1975; Rao and Rao, 1955).

There is no reliable means of determining the levels of sulphite at low concentrations. Therefore, a sample collected from water scrubbing must first be treated with hydrogen peroxide (30% by weight) to convert sulphite to sulphate before analysis. Such treatment thereby reduces the analysis to a single testing of total sulphate.

The procedure for determining sulphate is a modification of the barium sulphate turbidimetric method. A single, dry powder reagent named Sulfa Ver 4 Sulphate reagent will cause a milky precipitate to form if sulphate is present. This Sulfa Ver 4 Sulphate reagent also contains a stabilizing agent to hold the precipitate in suspension for turbidimetric analysis spectrophotometrically at 450 nm. The amount of turbidity formed is directly proportional to the amount of sulphate present (Hach Chemical, 1975). Additional details of the method are available in the literature (Hach Chemical, 1975; Rao and Rao, 1955). A summary is provided in Appendix C.

CHAPTER 5

RESULTS AND DISCUSSION

In this chapter, the results obtained according to the program outlined in Chapter 4 are presented and discussed. The water scrubbing data are interpreted in terms of the derived physical model which was developed from the stage concept and the residence time distribution function given by Van Swaaij et al. (1969). The liquid residence distribution function developed by Van Swaaij et al. (1969) was assumed to be valid under trickle flow conditions. The validity of this assumption is important to this work as far as the flow condition is concerned. Therefore, prior to the discussion of the results, the assumption of Van Swaaij et al. (1969) is reviewed and discussed.

5.1 Liquid Residence Time and the Assumption of Van Swaaij et al. (1969)

The mean liquid residence time, $\bar{t}$, in a stage of height, ΔZ, can be determined either from Equation 3.12 or 3.33. The evaluation of $\bar{t}$ from Equation 3.12 requires prior knowledge of h_t and ΔZ. Values of h_t can be

obtained according to the discussion in Appendix D. However, the value of ΔZ for Pall rings (5/8") is not available in the literature. A value of 3.6×10^{-2} m was assumed on the basis of the Raschig ring data given by Sicardi and Baldi (1976), Van Swaaij et al. (1969), and De Waal and Van Mameren (1965). Use of Equation 3.33 requires values of β, the liquid fraction passing through the stagnant region. The value for β can be estimated according to the following procedure.

In principle, Equations 3.12 and 3.33 represent the same residence time measurement. However, due to the inherent errors introduced with h_t, h_d, h_s and v_L evaluations, these two expressions are expected to give results that differ from each other. The differences are important for small values of h_t, h_d, and h_s. To account for the possible errors in determinations, an adjustable parameter, γ, is introduced to force the two expressions to represent the same time measurement. As a result,

$$\gamma = \frac{\bar{t}_{Eq.3.12}}{\bar{t}_{Eq.3.33}} \qquad .....(5.1)$$

where γ is defined as a residence time correction factor between the two

equations. A value of $\gamma = 1$ indicates perfect agreement between the two expressions. Substitution of Equations 3.8a and 3.8b into Equation 5.1 and subsequent simplification yields:

$$\left(\frac{4\gamma h_t}{\pi}\right)^{\frac{1}{2}} = (h_s\beta)^{\frac{1}{2}} + [(1-\beta)h_d]^{\frac{1}{2}} \qquad .....(5.2)$$

The values of h_d estimated from the Otake–Okada (1953) correlation agree with experimental data to within 20 per cent and the value of h_s determined by Shulman et al. (1955) is believed to be within the same degree of accuracy. Therefore, it is expected that for a given experimental condition, the correction factor, γ, will be a constant with a value of approximately 1 ± 0.2. In fact, γ is found to have a value 0.78 in this study.

Figure 5.1 illustrates values of β calculated from Equation 5.2, using an algorithm given by Forsythe et al. (1977), with γ equal to 0.78. Values of $\bar{t}$ evaluated from Equation 3.12 are shown in Figure 5.2. It is evident from Figure 5.2 that as the liquid flow rate increases, the mean residence time in a stage decreases toward a limiting value. This behaviour suggests that the system attains a limiting residence time at higher liquid rates. This trend agrees

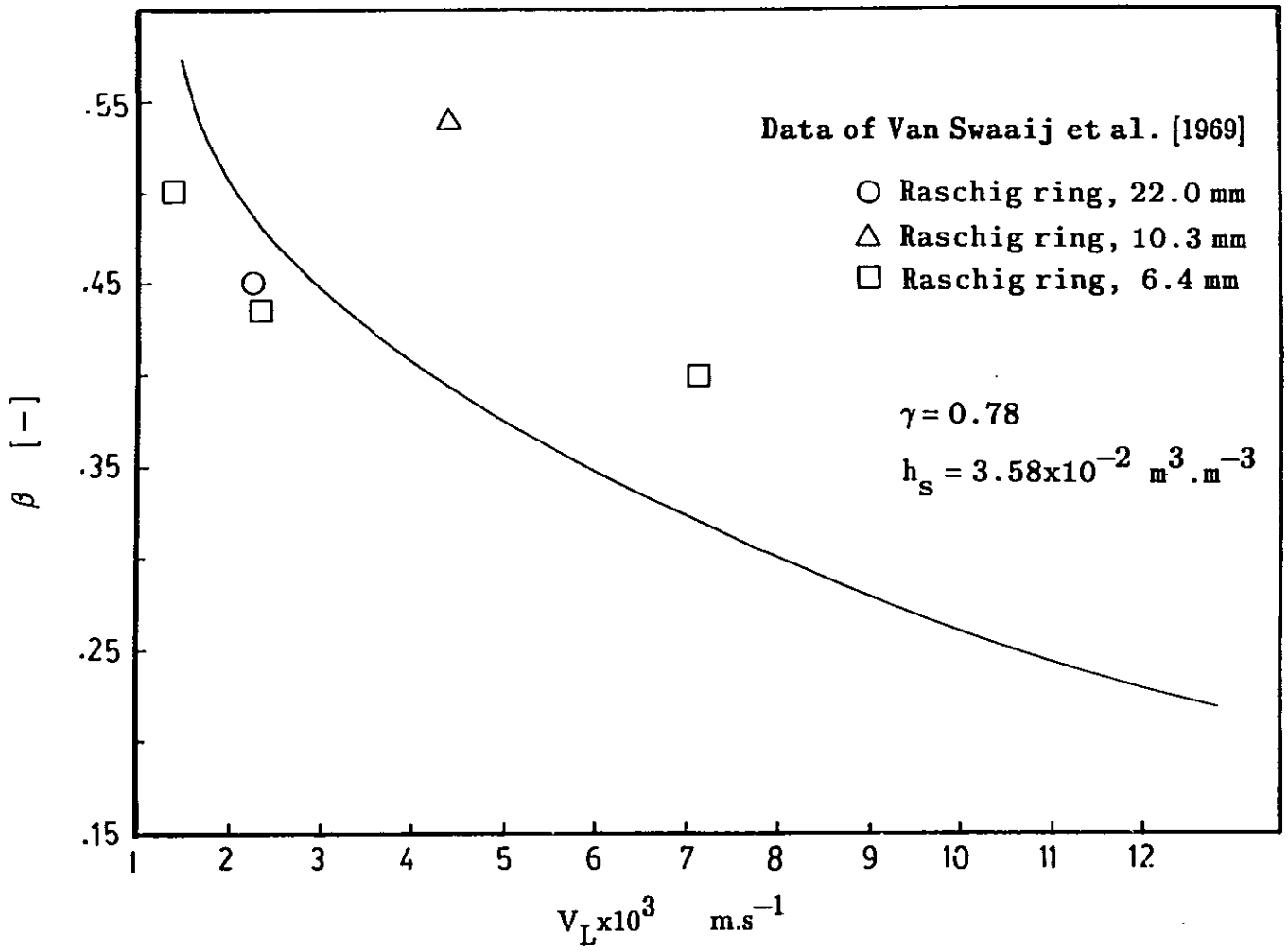

Figure 5.1 Liquid Fraction Through the Stagnant Region as a Function of Liquid Velocity

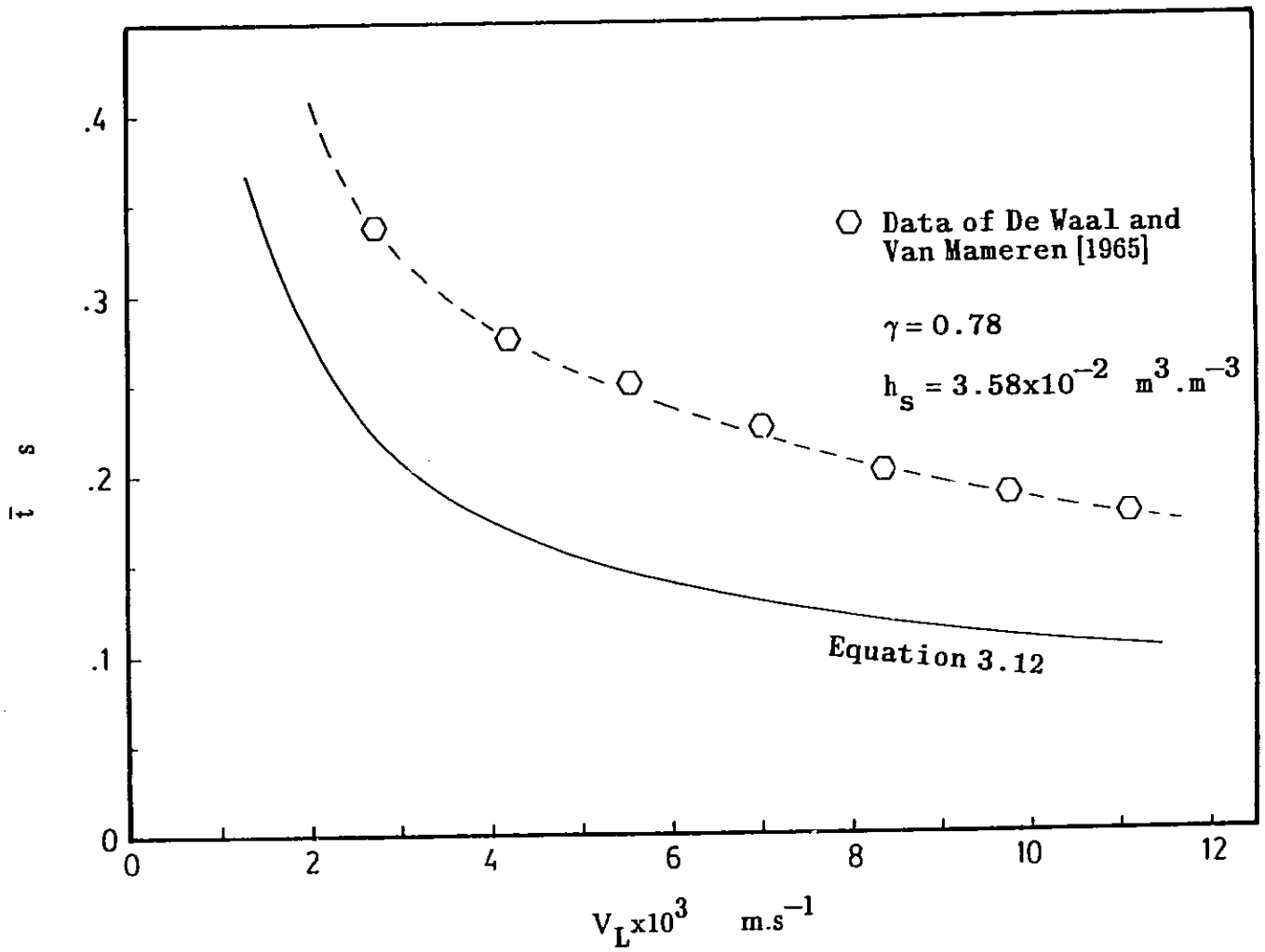

Figure 5.2 Liquid Residence Time in Packed Column as a Function of Liquid Velocity

qualitatively with the experimental observations of De Waal and Van Mameren (1965) as shown in Figure 5.2.

In deriving Equations 3.12 and 3.33, we adopted the liquid distribution function developed by Van Swaaij et al. (1969) (Equation 3.8). These authors assumed in their derivation that β was the same as h_s for trickle flow conditions. However, they were not certain whether the dynamic and static holdups were identical to the mobile phase and the stagnant regions as they had assumed. To test the validity of this parallel mixed cell assumption, two plots of $(\frac{1-\beta}{\beta})$ versus $\frac{h_d}{h_s}$ have been generated in accordance with the operating conditions of Whitney and Vivian (1949) and Chilton et al. (1937).

Theoretically, a plot of $(\frac{1-\beta}{\beta})$ versus $\frac{h_d}{h_s}$ should produce a 45 degree line passing through the origin if the Van Swaaij et al. (1960) assumption is correct. It is evident from Figures 5.3 and 5.4 that the experimental results of Whitney and Vivian (1949) and Chilton et al.(1937) are in excellent agreement with the theoretical line for liquid flow rates below 4.4×10^{-5} $m^3.s^{-1}$. Consequently, it can be concluded that the assumption made by Van Swaaij et al. (1969) is justified.

The maximum liquid flow rate in the present study was below 2×10^{-5}

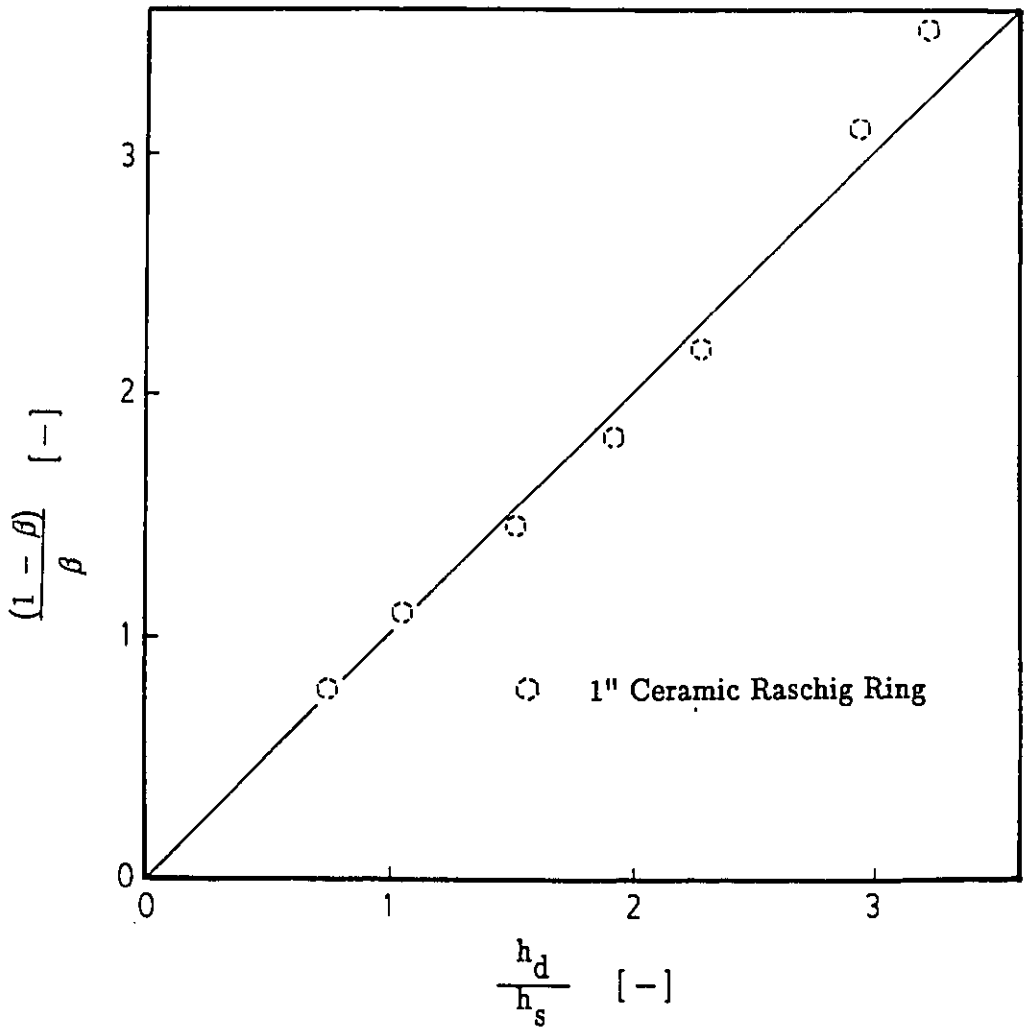

Figure 5.3 Ratio of Liquid Fraction for the Mobile Phase to the Stagnant Region vs Ratio of Dynamic Holdup to Static Holdup – Operating Condition According to Whitney and Vivian [1949]; 1" Ceramic Raschig Ring
$2.6 \leq Q_L x 10^5 \leq 22.4 \quad m^3.s^{-1}$

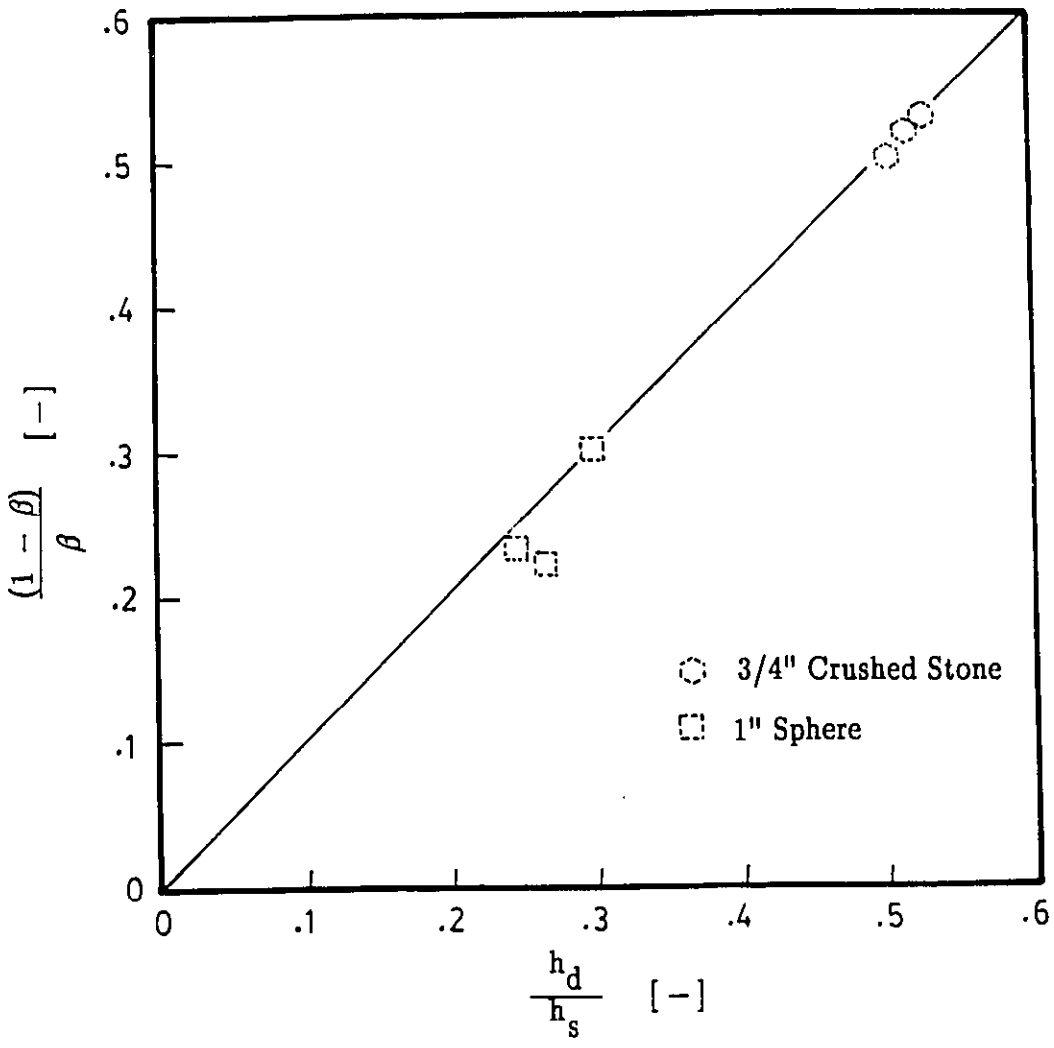

Figure 5.4 Ratio of Liquid Fraction for the Mobile Phase to the Stagnant Region vs Ratio of Dynamic Holdup to Static Holdup – Operating Condition According to Chilton et al. [1937]; $0.3 \leq Q_L x 10^5 \leq 4.4 \quad m^3.s^{-1}$

$m^3.s^{-1}$, a value well within the liquid range allowed. Therefore, it is concluded that the flow conditions prescribed by Van Swaaij et al. (1969) were complied with in this study. Further evidence on the trickle flow assumption was provided by Michell and Furzer (1972).

5.2 Absorption of NO_x into Water

The effects of scrubbing liquid flow rates, gas flow rates, and inlet NO_x levels on removal efficiency are shown in Figures 5.5 to 5.9.

5.2.1 Removal Efficiency

The absorption efficiency, defined as the percentage of nitrogen oxides removed from the inlet flue gas, was calculated from the following relationship:

$$X_{NO_x} = \left(1 - \frac{Y_{NO_x,out}}{Y_{NO_x,in}}\right)x100 \qquad .....(5.3)$$

where $Y_{NO_x,in}$ and $Y_{NO_x,out}$ represented the total mole fractions of nitrogen oxides in any oxidation state recorded by the NO_x/SO_2 analyzer at the inlet and outlet of the absorption column, respectively.

As shown in Figures 5.5 and 5.6, only limited improvement in removal efficiency is achieved with increasing liquid flow rate. The same effect was noted by Counce and Perona (1979). However, such small variations were not observed by Myerson and Sandy (1981) when water flow velocities varied from $4x10^{-6}$ to $1.25x10^{-5}$ $m^3.s^{-1}$. The effect of liquid flow rate on NO_x removal efficiency can be attributed to a better mass transfer condition occurring at the gas–liquid interface as the result of increased liquid rates. In fact, gas–liquid interfacial areas and liquid–phase mass transfer coefficients are known to increase with increasing liquid rates (Sherwood and Holloway, 1940; Yoshida and Koyanagi, 1958; Onda and co–workers, 1959, 1960; Yoshida and Miura, 1963; Semmelbauer, 1967; Jackson and Marchello, 1970; Puranik and Vogelpohl, 1974).

Variations of gas flow rate from $8.3x10^{-4}$ to $1.67x10^{-3}$ $m^3.s^{-1}$ had an adverse effect on the NO_x absorption efficiency. The results in Figure 5.7 show a steady linear decrease in the NO_x removal efficiency with increasing gas flow rate. Such an effect on absorption efficiency was confirmed by the recent studies of Counce and Perona (1979), and Myerson and Sandy (1981).

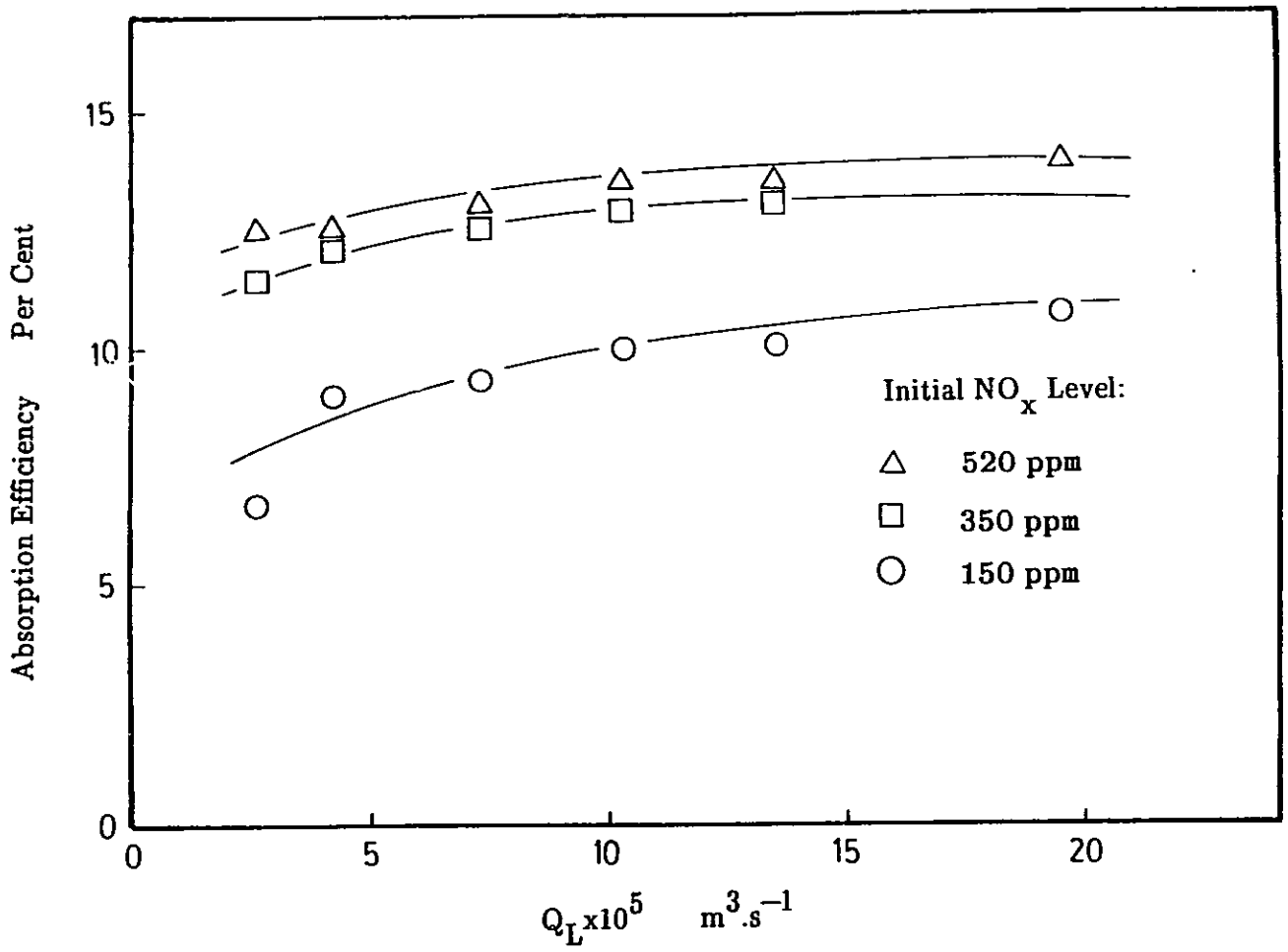

Figure 5.5 Absorption Efficiency vs Liquid Flow Rate – NO_x/H_2O System;
$Q_G = (1.07 \pm 0.05)x10^{-3}$ $m^3.s^{-1}$

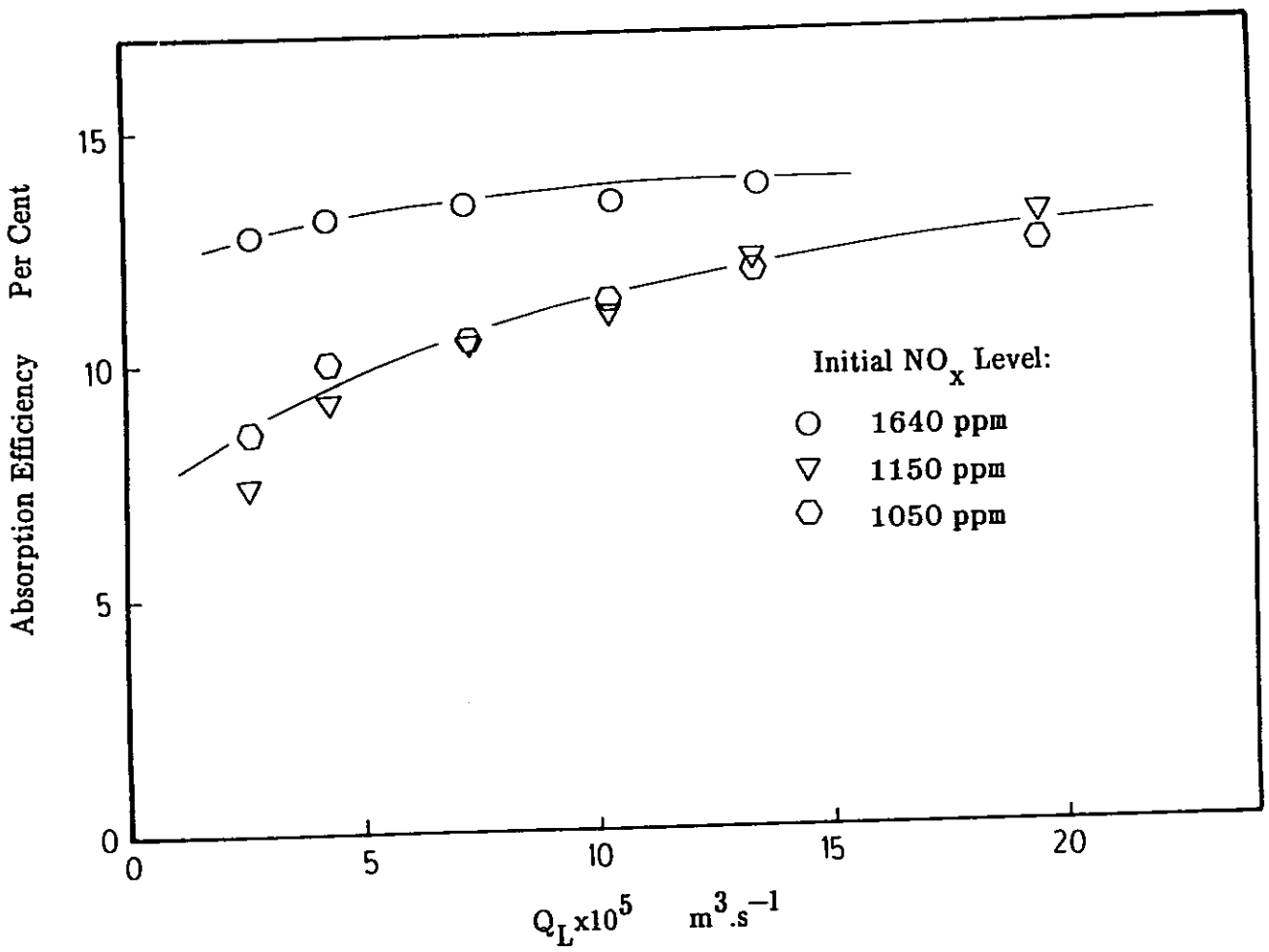

Figure 5.6 Absorption Efficiency vs Liquid Flow Rate – NO_x/H_2O System;
$Q_G = (1.6 \pm 0.2)x10^{-3}$ $m^3.s^{-1}$

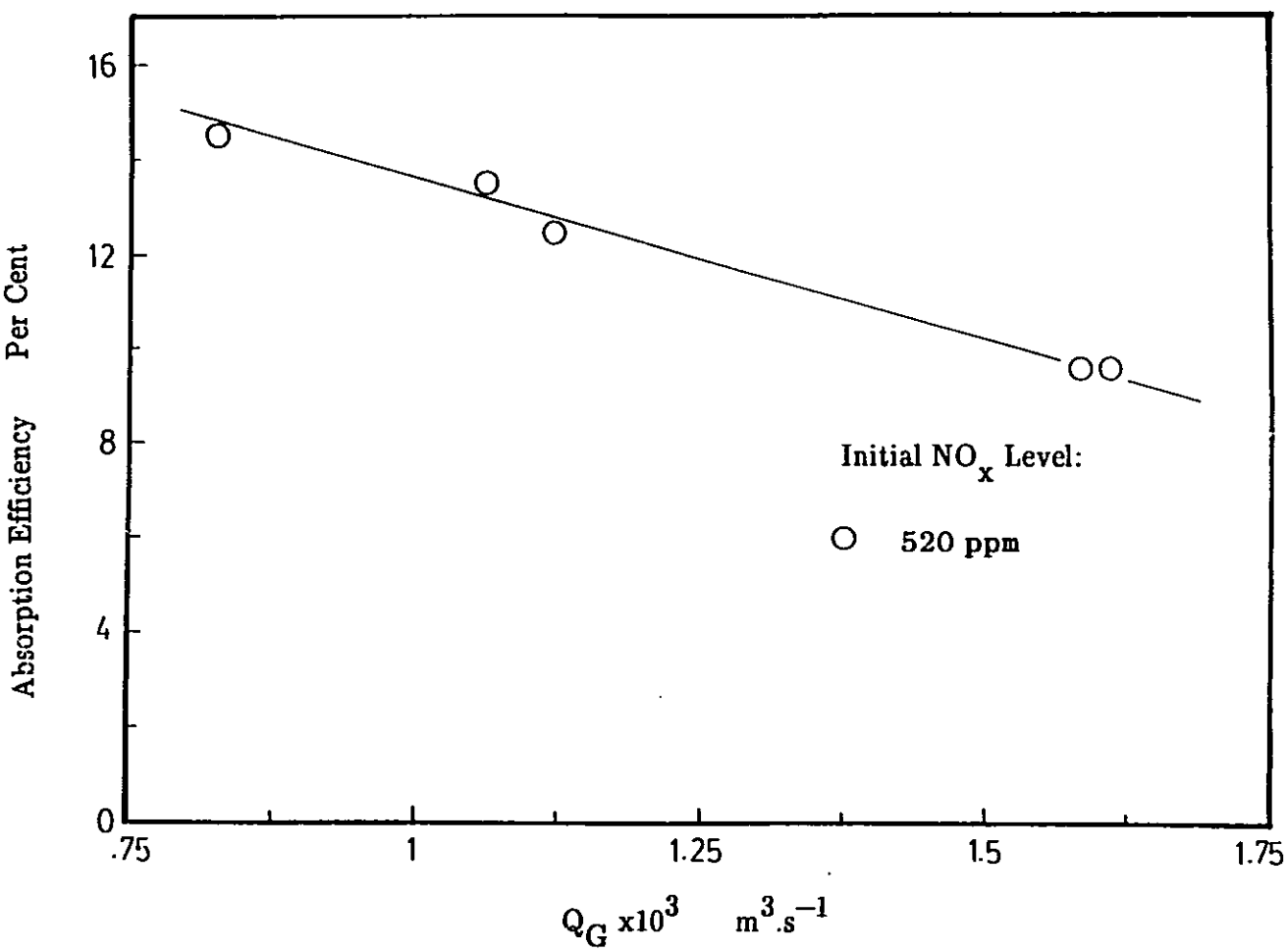

Figure 5.7 Absorption Efficiency vs Gas Flow Rate – NO_x/H_2O System;
$Q_L = (1.26 \pm 0.09)x10^{-3}$ $m^3.s^{-1}$

The decrease in absorption efficiency with increasing gas flow rate can be interpreted as a gas–liquid contact time effect. This effect was demonstrated by the work of Myerson and Sandy (1981). In their study, the reactor volume was varied to provide different residence times for the inlet flue gas. Absorption was found to increase rapidly with increasing reactor volume. In other words, the NO_x removal was inversely proportional to some function of gas flow rate.

As illustrated in Figures 5.8 and 5.9, higher removal efficiencies are obtained with higher inlet NO_x levels until the concentration exceeds 1000 ppm. This observed trend agrees with the recent findings of Myerson and Sandy (1981), who studied the absorption of NO_x in a column packed with limestone. They found that the absorption efficiency increased slightly with increasing inlet NO_x partial pressures up to 38 kPa. Counce and Perona (1979) also observed the same effect when they performed their absorption study on NO_x in a Sieve–Plate column. The NO_x removal efficiency reached a constant value for feed gas NO_x partial pressures greater than 0.05 atmosphere. However, no explanation for this behaviour was given by these researchers.

It is possible that a constant absorption efficiency is established when gas phase NO_x concentrations exceed 1000 ppm as a result of liquid film resistance control and perhaps because of the limitation of the physical solubility of NO_x in the liquid absorbent.

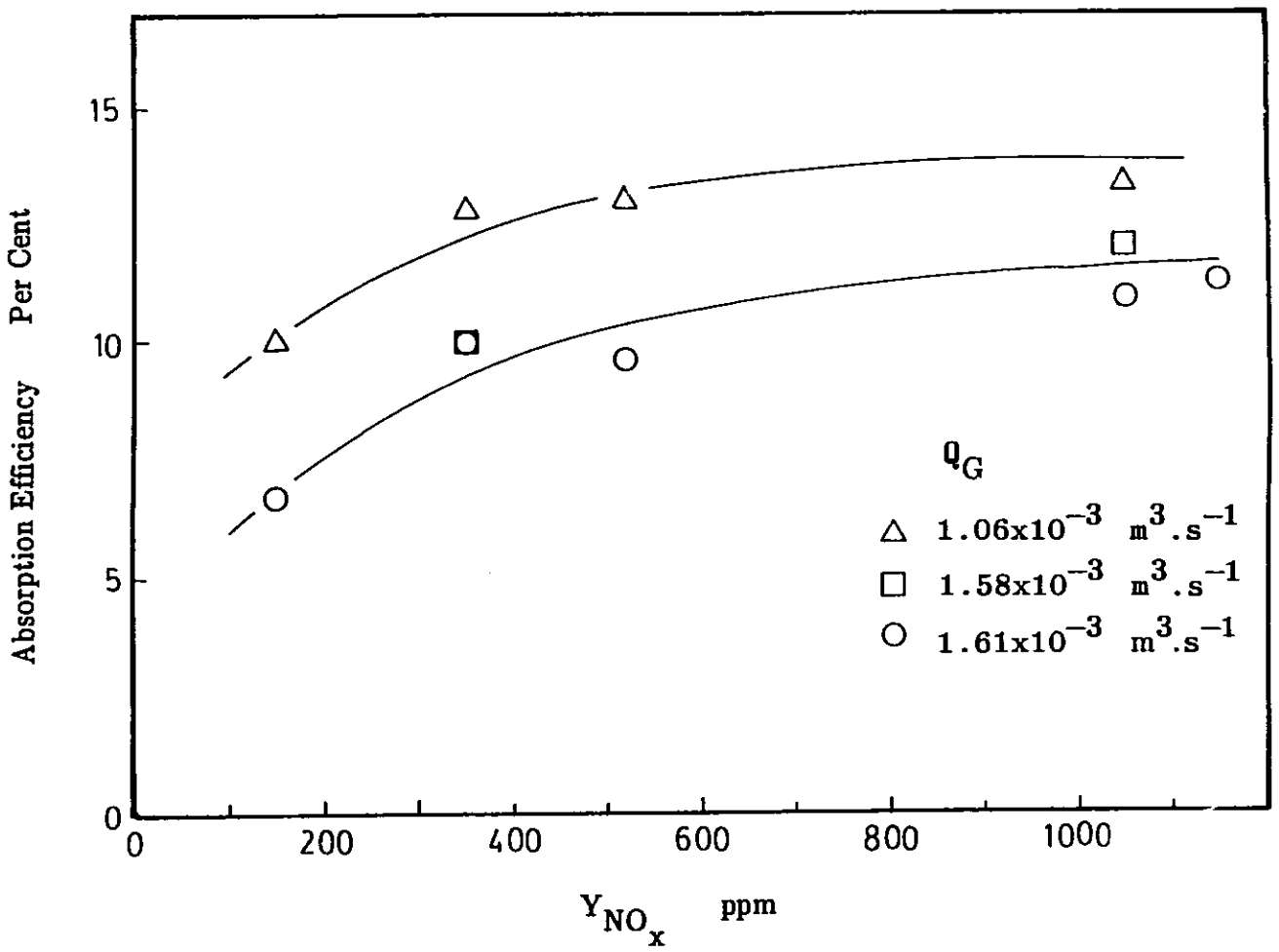

Figure 5.8 Absorption Efficiency vs Inlet NO_x Level – NO_x/H_2O System; $Q_L = 1.35x10^{-4}$ $m^3.s^{-1}$

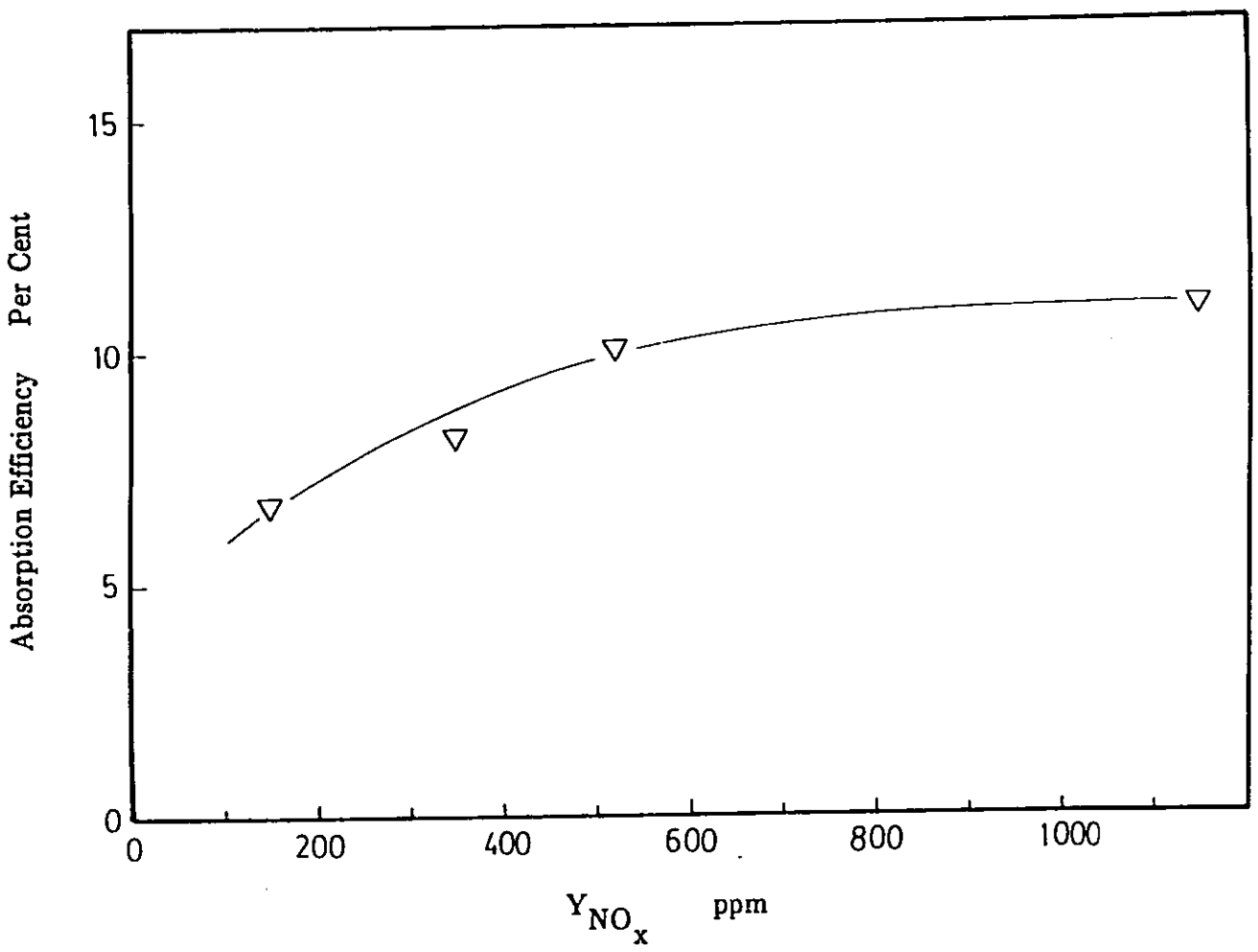

Figure 5.9 Absorption Efficiency vs Inlet NO_x Level – NO_x/H_2O System; $Q_L = 1.35 \times 10^{-4}$ $m^3.s^{-1}$; $Q_G = 1.82 \times 10^{-3}$ $m^3.s^{-1}$

5.2.2 Comparison of Experimental Data with Model Prediction

To understand the model simulation scheme, some appreciation of the previously defined adjustable parameter, ζ, is essential. In their derivation, Baldi and Sicardi (1975, 1976) introduced the concept of the liquid stream mass transfer coefficient, $k'_{L,i}$, defined by:

$$k'_{L,i} = \frac{\zeta}{\sqrt{t_i}} \qquad \text{....(3.20a)}$$

From Higbie's penetration theory, the liquid phase mass transfer coefficient, k_L, can be expressed in the form:

$$k_L = 2\left(\frac{D_{AL}}{\pi \ \theta}\right)^{\frac{1}{2}} \qquad \text{.....(5.4)}$$

Where

k_L = liquid side mass transfer coefficient, $m.s^{-1}$

D_{AL} = liquid phase diffusivity of solute gas A, $m^2.s^{-1}$

θ = time during which an element of liquid surface is exposed to the gas solute A, s

A comparison of Equations 3.20a and 5.4, suggests that an initial estimate of ζ, would be represented by:

$$\zeta \cong 2 \left(\frac{D_{AL}}{\pi}\right)^{\frac{1}{2}} \qquad \text{.....(5.5)}$$

According to Equation 5.5, the adjustable parameter, ζ, which is to account for different hydrodynamic conditions, should have a constant value.

To determine the value and the trend of the dependence of ζ on liquid flow rate, the value calculated from Equation 5.5 was compared with the value that provided the fit of predicted scrubber outlet NO_3^- and SO_4^{2-} concentrations with experimental data. If ζ were a function of liquid flow rates under the operating condition, it would be likely that ζ would vary from test to test.

The results for NO, NO_2 and N_2O_3 absorption are shown in Figures 5.10, 5.11, and 5.12 respectively. It is evident from these data that ζ remains

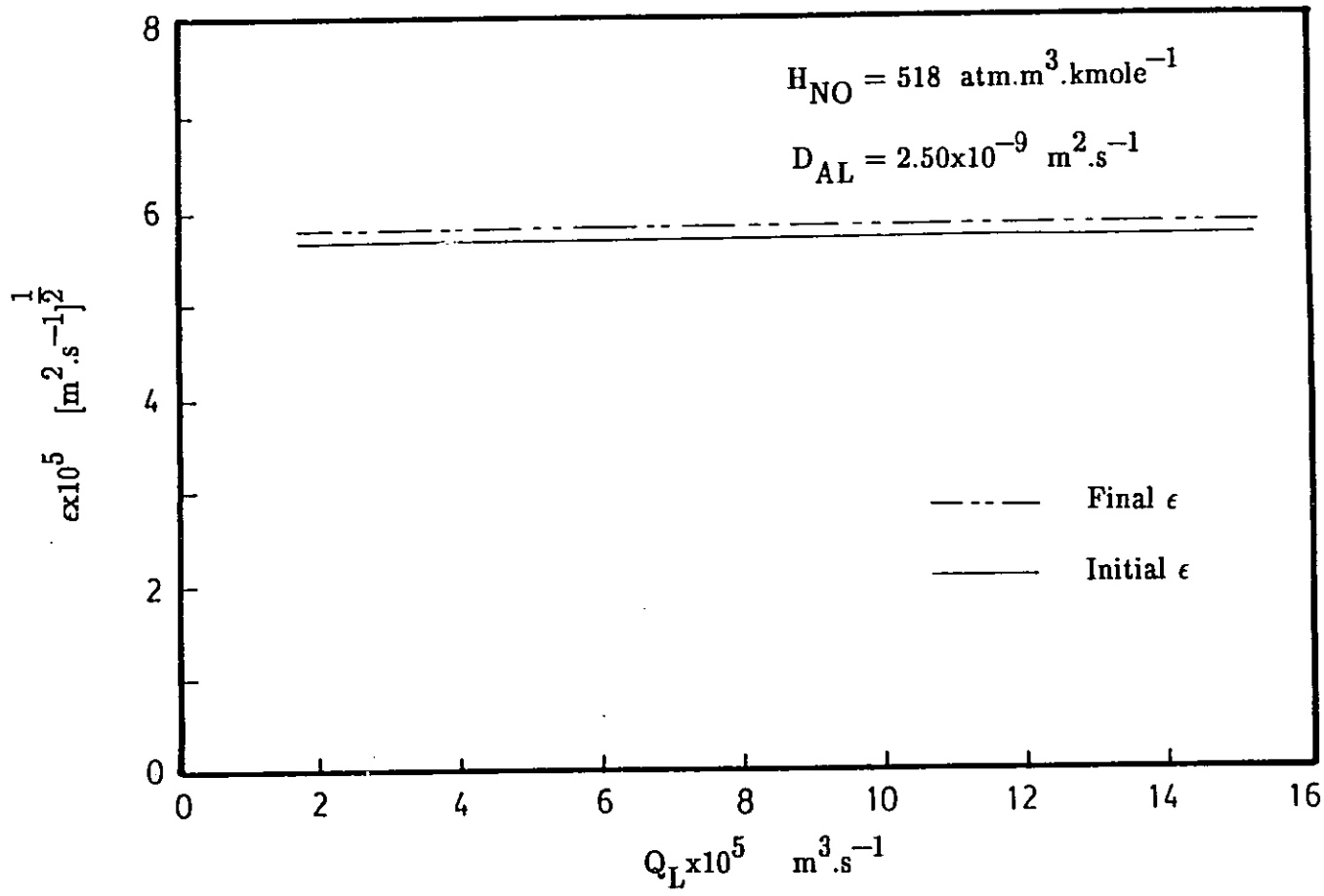

Figure 5.10 ϵ as a Function of Liquid Flow Rate – NO/H_2O System

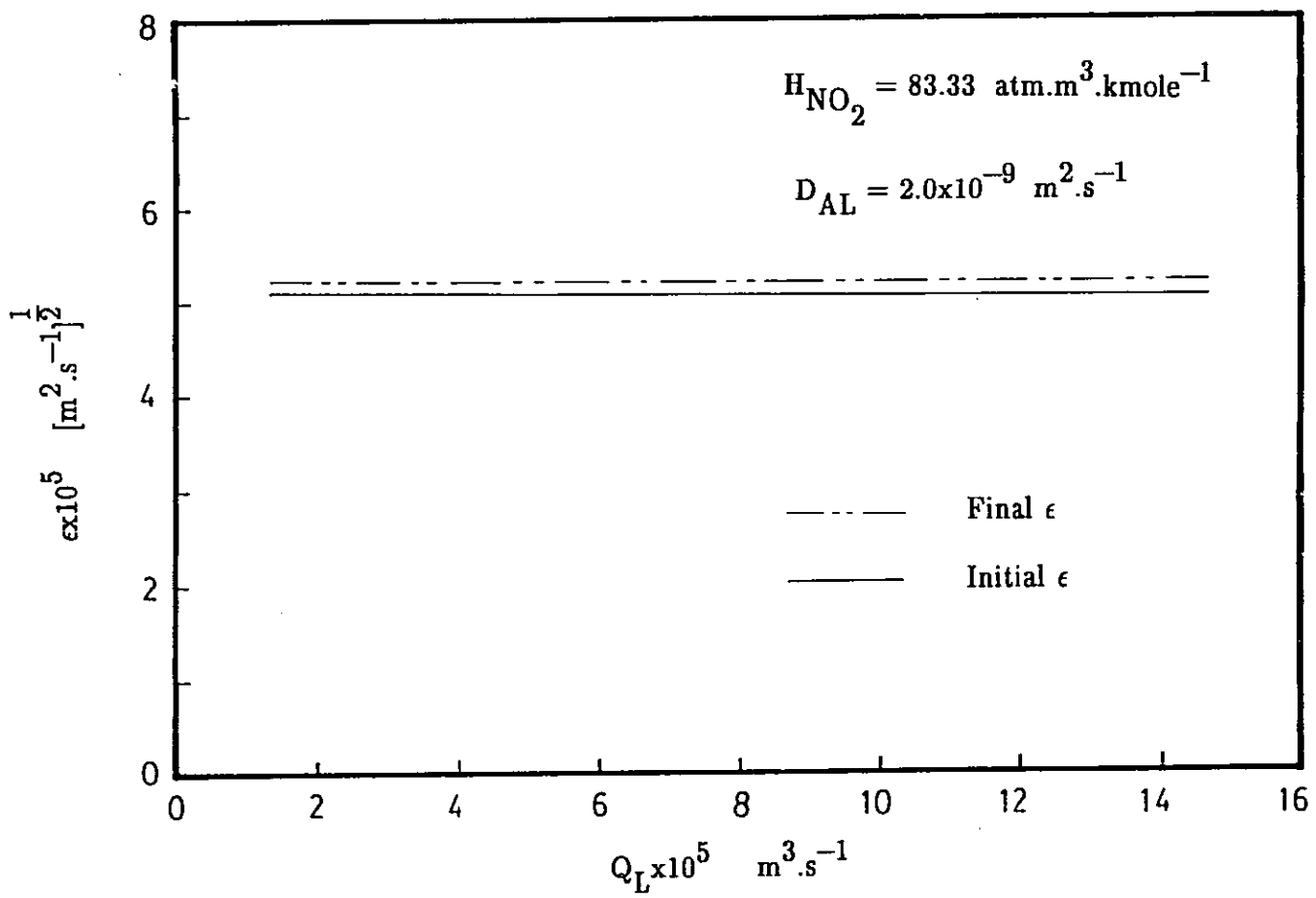

Figure 5.11 ϵ as a Function of Liquid Flow Rate – NO_2/H_2O System

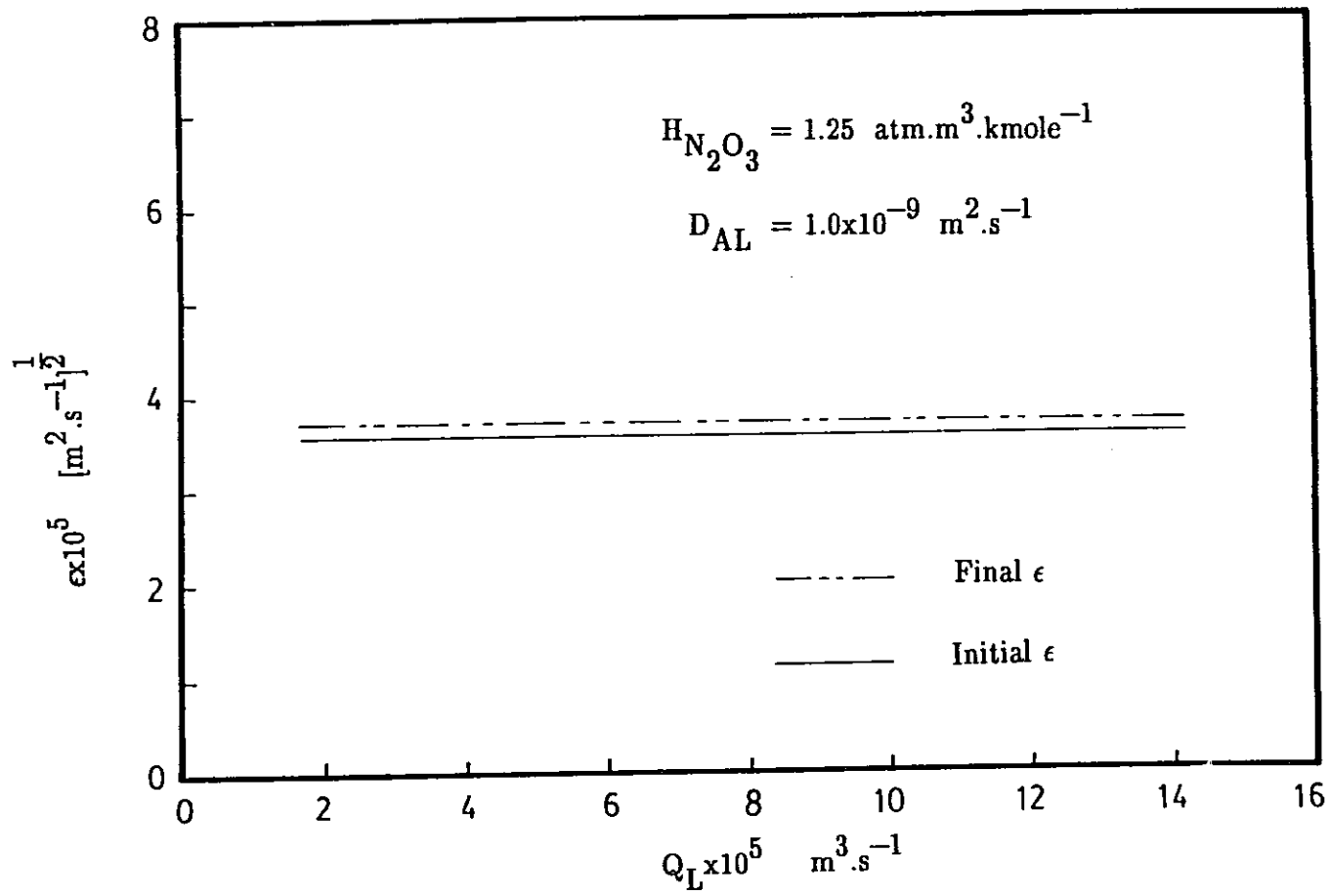

Figure 5.12 ϵ as a Function of Liquid Flow Rate – N_2O_3/H_2O System

constant irrespective of liquid flow rates for all measurements made under different flow conditions. King (1964) has argued that in any realistic mass transfer device, there will be local variations in $k'_{L,i}$ from point to point of the interface. Such behavior is predicted from both the penetration theory and by boundary–layer theory. It is evident from King's work that variations in $k'_{L,i}$ are accounted for by the stream exposure times, θ_i, only. Consequently, it is expected that ζ will be a constant for any specific gas solute. This impression is supported by the data in Figures 5.20, 5,21 and 5.22. They show that liquid flow rates have no effect on ζ values for the SO_2–H_2O system under the experimental conditions of this investigation. The data in Figures 5.10, 5.11, 5.12, 5.20, 5.21, and 5.22 emphasize that variations in hydrodynamic conditions are accounted for completely by the average residence time, $\bar{t}$. As a result the adjustable parameter, ζ, will have a constant value for each gas, as defined by Equation 5.5.

The literature review indicated that the absorption process of NO_x is very complex. Depending on the initial NO_x concentration, different reaction mechanisms and diffusing species must be considered. To establish an absorption model that will be valid for flue gas NO_x levels, reactions and diffusing species that prevail under the corresponding condition must be identified. Although the reaction mechanisms and diffusing species for high NO_x

levels are well documented and confirmed, considerable ambiguity still exists at low NO_x levels, especially when mixtures of NO and NO_2 are being absorbed.

An attempt was made to infer the most likely reactions and to identify the diffusing species through the application of the derived model. Initially, the diffusing species was assumed to be only NO. The nitrate concentrations predicted from Equation 3.13 were compared with the experimental values. The calculation was repeated for other species of NO_x (NO_2 and N_2O_3) until a reasonable agreement between experimental and predicted values was obtained.

Figures 5.13, 5.14, 5.15 and 5.16 compare predicted nitrate concentrations with experimental data when NO, NO_2 and N_2O_3 were assumed to be the major absorbing species. It is clearly demonstrated that only values predicted assuming N_2O_3 as the major transporting species agree with the experimental data for liquid rates exceeding $1x10^{-4}$ $m^3.s^{-1}$. Very poor agreement was found when NO or NO_2 were considered as the predominant absorbing species. However, examination of these graphs reveals that, even with N_2O_3 as the major diffusing species, significant disagreements between the experimental and predicted nitrate concentrations occur consistently at lower liquid rates. The positive deviations from model predictions suggest that additional reactions, other than those corresponding to the purely physical absorption assumed by the model, must occur at lower liquid rates. These

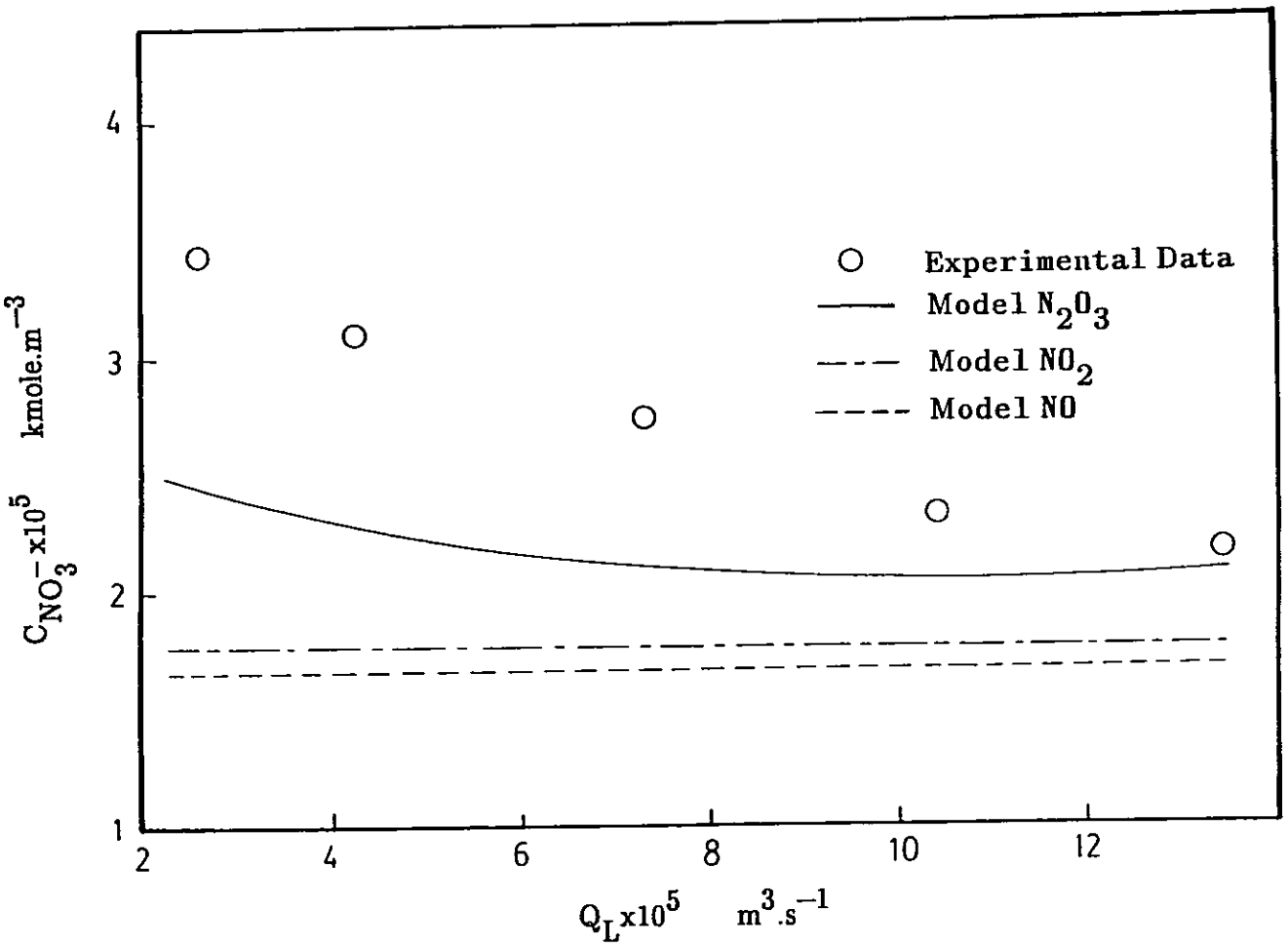

Figure 5.13 Experimental and Predicted $C_{NO_3^-}$ Values for Varying Liquid Flow Rate – NO_x/H_2O System; Y_{NO_x} = 150 ppm; $Q_G = 1.12x10^{-3}$ m^3.s^{-1}

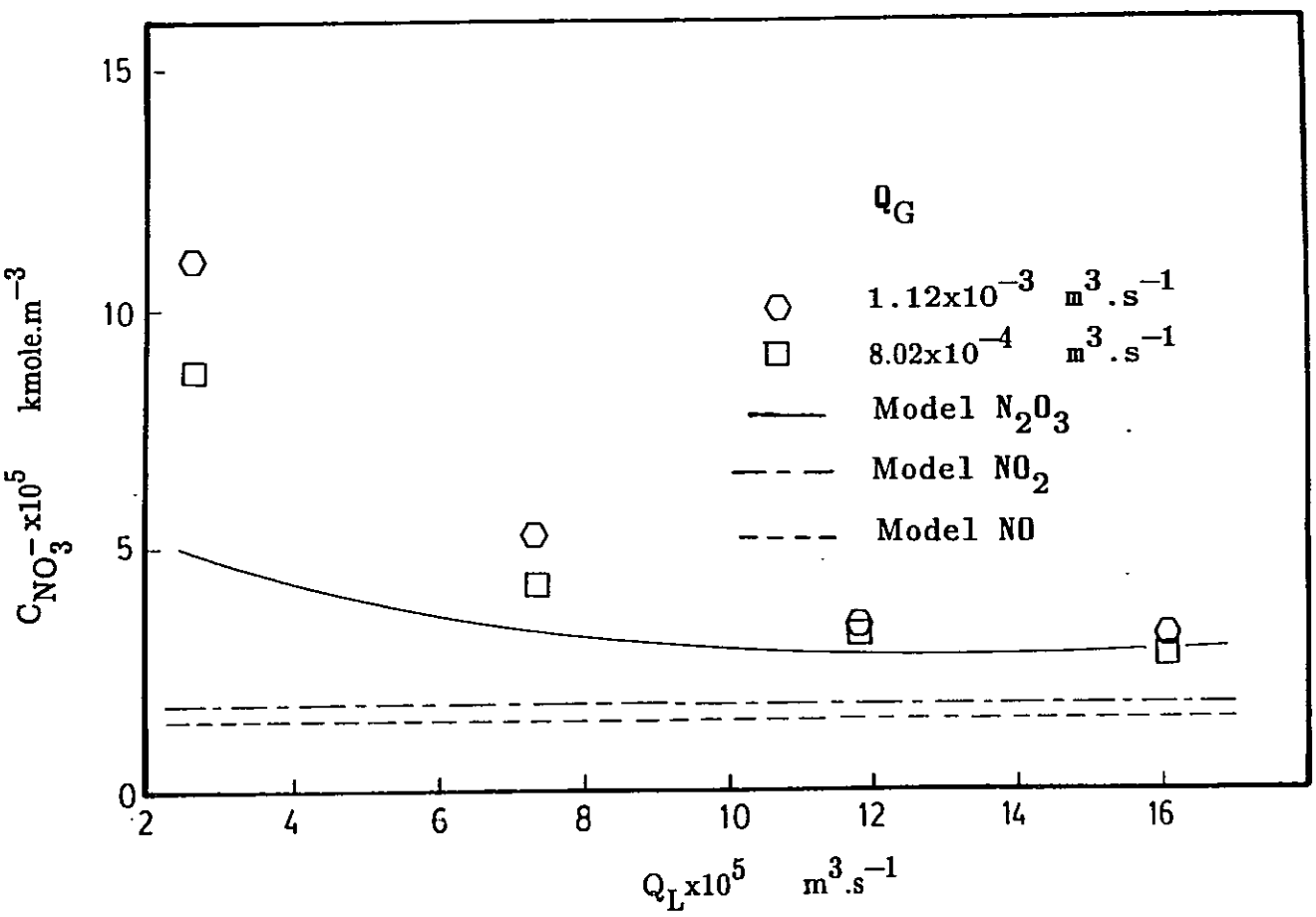

Figure 5.14 Experimental and Predicted $C_{NO_3^-}$ Values for Varying Liquid Flow Rate – NO_x/H_2O System; Y_{NO_x} = 500 ppm

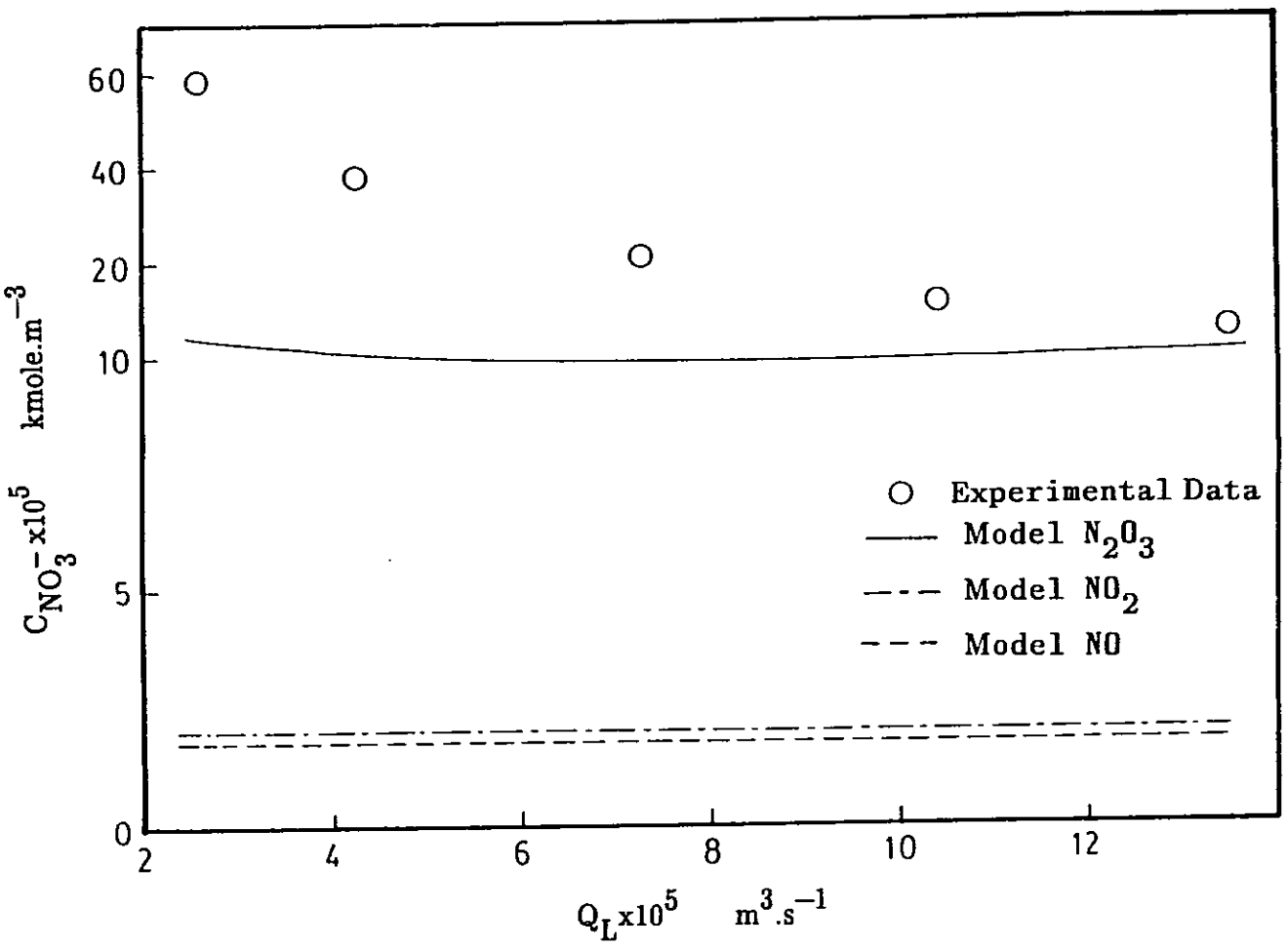

Figure 5.15 Experimental and Predicted $C_{NO_3^-}$ Values for Varying Liquid Flow Rate – NO_x/H_2O System; Y_{NO_x} = 1640 ppm; $Q_G = 1.58x10^{-3}$ m^3.s^{-1}

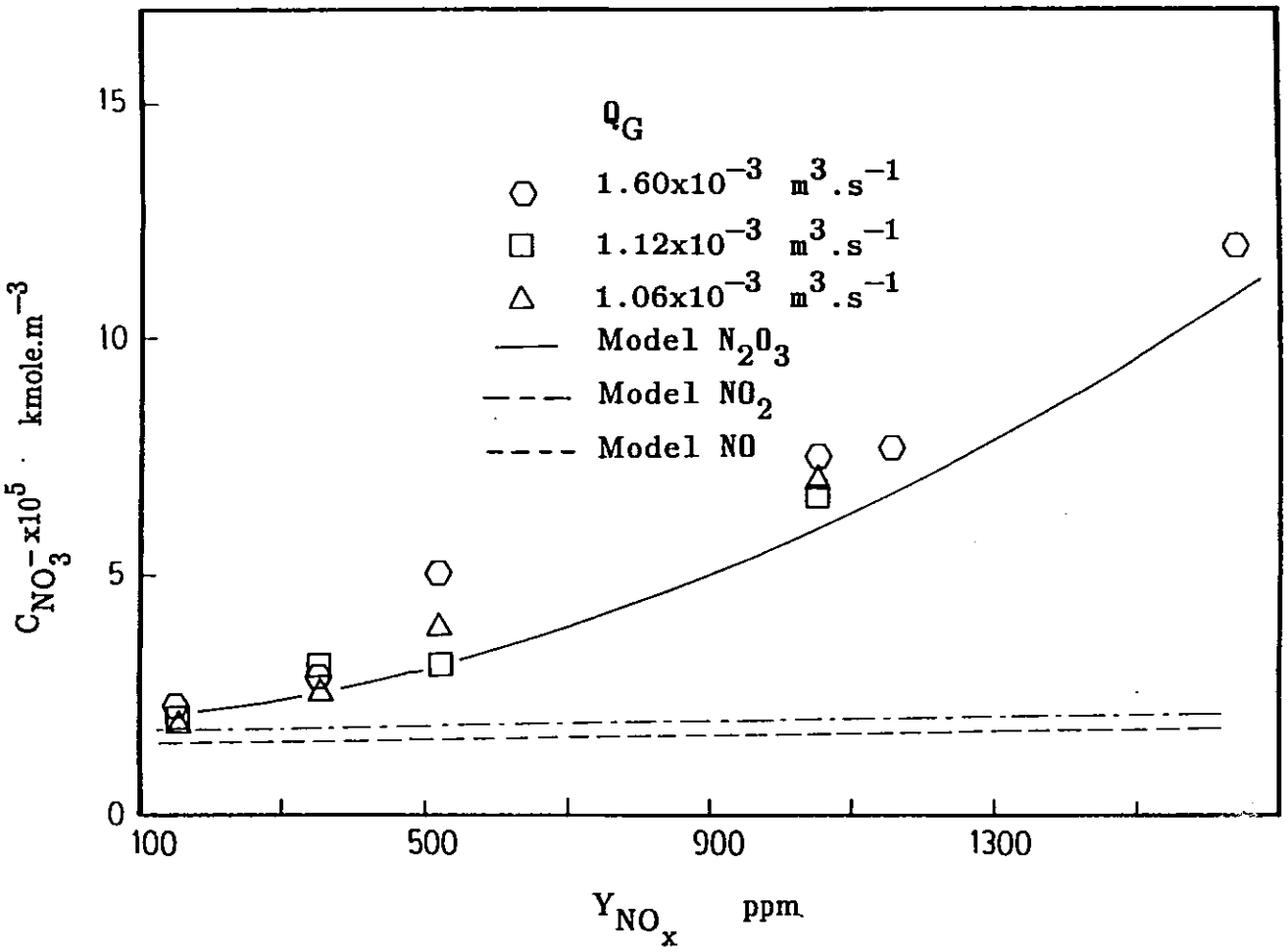

Figure 5.16 Experimental and Predicted $C_{NO_3^-}$ Values for Varying Inlet NO_x Level – NO_x/H_2O System; $Q_L = 1.35x10^{-4}$ $m^3.s^{-1}$

discrepancies might be attributed to absorbed NO_x accumulating in the scrubbing liquid in the form of nitrous and nitric acids which promote the absorption capacity of liquid water. As a result, higher nitrate concentrations will be measured at the column outlet. This interpretation was evident from an absorption study conducted by Carta and Pigford (1983), who observed that the rate of absorption of NO_x increased with increasing nitrous acid concentrations. Further evidence was provided by a recent study of Carta (1986), who employed aqueous nitric acid solution as scrubbing liquid.

Although pure NO was used in the experiments, there is no strong evidence that NO was the major species transported. According to the earlier literature (Caudle and Denbigh, 1953; Wendel and Pigford, 1958; Koval and Peter, 1960; Komiyama and Inoue, 1980), N_2O_3 appears to be the most probable transporting species under the current experimental conditions involving pure NO being released at high concentrations from a pressurized cylinder. It is suggested that the NO reacts readily with molecular oxygen in air to form NO_2 according to:

$$2NO_{(g)} + O_{2(g)} \longrightarrow 2NO_{2(g)} \qquad .....(2.19)$$

This newly oxidized $NO_{2(g)}$ reacts further with $NO_{(g)}$ to give $N_2O_{3(g)}$ according to:

$$NO_{2(g)} + NO_{(g)} \longrightarrow N_2O_{3(g)} \qquad .....(2.21)$$

Since the gas phase diffusivities of NO, NO_2 and N_2O_3 are essentially equal, all three species will diffuse to the gas–liquid interface where their fates will depend largely on their solubilities in water. Since $N_2O_{3(g)}$ is much more soluble than NO and NO_2, it readily establishes its equilibrium with liquid water and is absorbed to form nitrous acid according to:

$$N_2O_{3(g)} \rightleftharpoons N_2O_{3(l)} \qquad .....(2.45)$$

$$N_2O_{3(l)} + H_2O_{(l)} \longrightarrow 2HNO_{2(l)} \qquad .....(2.50)$$

Detection of nitrite in the liquid effluent provided support for the postulated nitrous acid formation. Although nitrite was found in the liquid effluent, no additional effort was made to quantify the amounts of nitrite and nitrate being

formed. The NO_x absorbed in the liquid effluent was determined as total nitrate. The total nitrate levels were checked closely with material balances of the solute gas. Agreement was, generally, within the range of 100 $\pm$ 15 % for all runs, except in a few cases where 25 % discrepancies were observed.

The oxidation of $NO_{(g)}$ by air according to Reaction 2.19 is a crucial step in the process of NO removal by water. However, this reaction does not occur to any great extent in a power plant boiler. The theoretical estimate of NO oxidation, based on the recommended rate constant (23.75 $atm^{-2}.s^{-1}$) (Nottingham, 1986), is about 80 per cent. This value excludes any dilution effects. However, it is a well recognized fact that when NO is present at low levels (< 1000 ppm), days are required for any significant oxidation of NO to occur under normal atmospheric conditions. Consequently, under the experimental conditions, Reaction 2.19 does not occur at a constant rate. The rate decreases quickly as dilution occurs.

The degree of NO oxidation at the column inlet was determined with a chemiluminescent analyzer. Measurements showed that about 10 per cent of the NO was oxidized when the inlet NO_x level was maintained at 500 ppm. This value was in good agreement with the observed removal efficiencies in the NO_x H_2O system, as discussed earlier. About 7 to 14% removal efficiency was obtained.

5.3 Absorption of SO_2 into Water

The absorption of SO_2 was studied for a range of liquid and gas flow rates and inlet SO_2 concentrations.

5.3.1 Removal Efficiency

Removal efficiencies, defined as the percentage of sulphur dioxide removed from the inlet gas stream, were calculated from Equation 5.3. The results of these evaluations are shown in Figures 5.17, 5.18 and 5.19 where the effects of liquid flow rate, gas flow rate and inlet SO_2 concentration are illustrated. As shown in Figure 5.17 the absorption efficiency was found to increase with increasing liquid flow rate. More than 20 per cent improvement in removal efficiency was observed when the liquid flow rate increased from $4x10^{-5}$ to $1.4x10^{-4}$ $m^3.s^{-1}$. Such an appreciable dependence on liquid flow rate was not observed with the $NO_x - H_2O$ system discussed previously.

The effect of gas flow rate on removal efficiency is illustrated in Figure 5.18. A decrease in efficiency occurs as gas flow rate is increased. A similar adverse effect of gas flow rate was observed with the $NO_x - H_2O$ system.

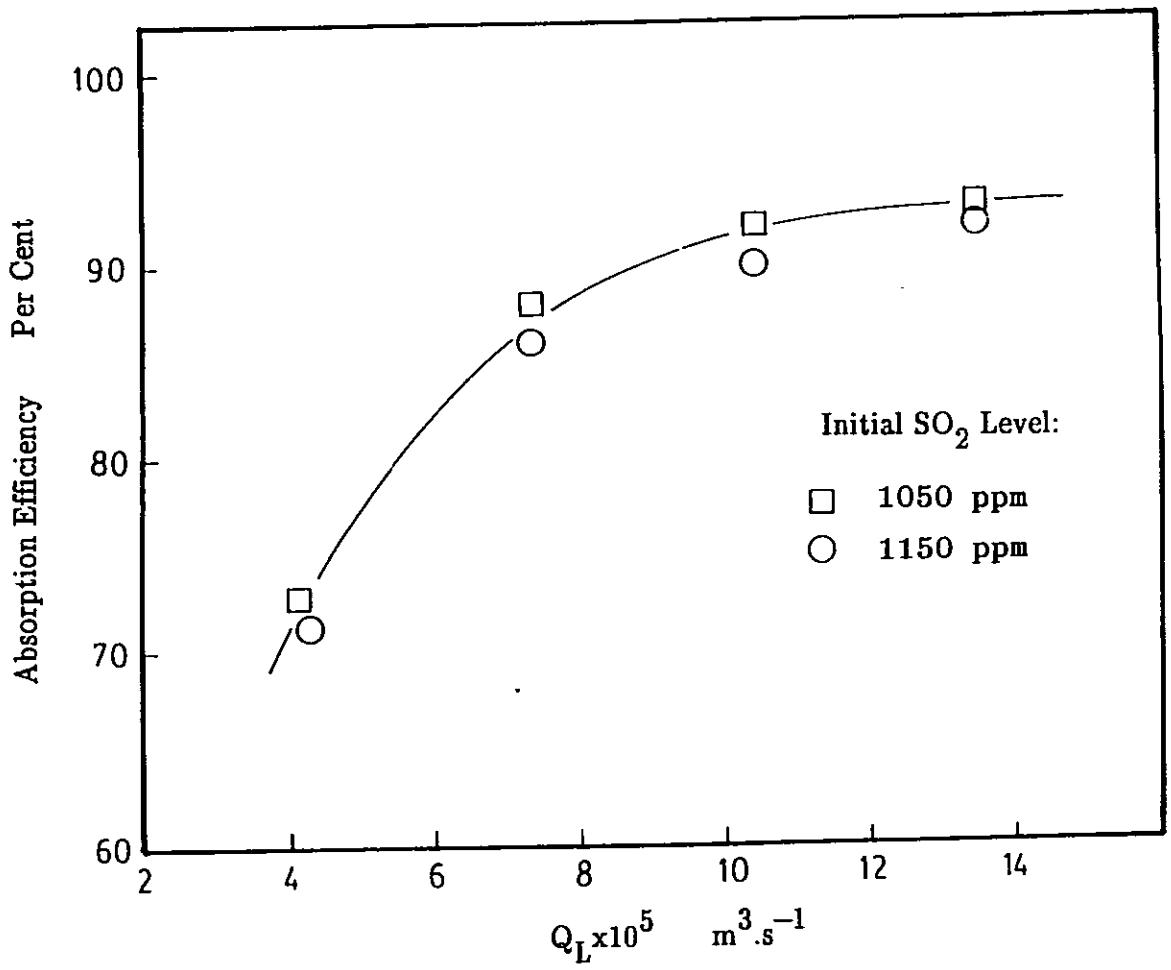

Figure 5.17 Absorption Efficiency as a Function of Liquid Flow Rate – SO_2/H_2O System; $Q_G = (1.2 \pm 0.1)x10^{-3}$ $m^3.s^{-1}$

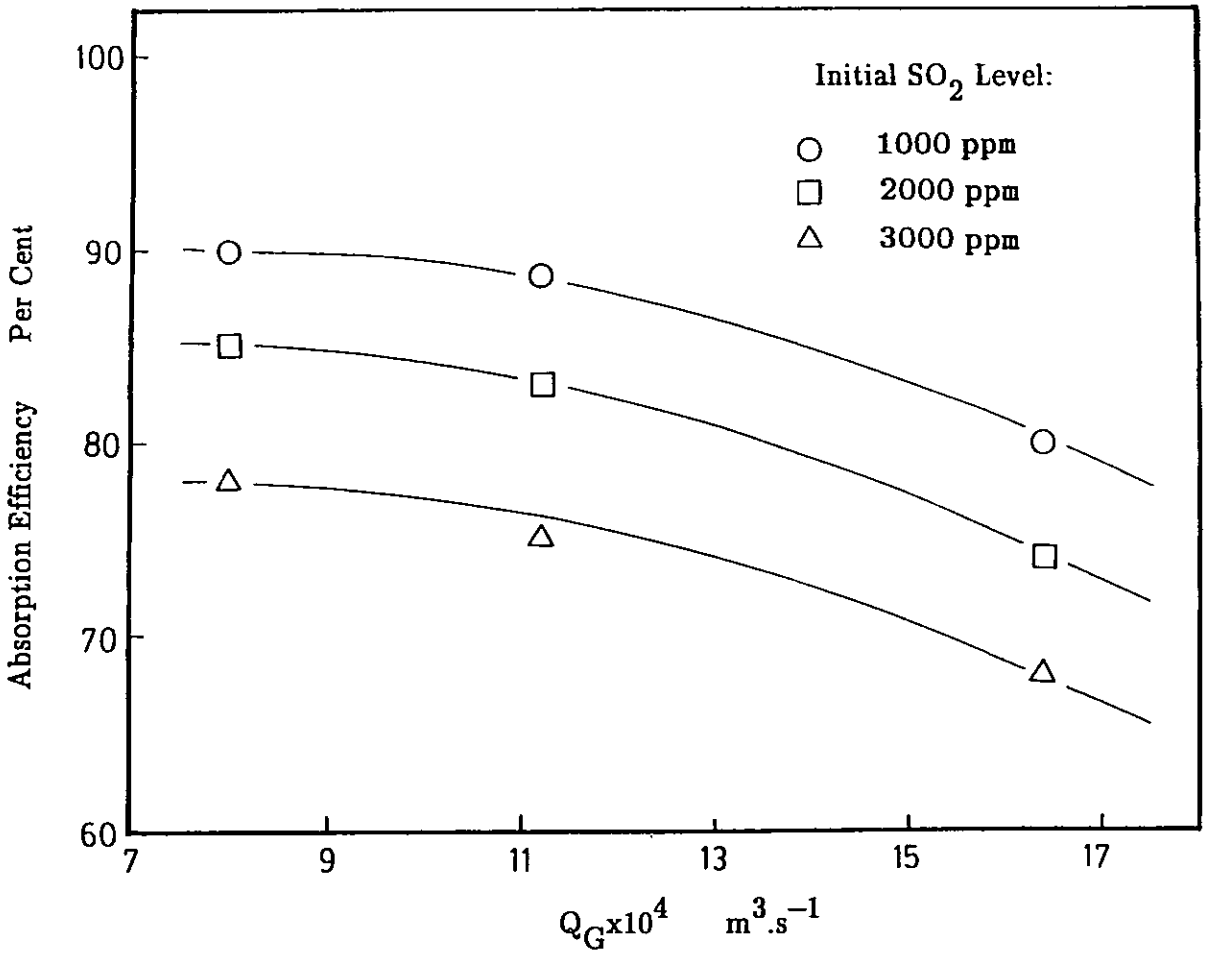

Figure 5.18 Absorption Efficiency as a Function of Gas Flow Rate – SO_2/H_2O System; $Q_L = 7.32x10^{-5}$ $m^3.s^{-1}$

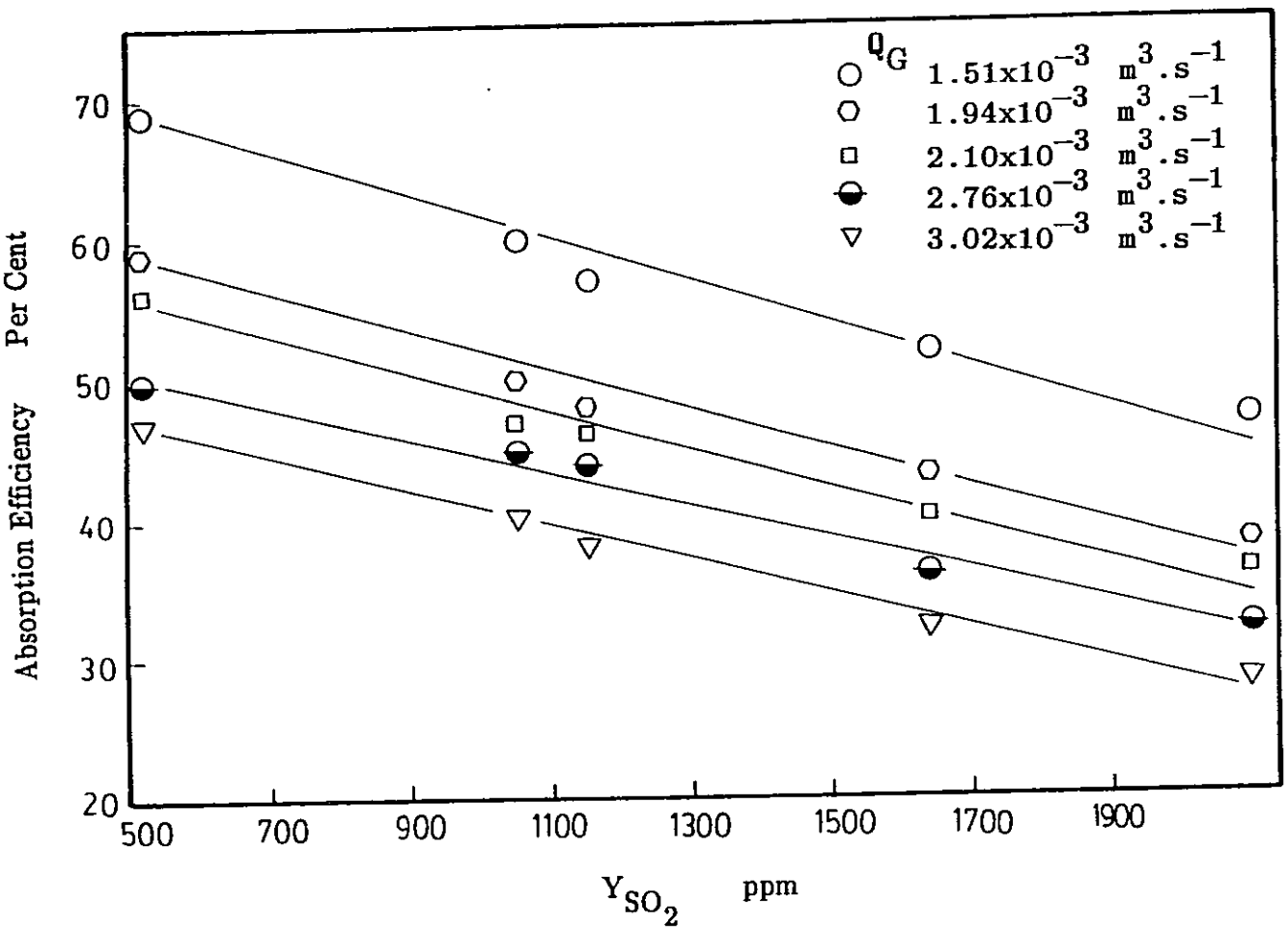

Figure 5.19 Absorption Efficiency as a Function of Inlet SO_2 Level – SO_2/H_2O System; $Q_L = 2.68x10^{-5}$ $m^3.s^{-1}$

Increasing inlet SO_2 levels decreases the efficiency of SO_2 removal. This effect, illustrated in Figures 5.18 and 5.19, conflicts with the result presented in Figures 5.8 and 5.9 which showed that the absorption efficiency increased slightly with increasing NO_x inlet levels. This difference can be explained by the fact that in the SO_2– H_2O system, the liquid absorbent is most likely near the point of saturation for the fairly soluble SO_2. Therefore, any additional SO_2 input will remain unabsorbed and pass through the scrubber. Rochelle and King (1977) observed a similar trend in their study. In the case of the NO_x– H_2O system, higher removal efficiencies with higher inlet NO_x levels perhaps result from more NO being oxidized during the dilution stage prior to the inlet of the column.

5.3.2 Comparison of Experimental Data with Model Prediction

A number of studies (Eriksen, 1969; Hikita et al., 1978; Roberts, 1980; Kaji et al., 1985), indicated that SO_2 undergoes significant hydrolysis when dissolved in water at low concentrations. The hydrolysis reaction increases greatly the capacity of water for SO_2 removal. More sophisticated studies (Hikita et al., 1978; Kaji et al., 1985) on SO_2 absorption into water regarded the SO_2 hydrolysis as an instantaneous, reversible, reaction as represented by

Equation 2.5. On this basis, SO_2 absorption into water is not a true physical process. Any model derived on the basis of strict physical absorption will underestimate the SO_2 removal.

This inference is confirmed in Figures 5.23 and 5.24, where the predicted SO_2 concentrations assuming no hydrolysis (represented by the dashed curves) are compared with those obtained experimentally. The model results agree qualitatively, but significant differences occur at higher liquid flow rates where the hydrolysis is extensive. Further evidence for the importance of hydrolysis is provided in Figures 5.25 and 5.26. In these diagrams, the predicted SO_2 concentrations are consistently below the experimental values when no corrections for hydrolysis are made.

Whitney and Vivian (1949) suggested that the absorption of SO_2 into water behaved like a purely physical absorption process with an effective Henry's law constant equal to 0.582 $atm.m^3.kmole^{-1}$. The same approach was taken by Goettler (1967) to explain the differences that he observed in his study.

Using the Whitney and Vivian (1949) and Goettler (1967) studies as a basis, the absorbed SO_2 concentrations were re–calculated from model Equation 3.13 with an effective Henry's law constant value of 0.582 $atm.m^3.kmole^{-1}$ as given by Whitney and Vivian (1949). Better agreement was obtained from these

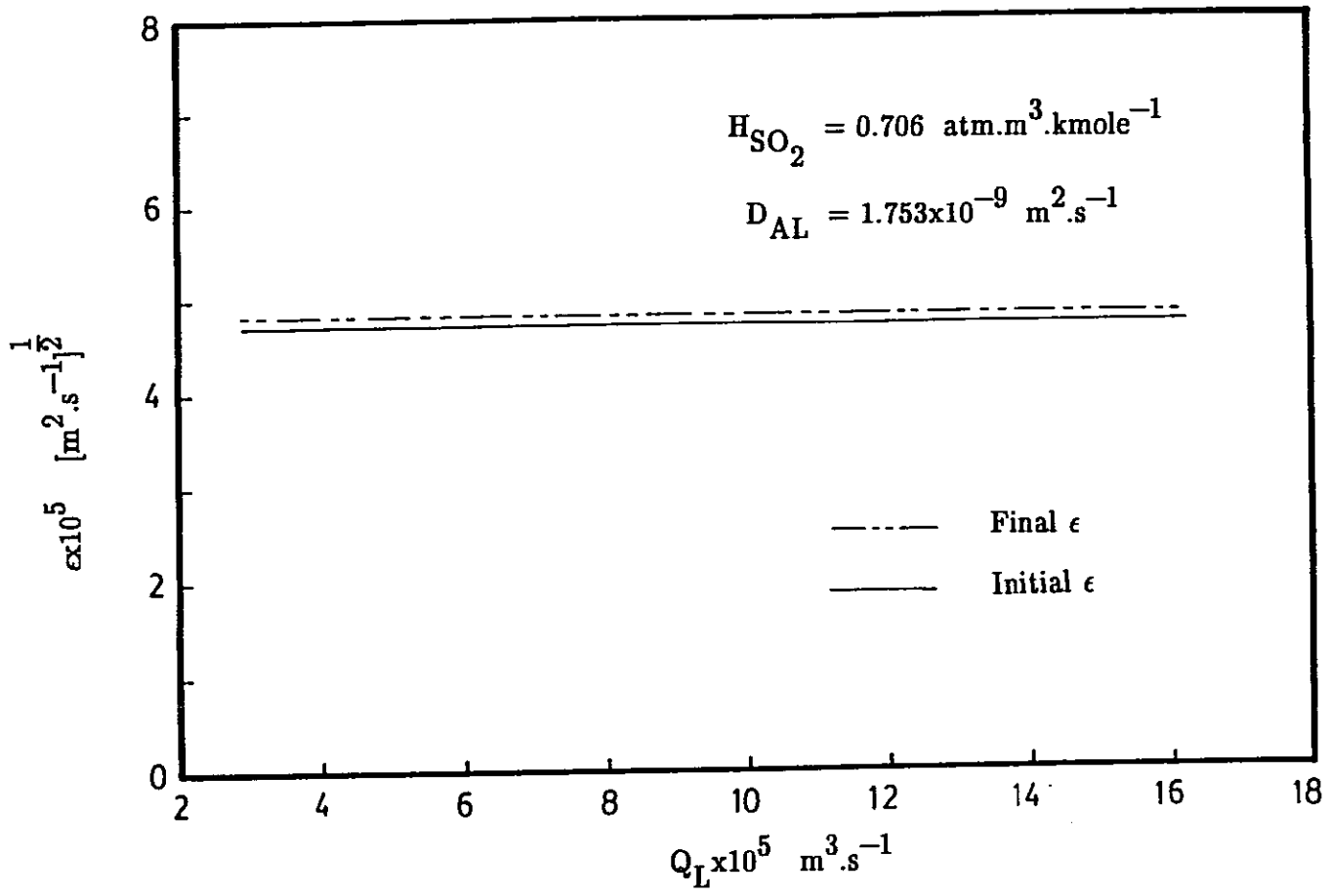

Figure 5.20 ϵ as a Function of Liquid Flow Rate – SO_2/H_2O System; Without Hydrolysis

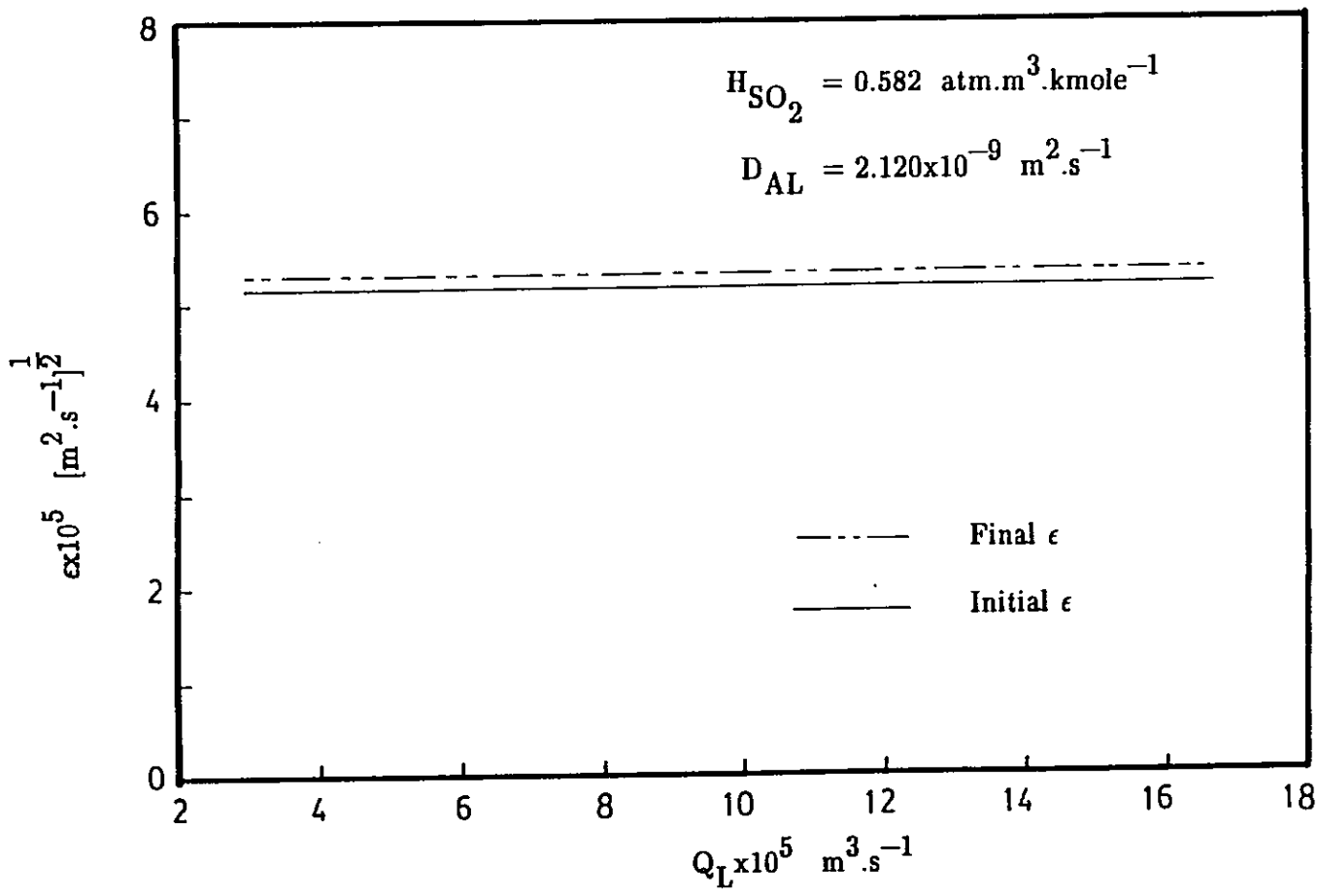

Figure 5.21 ϵ as a Function of Liquid Flow Rate – SO_2/H_2O System; With Hydrolysis

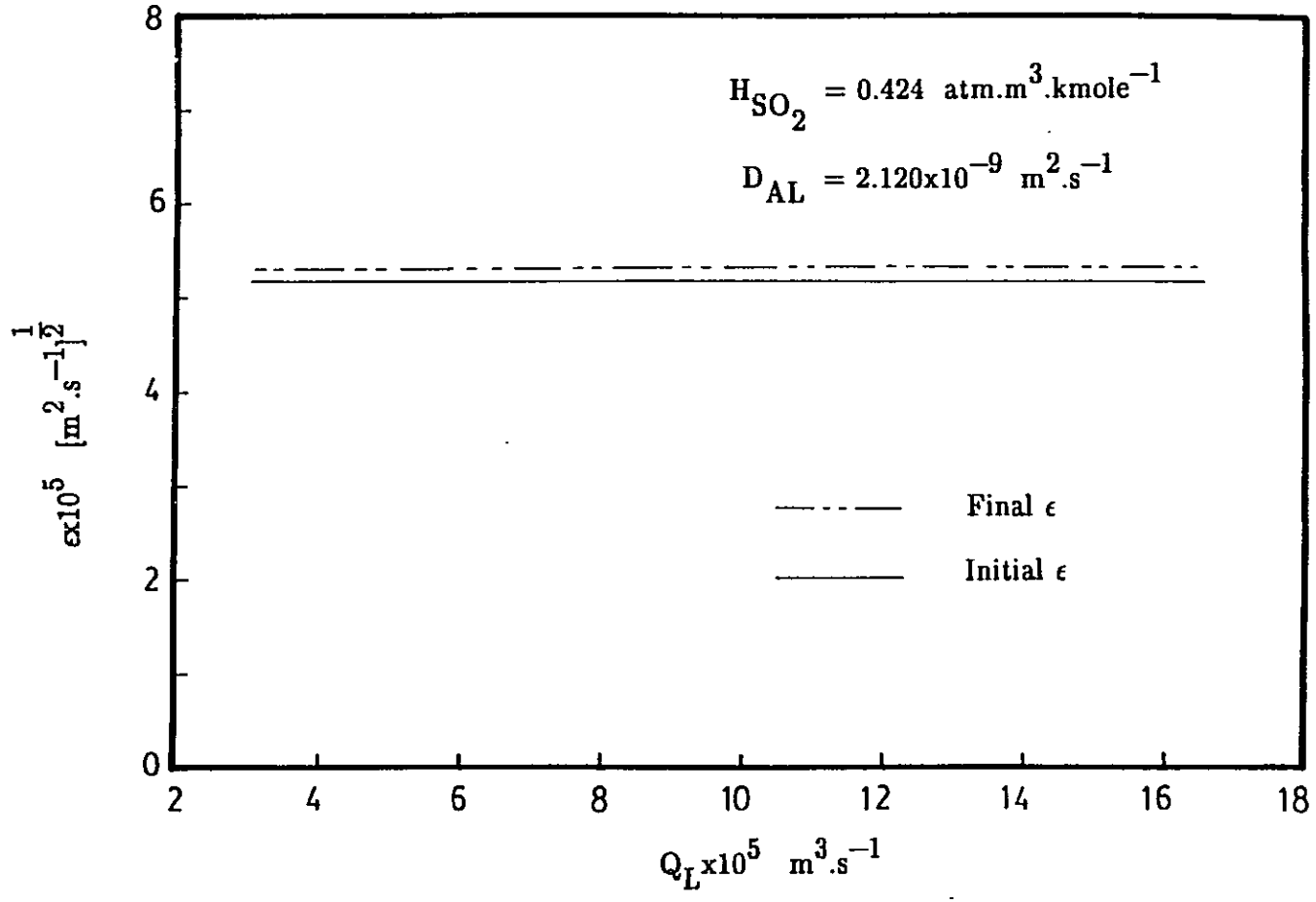

Figure 5.22 ε as a Function of Liquid Flow Rate – SO_2/H_2O System; With Hydrolysis

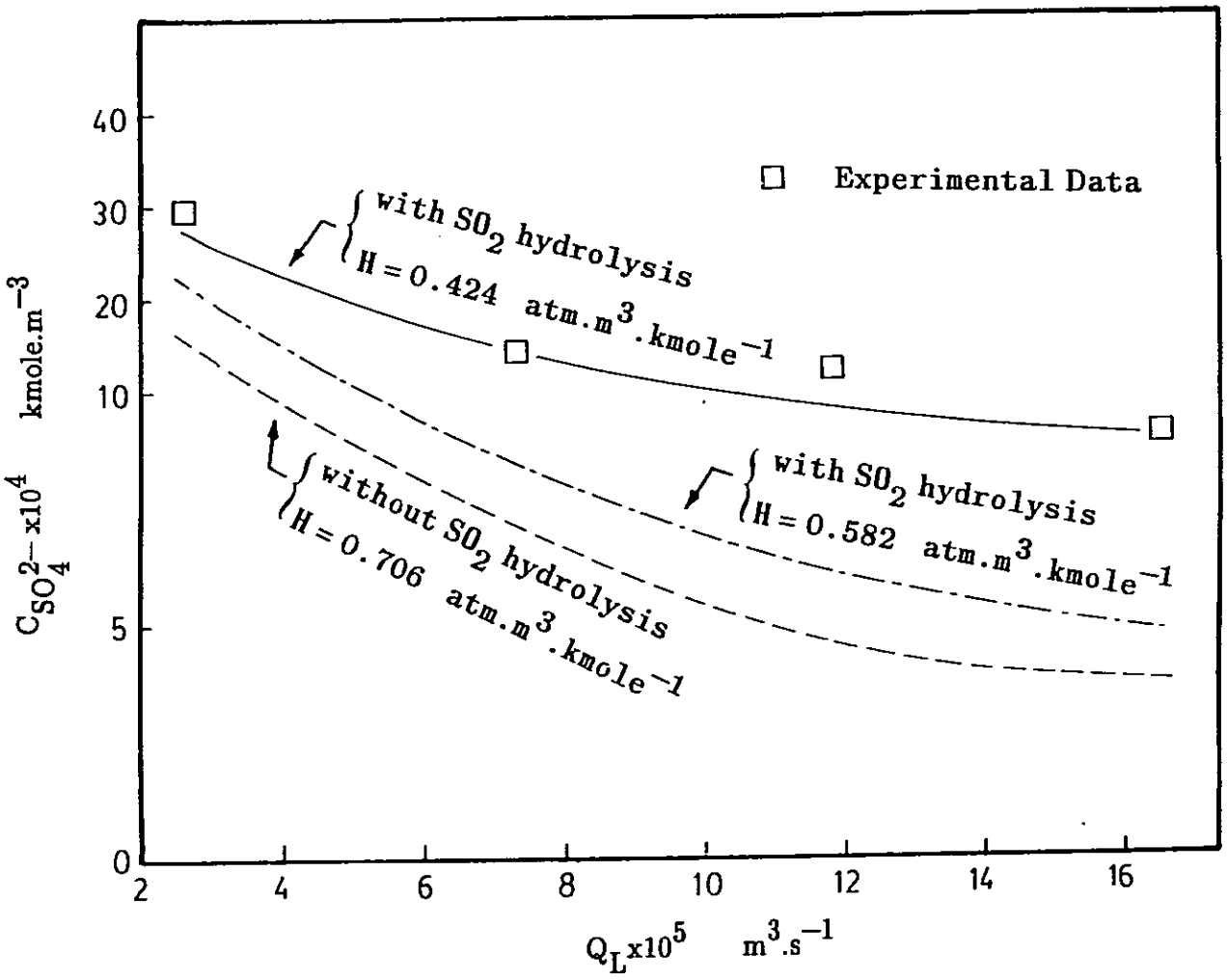

Figure 5.23 Experimental and Predicted $C_{SO_4^{2-}}$ Values for Varying Liquid Flow Rate – SO_2/H_2O System; $Q_G = 1.64 \times 10^{-3}$ m^3.s^{-1}; $Y_{SO_2} = 2000$ ppm

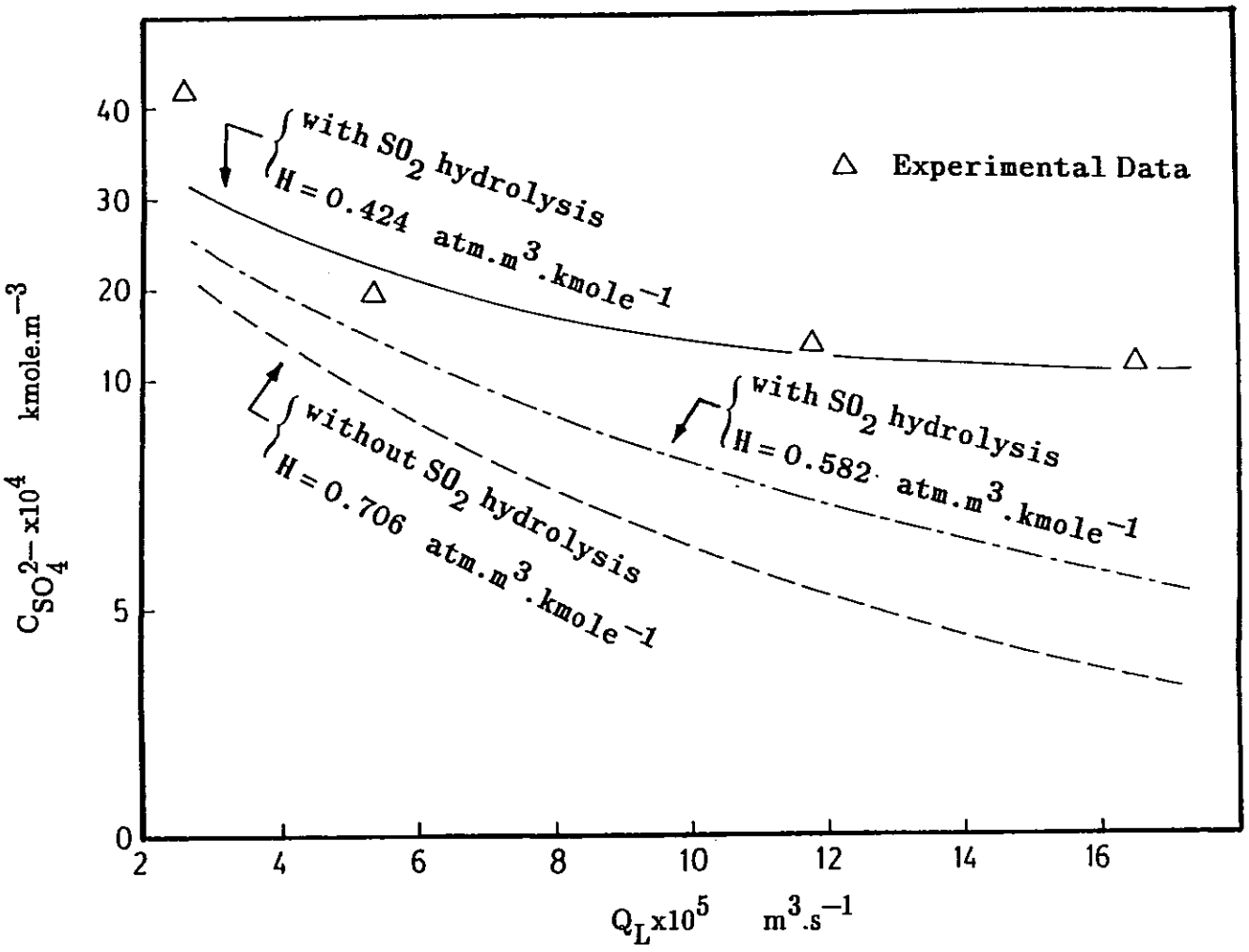

Figure 5.24 Experimental and Predicted $C_{SO_4^{2-}}$ Values for Varying Liquid Flow Rate – SO_2/H_2O System; $Q_G = 1.64 \times 10^{-3}$ m^3.s^{-1}; Y_{SO_2} = 3000 ppm

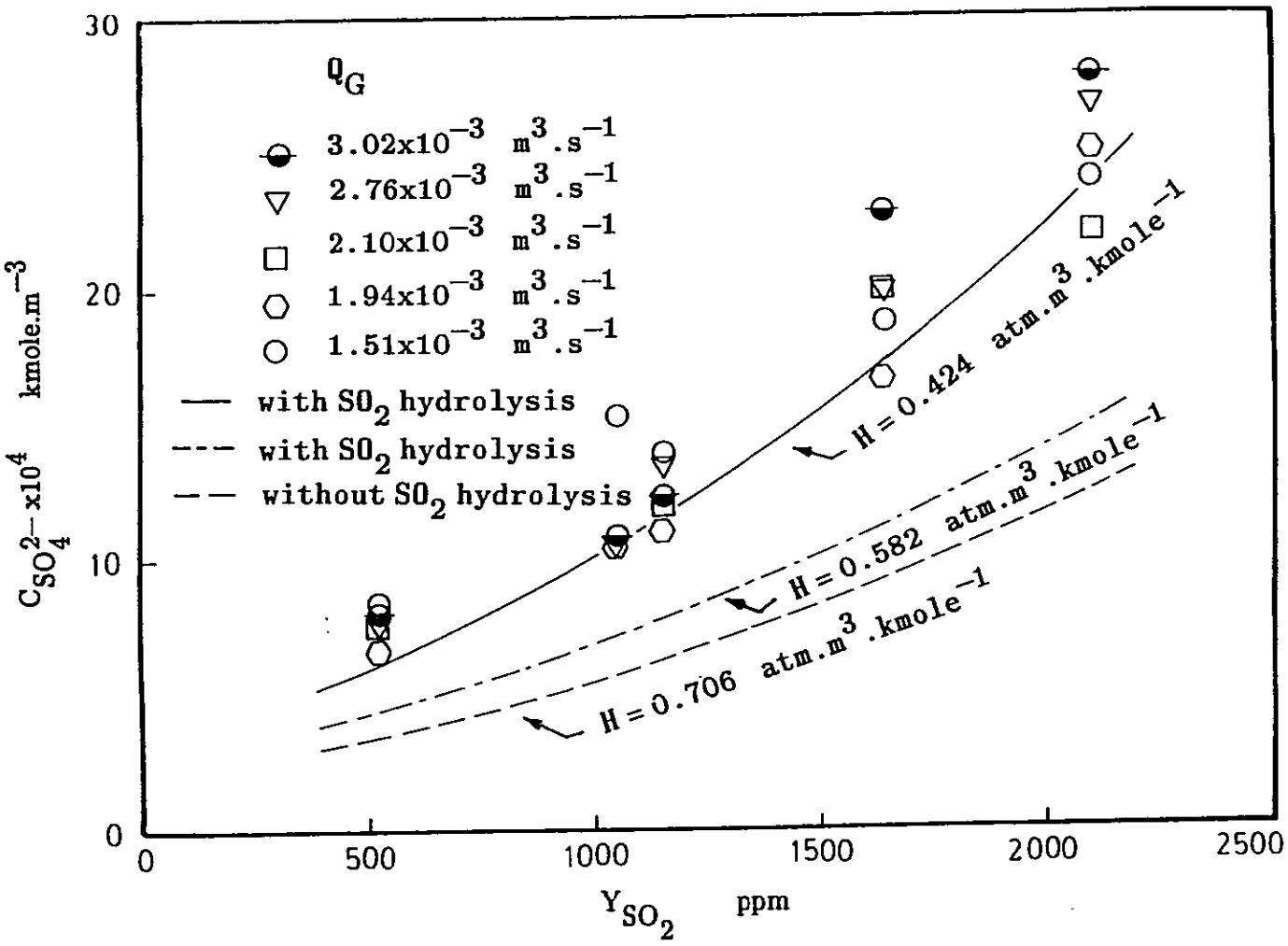

Figure 5.25 Experimental and Predicted $C_{SO_4^{2-}}$ Values for Varying Inlet SO_2 Level – SO_2/H_2O System; $Q_L = 2.60 \times 10^{-5}$ m^3.s^{-1}

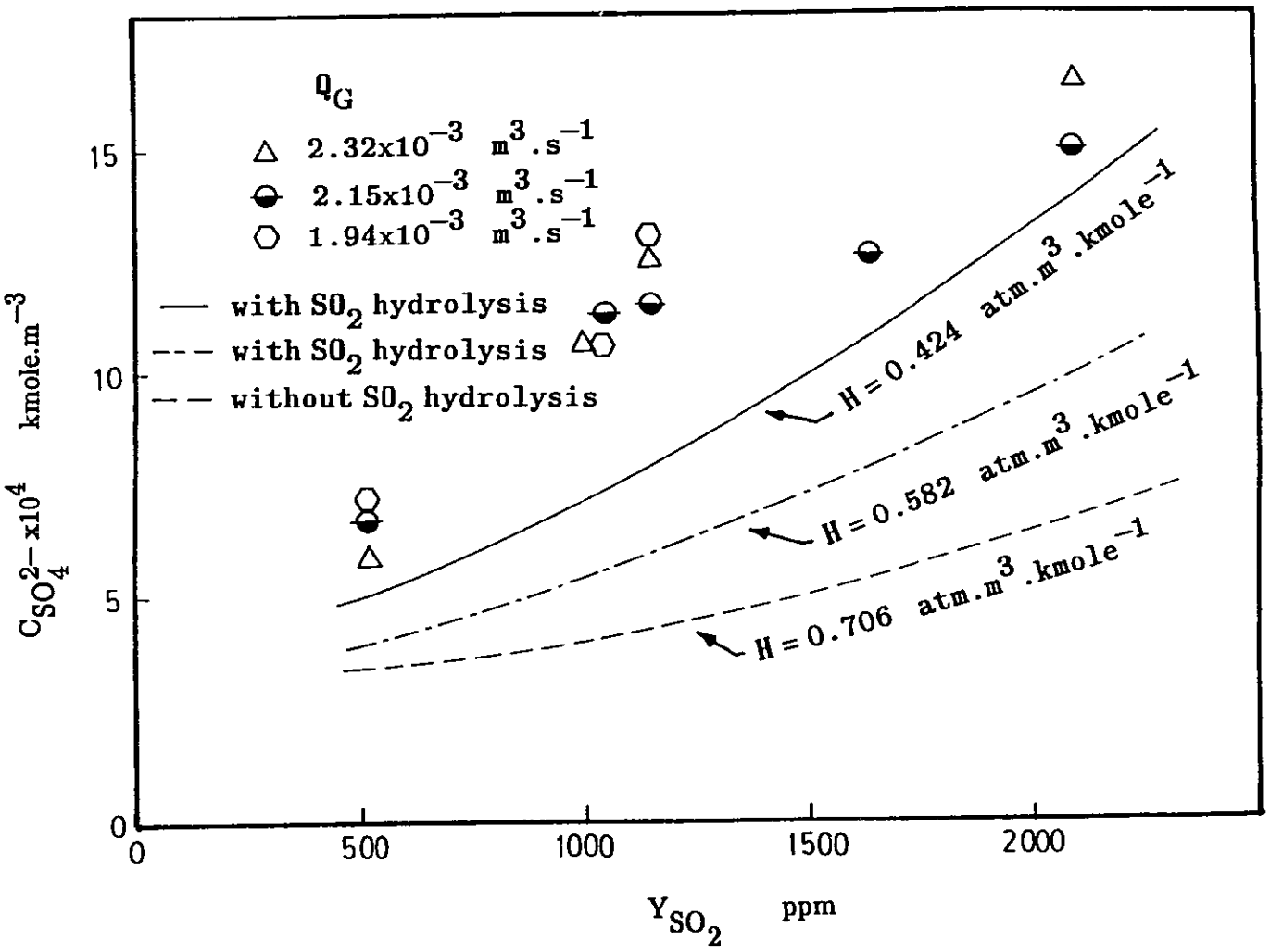

Figure 5.26 Experimental and Predicted $C_{SO_4^{2-}}$ Values for Varying Inlet SO_2 Level – SO_2/H_2O System; $Q_L = 1.34x10^{-4}$ $m^3.s^{-1}$

calculations. However, the predicted SO_2 concentrations again were still consistently lower than the measured values as shown in Figures 5.23 and 5.24. The discrepancies are most likely due to the degree of hydrolysis of the absorbed SO_2. To confirm this speculation, calculations were repeated with different assumed effective Henry's law constant values until reasonable agreement was obtained with the experimental results. When these predicted results are plotted in Figures 5.23 through 5.26 as indicated by the solid curves, there is close agreement with the observed data for an effective Henry's law constant equal to 0.424 $atm.m^3.kmole^{-1}$. This effective Henry's law constant is about 25 % lower than the value reported by Whitney and Vivian (1949).

As indicated by Goettler (1967), the effective Henry's law constant varies considerably with absorbed SO_2. It decreases as hydrolysis increases for lower SO_2 concentrations. Whitney and Vivian (1949) employed rather high SO_2 input levels, varying between 0.1 and 0.175 atmospheres; (corresponding to $1x10^5$ ppm and $1.75x10^5$ ppm respectively). Their gas phase concentrations were about 2 orders of magnitude higher than those in the present study using typical flue gas concentrations of 1000 ppm to 3000 ppm. Therefore, lower degrees of hydrolysis would be expected in the Whitney and Vivian study (1949) with correspondingly higher effective Henry's law constants than in the present study.

The effective liquid phase diffusivity of SO_2 tends to increase the predicted SO_2 concentrations by less than 2 per cent. Therefore, its effect on SO_2 absorption at flue gas SO_2 levels can be safely neglected. The diffusivity of molecular SO_2 can be used without introducing much error.

There are numerous ways to oxidize SO_2 in the gas phase under atmospheric condition. The gas phase oxidation of SO_2 depends solely on the availability of oxygen atoms and molecules. The sources of oxygen atoms are varied. For example, photo–decomposition of ozone through sunlight absorption in the short wave length region of the spectrum is one possibility. Since this possibility was not likely provided in the present study, oxidation of SO_2 by this reaction path was unimportant. Although oxidation of SO_2 by molecular oxygen is thermodynamically favorable at normal room conditions, the oxidation reaction is kinetically controlled under catalyst–free conditions. The gas phase reaction is so slow that it can be safely ignored. Therefore, it was assumed, that although pure SO_2 was used in the study, no oxidation occurred prior to the inlet of the absorption column. Only dilution with air occurred.

5.4 Absorption of NO_x into Alkaline Aqueous Sodium Chlorite Solution

Absorption of NO_x into alkaline aqueous sodium chlorite solutions was

studied experimentally over a concentration range of 0.05 to 0.67 M $NaClO_2$. The results are discussed in terms of the dependence of NO_x removal efficiency on nitrite concentration. The effects of liquid and gas flow rates and inlet NO_x concentrations on absorption efficiency were determined and are discussed as well.

5.4.1 Removal Efficiency

The definition provided by Equation 5.3 was used to determine the absorption efficiency of NO_x into alkaline sodium chlorite solutions. Calculations were made from the differences between inlet and outlet gas phase compositions recorded by the analyzer.

The influences of liquid and gas flow rates, inlet NO_x and aqueous chlorite concentrations on NO_x removal are illustrated in Figures 5.27 through 5.29.

Figure 5.27 shows how the absorption efficiency varied with liquid flow rate. It is obvious that no appreciable change in removal efficiency occurred as the liquid flow rate increased for constant inlet NO_x and aqueous chlorite concentrations. These data indicate that liquid flow rate had only a minor effect

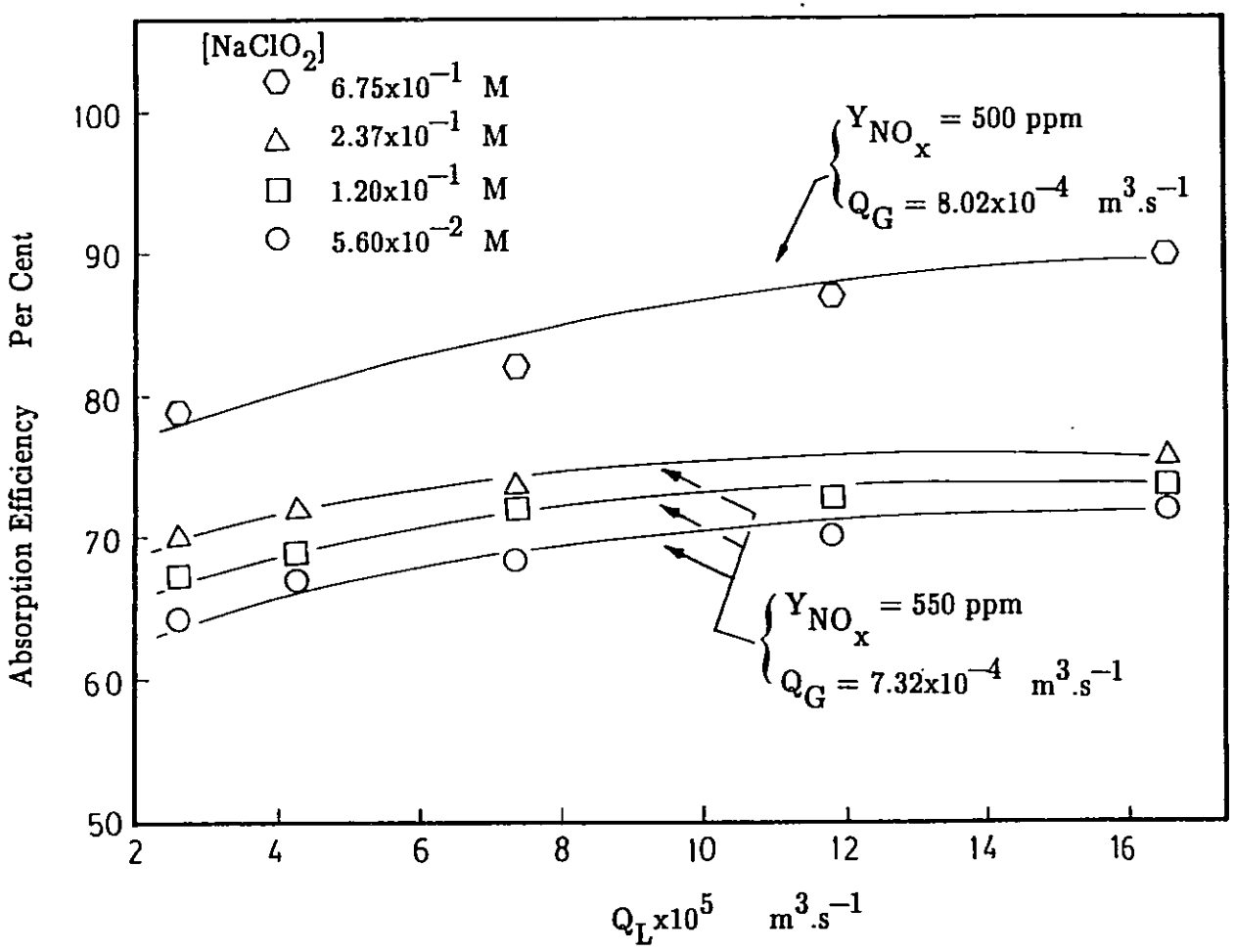

Figure 5.27 Absorption Efficiency as a Function of Liquid Flow Rate – $NO_x/NaClO_2$ System

on NO_x absorption. However, it appears that the absorption efficiency is improved slightly with increasing chlorite concentrations. According to the data in Figure 5.28, where the NO_x removal efficiency is plotted against the gas flow rate for several chlorite concentrations, there was a trend toward lower absorption with increasing gas flow rate. The same trend was observed previously for NO_x scrubbing with pure H_2O.

An examination of Figure 5.29 shows that a significant increase in NO_x absorption efficiency was achieved when NO_x inlet levels increased from 200 ppm to 500 ppm. However, improvement leveled off beyond 600 ppm. A possible explanation for the behaviour of this system can be related to the absorption control mechanism. As NO_x diffuses through the gas–liquid interface, it reacts instantaneously with chlorite ion, thus shifting the control mechanism to gas phase diffussion. Initially, the gas phase NO_x diffusion across the gas film is increased as the NO_x concentration in the bulk gas increases. However, this increase in diffusion, resulting from the concentration gradient, soon becomes gas film controlled. As a result the amount of NO_x passing through the gas film is limited.

The instantaneous reaction between absorbed NO_x and chlorite was evident from the work of Sada et al. (1978,1979), who studied the absorption of NO into alkaline sodium chlorite solutions and believed that the absorption was gas film controlled. A similar conclusion was also reached by Aoki et al. (1982),

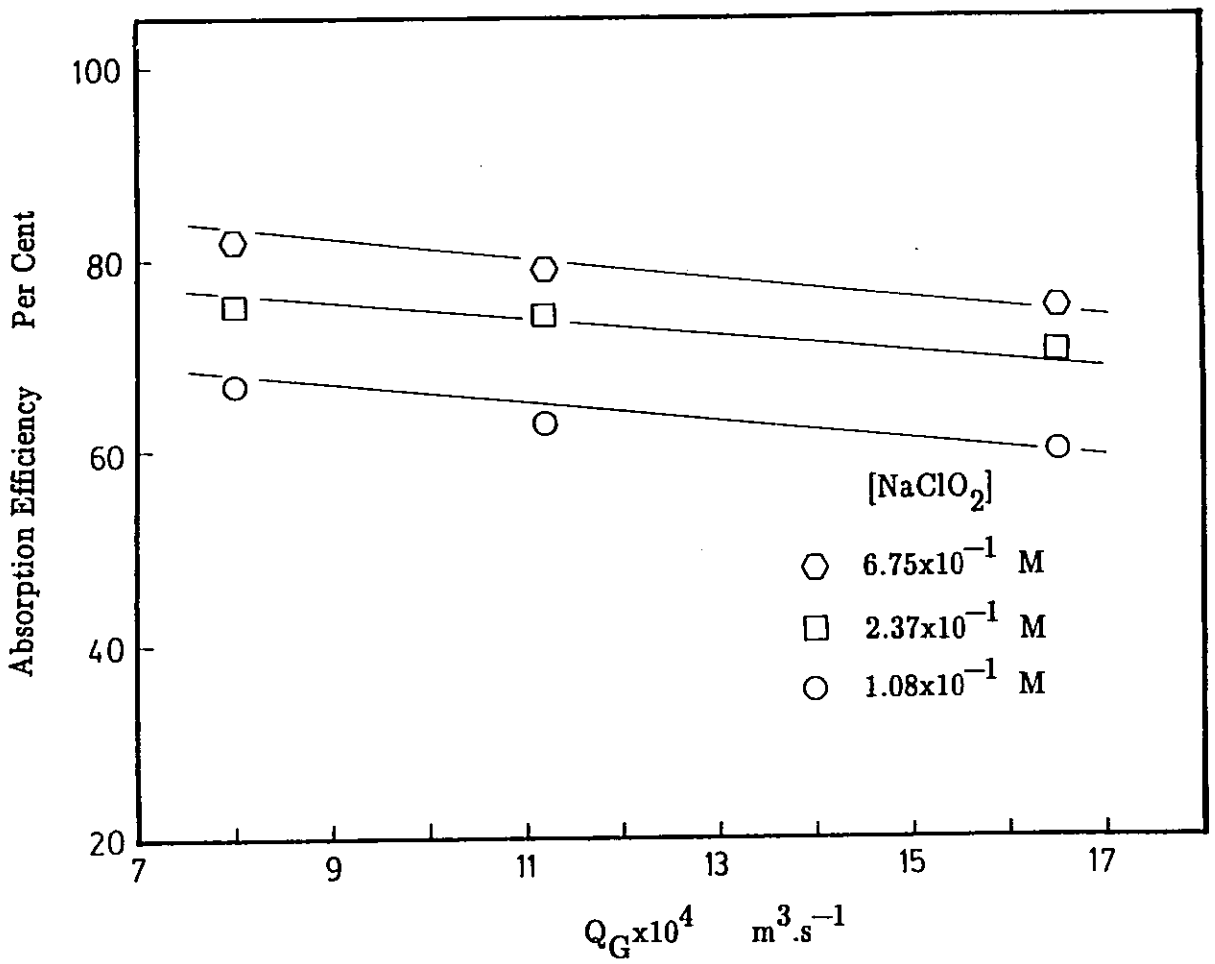

Figure 5.28 Absorption Efficiency as a Function of Gas Flow Rate – $NO_x/NaClO_2$ System;

$Q_L = 7.32x10^{-5}$ $m^3.s^{-1}$; $Y_{NO_x} = 500$ ppm

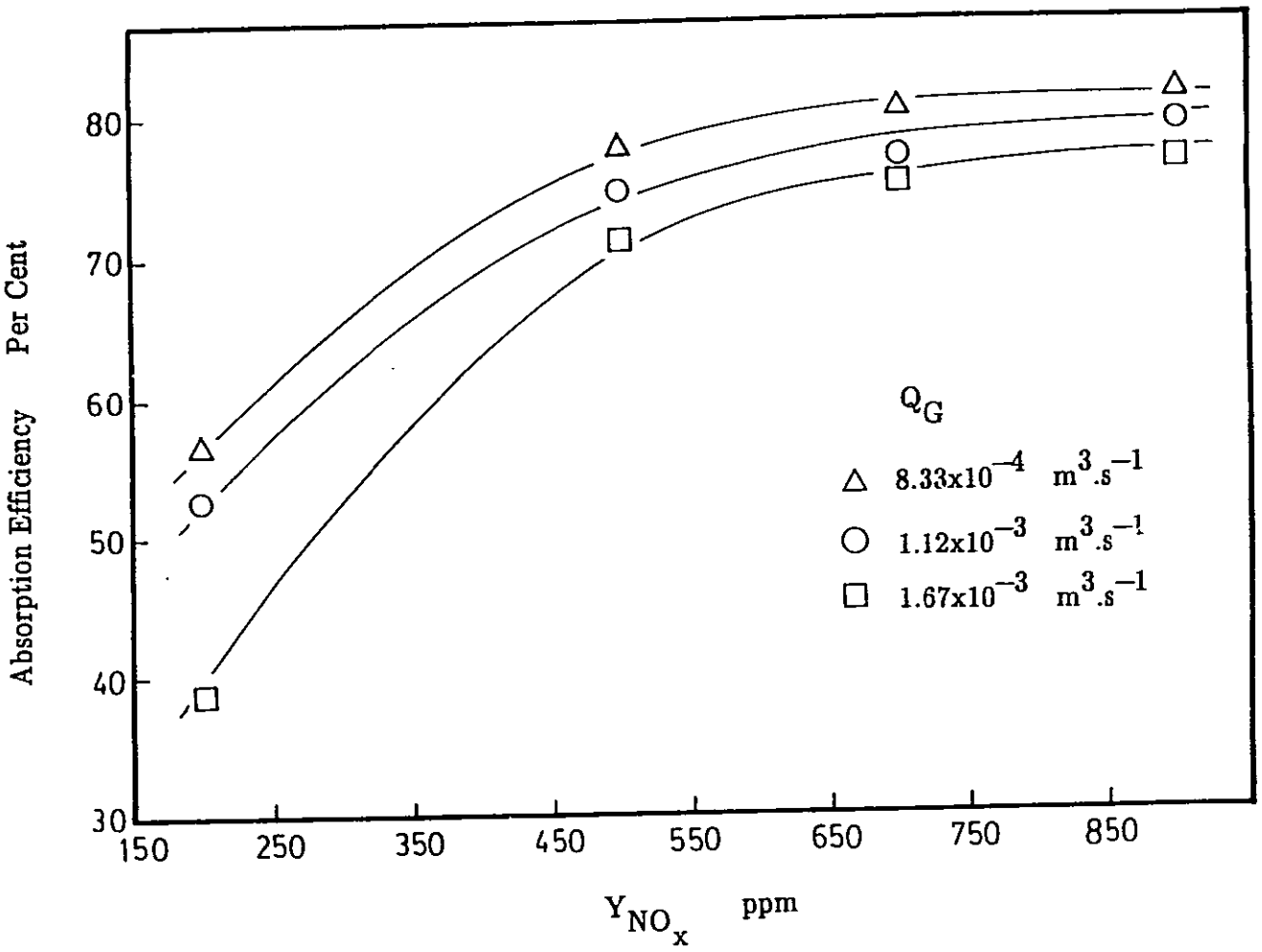

Figure 5.29 Absorption Efficiency as a Function of Inlet NO_x Level – $NO_x/NaClO_2$ System; $Q_L = 7.32x10^{-5}$ $m^3.s^{-1}$; $[NaClO_2] = 0.24$ M

who indicated that the controlling step was the diffusion of NO_x across the gas film.

A comparison between the NO_x removal efficiencies for the NO_x– H_2O and NO_x– $NaClO_2$ systems suggests that a significant portion of NO must be absorbed along with N_2O_3. The N_2O_3 is believed to be the major transporting species when water is the scrubbing liquid. As discussed earlier, about 14 per cent of the NO_x removed from the gas stream was in the form of N_2O_3 when scrubbed with water. However, more than 70 per cent absorption was achieved when $NaClO_2$ concentrations varied between 0.05 and 0.67 M. Therefore, the conclusion that can be drawn from these results is that a significant portion of the NO must be absorbed and become dominant in the alkaline sodium chlorite absorption process. A model based on NO as the predominant diffusing species was derived earlier and was used in the present section to interpret the results obtained.

5.4.2 Comparison of Experimental Data with Model Prediction

According to Sada et al. (1978), the absorption of NO by alkaline sodium chlorite solutions falls in the fast reaction regime. The rate of absorption is

given by:

$$N_{NO} = \sqrt{\left(\frac{2}{m+1}\right) k C_B^n C_{NO,i}^{m+1} D_{NO,L}} \qquad \text{.....(5.6)}$$

where

N_{NO} = absorption rate of NO, kmole.s^{-1}.m^{-2}

m = order of reaction relative to NO, dimensionless

k = rate constant of (m,n) order reaction, $(m^3.kmole^{-1})^{m+n-1}$ .s^{-1}

n = order of reaction relative to liquid phase reactant ($NaClO_2$), dimensionless

$D_{NO,L}$ = liquid phase diffusivity of NO in a mixed salt solution, $m^2.s^{-1}$

$C_{NO,i}$ = concentration of NO at gas–liquid interface, kmole.m^{-3}

C_B = chlorite concentration, kmole.m^{-3}

This expression is valid for sodium chlorite concentrations greater than 0.8 M. The values of m and n were reported by Sada et al. (1978) to equal 2 and 1 respectively. On the basis of Equation 5.6, the flow model derived in Chapter 3 is applicable to higher scrubbing chlorite concentrations (> 0.8 M).

For lower chlorite concentrations (< 0.8 M), Sada et al. (1978) indicated that the absorption reaction is dominated by hydrolysis rather than oxidation. These authors also determined that the order of reaction relative to NO, (m), tends to decrease while the order of reaction relative to chlorite, (n), remains constant at 1. Their results, at lower chlorite concentrations were interpreted by the film theory under the fast reaction regime according to:

$$N_{NO} = \sqrt{\frac{2}{(m+1)} (k_{hyd} + kC_B) C_{NO,i}^{m+1} D_{NO,L}} \qquad .....(5.7)$$

where

k_{hyd} = rate constant for hydrolysis,
for second order reaction,

$k_{hyd} = 3.09 \times 10^8 \ (m^3.kmole^{-1}).s^{-1}$

k = third order rate–constant for reaction of NO, $(m^3.kmole^{-1})^2.s^{-1}$

Since the current experiments were conducted at chlorite concentrations below 0.8 M, a flow model valid for low chlorite concentrations was derived on the basis of Equation 5.7. This modified version, for lower chlorite concentrations takes the form:

$$\bar{C}_{B,j} = \frac{1}{k}\left[\sqrt{(k_{hyd} + kC_{B,j-1})} - \frac{k\bar{a}_L \bar{t} F_B \sqrt{\frac{2}{m+1} C_{NO,i}^{m+1} D_{NO,L}}}{2F_{NO}}\right]^2 - \frac{k_{hyd}}{k} \qquad .....(5.8)$$

where

$\bar{C}_{B,j}$ = mean chlorite concentration at stage j, $kmole.m^{-3}$

F_B = stoichiometric coefficient of chlorite, dimensionless

F_{NO} = stoichiometric coefficient of NO, dimensionless

Calculations were performed with k equal to 2.45×10^{12} $(m^3.kmole^{-1})^2.s^{-1}$ and m, as the variation parameter, assumed an initial value of 2 (Sada et al., 1978, 1979). A total of 13 stages were required for the calculation to terminate. The final value of m was expected to be within the range of 1 to 2 in accordance with Sada et al. (1979). The interfacial concentrations of NO and its physical solubilities in alkaline $NaClO_2$ solutions were estimated according to the discussion in Appendix D.

The results predicted from Equation 5.8 represent the exit chlorite concentrations at the bottom of the tower. The predicted concentrations were used to relate the nitrate concentrations being generated according to the stoichiometric relationships given by Equations 5.9 and 5.10.

$$4NO_{(l)} + 3ClO_{2(l)}^{-} + 4OH^{-}_{(l)} \longrightarrow 4NO_{3(l)}^{-} + 3Cl^{-}_{(l)} + 2H_2O_{(l)} \qquad .....(5.9)$$

$$\overline{C}_{NO_3^-} = \frac{4}{3}(\overline{C}_{ClO_2^-,in} - \overline{C}_{ClO_2^-,out}) \qquad \text{.....(5.10)}$$

Figures 5.30 to 5.34 compare typical results predicted from Equations 5.8 and 5.10, with experimental data. These graphs illustrate the dependence of nitrate concentrations on liquid and gas flow rates and sodium chlorite and inlet NO_x concentrations. The best agreement between predicted and experimental values was obtained with m equal to 1.8 ± 0.1. This order agrees with the findings of Sada et al. (1978, 1979) who studied NO absorption into chlorite solutions.

Figure 5.30 compares experimentally determined nitrate concentrations with those predicted from the model for two different liquid feed stream chlorite concentrations. The solid curves representing the model predictions agree very well with the experimental data.

The effect of gas flow rate on nitrate concentration was studied over the gas flow rate range from 8×10^{-4} to 1.65×10^{-3} $m^3.s^{-1}$. These values correspond to residence times in the absorption column of about 19 to 9 seconds. As shown in Figure 5.31, no appreciable change in nitrate concentration was found over the experimental gas flow rate range. The slight increases in nitrate concentrations with increasing gas flow rates provide evidence of the gas–film

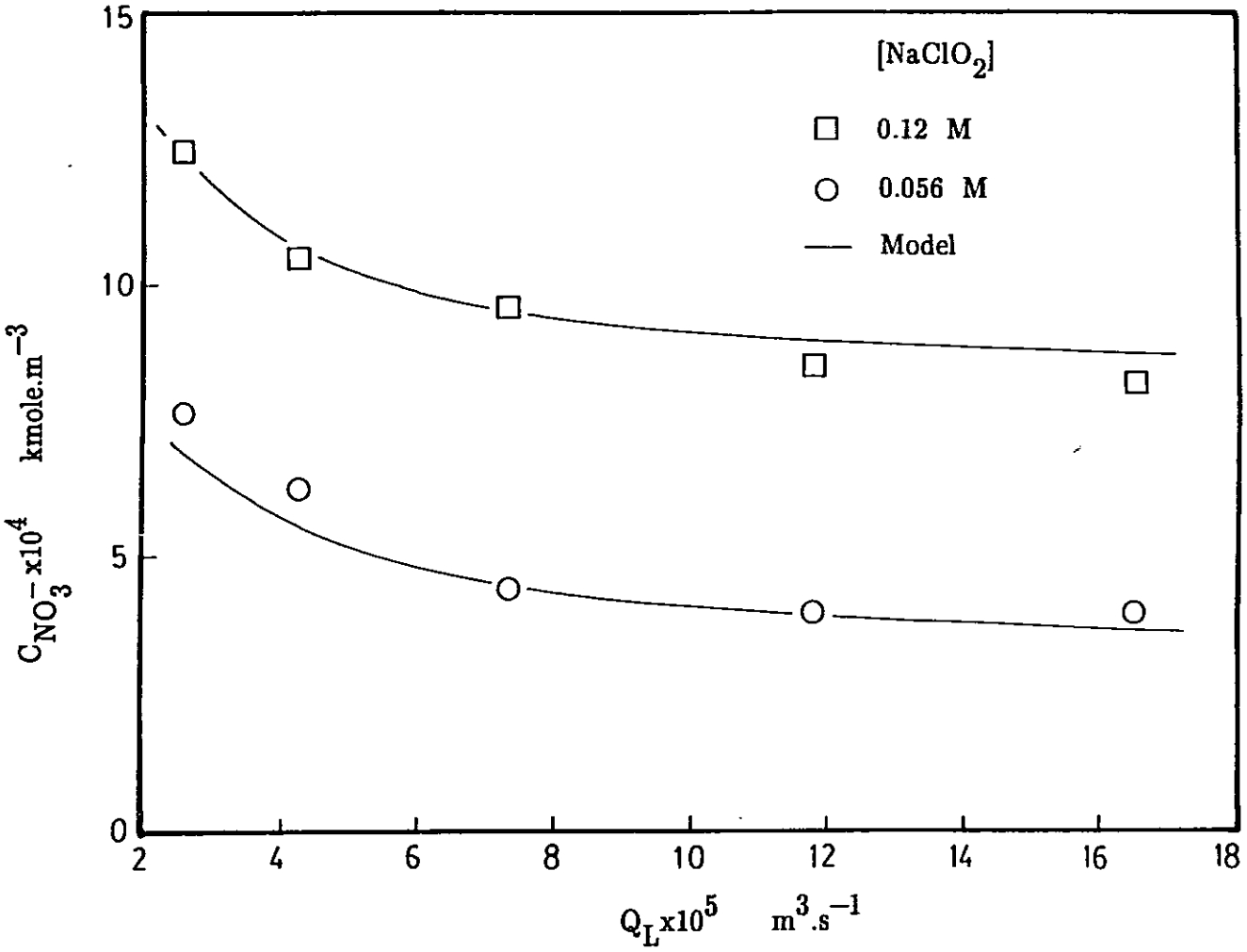

Figure 5.30 Experimental and Predicted $C_{NO_3^-}$ Values for Varying Liquid Flow Rate – $NO_x/NaClO_2$ System; $Q_G = 7.32 \times 10^{-4}$ $m^3.s^{-1}$; $Y_{NO_x} = 550$ ppm

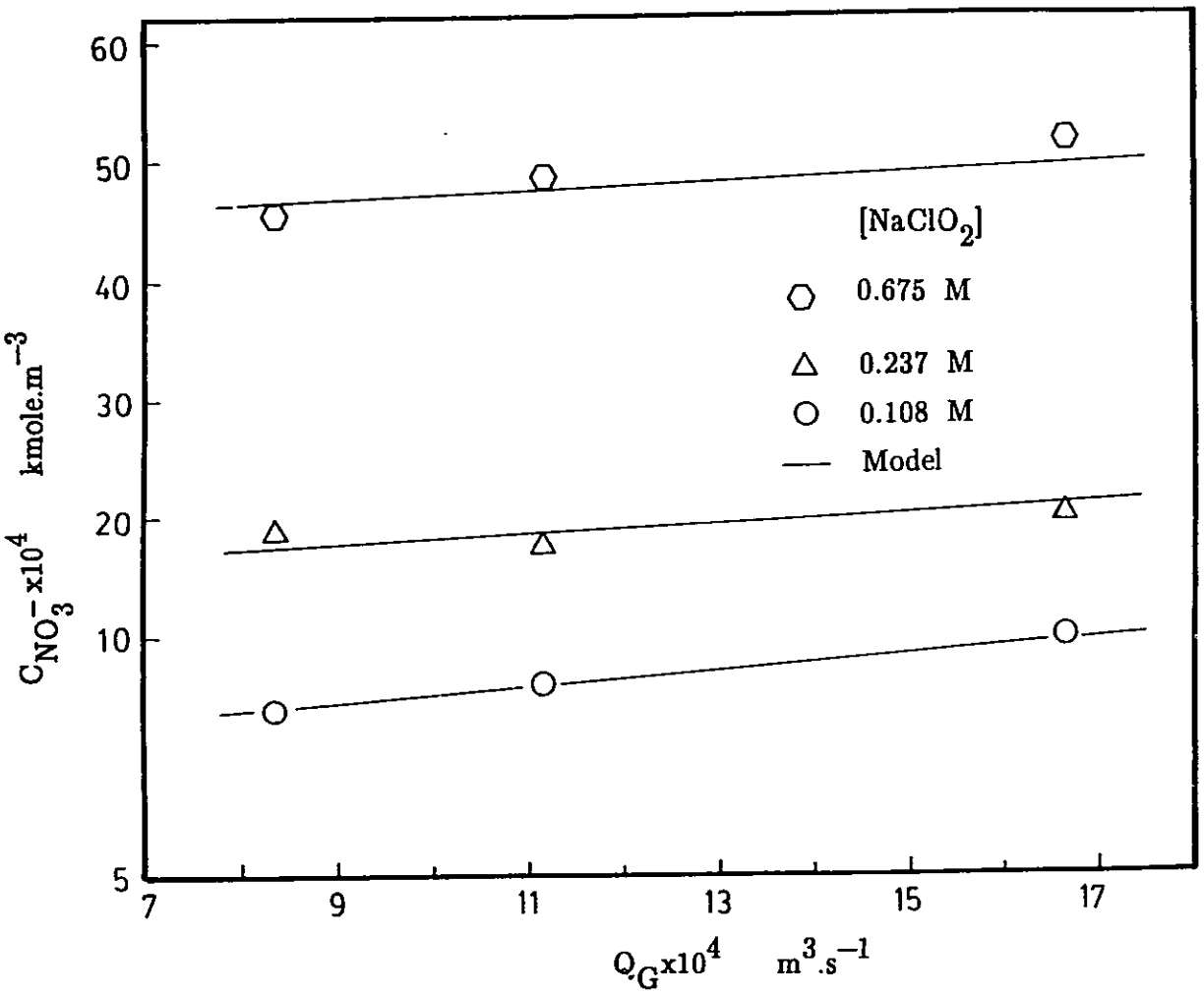

Figure 5.31 Experimental and Predicted $C_{NO_3^-}$ Values for Varying Gas Flow Rate – $NO_x/NaClO_2$ System; $Q_L = 7.32x10^{-5}$ m^3.s^{-1}; $Y_{NO_x} = 500$ ppm

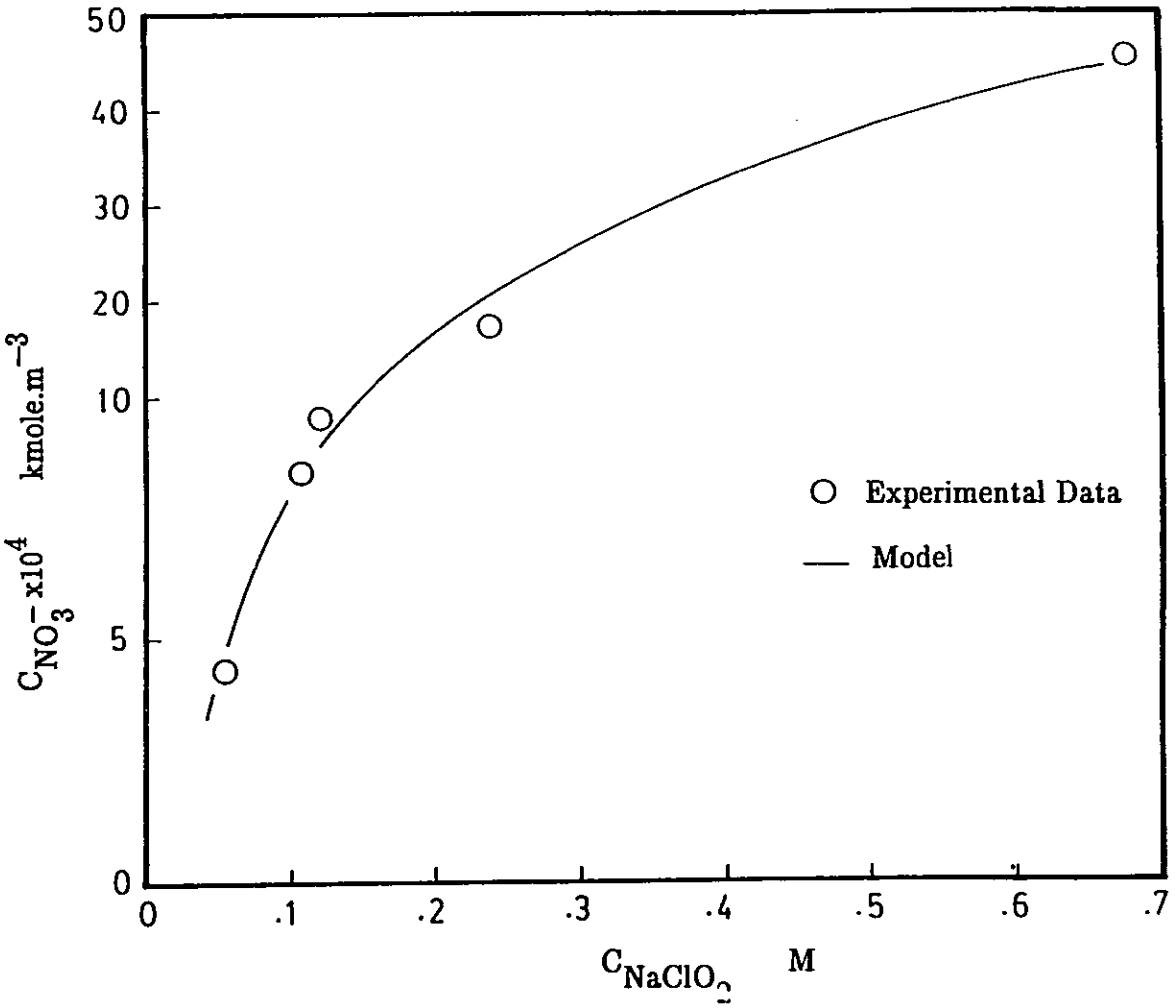

Figure 5.32 Experimental and Predicted $C_{NO_3^-}$ Values for Varying Scrubbing Liquid Concentration – $NO_x/NaClO_2$ System; $Q_L = 7.32 \times 10^{-5}$ $m^3.s^{-1}$; $Y_{NO_x} = 500$ ppm

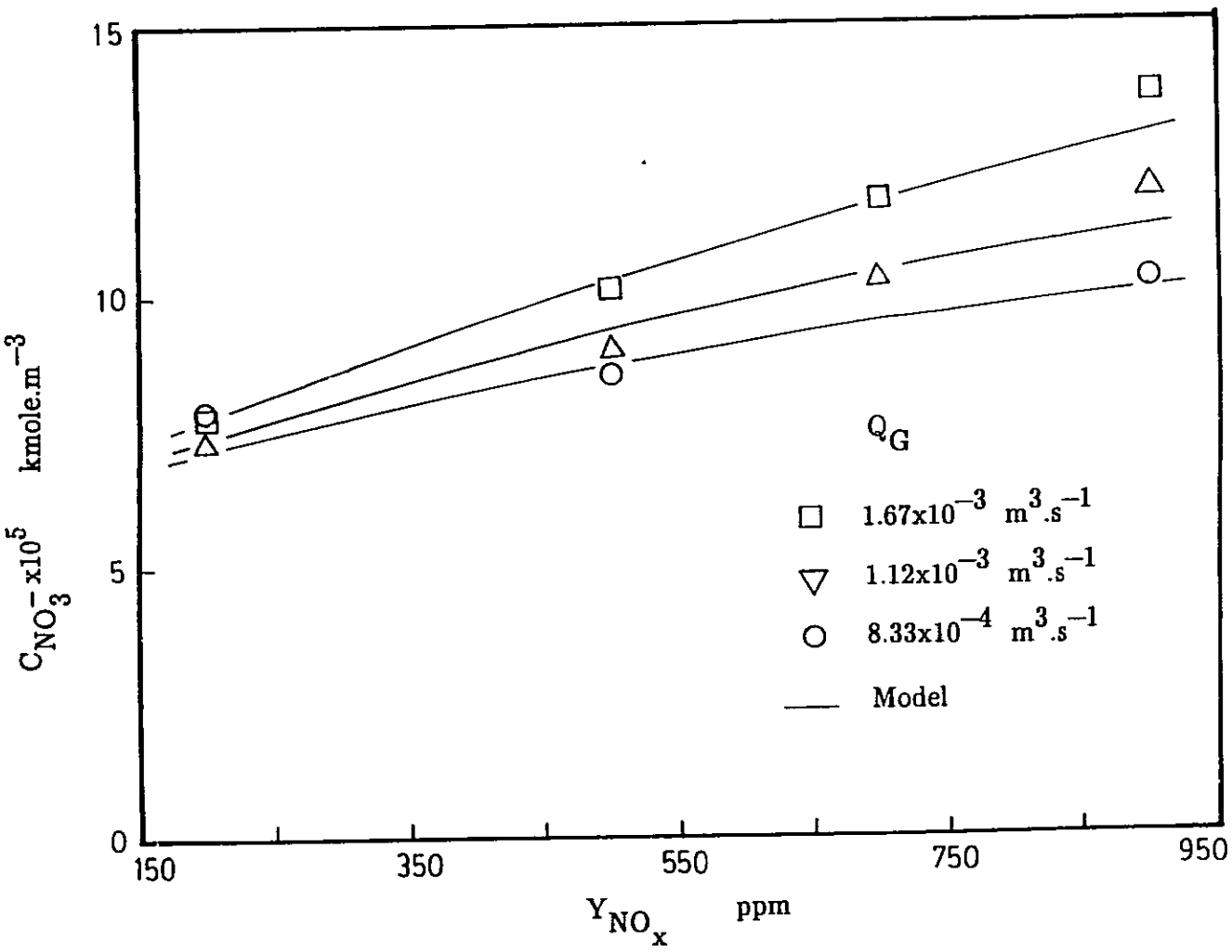

Figure 5.33 Experimental and Predicted $C_{NO_3^-}$ Values for Varying Inlet NO_x Level – $NO_x/NaClO_2$ System; $Q_L = 7.32 \times 10^{-5}$ m^3.s^{-1}; $[NaClO_2] = 0.11$ M

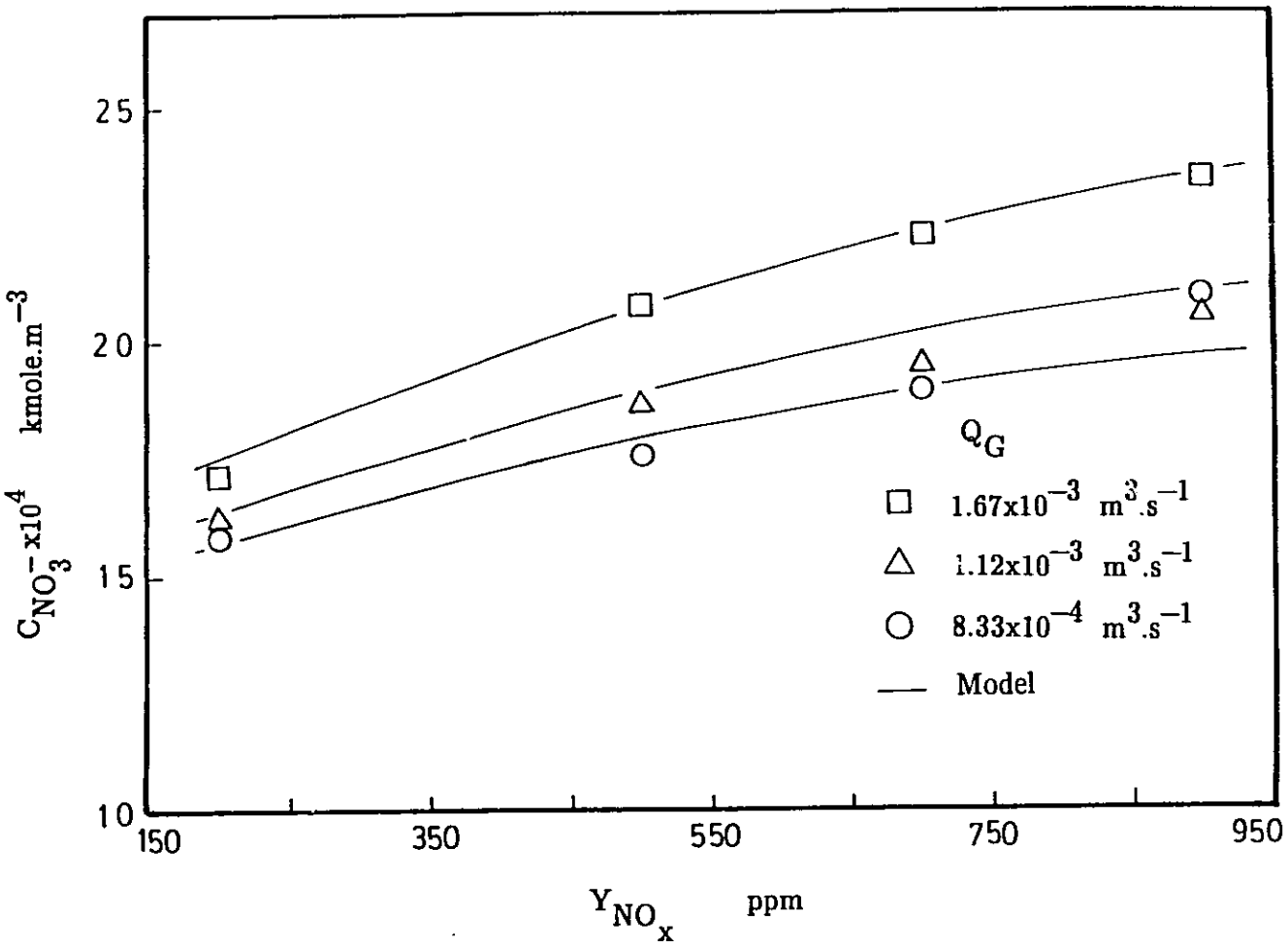

Figure 5.34 Experimental and Predicted $C_{NO_3^-}$ Values for Varying Inlet NO_x Level – $NO_x/NaClO_2$ System; $Q_L = 7.32 \times 10^{-5}$ $m^3.s^{-1}$; $[NaClO_2] = 0.24$ M

control prevailing in the system under study. An increase in the gas flow rate promotes turbulence in the bulk gas which would facilitate transport of NO_x through the gas film to promote higher NO_x absorption. As a result, higher nitrate concentrations would be measured in the liquid effluent.

Other comparisons between predicted and experimental nitrate concentrations for varying inlet chlorite and NO_x concentrations are given in Figures 5.32, 5.33 and 5.34. In general, the absorption of NO_x increases with increasing sodium chlorite concentrations and NO_x inlet levels. The good agreements between predicted and experimental values demonstrated in Figures 5.31 to 5.34 support the contention that NO is the major absorbing species rather than N_2O_3 as found for the $NO_x - H_2O$ system.

5.5 . Absorption of SO_2 Into Alkaline Sodium Chlorite Solution

To study the effect of liquid and gas flow rates on SO_2 removal, experiments were conducted with the SO_2 input level set at 2000 ppm and the alkaline sodium chlorite concentration maintained constant at 5.5×10^{-2} M. The choice of SO_2 input level was consistent with typical coal–fired thermal power plant emission levels.

5.5.1 Removal Efficiency

As shown in Figures 5.35 and 5.36, total absorption of SO_2 was achieved experimentally at fairly low sodium chlorite concentrations. Consequently, liquid and gas flow rates have no effect on SO_2 removal when scrubbing is conducted with aqueous sodium chlorite solutions.

5.5.2 Comparison With Model Prediction

When required for model prediction, the liquid phase diffusivity of SO_2 in mixed solutions was taken to be 1.90×10^{-9} $m^2.s^{-1}$ in accordance with Sada et al. (1978). The interfacial concentration of SO_2 was estimated according to the discussion in Appendix D.

A computation procedure similar to that used for the NO_x– $NaClO_2$ system was adopted for the SO_2 – $NaClO_2$ System. Five theoretical stages were equivalent to the packing of 33 inches of Pall rings. Predicted chlorite concentration is related to the exit sulphate concentration through the stoichiometry given by Equation 5.12.

$$2SO_{2(l)} + 4OH^-_{(l)} + ClO^-_{2(l)} \longrightarrow 2SO^{2-}_{4\,(l)} + Cl^-_{\,(l)} + 2H_2O_{\,(l)} \qquad .....(5.11)$$

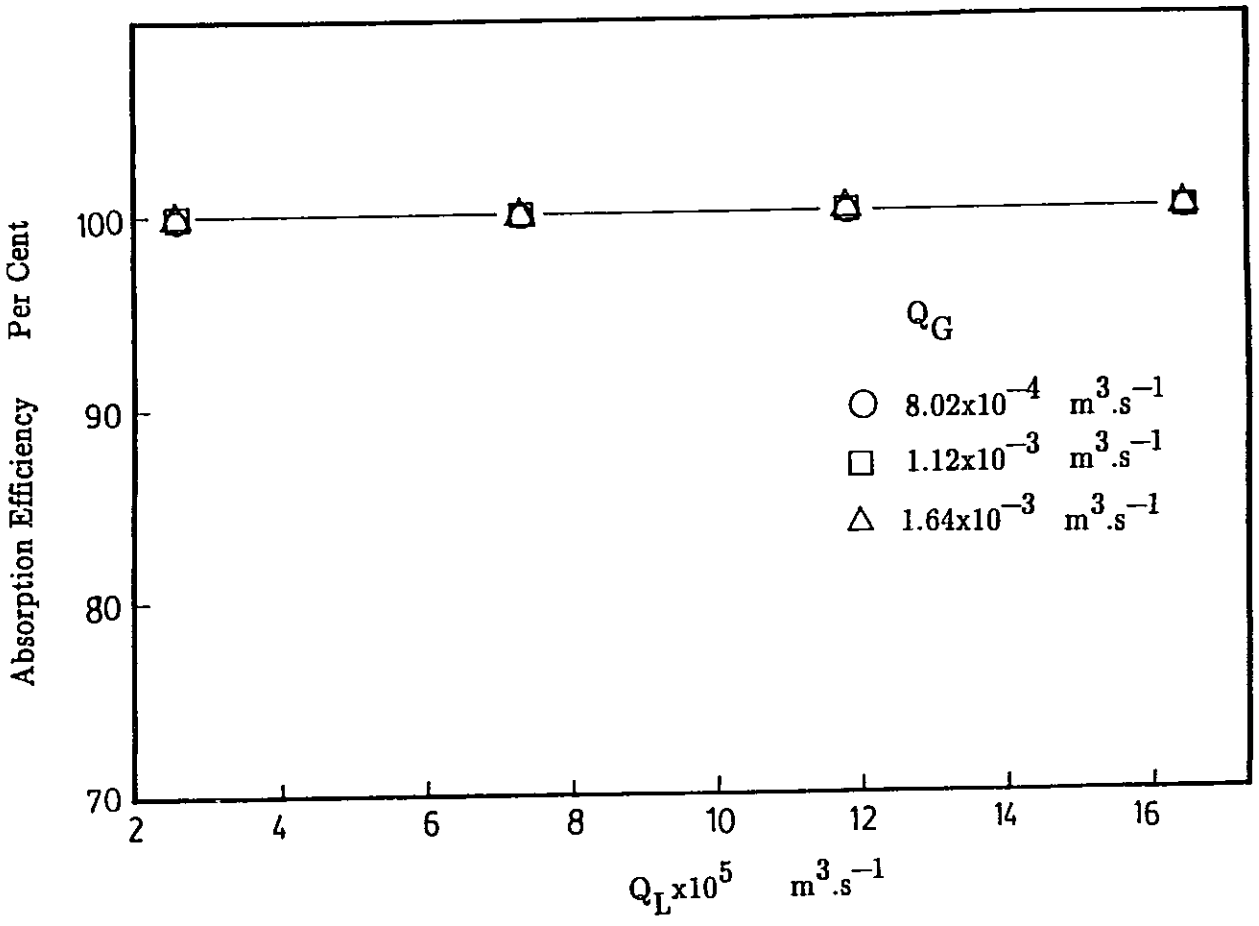

Figure 5.35 Absorption Efficiency as a Function of Liquid Flow Rate – $SO_2/NaClO_2$ System; Y_{SO_2} = 2000 ppm;

$[NaClO_2] = 5.50x10^{-2}$ M

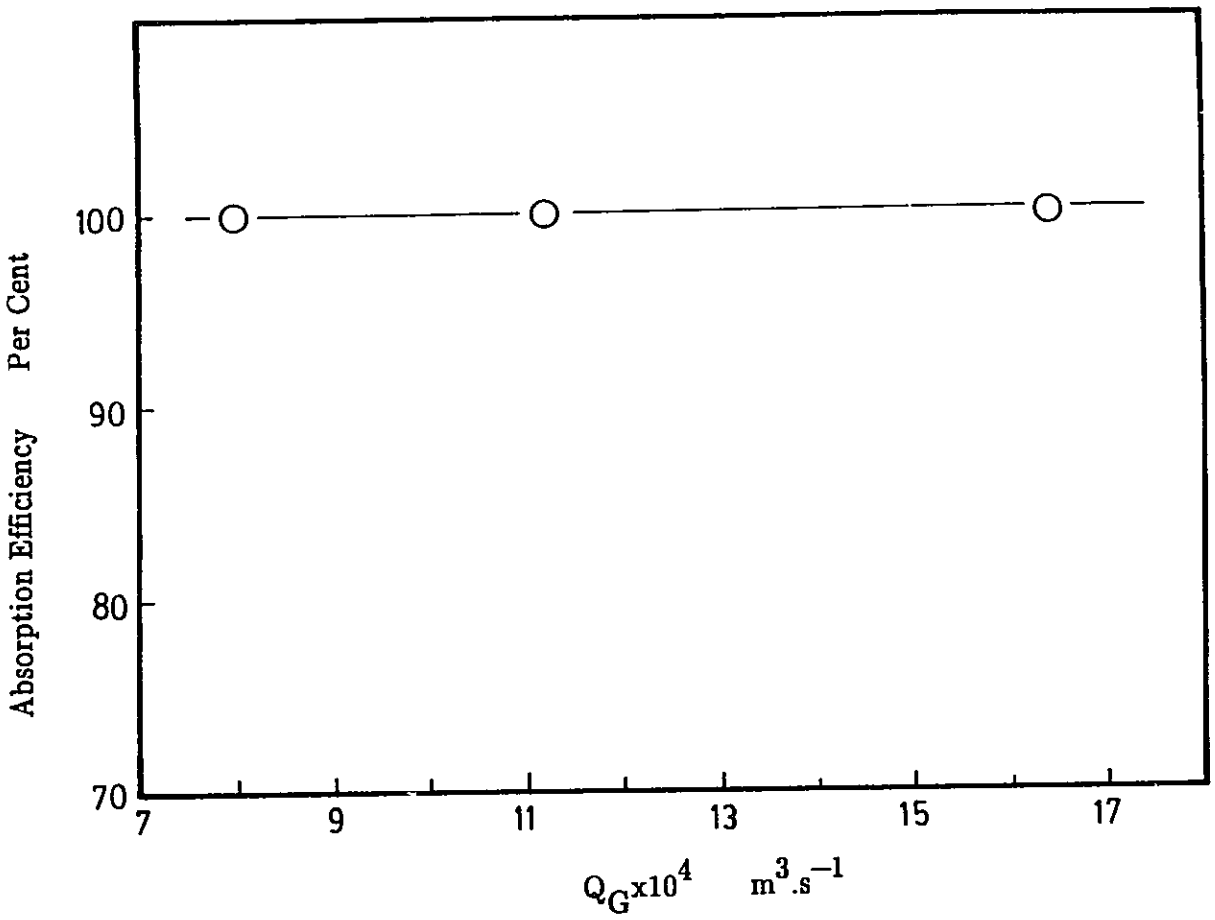

Figure 5.36 Absorption Efficiency as a Function of Gas Flow Rate – $SO_2/NaClO_2$ System;

Y_{SO_2} = 2000 ppm; $[NaClO_2] = 5.50x10^{-2}$ M;

$2.60x10^{-5} \leq Q_L \leq 1.35x10^{-4}$ $m^3.s^{-1}$

$$C_{SO_4^{2-}} = 2\,[\,\overline{C}_{ClO_2^-,in} - \overline{C}_{ClO_2^-,out}\,] \qquad .....(5.12)$$

The results of these calculations are illustrated in Figure 5.37 where sulphate concentrations are plotted against liquid flow rates for three different gas flow rates. Figure 5.37 shows that the predicted results agree fairly well with the experimental data at higher liquid flow rates. At lower liquid flow, the model agrees qualitatively for lower gas flow. A possible cause of the evident discrepancies may be due partly to the turbulent mixing effect induced at higher gas flow rates that the model was unable to account for. The uncertainty in the kinetic rate constant, k_2 , which was adopted from the work of Wang and Himmelblau (1964) might also account for part of the difference. Since no other reliable source for the value of k_2 was identified during the earlier literature search, no further improvement to the model could be attempted.

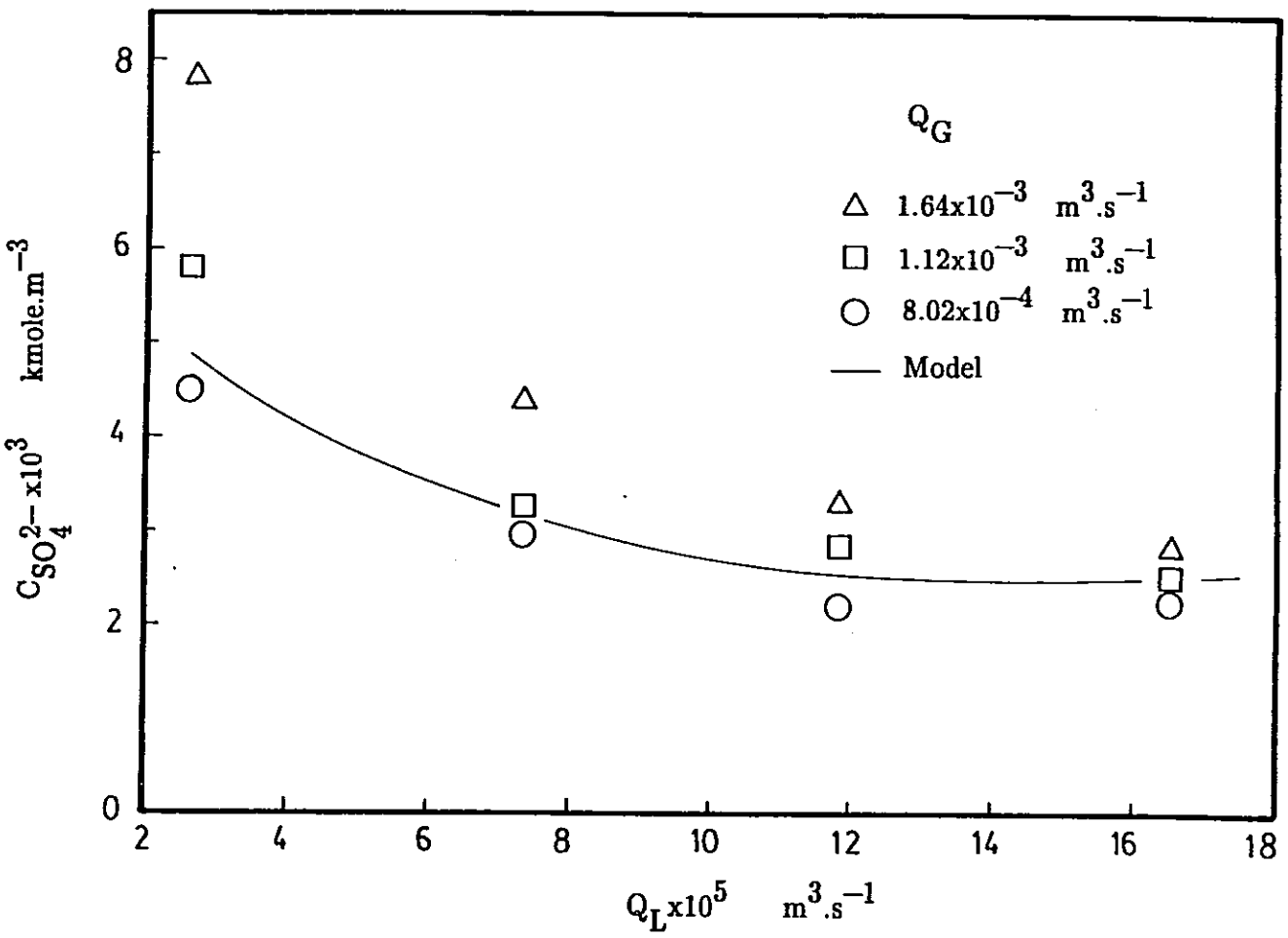

Figure 5.37 Experimental and Predicted $C_{SO_4^{2-}}$ Values for Varying Liquid Flow Rate – $SO_2/NaClO_2$ System; Y_{SO_2} = 2000 ppm

CHAPTER 6

CONCLUSIONS AND RECOMMENDATIONS

6.1 Conclusions

The following conclusions can be drawn from the results of this study:

6.1.1 Water Scrubbing of NO_x

The results of this investigation show that:

. Only a very small percentage of inlet NO_x is removed.

. The major absorbing species is N_2O_3 rather than NO_2 or NO.

. Water scrubbing is very inefficient unless the principal form of NO_x, which is NO, is effectively oxidized to its higher oxide form. Otherwise the absorption process is highly limited by the relatively inert nature of NO.

. Removal efficiency is adversely affected by low NO_x input levels and increasing gas flow rates.

. Varying liquid flow rates have only minor effects on the removal of NO_x.

. A maximum of only 14% absorption efficiency is achievable under the conditions studied. This limit corresponds to the NO oxidization during the dilution stage with air at the inlet to the absorption column.

. Re–circulation of the once–through scrubbing solution should provide a higher removal efficiency as demonstrated by Carta and Pigford (1983) and Carta (1986). Evidence was also provided by the present study at low liquid flow rates.

. The derived physical absorption model was confirmed qualitatively at higher liquid flow rates assuming N_2O_3 as the major diffusing species.

. The mechanism for the absorption of NO_x can be discussed in terms of:

$$2NO_{(g)} + O_{2(g)} \longrightarrow 2NO_{2(g)} \qquad \text{.....(2.19)}$$

$$NO_{2(g)} + NO_{(g)} \longrightarrow N_2O_{3(g)} \qquad \text{.....(2.21)}$$

$$N_2O_{3(g)} \rightleftharpoons N_2O_{3(l)} \qquad \text{.....(2.45)}$$

$$N_2O_{3(l)} + H_2O_{(l)} \longrightarrow 2HNO_{2(l)} \qquad \text{.....(2.50)}$$

6.1.2 Water Scubbing of SO_2

The experimental data indicate that:

. A high percentage of inlet SO_2 was absorbed over the range of parameters studied.

. Up to 90 % removal of SO_2 can be achieved.

. Water is an effective liquid absorbent for SO_2.

. Unlike the NO_x– H_2O system, the SO_2– H_2O system demonstrates adverse effects on removal efficiency when the input level of the gas to be removed is increased in the feed stream.

. Increasing gas flow rates have a negative effect on SO_2 absorption while increasing liquid flow rates show positive effects on SO_2 removal.

. The physical model predictions agreed with experimental data when hydrolysis was taken into into account. The hydrolysis was related to an effective Henry's law constant.

6.1.3 Alkaline Sodium Chlorite Scrubbing of NO_x

It is clearly evident that:

. $NaClO_2$ is more efficient in removing NO_x than H_2O under the same operating conditions.

. Removal efficiencies of NO_x can be as high as 80%.

. Significant proportions of NO_x are absorbed as NO.

. Liquid and gas flow rates show little effect on NO_x removal while increasing liquid chlorite concentrations enhance NO_x absorption.

. Absorption of NO_x tends to be totally gas–film controlled at all NO_x input levels.

. Model predictions based on NO as the predominant diffusing species agreed well with experimental data. With water scrubbing N_2O_3 was assumed to be the major transporting species.

. The overall third order reaction reported by Sada et al. (1978, 1979) was confirmed by this study.

6.1.4 Alkaline Sodium Chlorite Scrubbing of SO_2

The results of this investigation show that:

. SO_2 at typical flue gas levels can be totally removed from gas streams scrubbed with solutions containing fairly low $NaClO_2$ concentrations.

. Varying gas and liquid flow rates have no effect on SO_2 absorption over the ranges studied.

. The model predictions agree qualitatively with the experimental data obtained during this investigation.

6.2 Recommendations:

For practical application of the basic principles established during this

investigation, it is important to:

. Repeat the testing programme with:
  - different packing materials such as Raschig rings and Berl saddles and Leva pak.
  - re–circulation of scrubbing liquid.

. Investigate combined NO_x/SO_2 removal with H_2O and $NaClO_2$ solutions, both at ambient and elevated temperatures, and with simulated stack gases including CO_2 and reduced levels of O_2.

. Test solvents capable of regeneration (such as ethylenedimethyltetramine (EDTA)).

. Investigate the clean–up potential of waste water from the non–regenerable solvent process.

. Investigate the economic feasibility of this process as compared to other SO_2/NO_x removal processes.

REFERENCES

Abel, E., and H. Schmid, "Kinetics of Nitrous Acid III. Kinetics of Nitrous Acid Decomposition", Z. Physik. Chem., **134**, 279 (1928).

Abel, E., and E. Neusser, "The Vapor Pressure of Nitrous Acid", Monatashefte Chem., **53**, 855 (1929).

Andrew, S.P.S., and D. Hanson, "The Dynamics of Nitrous Gas Absorption", Chemical Engineering Science, **14**, 105 (1961).

Aoki, M., H. Tanaka, H. Komiyama, and H. Inoue, "Simultaneous Absorption of NO and NO_2 into Alkaline Solutions", Journal of Chemical Engineering of Japan, **15**, 362 (1982).

Armor, J.N., "Influence of pH and Ionic Strength Upon Solubility of NO in Aqueous Solution", Journal of Chemical and Engineering Data, **19**, 82 (1974).

Ashmore, P.G., and B.J. Tyler, "The Formation and Thermodynamic Properties of Nitrous Acid Vapor", Journal of Chemical Society, **1**, 1017 (1961).

Ashmore, P.G., M.G. Burnett and B.J. Tyler, "Reaction of Nitric Oxide and Oxygen", Trans. Faraday Soc., **58**, 685 (1962).

Baldi G. and S. Sicardi, "A Model for Mass Transfer with and without Chemical Reaction in Packed Towers", Chemical Engineering Science, **30**, 617 (1975).

Basu, R.K., and B.K. Dutta, "Kinetics of Absorption of Sulphur Dioxide in Dimethylaniline Solution", The Canadian Journal of Chemical Engineering, **65**, 27 (1987).

Beattie, I.R., and S.W. Bell, "Dinitrogen Trioxide", J. Chem. Soc., 2, 1681 (1957).

Beattie, I.R., "Dinitrogen Trioxide", Progress in Inorganic Chemistry, vol.5, Wiley, New York (1963).

Bird, R.B., W.E. Stewart, and E.N. Lightfoot, "Transport Phenomena", 510, John Wiley, New York, (1960).

Bjerle, I., S. Bengstsson and K. Farnkvist, "Absorption of SO_2 in $CaCO_3$–Slurry in a Laminar Jet Absorber", Chemical Engineering Science, 27, 1853 (1972).

Boslo, S., A. Ravella, G.B. Saracco, and G.Genon, "NO_x Absorption by Ferrous Sulfate Solution", Ind. Eng. Chem. Process Des. Dev., 24, 149 (1952).

Campbell, W.B., and O. Maass, "Equilibria in Sulphur Dioxide Solution", Canadian Journal of Research, 2, 42 (1930).

Carberry, J.J., "Some Remarks on Chemical Equilibrium and Kinetics in the Nitrogen Oxides – Water System", Chem. Eng. Sci., 9, 189 (1959).

Carta, G., and R.L. Pigford, "Absorption of Nitric Oxide in Nitric Acid and Water", Ind. Eng. Chem. Fundam., 22, 329 (1983).

Carta, G., "Scrubbing of Nitrogen Oxides with Nitric Acid Solutions", Chem. Eng. Commun., 42, 157 (1986).

Caudle, P.G., and K.G. Denbigh, "Kinetics of the Absorption of Nitrogen Peroxide into Water and Aqueous Solutions", Trans. Faraday Soc., 49, 39 (1953).

Chambers,F.S., and T.K. Sherwood, "The Equilibrium Between Nitrogen Peroxide and Aqueous Solutions of Nitric Acid", J. Am. Chem. Soc., 59, 316 (1937).

Chambers, F.S., and T.K. Sherwood, "Absorption of Nitrogen Dioxide by Aqueous Solutions" Ind. Eng. Chem., 29, 1415 (1937).

Chan, W.H., R.J. Nordstrom, J.G. Calvert and J.H. Shaw, "Kinetic Study of HONO Formation and Decay Reactions in Gaseous Mixtures of HONO, NO, NO_2, H_2O and N_2", Environ. Sci. Tech., **10**, 674 (1976).

Chan, K.F., "An Examination of Techniques for the Removal of NO_x and NO_x/SO_x from Flue Gases", M.A.Sc. Thesis, University of Windsor, Windsor (1983).

Chang, C.S., and G.T. Rochelle, "SO_2 Absorption into Aqueous Solutions", AIChE Journal, **27**, 292 (1981).

Chappell, G.A.,"Development of Aqueous Processes for Removing NO_x from Flue Gases", EPA–R2–72–051, U.S. Environmental Protection Agency, Washington D.C., 20460, (September, 1972).

Chappell, G.A., "Aqueous Scrubbing of Nitrogen Oxides from Stack Gases", Adv. Chem. Series **127**, Editors, Jimeson, R.M. and R.S. Spirint, Wash. D.C. Amer. Chem. Soc., Chapter 18, 206 (1973).

Charles, J.W. and C.S. Helen, "Indoor Ozone Exposures", JAPCA, **39**, No. 12, 1562 (1989).

Chen, R., "Investigation of Odor Control by Alkaline Potassium Permanganate Solutions", M.A.Sc. Thesis, University of Windsor, Windsor (1978).

Chilton, T.H., H.R. Duffey, and H.C. Vernon, "The Absorption of Gases in Packed Towers", Industrial and Engineering Chemistry, **29**, 298 (1937).

Counce, R.M., and J.J. Perona, "Gaseous Nitrogen Oxide Absorption in Sieve Plate Column", Ind. Eng. Chem. Fundam., **18**, 400 (1979).

Counce, R.M., and J.J. Perona, "A Mathematical Model for Nitrogen Oxide Absorption in a Sieve Plate Column", Ind. Eng. Chem. Process Des. Dev., **19**, 426 (1980).

Counce, R.M., "The Scrubbing of Gaseous Nitrogen Oxides in Packed Tower", Ph.D. Thesis, The University of Tennessee, Knoxville, Chapter 2, 13 (1980).

Counce, R.M., and J.J. Perona, "Scrubbing of Gaseous Nitrogen Oxides in Packed Towers", AIChE Journal, **29**, 26 (1983).

Danckwerts, P.V., "Gas–Liquid Reactions", 6–104, McGraw–Hill Book Co., New York, (1970).

Day, R.A. Jr., and A.L. Underwood, "Quantitative Analysis – Laboratory Manual", 3rd Ed., Prentice Hall Inc., New Jersey, (1980).

Dekker, W.A., E. Snoeck and H. Kramers, "The Rate of Absorption of NO_2 in Water", Chemical Engineering Science, **11**, 61 (1959).

DeMaine, P.A.D., "Interaction Between Sulfur Dioxide and Polar Molecules. I. Systems Containing Aliphatic Alcohols, Ethers, Or Benzene in Carbon Tetrachloride", J. Chem. Phys., **26**, 1036 (1957).

Denbigh, K.G., and A.J. Prince, "Kinetics of Nitrous Gas Absorption in Aqueous Nitric Acid", J. Chem. Soc., 790 (1947).

De Wall, Jr. K.J.A., and A.C. Van Mameren, "Pressure Drop, Liquid Hold–Up, and Distribution, Residence Time Distributions, and Interfacial Area Between Gas and Liquid in One Packed Column", AIChE Journal, Chem.E. Symposium Series, NO. 60 (1969).

Douabul, A., and J. Riley, "Solubility of Sulphur Dioxide in Distilled Water and Decarbonated Sea Water", Journal of Chemical and Engineering Data, **24**, 274 (1979).

Egan, B.Z., and L.K. Felker, "Removal of SO_2 from Simulated Flue Gas by Magnesia Spray Absorption: Parameters Affecting Removal Efficiency and Products", Ind. Eng. Chem. Process Des. Dev., **25**, 558 (1986).

Eigen, M., K.Kustin, and G.Maass, "Die Geschwindigkeit der Hydration Von SO_2 in Wassriger Losung", Z. Phys. Chem. Frankfurt, **30**, 130 (1961).

England, C., and W.H. Corcoran, "Kinetics and Mechanisms of the Gas Phase Reaction of Water Vapor and Nitrogen Dioxide", Ind. Eng.Chem., Fundam. **13**, 373 (1974).

Environmental Science & Engineering , 6 (September,1990).

Eriksen, T.E., "Diffusion Studies in Aqueous Solutions of Sulphur Dioxide", Chemical Engineering Science, **24**, 273 (1969).

Falk, M., and P.A. Giguere, "On the Nature of Sulphurous Acid", Can.J.Chem.,**36**, 1121 (1958).

Fan, L.S., C. Laohavichitra, K. Muroyama, and S.H. Wang,"Absorption of Sulfur Dioxide by Calcium Hydroxide in a Wetted–Wall Column: Effect of Magnesium Hydroxide, Magnesium Carbonate and Magnesium Sulfate Additives", Chemical Engineering Science, **37**, 1572 (1982).

Fogiel, M., "Handbook of Mathematical, Scientific, and Engineering Formulas, Tables, Functions, Graphs, Transform", 593–596, Research and Education Association, New York (1986).

Forsythe and Giauque, "The Entropies of Nitric Acid and its Mono– and Tri–Hydrates. Their Heat Capacities from 15 to 300 K. The Heats of Dilution at 298.1 K. The Internal Rotation and Free Energy of Nitric Gas. The Partial Pressures Over its Aqueous Solutions", J.Am.Chem.Soc. **64**, 48 (1942).

Forsythe, G.E., M.A. Malcom, and C.B. Moler, "Computer Methods for Mathematical Computations", Prentice–Hall Englewood Cliffs, N.J., (1977).

Galbally, I.E., and C.R. Ray, "Loss of Fixed Nitrogen from Soils by Nitric Oxide Exhalation", Nature, **275**, 734 (1978).

Goettler, L.A., "The Simultaneous Absorption of Two Gases in a Reactive Liquid", Ph.D. Dissertation, University of Delaware, p.136–140 (1967).

Goyer, G.G., "The Formation of Nitric Acid Mists", Journal of Colloid Science, **18**, 616 (1963).

Graedel, T.E., L.A. Farrow and T.A. Weber, "The Influence of Aerosols on The Chemistry of The Troposphere", Int. J. Chem. Kinetics Symposium, 1, 581 (1975).

Graham, R.F., and B.J. Tyler, "Formation of Nitrous Acid in a Gas–Phase Stirred Flow Reactor", J.Chem. Soc. **68**, 683 (1972).

Gratzel, M., A. Henglein, J. Lilie, and G. Beck, "Pulse Radiolytic Investigation of some Elementary Processes of Oxidation and Reduction of Nitrite Ion", Ber. Bunsenges, **73**, 646 (1969).

Greig, J.D., and P.G. Hall, "Thermal Oxidation of Nitric Oxide at Low Concentrations", Trans Faraday Soc., **63**, 655 (1967).

"Hach Water and Wastewater Analysis Procedures Manual", Hach Chemical Company, Ames, Iowa (1975).

Handles,A.E., and T. Baron, "Mass and Heat Transfer from Drops in Liquid–Liquid Extraction", AIChE Journal,**3**, 127 (1959).

Hasche, R.L., and W.A. Patric, "Studies on the Rate of Oxidation of Nitric Oxide. II. The Velocity of the Reaction Between Nitric Oxide and Oxygen at 0^{o} and 30^{o}C", J. Am. Chem. Soc., **47**, 1207 (1925).

Hikita, H., S. Asai, and H. Nose, "Absorption of Sulphur Dioxide into Water", AIChE Journal, **24**, 147 (1978).

Hisatune, I.C., and L.Zafonte, "A Kinetic Study of Some Third–Order Reactions of Nitric Oxide", J. Phys. Chem., **73**, 2980 (1969).

Ho, M.P., and G.E.Klinzing, "Absorption of Sulphur Dioxide and Nitric Oxide by Some Amines and N–Cyclohexyl–2–Pyrrolidone", The Canadian Journal of Chemical Engineering, **64**, 243 (1986).

Hoftyzer, P.J., and F.J.G. Kwanten, Processes for Air Pollution Control, 2nd Ed., Chemical Rubber Co., Cleveland, Chapter 5B (1972).

Huss, A., and C.A. Eckert, "Equilibria and Ion Activities in Aqueous Sulphur Dioxide Solutions", J. Phys. Chem., 81, 2268 (1977).

Hutchings, L.E., L.F. Stutzman, and A.K.J. Howard, "Gas Absorption : Mass Transfer Coefficients as Functions of Liquid, Gas Rates, Tower Packing Characteristics", Chem. Eng. Progr., 45, 253 (1949).

Iya, K.S., "Reduce NO_x in Stack Gases", Hydrocarbon Processing, 163 (Nov. 1972).

Jackson, G.S. and J.M. Marchello, "Effective and Wetted Areas for Absorption in Packed Columns", Journal of Chemical Engineering of Japan, 3, 263 (1970).

JANAF, Thermochemical Tables, 3rd Ed., The Dow Chemical Company, Midland, Michigan (1985).

Johnstone, H.F., and P.W. Leppler, "The Solubility of Sulphur Dioxide at Low Partial Pressures. The Ionization Constant and Heat of Ionization of Sulfurous Acid", J. Am. Chem. Soc., 56, 2233 (1934)

Johnstone, H.F., and A.D.Singh, "Recovery of Sulphur Dioxide from Waste Gases", Industrial and Engineering Chemistry, 29, 286 (1937).

Joosten, G.E.H., and P.V. Danckwerts, "Solubility and Diffusivity of Nitrous Oxide in Equimolar Potassium Carbonate – Potassium Bicarbonate Solutions at 25°C and 1 Atmosphere", Journal of Chemical Engineering Data, 17, 452 (1972).

Jones, L.H., and E.McLaren, "Infrared Absorption Spectra of SO_2 and CO_2 in Aqueous Solution", J. Chem. Phys.,28, 995 (1958)

Joshi, J.B., V.V.Mahajani, and V.A. Juvekar, "Invited Review – Absorption of NO_x Gases", Chem. Eng. Commum., **33**, 1 (1985).

Kaiser, E.W., and C.H. Wu, "A Kinetic Study of the Gas Phase Formation and Decomposition Reactions of Nitrous Acid", J.Phys.Chem. **81**, 1701 (1977).

Kaji, R., Y. Hishinuma, and H. Kuroda, "SO_2 Absorption by Water Droplets", Journal of Chemical Engineering of Japan, **18**, 169 (1985).

Kassel, L.S., "The Theory of Third–Order Gas Reactions", J. Phys. Chem., **34**, 1777 (1930).

King, C.J., "The Additivity of Individual Phase Resistance in Mass Transfer Operations", AIChE Journal, **10**, 671 (1964).

Komiyama, H. and H.Inoue, "Absorption of Nitrogen Oxides into Water", Chemical Engineering Science, **35**, 154 (1980).

Koval, E.J., and M.S. Peters, "How Does Nitric Oxide Affect Reactions of Aqueous Nitrogen Dioxide?", Industrial and Engineering Chemistry, **52**, 1011 (1960)

Kramers, H., M.P.P. Blind, and E. Snoeck, "Absorption of Nitrogen Tetroxide by Water Jets", Chem. Eng. Sci., **14**, 115 (1961).

Laohavichitra, C., K. Muroyama, S.H. Weng and L.S. Fan, "Absorption of Sulphur Dioxide by Calcium Hydroxide Solution in a Wetted–Wall Column: Effect of Magnesium Hydroxide, Magnesium Carbonate and Magnesium Sulfate Additives", Chemical Engineering Science, **37**, 1572 (1982).

Leaist, D.G., "Diffusion with Hydrolysis Equilibria : Transport Coefficients of Aqueous SO_2, NH_3 and Na_2CO_3", Can. J. Chem., **61**, 1494 (1983).

Leaist, D.G., "Diffusion Coefficient of Aqueous Sulphur Dioxide at 15^{o}C", Journal of Chemical and Engineering Data, **29**, 281 (1984).

Lee, Y.N., and S.E. Schwartz, "Reaction Kinetics of Nitrogen Dioxide With Liquid Water at Low Partial Pressure", J.Phys.Chem., **85**, 840 (1981).

Levaggi, D.A., R. Zerrudo, G. Karels, W. Oyung, and M. Feldstein, "An Integrated Manual Impinger Method for the Simultaneous Determination of NO_x and SO_x in Source Effluents", Journal of Air Pollution Control Association, **26**, 783 (1976).

Michell, R.W., and I.A. Furzer, "Trickle Flows in Packed Beds", Trans. Instn. Chem. Engrs, **50**, 334 (1972).

McMichael, W.J., L.S.Fan and C.Y.Wen, "Analysis of Sulphur Dioxide in Limestone Data from Pilot Plant Spray and TCA Scrubbers", Ind. Eng. Chem., Process Des. Dev., **15**, 459 (1976).

Mohamed, R.S., and G.E.Klinzing, "Absorption of Nitrogen Dioxide and Sulphur Dioxide in Methanol", The Canadian Journal of Chemical Engineering, **62**, 99 (1984).

Mohunta, D. M., A.S. Vaidyanathan and G.S. Laddha, "Prediction of Liquid–Phase Mass Transfer Coefficients in Columns Packed with Raschig Rings", Indian Chemical Engineer, 73–79 (July, 1969).

Monthly Report, ECO/LOG Canadian Pollution Legislation volume 7, Number 9, (September, 1990).

Morgan, O.M., and O.Maass, "An Investigation of the Equilibria Existing in Gas–Water Systems Forming Electrolytes", Can. J. Res., 5, 162 (1931).

Morrison, M.E., R.C. Rinker, and W.H. Corcoran, "Wall Effect in Couette Flow of Non–Newtonian Suspensions", Ind. Eng. Chem. Fundam.,, 5, 175 (1966).

Myerson, A.S., and C.W. Sandy, "Nitric Oxide Gas Absorption in a Limestone Packed Column", AIChE Journal, 27, 518 (1981).

NBS, "Selected Values of Chemical Thermodynamic Properties, Tables for the First Thirty Four Elements in the Standard Order of Arrangement", US, NBS, Technical Note, 273 (1968).

Newman, B.L. and G. Carta, "Mass Transfer in the Absorption of Nitrogen Oxides in Alkaline Solutions", AIChE Journal, 34, No.7, 1190 (1988).

Nottingham, W.C., and J.R. Sutter, International J. of Chemical Kinetics, 18, 1289 (1986).

Onda, K., E. Sada and Y. Murase, "Liquid–Side Mass Transfer Coefficients in Packed Towers", AIChE Journal, 5, 235 (1959).

Onda, K., T. Okumoto and H. Honda, "Liquid–Side Mass Transfer Coefficient in a Tower Packed with Berl Saddles", Chem. Eng. of Japan, 24, 490 (1960).

Onda, K., E. Sada, C. Kido, and A. Tanaka, "Liquid–Side and Gas–Side Mass Transfer Coefficients in Towers Packed with Spheres", Chem. Eng. of Japan, 27, 140 (1963).

Onda, K., H. Takeuchi, and Y. Koyama, "Effect of Packing Materials on the Wetted Surface Area", Kagaku Kogaku, 31, 126 (1967).

Onda, K., H. Takeuchi and Y. Okumoto, "Mass Transfer Coefficients Between Gas and Liquid Phases in Packed Columns", Journal of Chemical Engineering of Japan, 1 56 (1968)

Onda, K., E. Sada, T. Kobayashi, S. Kito, and K.K. Ito, "Solubility of Gases in Aqueous Solutions of Mixed Salts", Journal of Chemical Engineering of Japan, 3, 137 (1970).

Otake, T., and K. Okada, "Liquid Hold–Up in Packed Columns", Journal of Chemical Engineering of Japan, 17, 176 (1953).

Peaceman, D.W., "Liquid– Side Resistance in Gas Absorption with and without Chemical Reaction", Sc. D. Thesis, Mass. Inst. Technol., Cambridge (1951).

Peter, M.S., C.P.Ross and J.E. Klein, "Controlling Mechanism in the Aqueous Absorption of Nitrogen Oxides", AIChE Journal, 1, 105 (1955).

Peters, M.S., and E.J. Koval, "Nitrogen Oxide Absorption in an Agitated Reactor", Ind.Eng.Chem., 55, 577 (1959).

Pruce, L., "Reducing NO_x Emissions at the Burner,in the Furnace, and after Combustion", Power, 125, 33 (1981).

Puranik, S.S. and A. Vogelpohl, "Effective Interfacial Area in Irrigated Packed Columns", Chemical Engineering Science, 29, 501 (1974).

Rabe, A.E., and J.F. Harris, "Vapor Liquid Equilibrium Data for the Binary System: Sulphur Dioxide and Water", Journal of Chemical and Engineering Data, 8, 333 (1963)

Rao, K.B., and G.G. Rao, "Oxidation Methods for the Volumetric Estimation of Sulphite", Analytica Acta, 13, 313 (1955).

Reid, R.C., J.M. Prausnitz and T.K. Sherwood, "The Properties of Gases and Liquids", McGraw–Hill Book Company, 3rd Ed., 554–567, New York (1977).

Riesenfeld, F.C., and A.L. Kohl, "Gas Purification", Gulf Publ. Co., Houston, 267 (1974).

Roberts, D.L., "Sulphur Dioxide Transport Through Aqueous Solutions", Ph.D. Dissertation, California Institute of Technology, Pasadena (1979).

Roberts, D.L., and S.K. Friedlander, "Sulphur Dioxide Transport Through Aqueous Solutions: Part I. Theory", AIChE Journal, 26, 593 (1980).

Roberts, D.L., and S.K. Friedlander, "Sulphur Dioxide Transport Through Aqueous Solutions: Part II. Experimental Results and Comparison with Theory", AIChE Journal, 26, 602 (1980).

Rochelle, G.T., and C.J. King, "The Effect of Additives on Mass Transfer in $CaCO_3$ or CaO Slurry Scrubbing of SO_2 from Waste Gases", Ind. Eng. Chem. Fundam., **16**, 67 (1977).

Sada, E., H. Kumazawa, N. Hayakawa, I. Kudo, and T. Kondo, "Absorption of NO in Aqueous Solutions of $KMnO_4$", Chemical Engineering Science, **32**, 1171 (1977).

Sada, E., H. Kumazawa, I. Kudo, and T. Kondo, "Absorption of NO in Aqueous Mixed Solutions of $NaClO_2$ and NaOH", Chemical Engineering Science, **33**, 315 (1978).

Sada, E., H. Kumazawa, Y. Yamanaka, I. Kudo, and T. Kondo, "Kinetics of Absorption of Sulphur Dioxide and Nitric Oxide in Aqueous Mixed Solutions of Sodium Chlorite and Sodium Hydroxide", Journal of Chemical Engineering of Japan, **11**, 276 (1978).

Sada, E., H. Kumazawa, and M.A. Butt, "Single and Simultaneous Absorptions of Lean SO_2 and NO_2 into Aqueous Slurries of $Ca(OH)_2$ or $Mg(OH)_2$ Particles", Journal of Chemical Engineering of Japan, **12**, 111 (1979).

Sada, E., H. Kumazawa, I. Kudo, and T. Kondo, "Absorption of Lean NO_x in Aqueous Solutions of $NaClO_2$ and NaOH", Ind. Eng. Chem. Process Dev. Des., **18**, 275 (1979).

Sada, E., H. Kumazawa, I. Hashizume, and H. Nishimura, "Absorption of Dilute SO_2 into Aqueous Slurries of $CaSO_3$", Chemical Engineering Science, **37**, 1423 (1982).

Schuck, E.A.,, and E.R.Stephens, "Oxides of Nitrogen", Advances in Environmental Science, Ed. by J.N. Pitts, Jr. and R.L. Metcalf, vol.1, Wiley–Interscience (1980)

Schwartz, S.E., and W.H. White, "Solubility Equilibria of the Nitrogen Oxides and Oxyacids in Dilute Aqueous Solutions", Advances in Environmental Science and Engineering, Vol.4, Pfafflin, J.R. and E.N. Ziegler (Ed.) Gordon and Breach Science Publishers, New York (1981).

Semmelbauer, R., "Die Berechnung der Schutthohe bei Absorptions Vorgangen in Fullkooperkolonnen", Chemical Engineering Science, **23**, 1237 (1967).

Sherwood, T.K., and F.A.L. Holloway, "Performance of Packed Towers – Liquid Film Data for Several Packings", Trans. Am. Inst. Chem. Engrs., **36**, 39 (1940)

Shulman, H.L., C.F. Ullrich, and N. Wells, "Performance of Packed Columns – I. Total, Static, and Operating Holdups", AIChE Journal, **1**, 247 (1955).

Shulman, H.L., C.F. Ullrich, A.Z. Proulx, and J. O. Zimmerman, Performance of Packed Columns – II. Wetted and Effective–Interfacial Areas, Gas and Liquid Phase Mass Transfer Rates", AIChE Journal, **1**, 253 (1955).

Shulman, H.L., C.G. Savini, and R.V. Edwin, "Performance of Packed Columns – VII. The Effect of Holdup on Gas–Phase Mass Transfer Rates", AIChE Journal, **9**, 479 (1963).

Shulman, H.L., W.G. Wellish and W.H. Lyman, "Performance of Packed Columns : IX. Simulation of a Packed Column", AIChE Journal, **17**, 631 (1971).

Sicardi, S., and G. Baldi, "A Model for Mass Transfer in Packed Towers : Mass Transfer with Controlling Resistance in the Gas Phase", Chemical Engineering Science, **31**, 651 (1976)

Smith, J.H., "A Rate Study of the Oxidation of Nitric Oxide with Nitric Acid Vapor", J.Am.Chem.Soc., **69**, 1941 (1947).

Takeuchi, H., M. Ando, and N. Kizawa,"Absorption of Nitrogen Oxides in Aqueous Sodium Sulfite and Bisulfite Solutions", Ind. Eng. Chem. Process Des. Dev., **16**, 303 (1977).

Teramoto, M., S. Hiramine, Y. Shimada, Y. Sugimoto, and H. Teranishi,"Absorption of Dilute Nitric Monoxide in Aqueous Solutions of Fe(II) – EDTA and Na_2SO_3", Journal of Chemical Engineering of Japan, **11**, 405 (1978).

Tipper, C.F.H., and R.K. Williams, "The Effect of Sulphur Dioxide on the Combustion of Some Inorganic Compounds", Trans. Faraday Soc., **77**, 2033 (1955)

Treacy, J.C., and F. Daniels, "Kinetic Study of the Oxidation of Nitric Oxide with Oxygen in the Pressure Range 1 to 20 Mm", J. Am. Chem. Soc., **77**, 2033 (1955).

Uchida, S., T. Kobayashi, and S. Kageyama,"Absorption of Nitrogen Monoxide into Aqueous $KMnO_4$/NaOH and $Na_2SO_3/FeSO_4$ Solutions", Ind. Eng. Chem. Process Des. Dev., **22**, 323 (1983).

Uchida, S., M. Miyazaki, and S. Masumoto,"Absorption of Sulfur Dioxide into Melamine Slurry", Chemical Engineering Science, **39**, 1527 (1984).

Van Krevelen, D.W., and P.J. Hoftijzer, "Kinetics of Simultaneous Absorption and Chemical Reaction", Chem. Eng. Progr., **44**, 529 (1948).

Van Swaaij, W.P.M., J.C. Charpentier, and J. Villermaux, "Residence Time Distribution in Liquid Phase of Trickle Flow in Packed Columns", Chemical Engineering Science, **24**, 1083 (1969).

Verhoek, F.M., and F.J. Daniels, "The Dissociation Constants of Nitrogen Tetroxide and of Nitrogen Trioxide", J. American Chemical Society, **53**, 1250 (1931).

Vivian, J.E., and R.P. Whitney, "Absorption of Chlorine in Water", Chem. Eng. Progr., **43**, 691 (1947).

Vosper, A.J., "Dinitrogen Trioxide, Part XIII, Hydration of Gaseous Dinitrogen Trioxide and a Reinvestigation of Its Dissociation", J. Chem. Soc.(Dalton), 135 (1976).

Waldorf, D.M., and A.L. Babb, "Vapor–Phase Equilibrium of NO, NO_2, H_2O and HNO_2", The Journal of Chemical Physics, **39**, 432 (1963).

Wang, J.C., and D.M. Himmelblau, "A Kinetic Study of Sulphur Dioxide in Aqueous Solution with Radioactive Tracer", AIChE Journal, **10**, 574 (1964).

Wayne, L.G., and D.M. Yost, "Kinetics of the Rapid Gas Phase Reaction Between NO, NO_2 and H_2O", The Journal of Chemical Physics, **19**, 41 (1951).

Wendel, M.M., and R.L. Pigford, "Kinetics of Nitrogen Tetroxide Absorption in Water", AIChE Journal, **4**, 249 (1958).

Wetters, J.H., and K.L. Uglum, "Direct Spectrophotometric Simultaneous Determination of Nitrite and Nitrate in the Ultraviolet", Analytical Chemistry, **42**, 335 (1970).

Whitney, R.P., and J.E. Vivian, "Absorption of Sulphur Dioxide in Water", Chemical Engineering Progress, **45**, 323 (1949).

Wilke, C.R. and P. Chang, "Correlation of Diffusion Coefficients in Dilute Solution", AIChE Journal, **1**, 264 (1955).

Wise, D.L., and G. Houghton, "Diffusion Coefficients of Neon, Krypton, Xenon, Carbon Monoxide and Nitric Oxide in Water at 10 – 60 °C", Chemical Engineering Science, **23**, 1211 (1968).

Yoshida, F. and T. Koyanagi, "Liquid Phase Mass Transfer Rates and Effective Interfacial Area in Packed Absorption Columns", Industrial and Engineering Chemistry, **50**, 365 (1958).

Yoshida, F., and Y. Miura, "Effective Interfacial Area in Packed Columns for Absorption with Chemical Reaction", AIChE Journal, **9** 331 (1963).

APPENDIX – A

CALIBRATION CURVES

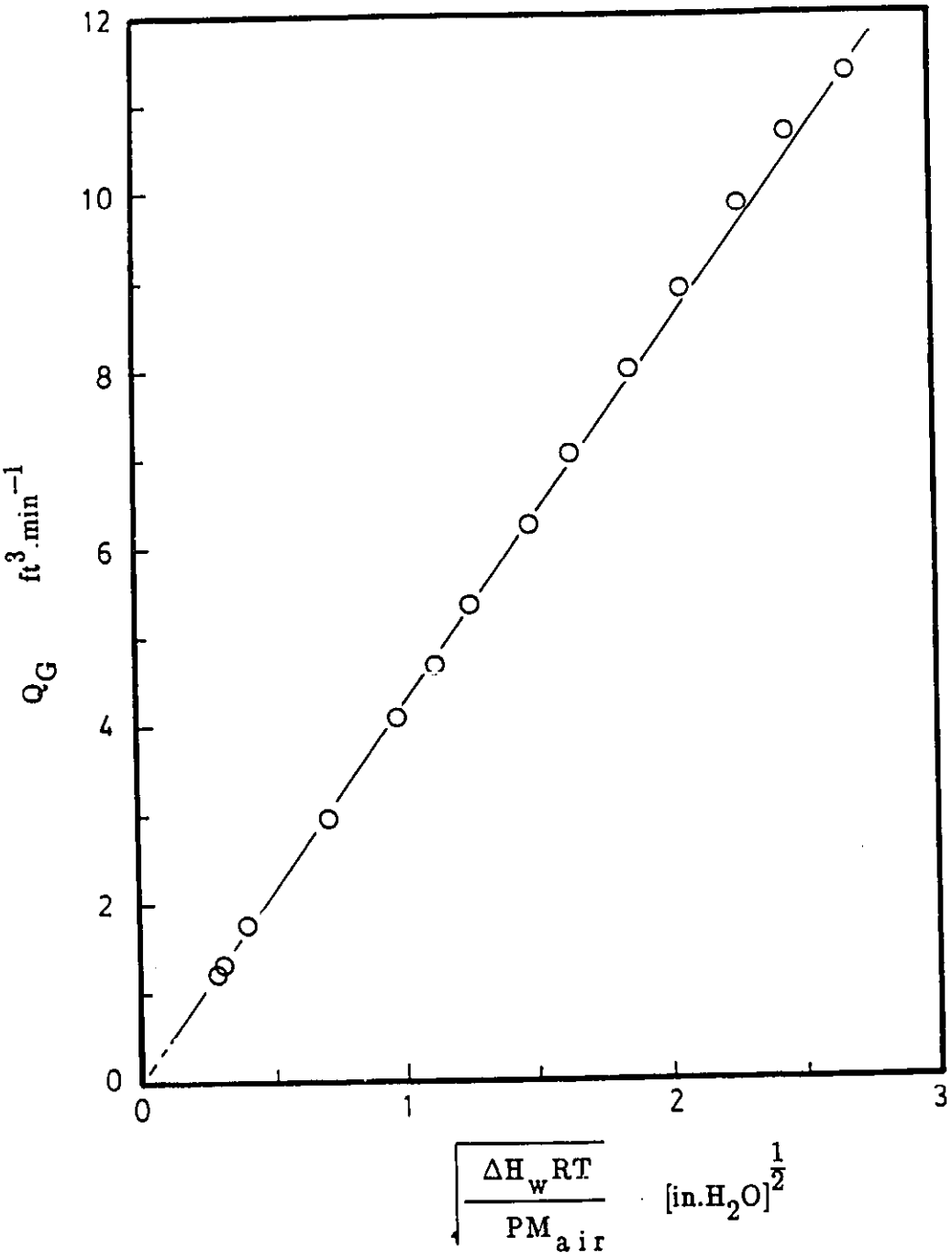

Figure A.1 Air Flow Rate Calibration – Orifice Meter

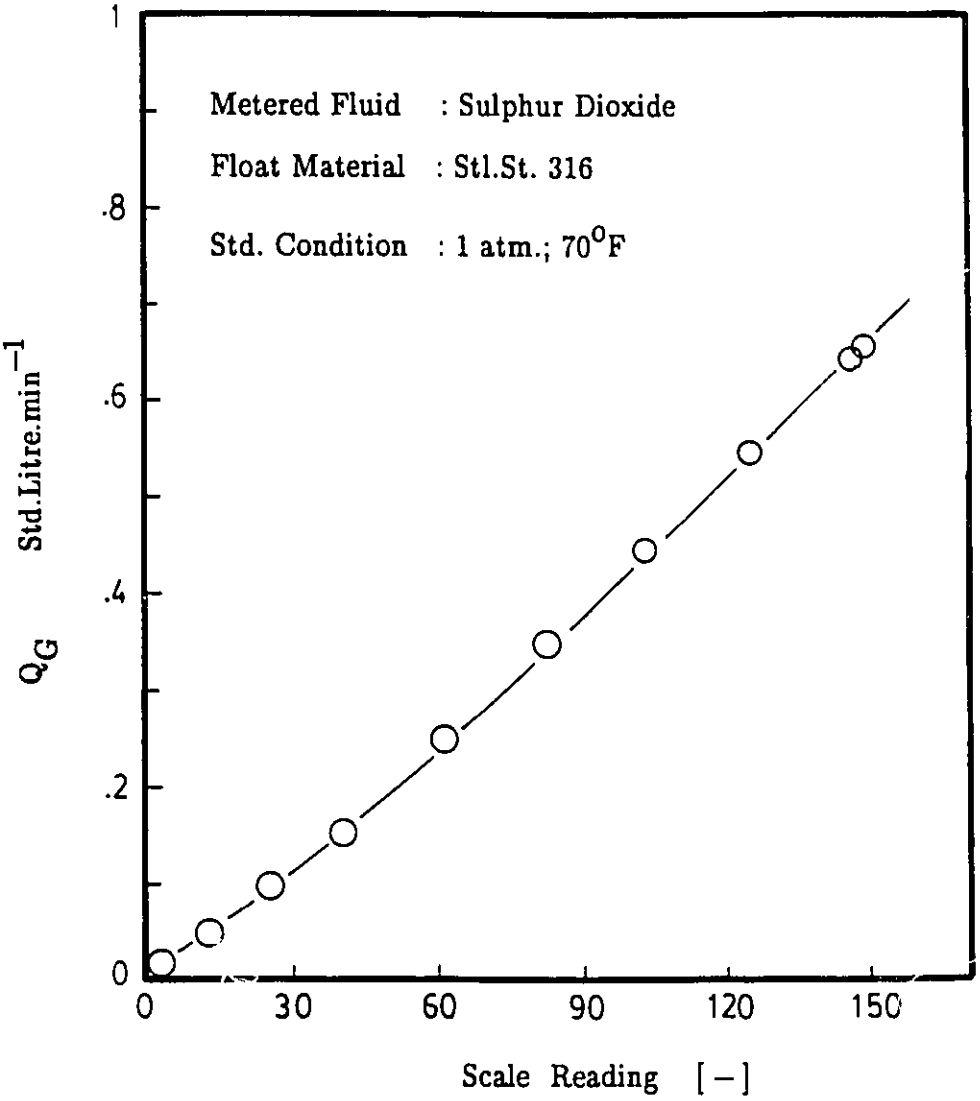

Figure A.2 SO_2 Flow Rate Calibration – Gas Proportioner; Data Obtained from Supplier

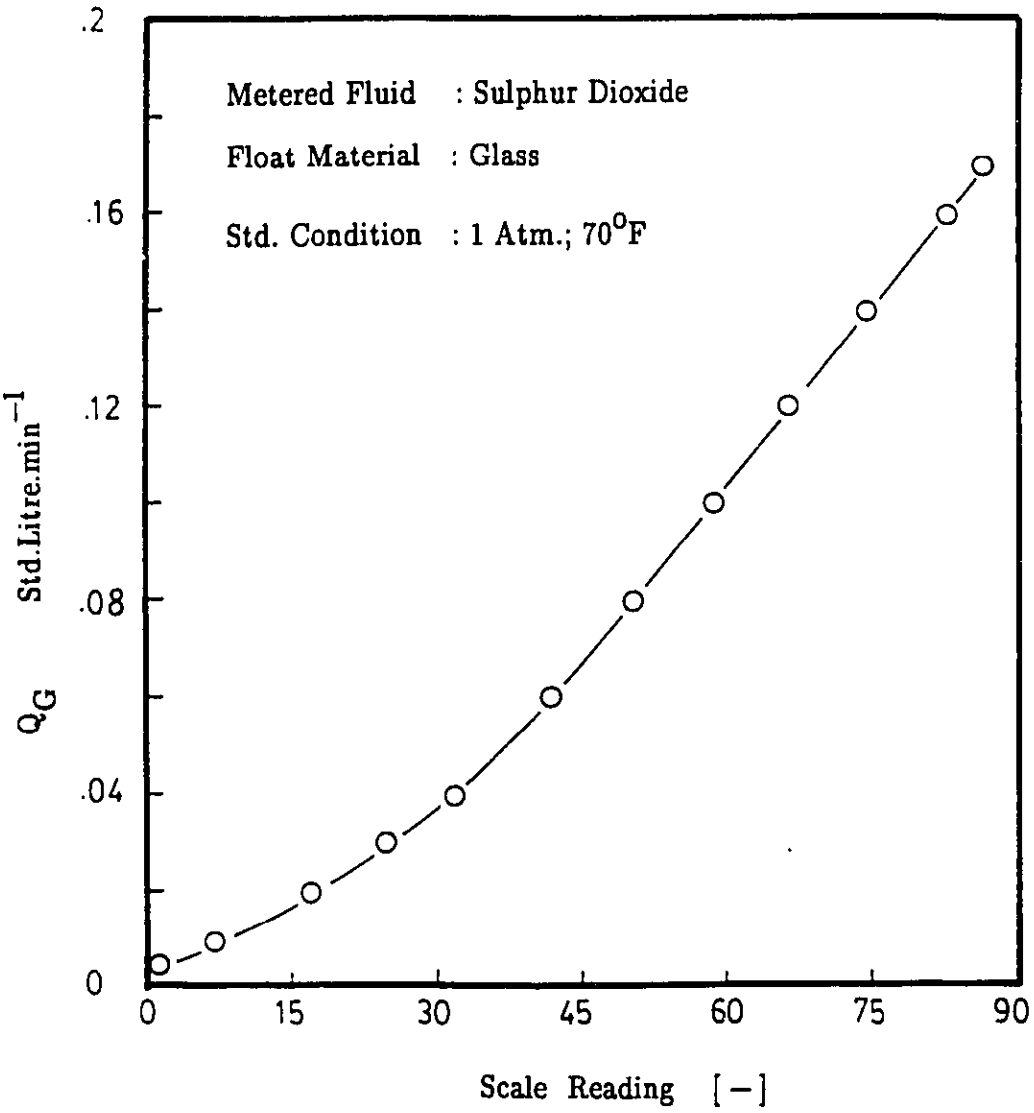

Figure A.3 SO_2 Flow Rate Calibration – Gas Proportioner; Data Obtained from Supplier

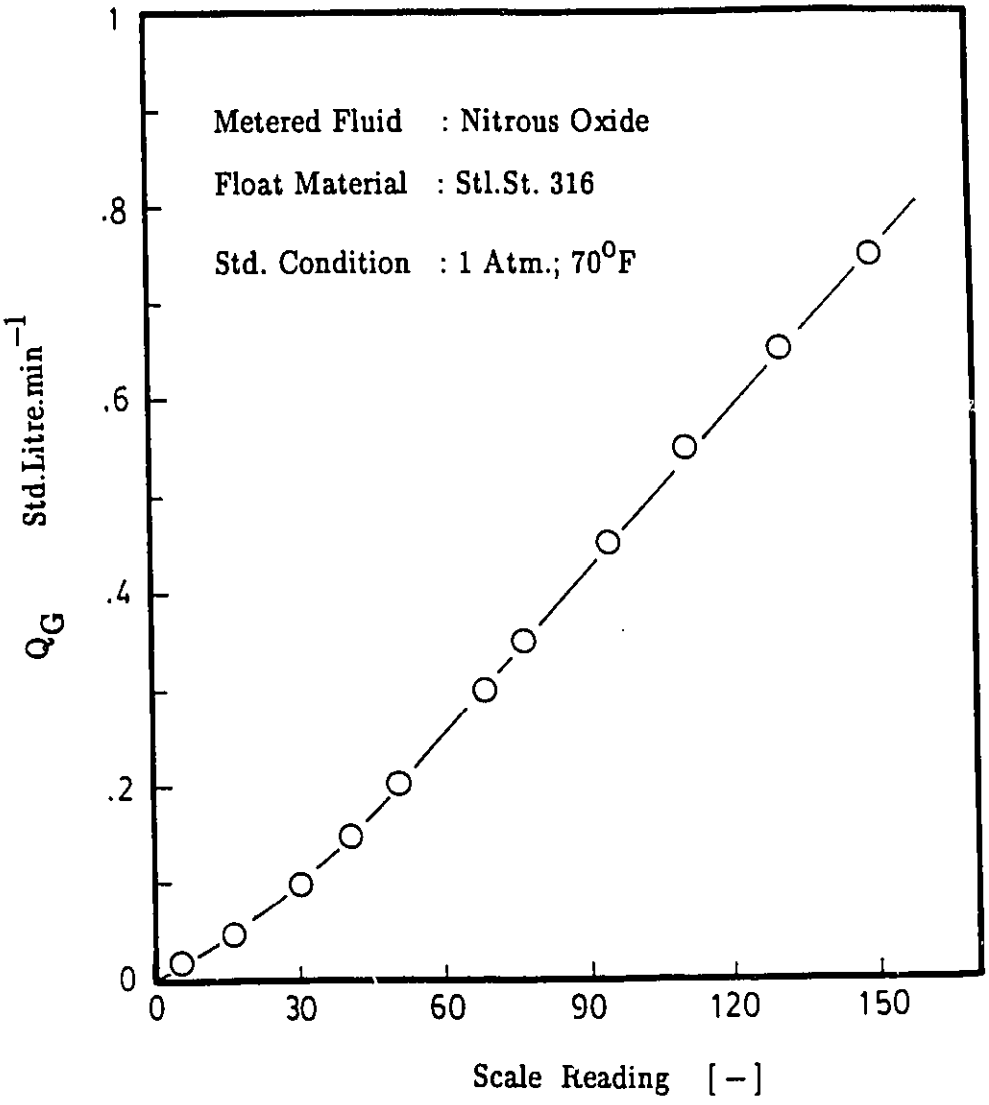

Figure A.4 N_2O Flow Rate Calibration – Gas Proportioner; Data Obtained from Supplier

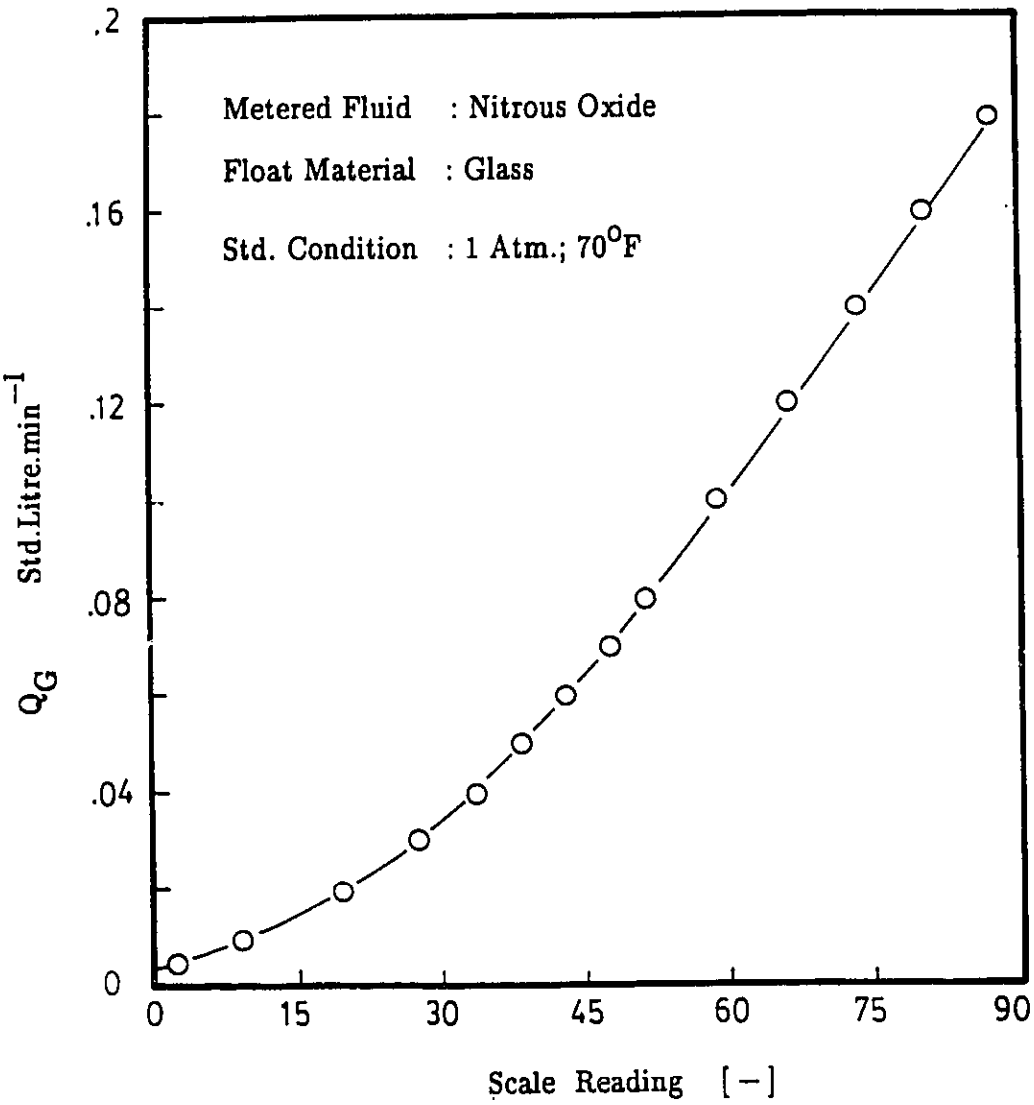

Figure A.5 N_2O Flow Rate Calibration – Gas Proportioner; Data Obtained from Supplier

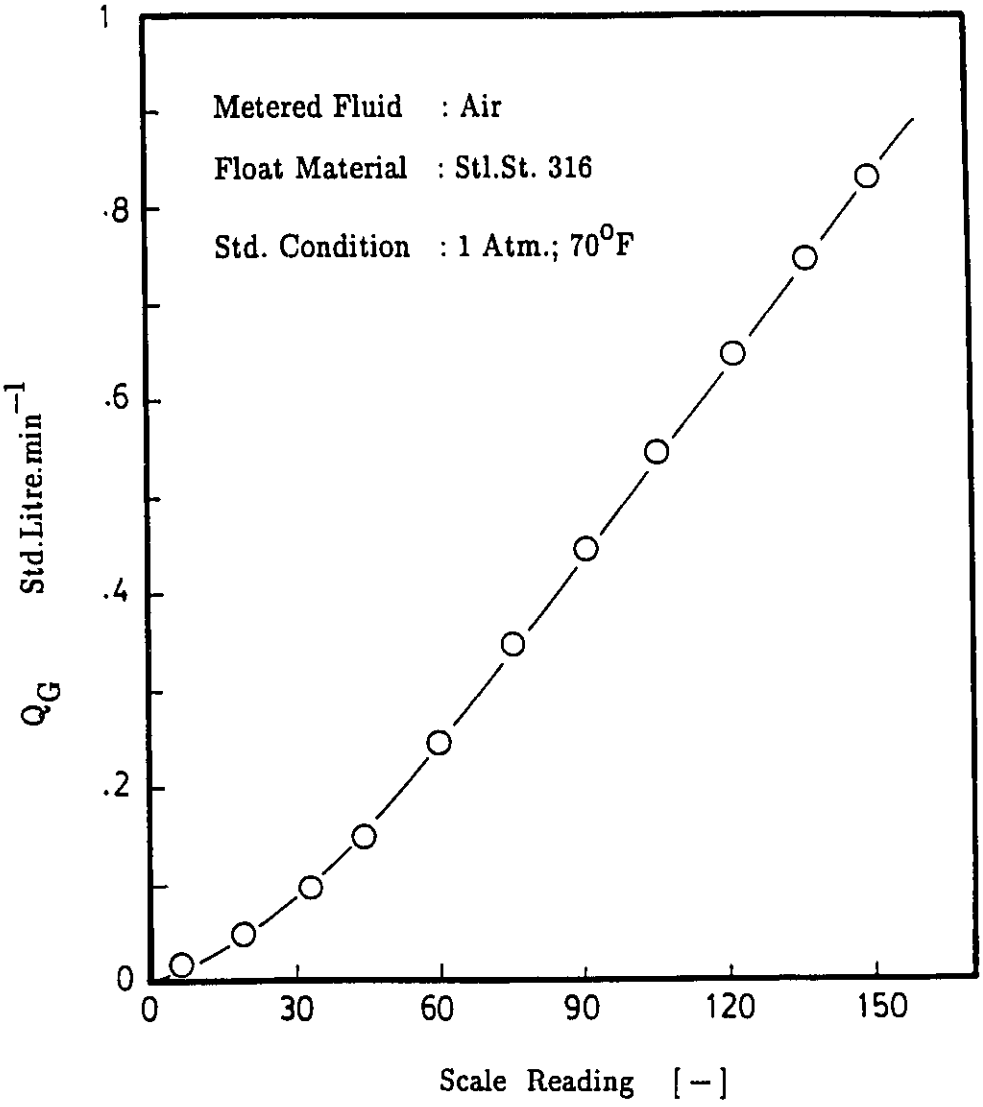

Figure A.6 Air Flow Rate Calibration – Gas Proportioner
Data Obtained from Supplier

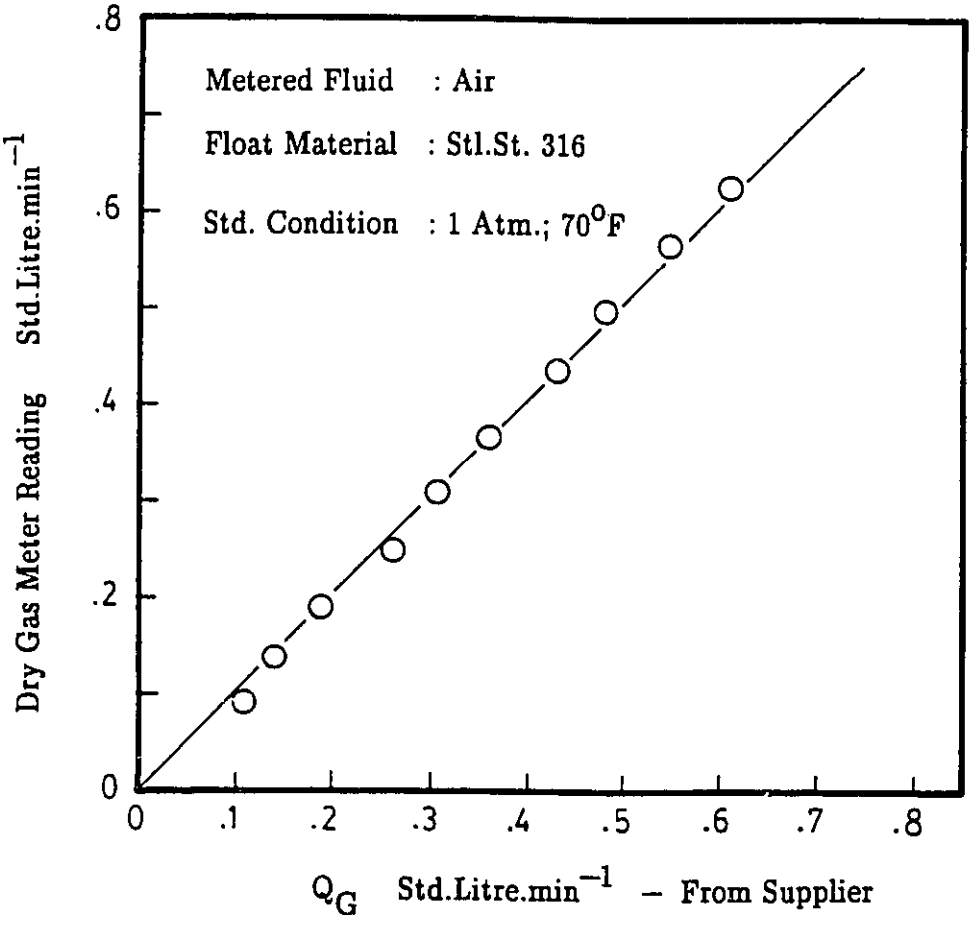

Figure A.7 A Check of Air Calibration Data from Supplier vs Measurement with Dry Gas Meter – Gas Proportioner

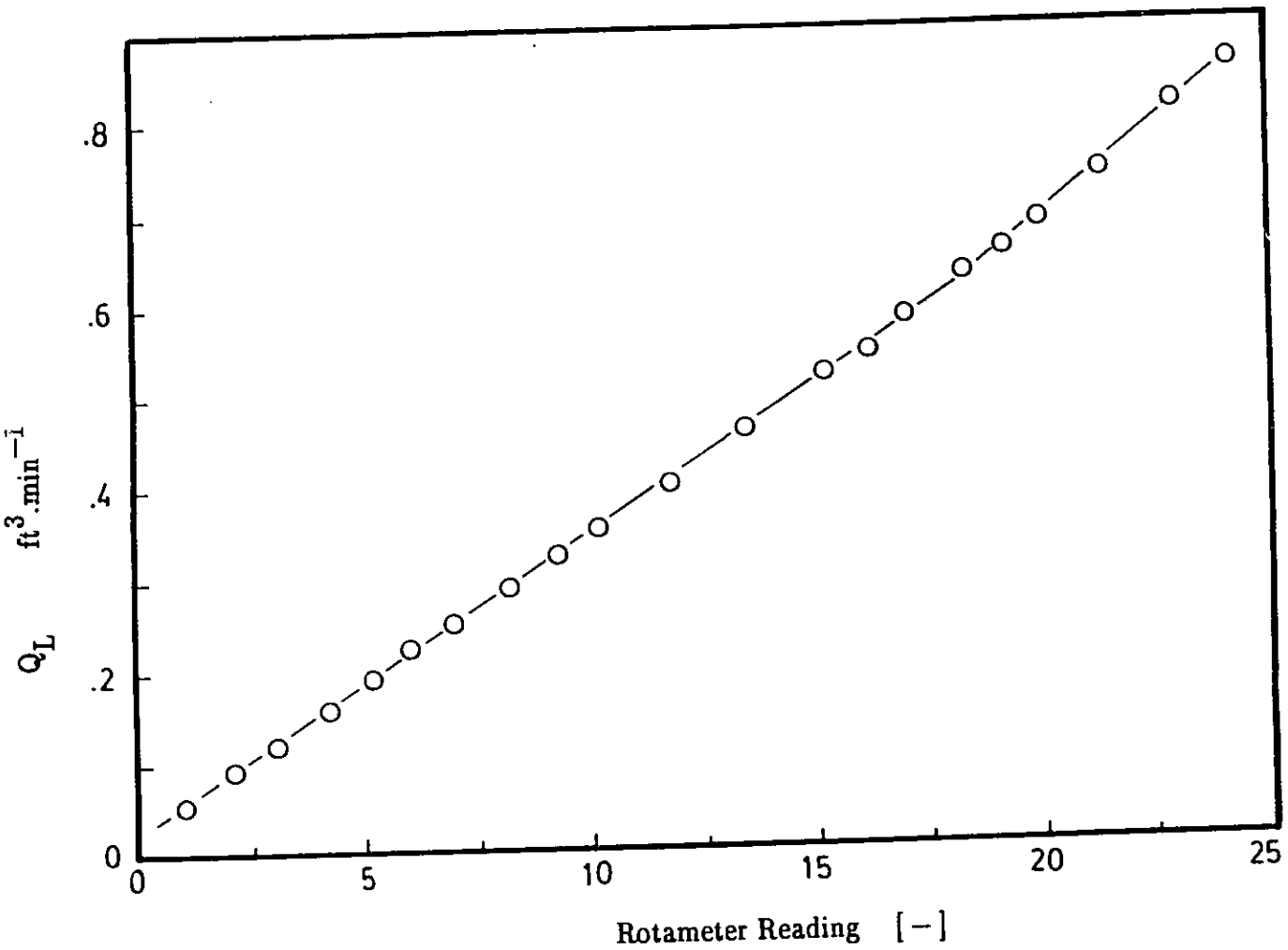

Figure A.8 Water Flow Rate Calibration – Liquid Rotameter

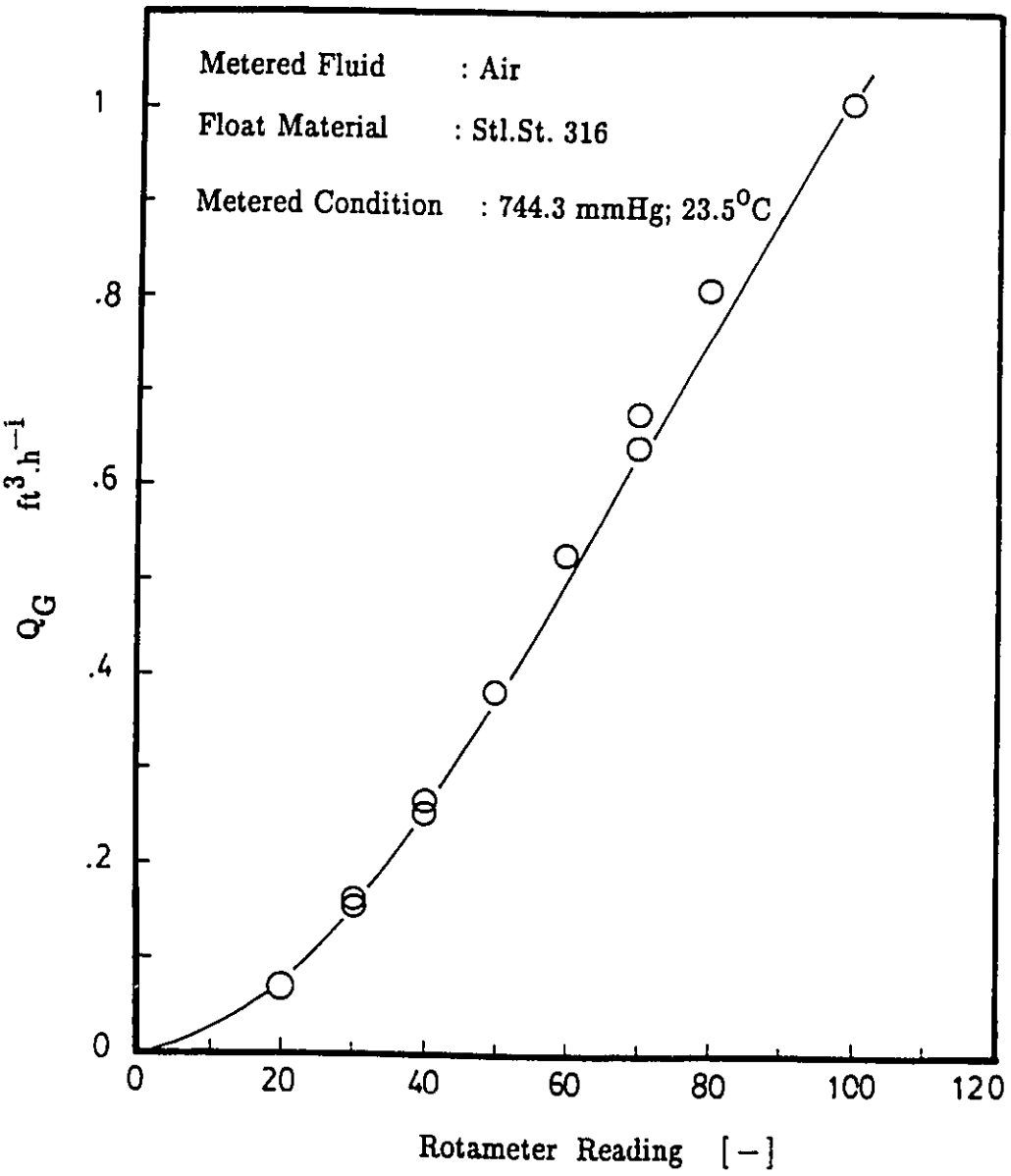

Figure A.9 Air Flow Rate Calibration – Rotameter for NO_x/SO_2 Analyzer

APPENDIX – B

LIST OF CHEMICALS

Chemical	Remarks	Supplier
Pure Gas:		
Nitric Oxide (NO)	99.0% (Min.)	Matheson Canada
Sulphur Dioxide (SO_2)	99.98% (Min.)	:
Span Gas:		
Nitric Oxide	Certified standard NO in N_2 50 ppm; 250 ppm 400 ppm; 450 ppm 700 ppm	:
Sulphur Dioxide	Certified standard SO_2 in N_2 100 ppm; 500 ppm 700 ppm; 1000 ppm 2000 ppm (0.2%)	:
Scrubbing Solution:		
Sodium Chlorite ($NaClO_2$)	powder; 80% by weight	Van Waters & Rogers 927 St.Luke Rd. Windsor, Ontario

Reagents:

Nitri Ver 3	Nitrite reagent Powder pillow Cat.# 14065	Fryston Canada Inc. 1515 Matheson Blvd. Suite B–10, Mississauga, Ont. (416) 629–4421
Nitra Ver 6	Nitrate reagent Powder pillow Cat.# 14119	:
Sulfa Ver 4	Sulfate reagent Powder pillow Cat.# 12065	:
Buffer Solution	Fisher certified pH 4; pH 7.2	Fisher Scientific
Starch Indicator		:
Sodium Thiosulphate Solution	0.025 N	:
Potassium Dichromate Solution	0.1 N	:
Potassium Permanganate Crystal	Fisher certified ACS	:
Potassium Nitrate	Fisher certified ACS	:
Potassium Nitrite	Fisher certified ACS	:

Sodium Hydroxide	Fisher certified ACS	:
Sodium Nitrate	Fisher certified ACS	:
Sodium Nitrite	Fisher certified ACS	:
Sodium Carbonate	Fisher certified ACS	:
Sodium Sulphate	Fisher certified ACS	:
Sodium Sulphite	Fisher certified ACS	:
Sulphuric Acid	Fisher reagent ACS	:
Oxalic Acid Crystal	Fisher certified ACS	:
Hydrochloric Acid	Fisher reagent ACS	:
Chloroform	Fisher reagent ACS	:
Hydrogen Peroxide Solution (30%)	Fisher reagent ACS	:
Potassium Iodide	ACS	J.T.Baker Chemical Co.
Sodium Thiosulphate	5–Hydrate crystal ACS	J.T.Baker Chemical Co.

APPENDIX – C

ANALYTICAL METHODS:

C.1 Determination of $NaClO_2$ Concentrations

C.2 Determination of NO_3^- and SO_4^{2-} Concentrations

C.1 Determination of $NaClO_2$ Concentrations

C.1.1 Preparation and Standardization of 0.1 N Sodium Thiosulphate Solution

Theory

In acidic solution, potassium iodide is oxidized to liberate iodine by a strong oxidizing agent (potassium dichromate) according to:

$$K_2Cr_2O_7 + 6I^- + 14H^+ \longrightarrow 2K^+ + 2Cr^{3+} + 3I_2 + 7H_2O \qquad \text{.....(C.1)}$$

The liberated iodine then oxidizes thiosulphate to tetrathionate ion in strongly acidic solutions of iodine, provided the solutions are well stirred, as shown by:

$$I_2 + 2S_2O_3^{2-} \longrightarrow 2I^- + S_4O_6^{2-} \qquad \text{.....(C.2)}$$

This reaction is fast and goes well to completion. The overall reaction is given by:

$$K_2Cr_2O_7 + 6I^- + 14H^+ + 6S_2O_3^{2-} \longrightarrow 2K^+ + 2Cr^{3+} + 7H_2O + 6I^- + 3S_4O_6^{2-} \quad \text{.....(C.3)}$$

When $S_2O_3^{2-}$ solution is added to a mixture of $K_2Cr_2O_7$ and KI, the $S_2O_3^{2-}$ ion will reduce I_2 to give colorless iodide. As the yellowish color of the solution of iodine nearly disappears, addition of starch as indicator at this point will produce a blue colored starch–iodine complex. At the end point of titration, one drop of $S_2O_3^{2-}$ (titrant) will remove the blue color so that excess $S_2O_3^{2-}$ will react with potassium dichromate directly producing an emerald green chromic ion, a reduced form of dichromate.

It must be noted that starch should not be added to a solution that contains a large quantity of iodine. The starch may be coagulated and the complex with iodine may not easily break up. A recurring end point will then result.

Calculation

The molarity of $S_2O_3^{2-}$ can be found from:

$$M_{S_2O_3^{2-}} = \frac{6000\ X_{K_2Cr_2O_7}}{294.17\ V_{S_2O_3^{2-}}} \qquad \text{.....(C.4)}$$

where

$M_{S_2O_3^{2-}}$ = Molarity of $S_2O_3^{2-}$, M

$V_{S_2O_3^{2-}}$ = Volume of titrant ($S_2O_3^{2-}$), mL

$X_{K_2Cr_2O_7}$ = weight of $K_2Cr_2O_7$, g

Procedure

. Weigh out 24.82 g $Na_2S_2O_3.5H_2O$ and dissolve it in a 1–litre volumetric flask with freshly boiled deionized water.

. Add 0.2 g Na_2CO_3 and a few drops of chloroform as preservative and make up the solution to one litre.

. To each of three prepared conical flasks add:

  . 0.2 g $K_2Cr_2O_7$

  . 4 ml concentrated H_2SO_4

  . 100 ml deionized water

  . 2g Na_2CO_3

  . 5 g KI

. Swirl to dissolve the additives and then cover the solution with a watch glass and let stand for about 3 minutes.

. Titrate with the prepared $Na_2S_2O_3$ until the yellowish color disappears, then add 5 ml starch solution as indicator. The final end point is reached when an emerald green color is observed.

. Calculate the molarity of $S_2O_3^{2-}$ from expression C.4.

A more detailed discussion of the method is given by Day and Underwood (1980).

C.1.2 Determination of $NaClO_2$ Concentration.

Theory:

A similar reaction occurs in the determination of sodium chlorite concentrations as with the standardization of sodium thiosulphate solution.

In acidic medium, sodium chlorite oxidizes potassium iodide to give iodine according to the reaction:

$$2ClO_2^- + 6I^- + 8H^+ \longrightarrow Cl_2 + 3I_2 + 4H_2O \qquad \text{.....(C.5)}$$

The liberated iodine is further reacted with standardized sodium thiosulfate solution as titrant according to:

$$I_2 + 2S_2O_3^{2-} \longrightarrow 2I^- + S_4O_6^{2-} \qquad \text{.....(C.6)}$$

The overall reaction is:

$$2ClO_2^- + 8H^+ + 6S_2O_3^{2-} \longrightarrow Cl_2 + 4H_2O + 3S_4O_6^{2-}$$

.....(C.7)

As titration continues, the brown color of iodine gradually fades. At the point when the brown color has almost disappeared, addition of 5 mL of starch solution causes a deep blue colored starch–iodine complex to form.

At the end point, the dark blue color disappears and the solution becomes clear and colorless.

Calculation

The oxidizing ability of $NaClO_2$ is calculated from,

$$C_{NaClO_2} = \frac{C_{S_2O_3^{2-}} \; V_{S_2O_3^{2-}}}{3V_{NaClO_2}} \qquad \text{.....(C.8)}$$

where

C_{NaClO_2} = concentration of $NaClO_2$, M

$C_{S_2O_3^{2-}}$ = concentration of standard thiosulphate solution, M

$V_{S_2O_3^{2-}}$ = volume of titrant (thiosulphate), mL

V_{NaClO_2} = volume of chlorite solution, mL

or it can be reported as percent chlorine by:

$$\text{Wt \% } Cl_2 = 0.5909\ C_{S_2O_3^{2-}} \frac{V_{S_2O_3^{2-}}}{V_{NaClO_2}} \qquad \text{.....(C.9)}$$

C.2 Determination of Nitrate and Sulphate

C.2.1 Nitrate Determination

Two methods have been examined for nitrate determination. The first is based on the work of Wetters and Uglum (1970). The second procedure was suggested by Levaggi et al. (1976).

C.2.1.1 The Method of Wetters and Uglum (1970)

The present method is based on the following findings of Wetters and Uglum (1970):

. The ratio of the absorbance of aqueous nitrite solution at 355 nm to that at 302 nm is 2.5.

. Nitrate does not absorb at 355 nm but absorbs only at 302 nm.

. Both nitrite and nitrate absorb at 302 nm.

These statements are expressed mathematically according to:

$$\frac{A_{NO_2^-}^{355}}{A_{NO_2^-}^{302}} = 2.5 \qquad \text{.....(C.10)}$$

$$A_{tot}^{302} = A_{NO_3^-}^{302} + A_{NO_2^-}^{302} \qquad \text{.....(C.11)}$$

where

$A_{NO_2^-}^{355}$; $A_{NO_2^-}^{302}$ = absorbance of NO_2^- at 355 nm and 302 nm respectively

A_{tot}^{302} = total absorbance of NO_3^- and NO_2^- at 302 nm

$A_{NO_3^-}^{302}$ = absorbance of NO_3^- at 302 nm

A direct measurement of a sample at 302 nm and 355 nm will permit evaluation of the nitrite and nitrate levels from Equations C.10 and C.11 if the concentration levels of NO_2^- and NO_3^- exceed 20. $\mu gNO_2^-/mL$ and 90. $\mu gNO_3^-/mL$ respectively.

This procedure is described in detail in the following section.

Experiment

Apparatus: Pye Unicam 8600UV/VIS spectrophotometer with 1–cm quartz cell.

Reagents: Sodium nitrite and sodium nitrate.

Objectives:

. To prepare standard absorbance curves for nitrite and nitrate of various concentrations.

. To evaluate the method by analyzing known NO_3^- and NO_2^- levels in mixed solutions.

Procedure: The nitrate and nitrite solutions were required in the experiment. Their preparation were described in the following sections.

a. Preparation of standard solutions of NO_3^- with the following concentrations:

. For lower concentration range.

0.3, 0.6, 0.9, 1.2, 1.5 g–$NaNO_3$.litre^{-1}

. For upper concentration range.

2.0, 4.0, 6.0, 8.0, 10.0 g–$NaNO_3$.litre^{-1}

. Weigh out exactly 100.0 g$NaNO_3$ and dissolve it in a volumetric flask. Make up to one litre with deionized water or distilled water.

. Desired concentrations for the lower detection limit can be prepared by diluting the stock solution with deionized water.

. For upper concentration range, a similar procedure is adopted as for the lower concentration range.

. Prior to sample measurement, the spectrophotometer is warmed up for at least half an hour to stabilize its operation.

. Set the corresponding wavelength (302 nm) for maximum absorbance of NO_3^-.

. Construct the standard curve by plotting the concentrations of NO_3^- vs absorbance.

b. **Preparation of standard solutions of NO_2^- with the following concentrations:**

0.6, 0.9, 1.2, 1.5, 2.0, 2.5, 3.0 g–$NaNO_2$.litre^{-1}

. Weigh out exactly 100.0 g–$NaNO_2$ and dissolve it in a volumetric flask. Make up to one litre with deionized water or distilled water.
. Measure 6, 9, 12, 15, 20, 25, 30 mL of the prepared stock solution and dilute to one litre.
. Measure the absorbance with wavelengths set at 302 nm and 355 nm.
. Construct the standard curve for nitrite by plotting the concentrations of NO_2^- vs absorbance.

c. **Preparation of a mixed solutions of NO_3^- and NO_2^- for method evaluation**

. Prepare a solution of 0.357 mole $NaNO_2$.litre^{-1} by diluting 246.3 mL stock solution prepared in Part b in a litre flask.

. Prepare a solution of 1.177 mole $NaNO_3$.litre^{-1} by dissolving 100.0 g$NaNO_3$ in a litre volumetric flask or use stock solution prepared in Part a.

. Prepare mixed solutions of NO_2^- and NO_3^- with the ratio of concentrations of NO_2^- to NO_3^- varying between 0.3 to 2.

Results and Discussion:

Tables C.1, C.2 and C.3 provide absorbances of nitrate and nitrite solutions of various concentrations. These values are in good agreement with those obtained by Wetters and Uglum (1970). The relationships between absorbance values and solution concentrations are illustrated in Figures C.1, C.2 and C.3.

The ratio of the absorbance of nitrite at 355 nm to that at 302 nm was found to be 2.3 $\pm$ 0.1, a value slightly lower than 2.5 $\pm$ 0.02 obtained by Wetters and Uglum (1970).

A study was performed to evaluate the method by determining known concentrations of nitrate and nitrite in mixed solutions. The results obtained

Table C.1 Nitrate Absorbance at Various Concentrations

Lower concentration range			Upper concentration range		
Nitrate Concentration	Absorbance at 302 nm Measured	Average	Nitrate Concentration	Absorbance at 302 nm Measured	Average
$[gNO_3^-.litre^{-1}]$	[–]	[–]	$[gNO_3^-.litre^{-1}]$	[–]	[–]
0.219	0.045 0.046 0.051 0.053	0.048	1.459	0.188 0.184 0.187 0.196	0.189
0.438	0.074 0.074 0.072 0.072	0.073	2.918	0.351 0.351 0.360 0.356	0.355
0.657	0.097 0.098 0.110 0.106	0.103	4.378	0.513 0.512 0.524 0.526	0.519
0.876	0.119 0.119 0.125 0.127	0.123	5.837	0.669 0.673 0.689 0.690	0.680
1.094	0.146 0.144 0.155 0.155	0.150	7.296	0.826 0.810 0.838 0.848	0.831

Table C.2 Nitrite Absorbance at Various Concentrations

Nitrite Concentration	Absorbance at 302 nm		355 nm		
	Measured	Average	Measured	Average	$A^{355}_{NO_2^-}/A^{302}_{NO_2^-}$
$[gNO_2^-.litre^{-1}]$	[–]	[–]	[–]	[–]	[–]
0.400	0.110 0.113		0.233 0.230 0.230 0.236		
		0.112		0.232	2.07
0.600	0.147 0.157		0.331 0.328 0.331 0.329		
		0.152		0.330	2.17
0.800	0.186 0.198		0.423 0.424 0.412 0.431		
		0.192		0.426	2.20
1.000	0.226 0.236		0.522 0.521 0.534 0.532		
		0.231		0.527	2.28
1.334	0.291 0.300		0.676 0.679 0.675 0.687		
		0.296		0.679	2.29
1.667	0.360 0.357		0.840 0.839 0.843 0.844		
		0.359		0.842	2.35
2.000	0.423 0.418		0.994 0.992 0.999 0.994		
		0.421		0.995	2.36
				Average:	2.25

Table C.3 Absorbance of Nitrate and Nitrite in Mixed Solutions of NO_3^- and NO_2^- with Various Concentration Ratios

Total solution volume = 250 mL

Nitrite	Nitrate	$[NO_2^-]/[NO_3^-]$	Absorbance at 302 nm		Absorbance at 355 nm	
$[gNO_2^-]$	$[gNO_3^-]$	[–]	Measured	Average	Measured	Average
0.2464	1.0944	0.2251	0.700 0.673 0.699 0.708	0.695	0.513 0.512 0.517 0.515	0.514
1.2320	1.0944	1.1257	1.409 1.409 1.414 1.417	1.412	2.002 2.004 2.000 2.005	2.003
1.7248	1.0944	1.5761	1.690 1.688 1.687 1.700	1.691	2.161 2.204 2.154 2.199	2.180
2.4640	1.0944	2.2510	1.965 1.976 1.963 1.953	1.964	2.197 2.171	2.185

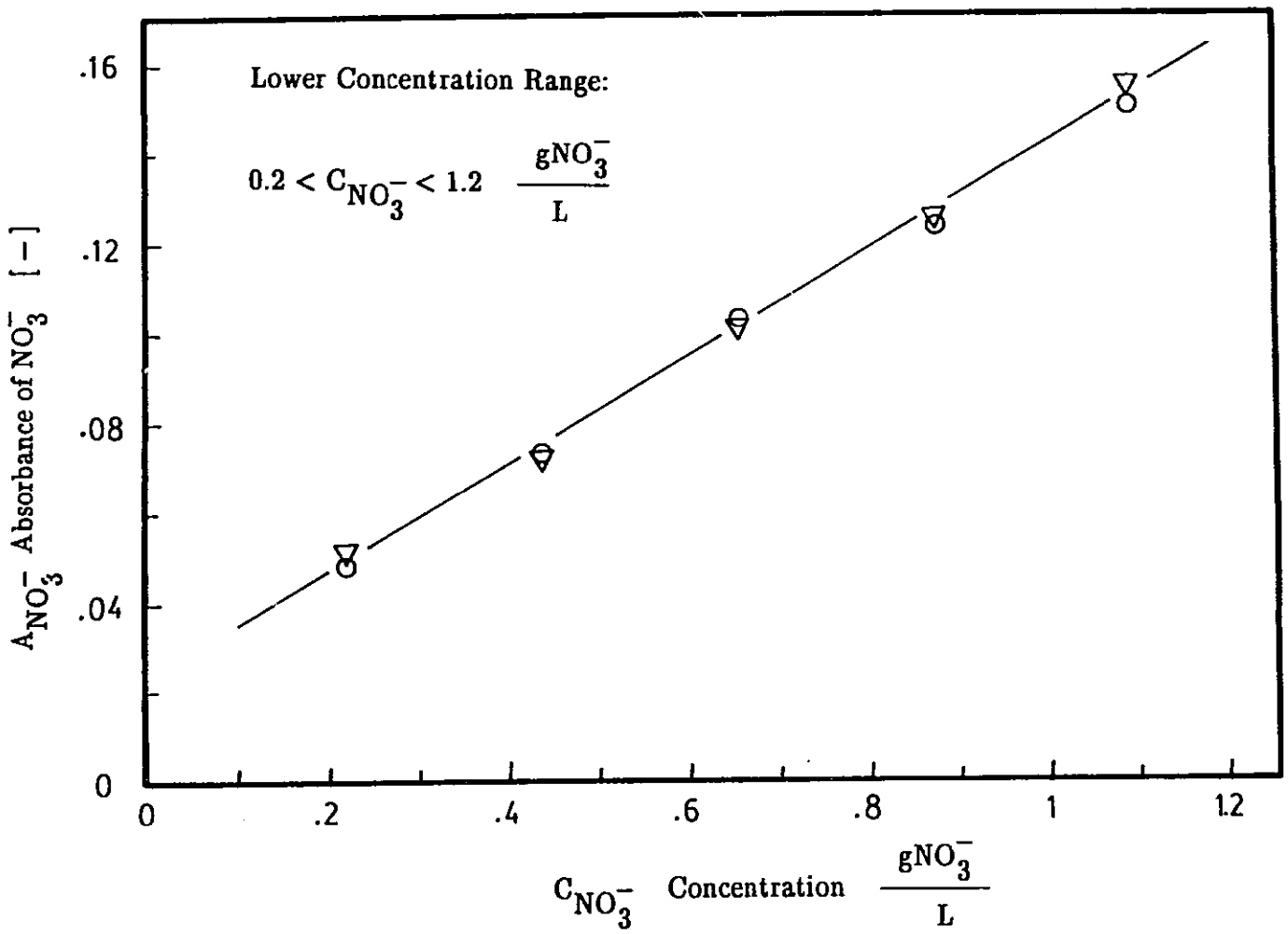

Figure C.1 Standard Curve for $NaNO_3$ Absorption vs $NaNO_3$ Concentration for $\lambda = 302$ nm; (with built in instrument zero function)

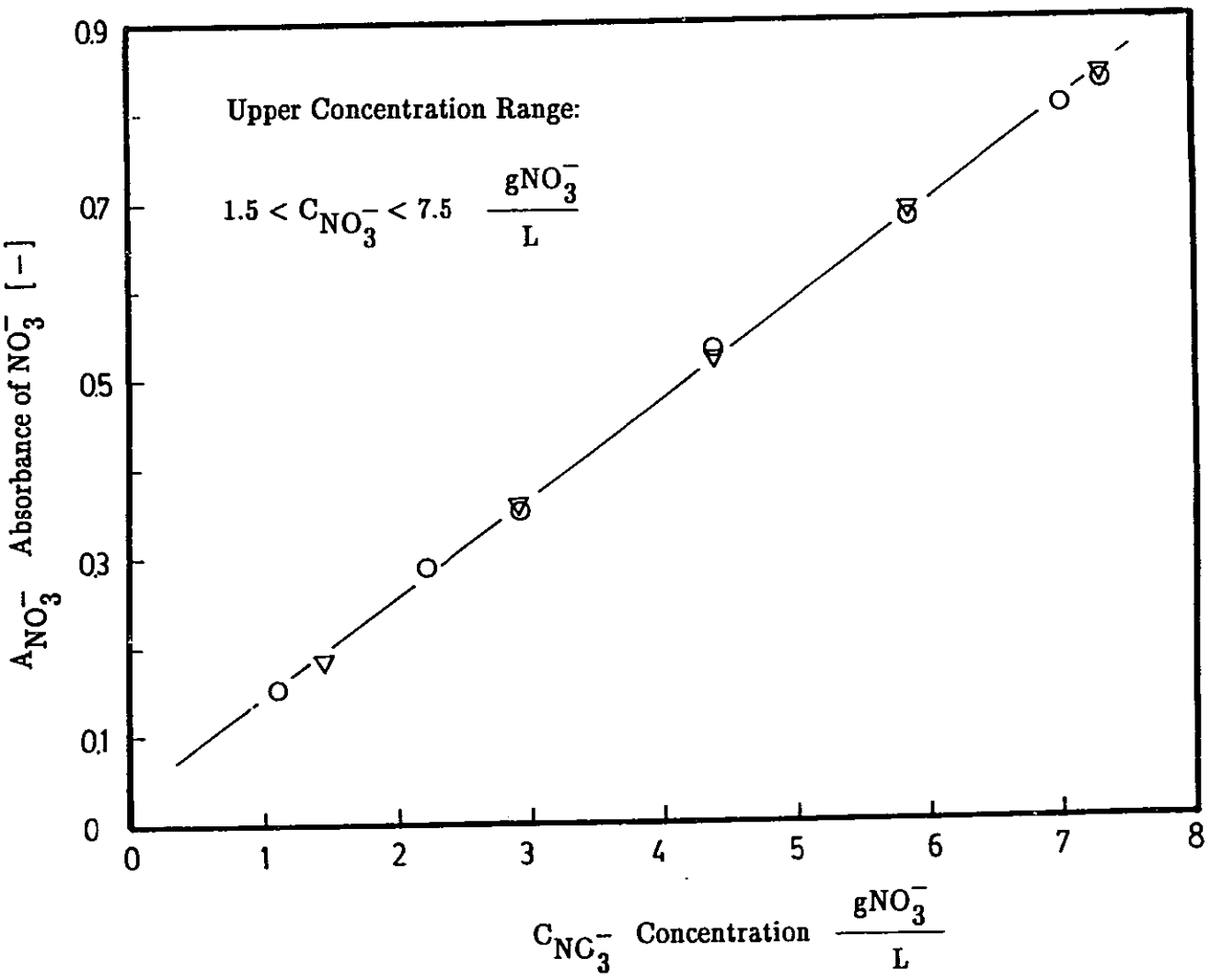

Figure C.2 Standard Curve for $NaNO_3$ Absorbance vs $NaNO_3$ Concentration for $\lambda = 302$ nm (with built in instrument zero function)

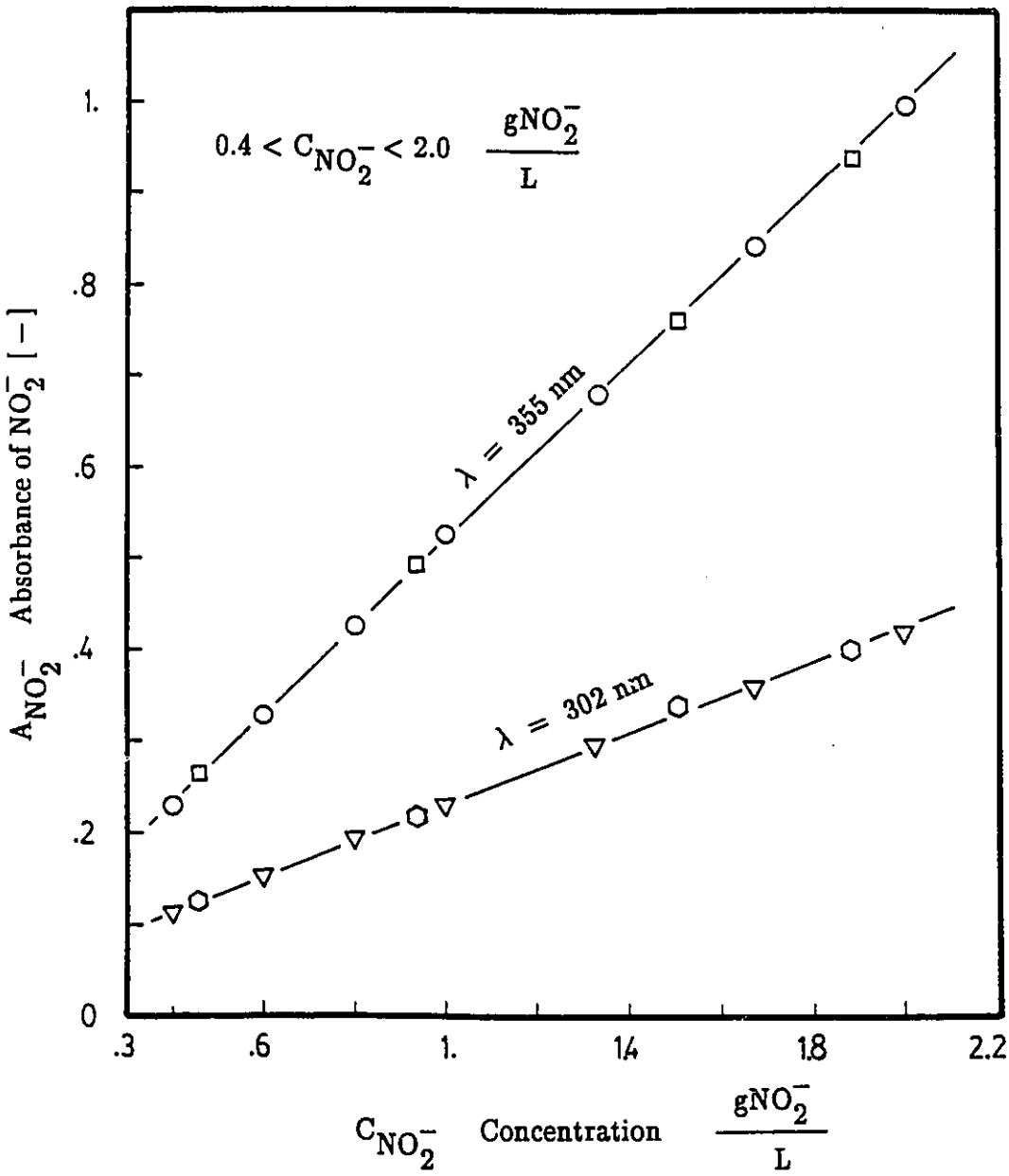

Figure C.3 Standard Curve for $NaNO_2$ Absorbance vs $NaNO_2$ Concentration for $\lambda = 302$ nm and $\lambda = 355$ nm (with built in instrument zero function)

from this study are shown in Tables C.4, C.5 and C.6. They are illustrated graphically in Figures C.4, C.5 and C.6.

Figure C.4 shows that this procedure is valid for $[NO_2^-]/[NO_3^-]$ ratios less than unity. If the concentration ratio exceeds this limit, the nitrite absorbance curve levels off to render the method inapplicable. Figures C.5 and C.6 illustrated that if concentration ratios are kept below unity, there is excellent agreement between actual nitrite and nitrate concentrations and values determined from the Wetters and Uglum method (1970). In spite of its simplicity, the Wetters and Uglum method (1970) could not be used for the low concentrations of NO_x in the liquids associated with this investigation.

C.2.1.2 Cadmium Reduction Method (Levaggi et al., 1976; Hach Chemical, 1975)

This method was suggested by Levaggi et al. (1976). It was tested during field sampling. The results obtained using this procedure are reported to be comparable to those provided by the instrumental chemiluminescence and the phenoldisulphonic acid procedures. The detection limit for nitrate is 2. μg/mL or slightly lower.

In the absorption of NO_x, nitrite and nitrate probably exist in the liquid

Table C.4 Absorbance of Nitrate and Nitrate in Mixed Solutions of NO_3^- and NO_2^-

Total solution volume = 250 mL

Concentration ratio = $0. < [NO_2^-]/[NO_3^-] < 1.$

Nitrite	Nitrate	$[NO_2^-]/[NO_3^-]$	Absorbance at 302 nm		Absorbance at 355 nm	
$[gNO_2^-]$	$[gNO_3^-]$	[–]	Measured	Average	Measured	Average
0.2464	1.0944	0.2257	0.700 0.699	0.700	0.531 0.512	0.513
0.3280	1.0944	0.2997	0.752 0.765	0.759	0.677 0.675	0.676
0.4921	1.8240	0.2698	1.196 1.199	1.198	0.985 0.986	0.986
0.6725	1.0944	0.6145	1.021 1.035	1.028	1.299 1.296	1.298
0.8202	2.5537	0.3212	1.657 1.652	1.655	1.544 1.544	1.544
0.9842	1.0944	0.8993	1.248 1.245	1.247	1.764 1.760	1.762

Table C.5 Actual Nitrite and Nitrate Levels Compared to Values Determined from the Method of Wetters and Uglum (1970) – Based on Absorbance Measurements Given in Table C.4.

Concentration of Nitrite			Concentration of Nitrate		
Actual amount	Calculated from Wetter and Uglum method	Error	Actual amount	Calculated from Wetters and Uglum method	Error
$[gNO_2^-.litre^{-1}]$		%	$[gNO_3^-.litre^{-1}]$		%
0.986	0.98	–0.6	4.378	4.10	–6.3
1.312*	1.32	+0.6	4.378	4.10	–6.3
1.968	1.96	–0.4	7.296	7.02	–4.0
2.679	2.64	–1.5	4.360	4.33	–0.6
3.281	3.15	–4.0	10.215	9.70	–5.0
3.937	3.76	–4.5	4.533	4.533	+3.5

* Sample Calculation:

Step 1:

$C_{NO_2^-} = 0.328\ [gNO_2^-] \times (1000/250)\ [litre^{-1}] = 1.312\ gNO_2^-.litre^{-1}$

Step 2:

For $A^{3\,5\,5}_{NO_2^-} = 0.676$ check from standard curve of nitrite, we have

$C_{NO_2^-} = 1.320\ \ gNO_2^-.liter^{-1}$

Step 3:

Use expressions C.10 and C.11 to get $A^{3\,0\,2}_{NO_3}$ and check for nitrate level from standard curve of nitrate, $C_{NO_3^-} = 4.10\ \ gNO_3^-.liter^{-1}$.

Table C.6 Total Nitrate Levels Compared to Values Determined from the Method of Wetters and Uglum (1970) – in Mixed Solutions of NO_3^-, NO_2^- and ClO_2^-; Treated with 6.3 % Oxalic Acid

Concentration of $NaClO_2$ = 0.448 M

Concentration of Nitrite	Concentration of Nitrate	Absorbance at 302 nm	Absorbance at 355 nm	Concentration of Nitrate Total	Concentration of Nitrate Calculated	Error
[gNO_2^-/L]	[gNO_3^-/L]	[–]	[–]	[gNO_3^-/L]		%
0.10*	0.2*	0.079	0.034	0.335*	0.32	–4.4
0.25	0.5	0.147	0.035	0.837	0.86	+3.5
0.50	1.0	0.256	0.035	1.674	1.73	+3.4
1.50	3.0	0.655	0.035	5.022	5.23	+4.1
2.50	5.0	1.113	0.036	8.369	8.50	+1.6
3.50	7.0	1.407	0.040	11.717	11.63	–0.7

* Sample Calculation:

In one litre of mixed solution when NO_2^- is totally converted to NO_3^-

there will be (0.1x62)/46 + 0.2 = 0.335 g–NO_3^- presence in the final solution

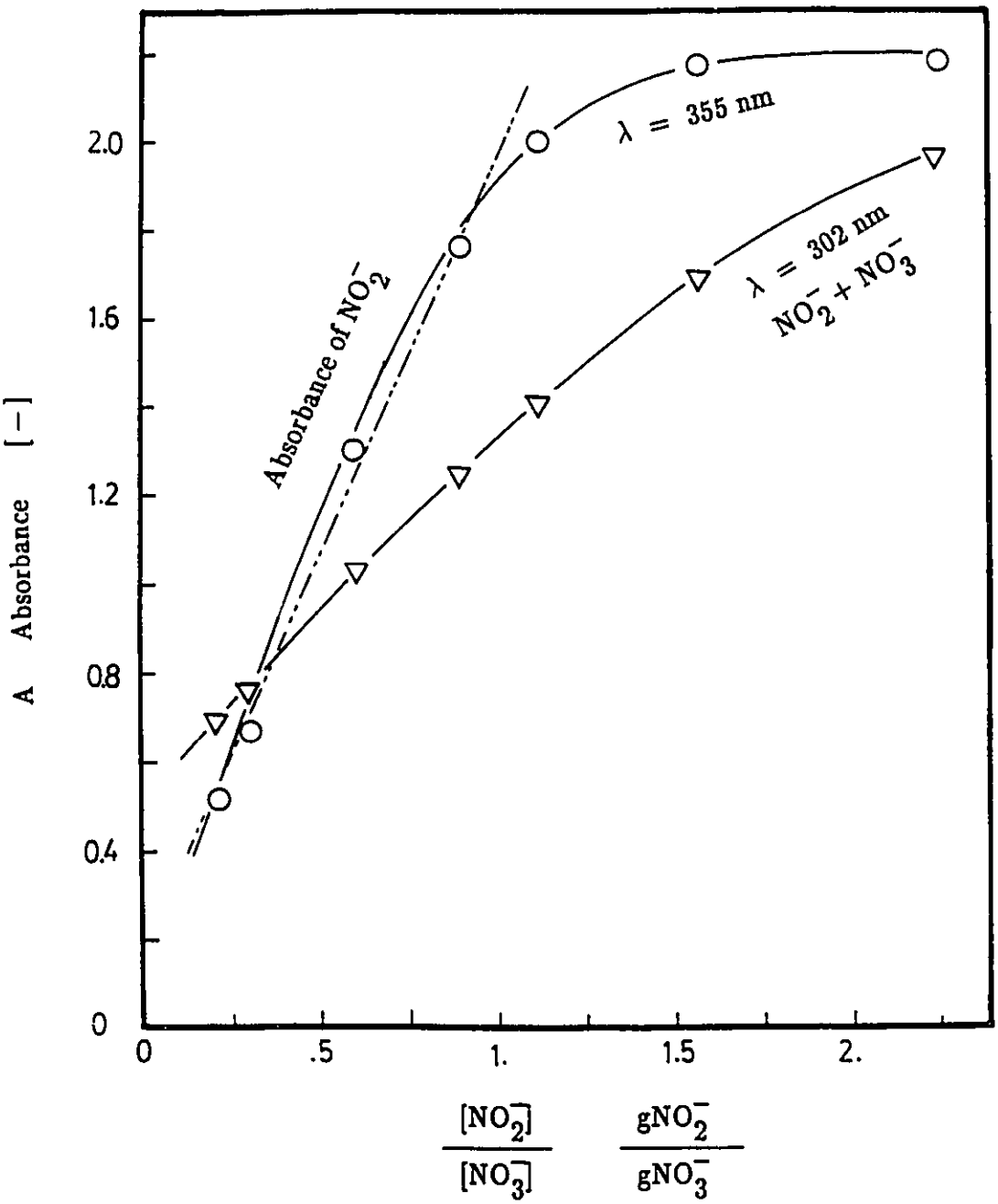

Figure C.4 Dependence of the Absorbance of Mixed Solutions of $NaNO_2 + NaNO_3$ on $[NO_2^-]/[NO_3^-]$ for $\lambda = 302$ nm and $\lambda = 355$ nm

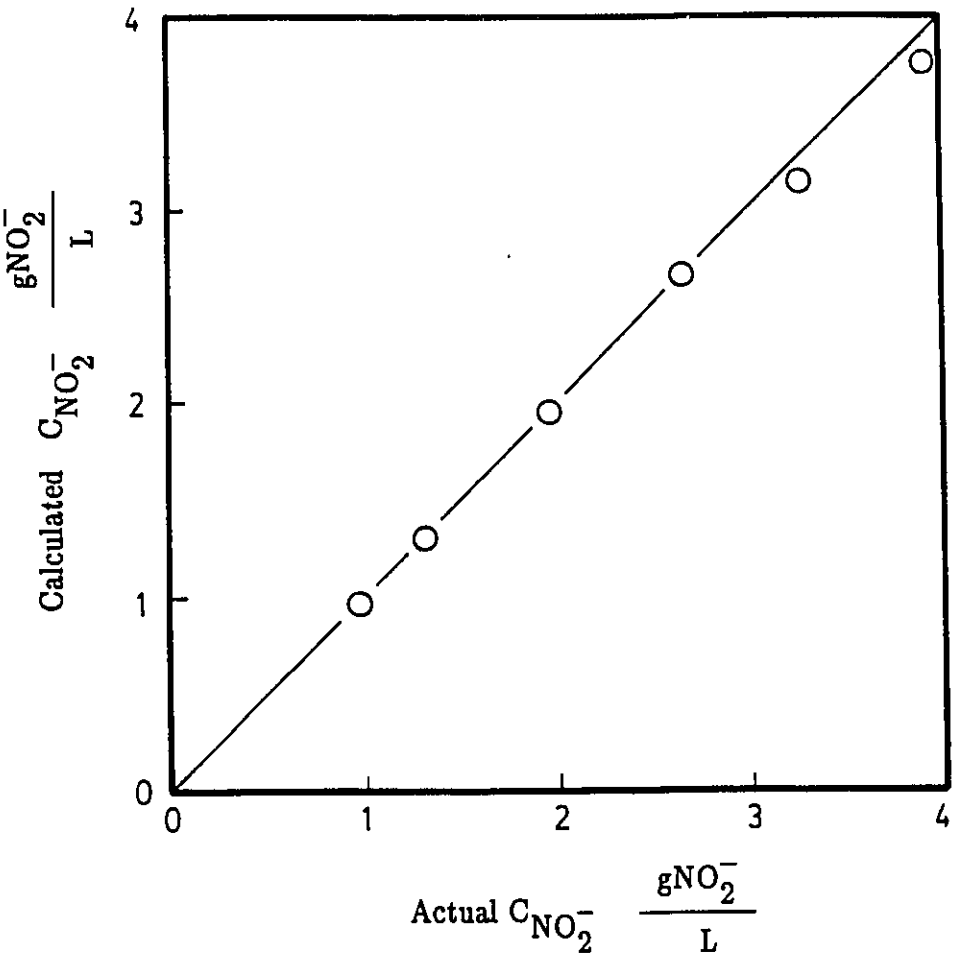

Figure C.5 Calculated $C_{NO_2^-}$ (from Wetters and Uglum Method [1970]) vs Actual $C_{NO_2^-}$ Values

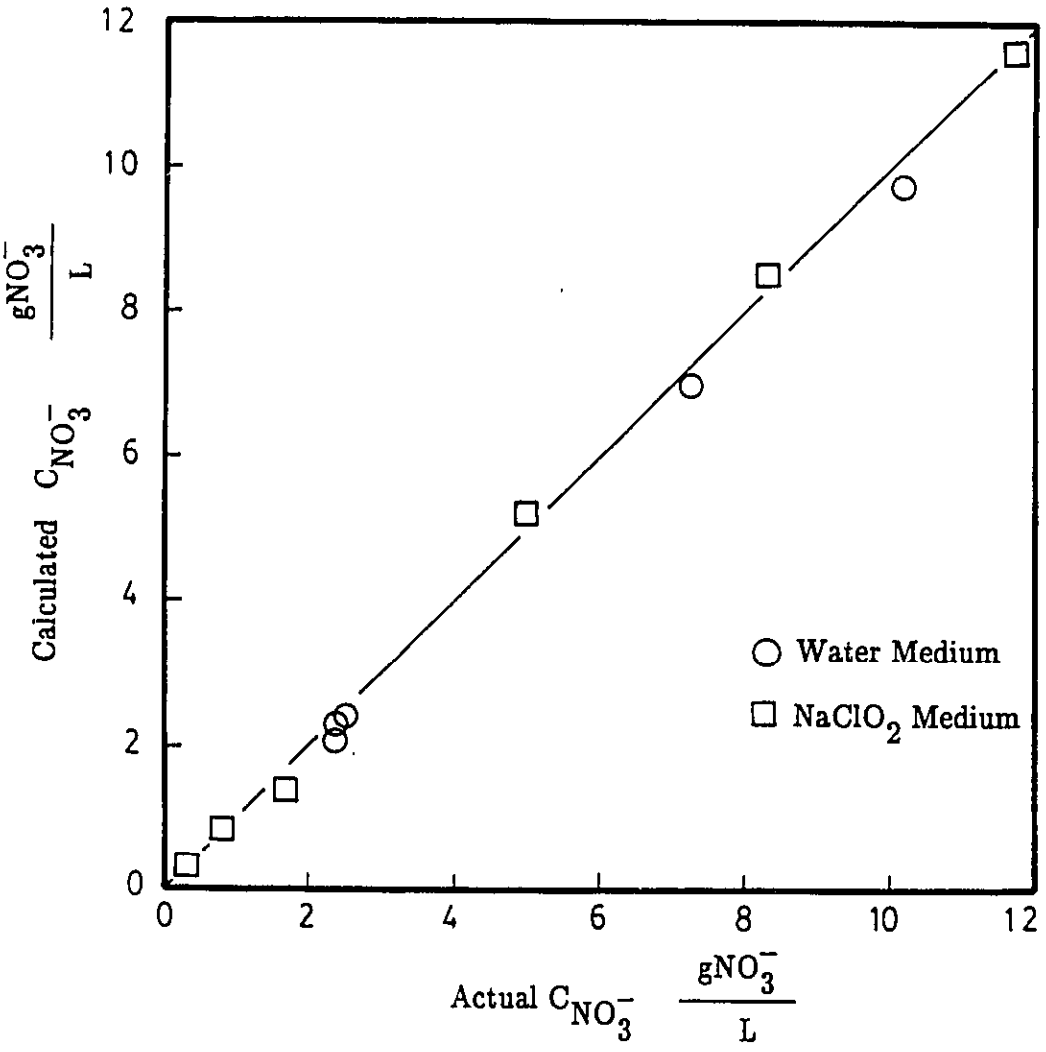

Figure C.6 Calculated $C_{NO_3^-}$ Values (from Wetters and Uglum Method [1970]) vs Actual $C_{NO_3^-}$ Values

sample. Consequently a common base point is needed for this procedure to apply. It can be achieved by adding Nitra Ver 6 – Nitrate reagent to reduce nitrate to nitrite. This nitrite is then reacted with Nitri Ver 3 – Nitrite reagent, diazotized and coupled to form a red dye compound which exhibits a characteristic absorbance at $\lambda = 500$ nm. However, the presence of an oxidizing agent might slow down the Nitra Ver 6 reduction capability. This possible interference is discussed in more detail in a later section.

Experiment

Apparatus: Pye Unicam 8600UV/VIS spectrophotometer with 1–cm quartz cell.

Reagents: Sodium nitrite, sodium nitrate, Nitra Ver 6 – Nitrate reagent and Nitri Ver 3 – Nitrite reagent.

Objectives:

. To prepare standard absorbance curve for nitrate using Nitra Ver 6 Nitrate reagent.

. To test for nitrate and nitrite in scrubbing water.

. To evaluate the method by analyzing known NO_3^- levels in mixed solutions of NO_2^-, SO_3^{2-}, and SO_4^{2-}.

. To determine NO_3^- levels in the presence of an oxidizing agent – sodium chlorite.

a. Preparation of standard curve for nitrate using Nitra Ver 6 – Nitrate reagent.

The low range nitrate test is a modification of the cadmium reduction method using a very sensitive chromotropic acid indicator. This procedure determines both nitrates and nitrites. The high range test is also a modification of the cadmium reduction method using gentistic acid instead of 1–naphthylamine. The test determines both nitrates and nitrites present in the sample and eliminates the need for dilutions by operating in a very useful range. All the necessary reagents have been combined into a single stable powder pillow named Nitra Ver 6 – Nitrate reagent.

The following procedure was adopted: A Nitra Ver 6 – Nitrate reagent pillow was added to the prepared nitrate solution which was immediately stoppered and shaken for exactly 3 minutes. The sample was allowed to stand for 30 seconds before a Nitri Ver 3 – Nitrite reagent pillow was added. The solution was shaken for another 30 seconds and then left undisturbed for proper

color development. At least 10 minutes standing time was required for the sample, but no more than 20 minutes was allowed. The sample was then analyzed spectrophotometrically for absorbance values at a wavelength of 500 nm.

The results are plotted in Figure C.7.

b. Use of Nitra Ver 6 reagent to test for nitrate and nitrite in tap water.

This procedure was used to test for nitrate and nitrite in tap water from the laboratory. Typical results are shown in Table C.7. The average nitrate level was found to be 1.68 $\mu g NO_3^-$/mL. There was no nitrite detected as indicated by the absence of the characteristic pink color development. The same procedure was used to determine nitrate levels when water scrubbing experiments were performed.

c. Nitrate determination in the presence of oxidizing agent – sodium chlorite

The presence of an oxidizing agent might interfere with the reduction

Table C.7 Nitrate and Nitrite Levels in Tap Water

Sample Number	Absorbance at 500 nm		Amount of	
	Nitrate	Nitrite	Nitrate [$\mu gNO_3^-/mL$]	Nitrite [$\mu gNO_2^-/mL$]
1	0.318	0.041	1.68	–
2	0.321	0.042	1.68	–
3	0.318	0.040	1.68	–
		Average =	1.68	–

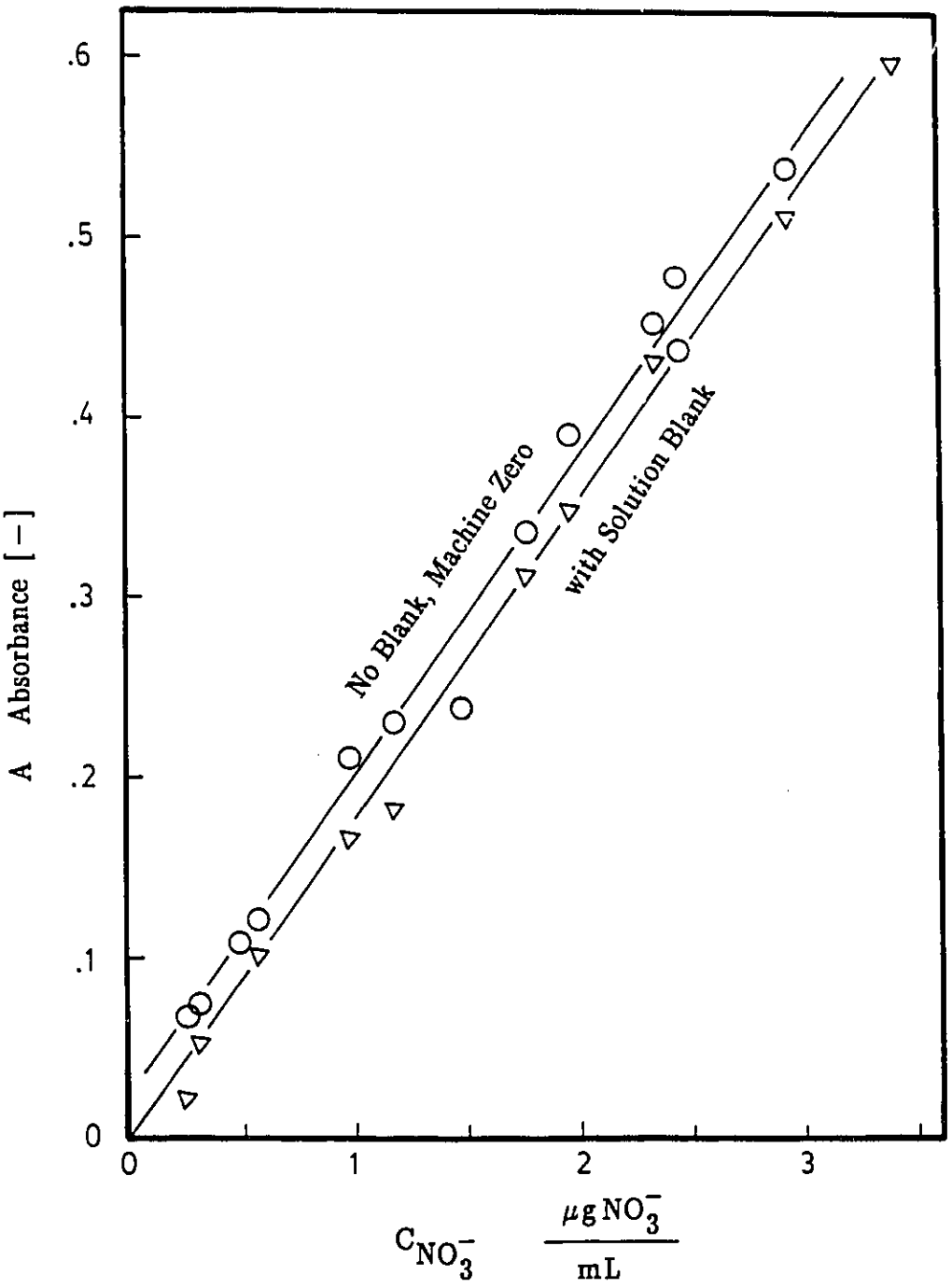

Figure C.7 Standard Curve for NO_3^- Absorbance vs Concentration at $\lambda = 500$ nm

step in the nitrate determination. In a series of experiments, this procedure was applied to nitrate determination in the presence of sodium chlorite by successive measurement of absorbance with time. Aliquots of 8 mL each of nitrate (4.5 $\mu gNO_3^-.mL^{-1}$) and nitrite (1.4 $\mu gNO_2^-.mL^{-1}$) solution were added to 17 mL of sodium chlorite solution of concentration $1.3x10^{-2}$ M. The procedure for testing was similar to that described in the previous experiments.

Preliminary experiments on the effect of chlorite ion during nitrate determination provided the data in Figure C.8, and Table C.8. It is evident that the presence of chlorite ion does interfere with the procedure by slowing down the formation of the red nitrite dye compound. It also appears that as the holding time increased, the measured nitrate concentration approached the actual value. The nitrate concentration reached 98.5% of the actual value after 20 hours had elapsed.

This test procedure took too long to produce the required results. Consequently, development of ways to speed up the reaction was essential. Oxalic acid was tested as an agent for accelerating the desired process. The experimental results are given in Table C.9 and illustrated in Figure C.8 for comparison. It is evident from the data in Figure C.8 that the addition of oxalic acid speeded up the reaction remarkably. The time taken to reach 98.5% of the actual value was reduced from 20 hours to 10 hours. It must be emphasized that the chlorite concentration in this later test (0.5 M) was much higher than the

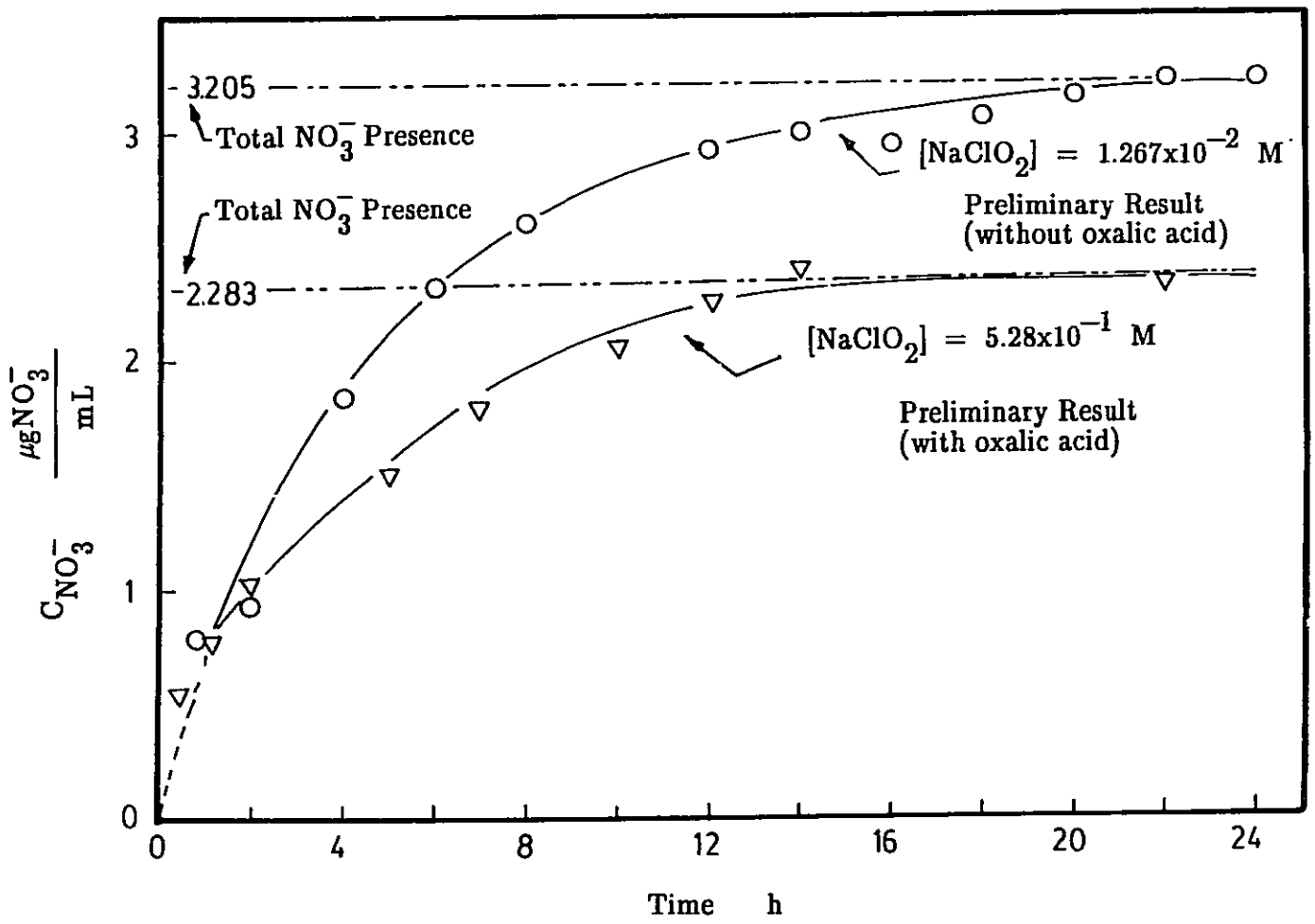

Figure C.8 Measured NO_3^- Levels as a Function of Time in $NaClO_2$ Medium

Table C.8 Preliminary Nitrate Determination in the Presence of Sodium Chlorite

Sodium Chlorite Concentration = 1.27×10^{-2} M

Amount of nitrate taken = 3.205 $\mu g NO_3^-/mL$

Time	Sample 1		Sample 2		Sample 3		Sample 4	
	Amount found	Error	Amount found	Error	Amount found	Error	Amount found	Error
[h]	[$\mu g NO_3^-/mL$]	%	[$\mu g NO_3^-/mL$]	%	[$\mu g NO_3^-/mL$]	%	[$\mu g NO_3^-/mL$]	%
0.75	0.88	−72.5	0.66	−79.4	0.87	−72.8	0.86	−73.2
2.00	0.93	−71.0	0.93	−71.0	0.95	−70.3	0.92	−71.3
4.00	1.86	−42.0	1.90	−40.7	1.96	−38.8	1.84	−42.6
6.00	2.33	−27.0	2.43	−24.2	2.46	−33.2	2.33	−27.0
8.00	2.73	−14.8	2.72	−14.8	2.73	−14.8	2.62	−18.3
12.0	2.88	−10.1	2.98	−7.02	2.97	−7.02	2.97	−7.02
14.0	3.02	−5.77	3.04	−5.14	3.06	−4.52	3.08	−3.90
16.0	3.04	−5.14	3.06	−4.52	3.07	−4.20	3.09	−3.59
18.0	3.08	−3.90	3.10	−3.27	3.12	−2.65	3.12	−2.65
20.0	3.14	−2.03	3.16	−1.40	3.14	−2.03	3.16	−1.40
22.0	3.23	+1.1	3.22	+0.5	3.20	+0.2	3.23	+0.8
24.0	3.23	+1.1	3.24	+1.1	3.22	+0.5	3.23	+0.8

Table C.9 Preliminary Nitrate Determination in the Presence of Sodium Chlorite When Sample is Treated with Oxalic Acid

Sodium Chlorite Concentration = 5.28×10^{-1} M

Amount of nitrate taken = 2.283 $\mu g NO_3^-/mL$

Time	Sample 1		Sample 2		Sample 3		Sample 4	
	Amount found	Error	Amount found	Error	Amount found	Error	Amount found	Error
[h]	[$\mu g NO_3^-/mL$]	%	[$\mu g NO_3^-/mL$]	%	[$\mu g NO_3^-/mL$]	%	[$\mu g NO_3^-/mL$]	%
0.25	0.70	−69.3	0.73	−68.0	0.70	−69.3	0.72	−68.0
1.00	0.95	−58.4	0.97	−57.5	0.94	−58.8	0.97	−57.5
2.00	1.00	−56.2	1.25	−45.3	1.23	−46.1	1.25	−45.3
5.00	1.68	−26.4	1.73	−24.2	1.68	−26.4	1.80	−21.2
7.00	1.92	−15.9	2.01	−12.0	1.95	−14.9	2.06	−9.77
10.0	2.14	−6.26	2.20	−3.66	2.18	−4.51	2.23	−2.32
12.0	2.25	−1.44	2.29	+0.30	2.21	−3.19	2.29	+0.30
14.0	2.29	+0.30	2.33	+2.06	2.24	−1.88	2.34	+2.06
22.0	2.21	−3.20	2.30	+0.74	2.27	−0.57	2.31	+1.18

earlier values ($1.3x10^{-2}$ M). To confirm the valid use of oxalic acid, further tests were conducted. The results will be discussed in a later section.

When oxalic acid is added to a sample solution containing chlorite ion, a greenish yellow color is produced, indicating that chlorite ion is being oxidized to chlorine. This dissolved chlorine must be expelled from the sample solution by gentle boiling until a colorless solution is obtained. The sample solution must be chilled to room temperature and readjusted to its original volume prior to testing by the cadmium reduction procedure. The boiling step is important because the dissolved chlorine in the sample solution might hinder the proper formation of the nitrite compound and color development.

e. Nitrate determination in various chlorite concentrations with oxalic acid addition

The applicability of oxalic acid as a reducing agent to counteract excess chlorite ion was examined in more detail. Initially, a sample solution was prepared from 3.749 g–$NaNO_2$ (5.0 g–NO_2^-/L) and 6.856 g$NaNO_3$ (10.0 g–NO_3^-/L) in 500 mL of 0.448 M sodium chlorite solution. This sample solution was diluted to provide solutions containing 0.2, 0.5, 1.0, 3.0, 5.0, 7.0, and 10.0 g–NO_3^-/L. The sodium chlorite concentration was determined by titration with

standard sodium thiosulphate. On this basis, the volume of oxalic acid required to react with the chlorite was calculated. About 5% excess of the calculated volume was added to the solution. After gentle boiling and sample volume re–adjustment, the solution was analyzed for nitrate by the cadmium reduction method. The results are shown in Figure C.9 and given in Table C.10. The measured values show good agreement with the amounts taken. These data confirm the use of oxalic acid for nitrate determinations in the presence of chlorite.

Conclusions

1. The cadmium reduction method has been tested for nitrate determinations and its validity was confirmed for use during this investigation.

2. The presence of chlorite ion interferes with the procedure, but problems can be avoided by the addition of oxalic acid.

3. A brief review of the modified procedure shows that the excess chlorite in the liquid sample must be eliminated prior to the addition of Nitra Ver 6 and Nitri Ver 3 reagents by introducing a slightly excess amount

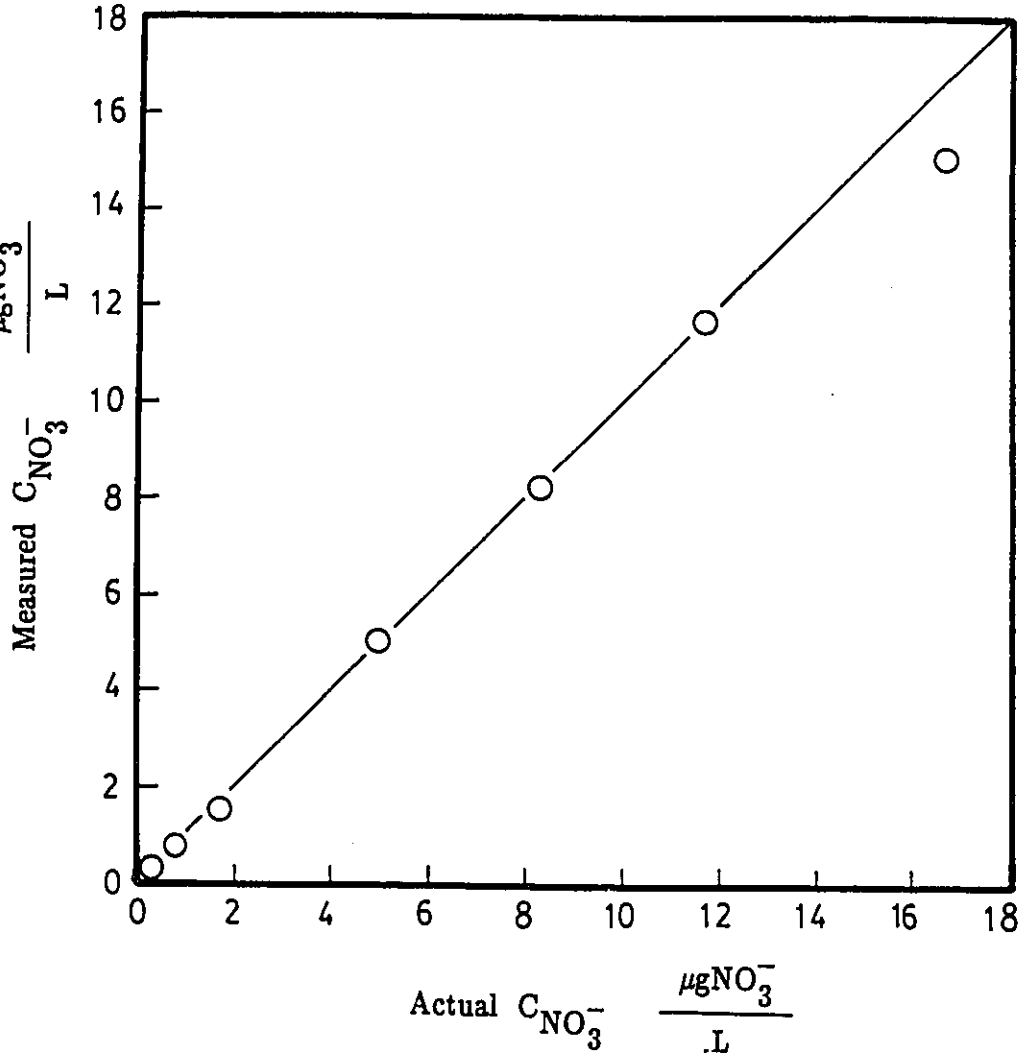

Figure C.9 Measured $C_{NO_3^-}$ vs Actual $C_{NO_3^-}$ with Cadmium Reduction Method at $\lambda = 500$ nm; solution mixture has been treated with 6.3% Oxalic acid (measurement taken when sample was boiled and chilled – 2 hours)

Table C.10 Nitrate Determination in Various Sodium Chlorite Concentrations When Sample is Treated With Oxalic Acid

Sample number	Sodium Chlorite concentration	Amount taken		Total amount taken	Amount found	Error
	[M]	[gNO_3^-/L]	[gNO_2^-/L]	[gNO_3^-/L]	[gNO_3^-/L]	%
1	$4.0x10^{-3}$	0.2	0.10	0.335	0.330	−1.5
2	$1.0x10^{-2}$	0.5	0.25	0.837	0.821	−1.9
3	$1.7x10^{-2}$	1.0	0.50	1.674	1.667	−0.4
4	$5.0x10^{-2}$	3.0	1.50	5.022	5.08	+1.1
5	$8.4x10^{-2}$	5.0	2.50	8.369	8.167	−2.4
6	$1.2x10^{-1}$	7.0	3.50	11.717	11.726	+0.1
7	$1.7x10^{-1}$	10.0	5.00	16.742	15.651	−6.5

of oxalic acid to reduce the chlorite ion to chlorine according to:

$$C_2O_4^{2-} + 2ClO_2^- + 4H^+ \longrightarrow 2H_2O + Cl_2 + 2CO_2 + O_2$$

.....(C.12)

4. The solution is boiled gently to expel the dissolved chlorine before the standard procedure is applied.

C.2.2 Sulphate Determination (Levaggi et al. 1976)

When compared to sulphite analysis, the procedure for sulphate determination is well established. To test for sulphate, a modification of the barium sulphate turbidimetric method was selected for its simplicity and accuracy. In this procedure, a ready made Sulfa Ver 4 Sulphate reagent will cause a milky precipitate to form if sulphate is present. According to the procedure a Sulfa Ver 4. Sulphate reagent was added to the sample solution which was stoppered immediately and inverted several times to ensure good mixing. The solution was left undisturbed for at least 5 minutes for full

turbidity to develop (but no more than 10 minutes). The absorbance was determined in a 1–cm cell at wavelengths of 450 nm and 500 nm.

a. Preparation of standard curve for sulphate absorbance using Sulfa Ver 4 reagent

Typical results for sulphate absorbance are given in Table C.11. These results are plotted in Figure C.10 to give the standard absorbance curve for sulphate for later use. According to the data in Figure C.10, a higher absorbance occurred at 450 nm rather than 500 nm as reported by Levaggi et al. (1976). This discrepancy is consistent with the original document provided by Hach Chemical Company (1975). Therefore, all later absorbance measurements concerned with sulphate determination were conducted at 450 nm instead of 500 nm.

b. Use of Sulfa Ver 4 to test for sulphate in tap water

The results for tap water testing are reported in Table C.12. The average sulphate level was determined to be 23.30 $\mu g SO_4^{2-}$/mL. This value was obtained

Table C.11 Sulphate Absorbance at Various Concentrations

Sulphate Concentration [$\mu g SO_4^{2-}.mL^{-1}$]	Absorbance (No Blank) 450 nm [–]	500 nm [–]
0.24	0.049	0.044
3.36	0.053	0.050
4.80	0.059	0.052
7.20	0.061	0.054
9.60	0.075	0.064
14.4	0.093	0.079
19.2	0.128	0.108
24.0	0.159	0.135
28.8	0.198	0.160
33.6	0.252	0.203
38.8	0.297	0.225
43.2	0.365	0.288
48.0	0.420	0.334

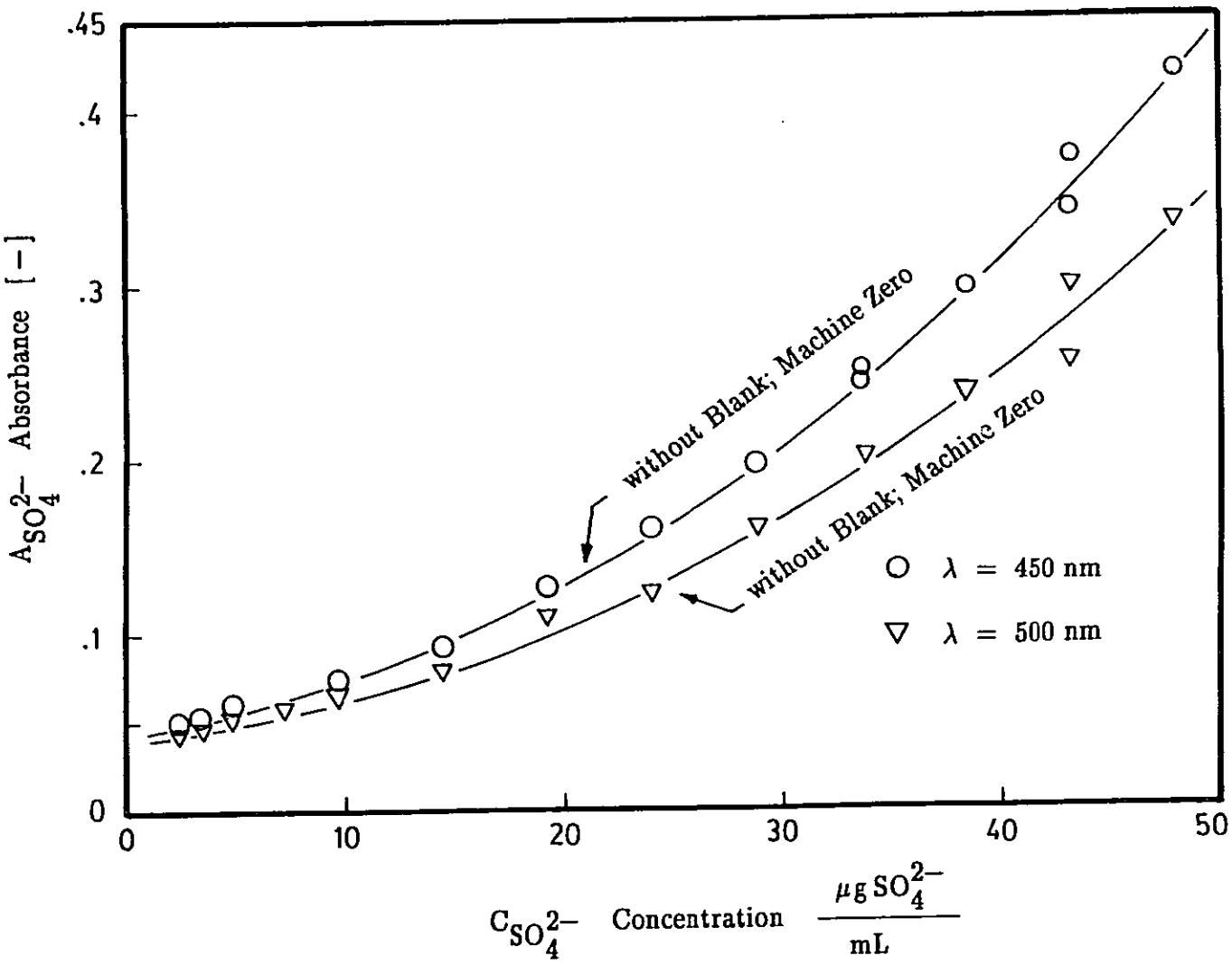

Figure C.10 Standard Curve for SO_4^{2-} Absorbance vs Concentration at $\lambda = 450$ nm (Turbidimetric Method)

Table C.12 Sulphate Levels in Tap Water

Sample Number	Absorbance at 450 nm		Amount of Sulphate found Without H_2O_2	With H_2O_2
	Without H_2O_2	With H_2O_2	[$\mu g SO_4^{2-}$/mL]	[$\mu g SO_4^{2-}$/mL]
1	0.155	0.148	23.40	22.7
2	0.148	0.154	22.80	23.40
3	0.157	0.150	23.60	23.00
4	0.155	0.156	23.40	23.50
		Average	23.30	3.15

from immediate sample analysis without hydrogen peroxide addition. Other solution samples were treated with 2 mL of hydrogen peroxide (30%) and left overnight. The same procedure was applied for sulphate determination. The average sulphate concentration obtained after such treatment was 23.15 μgSO_4^{2-}/mL. This value provided a good check of the earlier data.

Obviously, there is no or insignificant amount of sulphite present in the tap water samples, otherwise, higher values would be obtained from the later analysis involving peroxide addition. The average value of these two determinations, 23.24 μgSO_4^{2-}/mL represented the inlet sulphate level in the water scrubbing experiments. This value was checked during the course of the water scrubbing experiments.

c. Estimation of sulphite conversion at various pH levels

"Sulphite is most commonly found in boiler and boiler feed waters where it is used to inhibit corrosion by reducing dissolved oxygen. It may be found in industrial wastes such as paper mill effluents. Sulphite is not normally present in natural water since it readily oxidizes to sulphate." (Hach Chemical, 1975). However, these statements are true for sulphite in alkaline or neutral media as indicated by Rao and Rao (1955). Rao and Rao (1955) further showed that

sulphite is not oxidized to sulphate completely, by permanganate in acid medium, but approaches 90.0% to 97.2% completion.

In the absorption of SO_2 by water, sulphite is probably produced in the liquid effluent and must be taken into account for material balances. Estimation of sulphite can be achieved through sulphite conversion to sulphate, followed by total sulphate determination. In the following experiments, known amounts of sulphite were treated with hydrogen peroxide (30%) at different pH levels. The reaction is given as:

$$SO_3^{2-}{}_{(l)} + H_2O_{2(l)} \longrightarrow SO_4^{2-}{}_{(l)} + H_2O_{(l)} \qquad .....(C.13)$$

The pH of the solution was adjusted by the addition of sodium hydroxide or hydrochloric acid. The solution was left overnight for subsequent sulphate analysis according to the turbidimetric method described earlier. The results are given in Figure C.11 and compared with data from the oxidimetric method suggested by Rao et al. (1955). A complete conversion of sulphite was obtained at all pH levels when solution samples were treated with hydrogen peroxide. Only about 85 % conversion was achieved by the oxidimetric method, suggested by Rao et al. (1955).

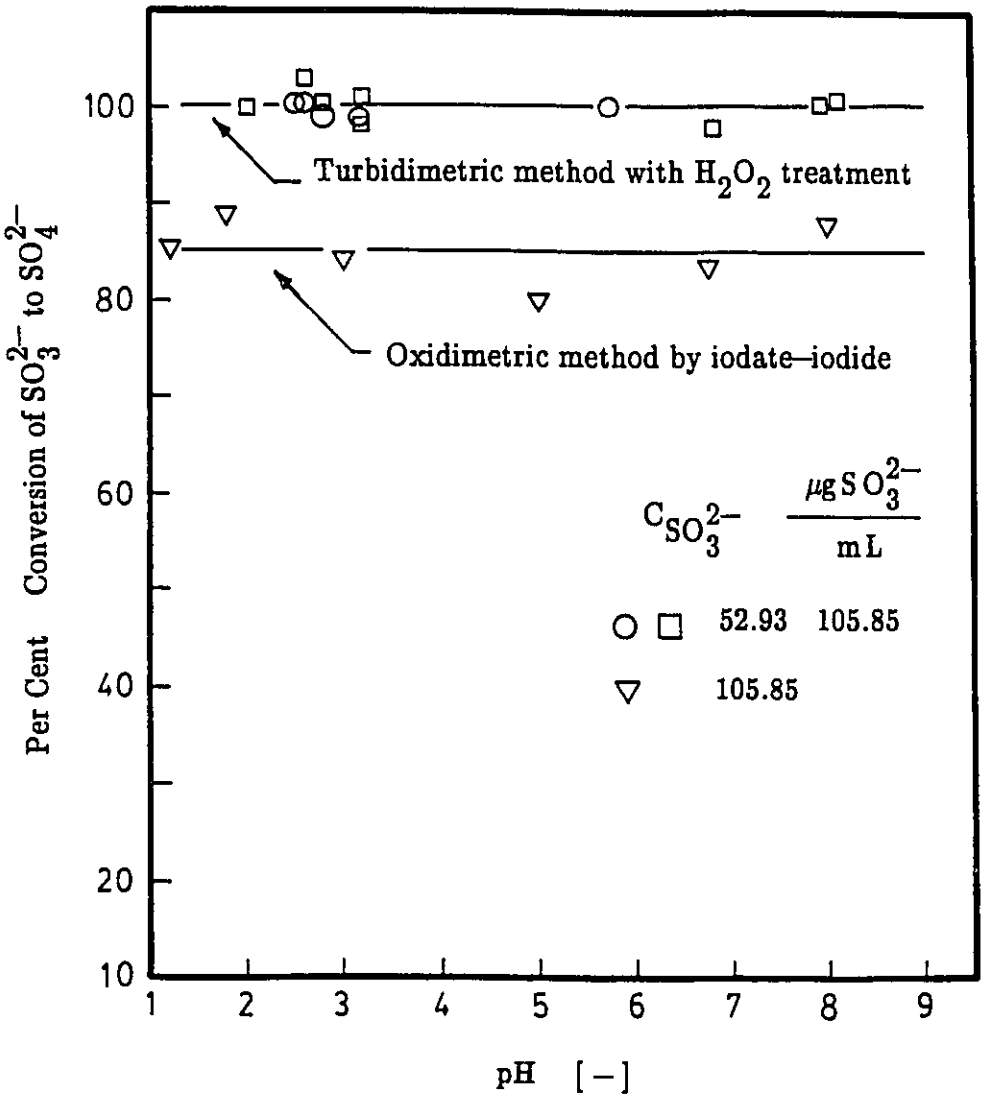

Figure C.11 The Conversion of Sulphite as a Function of pH

d. Sulphate determination in the presence of sodium chlorite

Preliminary experiments on sulphate determination in the presence of sodium chlorite provided higher sulphate levels than the actual value. This discrepancy suggested an unaccounted sulphate source, perhaps from sodium chlorite impurity.

A 0.2 M sodium chlorite solution was prepared in deionized water and tested for sulphate by the turbidimetric method. The results of this measurement indicated that the sodium chlorite contained a rather high sulphate level as impurity. The average sulphate impurity was determined to be 430.23 $\mu g SO_4^{2-}$/mL $NaClO_2$ solution or 2.28% by weight. Similar tests were performed on deionized water, hydrogen peroxide and oxalic acid, but all results were negative. No characteristic white turbidity was observed during these later tests. Therefore, it was concluded that the only possible source of sulphate was the sodium chlorite impurity.

Further tests were performed on sulphate with known amounts taken to evaluate the turbidimetric method. The results obtained with all sources of sulphate taken into account are listed in Table C.13. The measured values are in good agreement with the amounts taken. Consequently, the procedure is valid for sulphate determinations required during this investigation.

Table C.13 Sulphate Determinations in Sodium Chlorite Solution by Turbidimetric Method

Concentration of sodium chlorite = 0.209 M

Sample Number	Amount of Sulphate taken [$\mu g SO_4^{2-}$/mL]	Amount Sulphate found [$\mu g SO_4^{2-}$/mL]	Error %
1	28.484	30.750	+7.9
2	32.443	31.730	−2.2
3	34.203	35.330	+3.3
4	49.750	49.900	+0.31

APPENDIX – D

PHYSICO–CHEMICAL PROPERTIES AND THEIR PREDICTIONS

In order to compare experimental results with those predicted from models, values of the physical properties and hydrodynamic constants of the pertinent systems are required for quantitative calculations. These properties, which include gas and liquid phase diffusivities, mass transfer coefficients and liquid holdups, must be estimated from the best available correlations when experimental values have not been measured. The needed correlations were selected on the basis of :

. Number of data points correlated
. Number of systems investigated
. Experimental limitations
. Literature consistency.

D.1. Gas and Liquid Phase Mass Transfer Coefficients

D.1.1. Gas Side Mass Transfer Coefficient – k_G

A summary of gas–side mass transfer correlations is provided in Table D.1. According to this review, the recent correlation developed by Onda and Takeuchi (1968) appears to be the best. Its superiority is justified on the basis

Table D.1 **Summary of Correlations on Gas–Side Mass Transfer Coefficients**

There are ten correlations available for k_G prediction. Seven of these correlations were contributed by Onda et al. (1961, 1963, 1966, 1968), two by Van Krevelen and Hoftijzer (1948, 1953) and one by Whitney and Vivian (1949).

The correlations provided by Onda et al. (1961, 1963, 1966, 1968) are essentially modifications of a basic relationship that account for different solutions, solvents and packing materials. The equations presented by these authors take the general form,

$$Sh\ \# = c(Re\#)^{l}(Sc\#)^{m}(a_t d_p)^{n} \qquad .....D.1$$

where

c,l,m,n = constants of correlation, dimensionless

Sh # = modified Sherwood number, defined by

$$\frac{k_G RT}{a_t D_{AG}}, \quad \text{dimensionless}$$

Re# = modified Reynolds number for gas, defined by

$$\frac{G}{a_t \mu_G}, \quad \text{dimensionless}$$

Table D.1 **Summary of Correlations on Gas–Side Mass Transfer Coefficients** (continued)

Sc # = Schmidt number, defined by $\frac{\mu_G}{\rho_G D_{AG}}$, dimensionless

A correlation of similar form was developed by Van Krevelen and Hoftijzer (1948) in 1948. However, Whitney and Vivian (1949) suggested that the Van Krevelen and Hoftijzer (1948) expression was dimensionally unsound. Reasoning by analogy with the Gilliland wetted–correlation as cited by these authors, it appears likely that a term is missing from the left side of the equation. Van Krevelen and Hoftijzer (1953) modified their correlation on the analogy of tests on the rate of evaporation at the surface of solid substances. Their modified equation came closer to the form given by Equation D.1.

Summary of Published Gas–Side Mass Transfer Correlations – k_G

Investigator	System				
	Solute	Process	Liquid	Packing Material	Tower Diameter
Onda,Sada, and Saito (1961)	NH_3	Absorption	H_2O	1",1/2",3/8" Raschig Rings 1",1/2" Berl Saddles	10 cm

Table D.1 Summary of Correlations on Gas–Side Mass Transfer Coefficients (continued)

Correlation:

Raschig Rings

$$\frac{k_G RT}{a_t D_G} = 0.021 \left[\frac{G}{a_t \mu_G}\right]^{0.8} \left[\frac{\rho_G^2 g}{a_t^3 \mu_G^2}\right]^{0.16} \left[\frac{\mu_G}{\rho_G D_G}\right]^{\frac{1}{3}}$$

Accuracy: $\pm$ 25%

Berl Saddles

$$\frac{k_G RT}{a_t D_G} = 0.011 \left[\frac{G}{a_t \mu_G}\right]^{0.8} \left[\frac{\rho_G^2 g}{a_t^3 \mu_G^2}\right]^{0.22} \left[\frac{\mu_G}{\rho_G D_G}\right]^{\frac{1}{3}}$$

Accuracy: $\pm$ 25%

Generalized equation for both Raschig Rings and Berl Saddles:

$$\frac{k_G RT}{a_t D_G} = 0.014 \left[\frac{G}{a_t \mu_G}\right]^{0.8} \left[\frac{\rho_G^2 g}{\mu_G^2 a_t^3}\right]^{0.2} \left[\frac{\mu_G}{\rho_G D_G}\right]^{\frac{1}{3}}$$

Accuracy: $\pm$ 30%

Range of Variables in the Correlation:

$60 - 400$ kg.m^{-2}.h^{-1}

Table D.1 Summary of Correlations on Gas–Side Mass Transfer Coefficients (continued)

Investigator	System				
	Solute	Process	Liquid	Packing Material	Tower Diameter
Onda,Sada, Kido and Tanaka (1963)	NH_3	Absorption	H_2O	1/2",1",3/4" Spheres 30 cm packing height	$6 < D_t < 25$ cm

Sphere

$$\frac{k_G RT}{a_t D_G} = 2.15 \left[\frac{G}{a_t \mu_G}\right]^{0.8} \left[\frac{\rho_G^2 g}{a_t^3 \mu_G^2}\right]^{0.2} \left[\frac{\mu_G}{\rho_G D_G}\right]^{\frac{1}{3}} [a_t d]^{-3}$$

Accuracy : $\pm$ 30%

Range of Variables in the Correlation:

$$2 < \frac{G}{a_t \mu_G} < 1000$$

$10 < d < 38$ mm

Table D.1 **Summary of Correlations on Gas–Side Mass Transfer Coefficients** (continued)

Investigator	System				
	Solute	**Process**	**Liquid**	**Packing Material**	**Tower Diameter**
Onda,Sada, Kido and Kawatake (1966)	NH_3, SO_2 acetone	Absorption	H_2O	Not reported	10 cm

Correlation:

$$\frac{k_G RT}{a_t D_G} = 2.00 \left[\frac{G}{a_t \mu_G}\right]^{0.8} \left[\frac{\rho_G^2 g}{a_t^3 \mu_G^2}\right]^{0.2} \left[\frac{\mu_G}{\rho_G D_G}\right]^{\frac{1}{2}} [a_t d]^{-3}$$

Accuracy: $\pm$ 30%

Range of Variables in the Correlation:

24 – 8609 $kg.m^{-2}.h^{-1}$

Table D.1 Summary of Correlations on Gas–Side Mass Transfer Coefficients (continued)

Investigator	System				
	Solute	Process	Liquid	Packing Materia	Tower Diameter
Onda, Takeuki and Okumoto (1968)	NH_3 Acetone Methanol Ethanol	Absorption	H_2O	d > 15 mm d < 15 mm Raschig Rings Berl Saddles	Not reported

Generalized correlation:

Higher Group – d > 15mm

$$\frac{k_G RT}{a_t D_G} = 5.23 \left[\frac{G}{a_t \mu_G}\right]^{0.7} \left[\frac{\mu_G}{\rho_G D_G}\right]^{\frac{1}{3}} [a_t d]^{-2}$$

Lower Group – d < 15 mm

$$\frac{k_G RT}{a_t D_G} = 2.00 \left[\frac{G}{a_t \mu_G}\right]^{0.7} \left[\frac{\mu_G}{\rho_G D_G}\right]^{\frac{1}{3}} [a_t d]^{-2}$$

Accuracy: $\pm$ 30%

Range of Variables in the Correlation:

Not reported

Table D.1 Summary of Correlations on Gas–Side Mass Transfer Coefficients (continued)

Investigator	System				
	Solute	Process	Liquid	Packing Material	Tower Diameter
Van Krevelen and Hoftijzer (1948)	NH_3	Absorption	H_2O	Not reported	Not reported

Correlation:

$$\frac{k_G d}{D_G} = 0.20 \left[\frac{G}{a_t \mu_G}\right]^{0.8} \left[\frac{\mu_G}{\rho_G D_G}\right]^{\frac{1}{3}}$$

Accuracy: Not reported

Range of Variables in the Correlation:

Not reported

Table D.1 Summary of Correlations on Gas–Side Mass Transfer Coefficients (continued)

Investigator	System				
	Solute	Process	Liquid	Packing Material	Tower Diameter
Van Krevelen and Hoftijzer (1953)	–	–	–	Not reported	Not reported

Correlation:

$$\frac{k_G RT}{a_t D_G} = 0.22 \left[\frac{G}{a_t \mu_G}\right]^{0.8} \left[\frac{\mu_G}{\rho_G D_G}\right]^{0.4}$$

Accuracy: Not reported

Range of Variables in the Correlation:

Not reported

Table D.1 **Summary of Correlations on Gas–Side Mass Transfer Coefficients** (continued)

Investigator	System				
	Solute	Process	Liquid	Packing Material	Tower Diameter
Whitney and Vivian (1949)	SO_2	Absorption	H_2O	Not reported	Not reported

Correlation:

$$k_G a = 0.028 G^{0.7} L^{0.25}$$

Accuracy: Not reported

Range of Variables in the Correlation:

Not reported

of its ability to match the experimental values reported by Whitney and Vivian (1949) for SO_2 absorption into water. The data in Table D.2 indicate that values predicted from the Onda–Takeuchi correlation (1968) agree very well with the experimental data whereas the Van Krevelen–Hoftijzer correlation (1948) overpredicts by a factor of about three. On this basis, the Onda–Takeuchi correlation was selected for the present work. It takes the form,

$$\frac{k_G RT}{a_t D_{AG}} = 2.0\left(\frac{G}{a_t \mu_G}\right)^{0.7}\left(\frac{\mu_G}{\rho_G D_{AG}}\right)^{\frac{1}{3}}(a_t d_p)^{-2.0} \qquad .....(D.1)$$

where

k_G = gas–side mass transfer coefficient, $kmole.m^{-2}.s^{-1}.atm^{-1}$

R = gas constant, 8.2056×10^{-2} $atm.m^3.kmole^{-1}.K^{-1}$

T = absolute temperature, K

a_t = total surface area of packing per unit column volume, $m^2.m^{-3}$

Table D.2 Gas Side Mass Transfer Coefficient for SO_2/H_2O

Operating Condition: $Q_L = 1.364 \times 10^{-4}$ $m^3.s^{-1}$

$Q_G = 1.121 \times 10^{-4}$ $m^3.s^{-1}$

Correlations:	k_G $kmole.m^{-2}.s^{-1}.atm^{-1}$
Onda and Takeuchi (1968)	9.012×10^{-5}
Van Krevelen–Hoftijzer (1948)	3.040×10^{-4}
Whitney and Vivian (1949) (experimental value)	9.652×10^{-5}

D_{AG} = gas phase molecular diffusivity of component A, $m^2.s^{-1}$

G = superficial gas mass flow rate, $kg.s^{-1}.m^{-2}$

μ_G = gas viscosity, $kg.m^{-1}.s^{-1}$

ρ_G = gas density, $kg.m^{-3}$

d_p = packing diameter, m

D.1.2 Liquid–Side Mass Transfer Coefficient – k_L

Since the Sherwood–Holloway (1940) experimental equation on liquid phase mass transfer coefficients was reported, many investigators (Van Krevelen and Hoftijzer, 1948; Whitney and Vivian, 1949; Shulman el al. 1955; Onda et al. 1959, 1960, 1963, 1968; Mohunta et al. 1969) have been studying the relationship. The various published correlations are summarized in Table D.3. To select the best correlation, values predicted from these equations were compared with the actual experimental data on k_L in accordance with the experimental condition given in the literature.

In cases where data on overall mass transfer coefficients are given, the liquid side mass transfer coefficients are calculated from:

Table D.3 Summary of Correlations on Liquid–Side Mass Transfer Coefficients

Investigator	System				
	Solute	Process	Liquid	Packing Material	Tower Diameter
Sherwood and Holloway (1940)	O_2	Desorption	H_2O	$\frac{1}{2}$",1",1$\frac{1}{2}$",2" Raschig Rings Berl Saddles	20"

Correlation:

Below flooding point:

$$\frac{k_L a}{D_{AL}} = \alpha \left[\frac{L}{\mu_L}\right]^{0.75} \left[\frac{\mu_L}{\rho_L D_{AL}}\right]^{0.53}$$

Obtained by Van Krevelen and Hoftijzer (1953) based on Sherwood–Holloway (1940) data

$$\frac{k_L a}{a_p D_{AL}} = 5 \left[\frac{L}{a_t \mu_L}\right]^{\frac{2}{3}} \left[\frac{\mu_L}{\rho_L D_{AL}}\right]^{0.4}$$

Accuracy: Not reported

Table D.3 Summary of Correlations on Liquid–Side Mass Transfer Coefficients (continued)

Investigator	System				
	Solute	Process	Liquid	Packing Material	Tower Diameter
Van Krevelen and Hoftijzer (1948)	CO_2	Absorption	NaOH	1/2" Raschig Rings	3"

Correlation:

$$\frac{k_L\left(\frac{\mu_L^2}{g\rho_L^2}\right)^{\frac{1}{3}}}{D_{AL}} = 0.015\left[\frac{L}{a\mu_L}\right]^{\frac{2}{3}}\left[\frac{\mu_L}{\rho_L D_{AL}}\right]^{\frac{1}{3}}$$

Accuracy: Not reported

Range of Variables in the Correlation:

$$10 < \frac{L}{a_t \mu_L} < 100$$

Table D.3 Summary of Correlations on Liquid–Side Mass Transfer Coefficients (continued)

Investigator	System				
	Solute	Process	Liquid	Packing Material	Tower Diameter
Shulman et al. (1955)	CO_2	Absorption	–	Not reported	Not reported

Correlation:

$$\frac{k_L d_p}{D_{AL}} = 25.1 \left[\frac{d_p L}{\mu_L}\right]^{0.45} \left[\frac{\mu_L}{\rho_L D_{AL}}\right]^{0.5}$$

Accuracy: Not reported

Range of Variables in the Correlation:

Not reported

Table D.3 Summary of Correlations on Liquid–Side Mass Transfer Coefficients (continued)

Investigator	System				
	Solute	Process	Liquid	Packing Material	Tower Diameter
Whitney and Vivian (1949)	SO_2	Absorption	H_2O	1" Raschig Rings	4",14"

Correlation:

$$k_L a = 0.044 L^{0.82}$$

Accuracy: Not reported

Range of Variables in the Correlation:

$970 - 1600$ lbs.h^{-1}.ft^{-2}

Table D.3 Summary of Correlations on Liquid–Side Mass Transfer Coefficients (continued)

Investigator	System				
	Solute	Process	Liquid	Packing Material	Tower Diameter
Onda,Sada and Murase (1959)	SO_2 H_2	Absorption	H_2O	1/4",1/3",2/5" Ceramic Raschig Rings	2",4"

Correlation:

Two–film theory

$$k_L\left[\frac{\rho_L}{g\mu_L}\right]^{\frac{1}{3}} = 0.021\left[\frac{L}{a_t\mu_L}\right]^{0.49}\left[\frac{\mu_L}{\rho_L D_{AL}}\right]^{-0.5}$$

Penetration theory

$$k_L\left[\frac{\rho_L}{g\mu_L}\right]^{\frac{1}{3}} = 0.013\left[\frac{L}{a_t\mu_L}\right]^{0.5}\left[\frac{\mu_L}{\rho_L D_{AL}}\right]^{-0.5}$$

Accuracy: $\pm$ 20%

Table D.3 **Summary of Correlations on Liquid–Side Mass Transfer Coefficients** (continued)

Range of Variables in the Correlation:

$264 - 6847$ $lbs.h^{-1}.ft^{-2}$

Remarks: Data of Sherwood–Holloway (1940), Whitney–Vivian (1949) are included.

Table D.3 Summary of Correlations on Liquid–Side Mass Transfer Coefficients (continued)

Investigator	System				
	Solute	Process	Liquid	Packing Material	Tower Diameter
Onda,Okamoto and Honda (1960)	CO_2	Absorption	H_2O	25 mm Berl Saddles	10 cm

Correlation:

$$k_L\left[\frac{\rho_L}{g\mu_L}\right]^{\frac{1}{3}} = 0.018\left[\frac{L}{a_t\mu_L}\right]^{0.5}\left[\frac{\mu_L}{\rho_L D_{AL}}\right]^{-0.5}$$

Accuracy: $\pm$ 20%

Range of Variables in the Correlation:

$600 - 20000$ $kg.h^{-1}.m^{-2}$

Remarks: Data of Sherwood–Holloway (1940), Whitney–Vivian (1949) are included.
Packing materials included Berl Saddles and Raschig Rings.

Table D.3 **Summary of Correlations on Liquid–Side Mass Transfer Coefficients** (continued)

Investigator	System				
	Solute	Process	Liquid	Packing Material	Tower Diameter
Onda,Sada,Kido and Tanaka (1963)	CO_2 NH_3	Absorption	H_2O	1/2",1" Ceramic Spheres	$6 < d_t < 50$ cm

Correlation:

$$k_L\left[\frac{\rho_L}{g\mu_L}\right]^{\frac{1}{3}} = 0.11\left[\frac{L}{a_t\mu_L}\right]^{0.5}\left[\frac{\mu_L}{\rho_L D_{AL}}\right]^{-0.5}\left[a_t d_p\right]^{-1.0}$$

Accuracy: $\pm$ 20%

Range of Variables in the Correlation:

$$0.5 < \frac{L}{a_t\mu_L} < 500$$

Remarks: Data of Sherwood–Holloway (1940), Whitney–Vivian (1949) are included. Packing materials included Berl Saddles, Raschig Rings and Spheres.

Table D.3 Summary of Correlations on Liquid–Side Mass Transfer Coefficients (continued)

Investigator	System				
	Solute	Process	Liquid	Packing Material	Tower Diameter
Onda,Takeuchi and Okumoto (1968)	CO_2	Absorption	H_2O, CCl_4 CH_3COH	15 mm Ceramic Spheres 1/2",1" Ceramic Spheres Berl Saddles, Rods	12 cm

Correlation:

$$k_L\left[\frac{\rho_L}{g\mu_L}\right]^{\frac{1}{3}} = 0.0051\left[\frac{L}{a_w\mu_L}\right]^{\frac{2}{3}}\left[\frac{\mu_L}{\rho_L D_{AL}}\right]^{-0.5}[a_t d_p]^{0.4}$$

Accuracy: $\pm$ 20%

Range of Variables in the Correlation:

$400 - 4500\ \ kg.h^{-1}.m^{-2}$

Remarks: Generalized correlation included all previously published data.
Organic solvents were tested together with various packing materials.

Table D.3 Summary of Correlations on Liquid–Side Mass Transfer Coefficients (continued)

Investigator	System				
	Solute	Process	Liquid	Packing Material	Tower Diameter
Mohunta, Vaidyanathan and Laddha (1969)	O_2	Desorption	H_2O	3/8",1/2",3/4" Raschig Rings	3",4"

Correlation:

$$k_L a\left[\left(\frac{a_t \mu_L}{g\rho_L}\right)^{\frac{2}{3}}\left(\frac{\mu_L}{g^2\rho_L}\right)^{\frac{1}{9}}\right] = 0.0025\left[\frac{\mu_L U_L^3 a_t^3}{g^2\rho_L}\right]\left[\frac{\mu_L}{\rho_L D_{AL}}\right]^{-0.5}$$

Accuracy: $\pm$ 20%

Range of Variables in the Correlation:

8 to 10000 $lbs.h^{-1}.ft^{-2}$

Remarks: Generalized correlation included all previously published data. Effect of viscosity was tested. More than 80% of data points were found within 23% of correlation. Over 300 experimental data runs are included.

$$\frac{1}{K_L a} = \frac{1}{k_L a} + \frac{H}{k_G a} = \frac{H}{k_G a} \qquad \text{.....(D.2)}$$

where

K_L = overall liquid phase mass transfer coefficient, $m.s^{-1}$

K_G = overall gas phase mass transfer coefficient, $kmole.atm^{-1}.m^{-2}.s^{-1}$

k_L = liquid side mass transfer coefficient, $m.s^{-1}$

a = interfacial area per unit column volume, $m^2.m^{-3}$

H = Henry's law constant for the absorbed component, $kmole.atm^{-1}.m^{-3}$

The value of k_G was estimated from the Onda–Takeuchi correlation. The correlation of Puranik–Vogelpohl (1974) was used to obtain the interfacial area per unit column volumn, a. The choice of this correlation will be discussed in a later section.

Figures D.1, D.2, and D.3 show that the k_L values predicted from the

correlations given by Onda et al. (1968) and Mohunta et al. (1969), are in good agreement with the experimental data of Chilton et al. (1937), Vivian and Whitney (1947) and Hutchings et al. (1949). It appears that the Mohunta–Vaidyanathan correlation (1969) is slightly better than that of Onda et al. (1968), probably because it is based on more data. The Mohunta–Vaidyanathan correlation (1969) was selected for this work because of its apparent superiority.

The Mohunta–Vaidyanathan correlation has the form:

$$k_L a\left[\left(\frac{a_t \mu_L}{\rho_L g}\right)^{\frac{2}{3}}\left(\frac{\mu_L}{\rho_L g^2}\right)^{\frac{1}{9}}\right] = 0.0025\left(\frac{\mu_L U_L^3 a_t^3}{\rho_L g^2}\right)\left(\frac{\mu_L}{\rho_L D_{AL}}\right)^{-0.5} \qquad \text{.....(D.3)}$$

where

μ_L	=	liquid viscosity, $kg.m^{-1}.s^{-1}$
g	=	gravitational acceleration, 9.807 $m.s^{-2}$
U_L	=	velocity of liquid based on empty cross section of column, $m.s^{-1}$
ρ_L	=	liquid density, $kg.m^{-3}$
D_{AL}	=	liquid diffusivity, $m^2.s^{-1}$

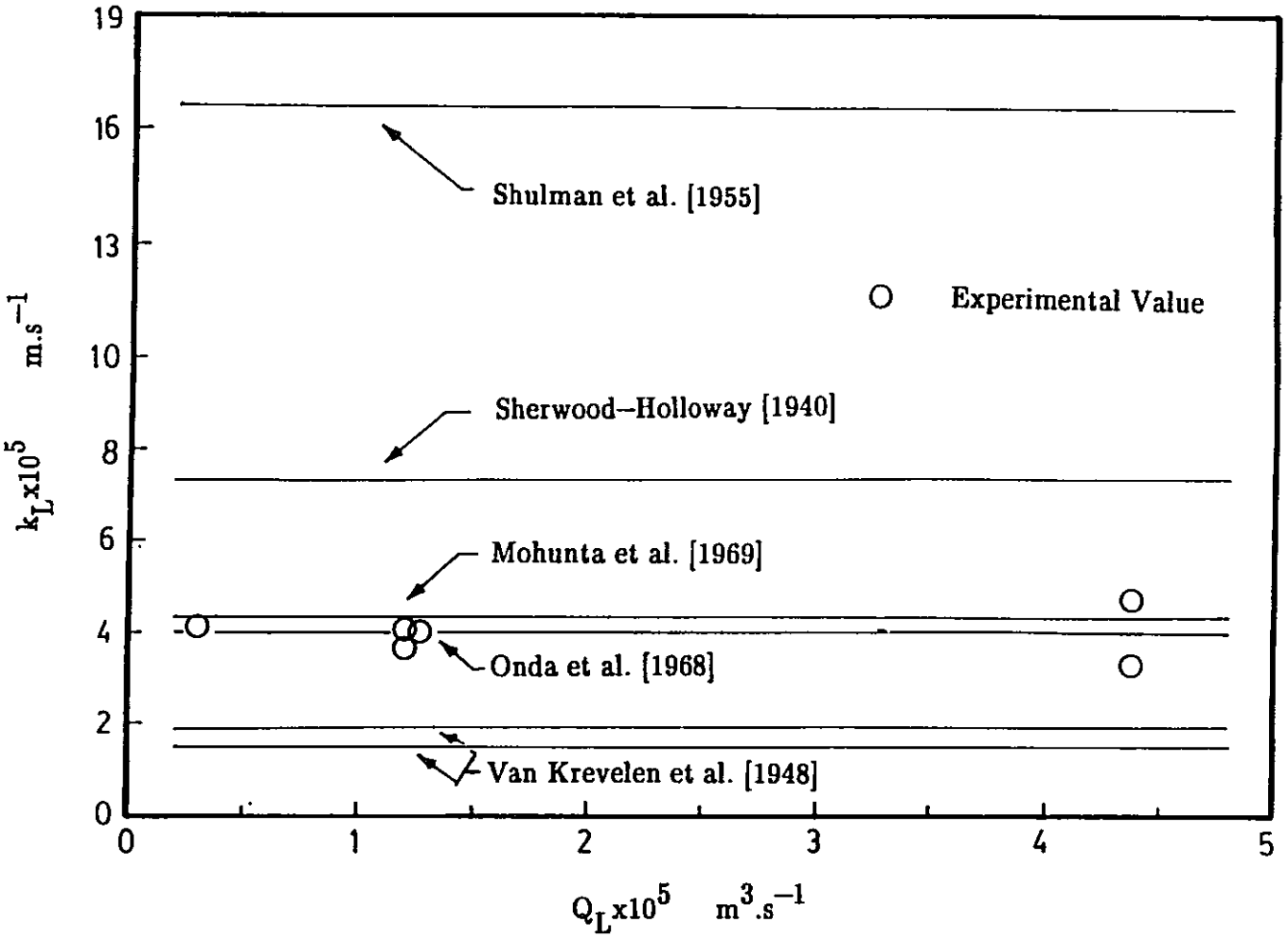

Figure D.1 k_L Values vs Liquid Flow Rate – NH_3/H_2O System; Operating Condition According to Chilton et al. [1937]; 6" Tower; 3/4" Crushed Stone

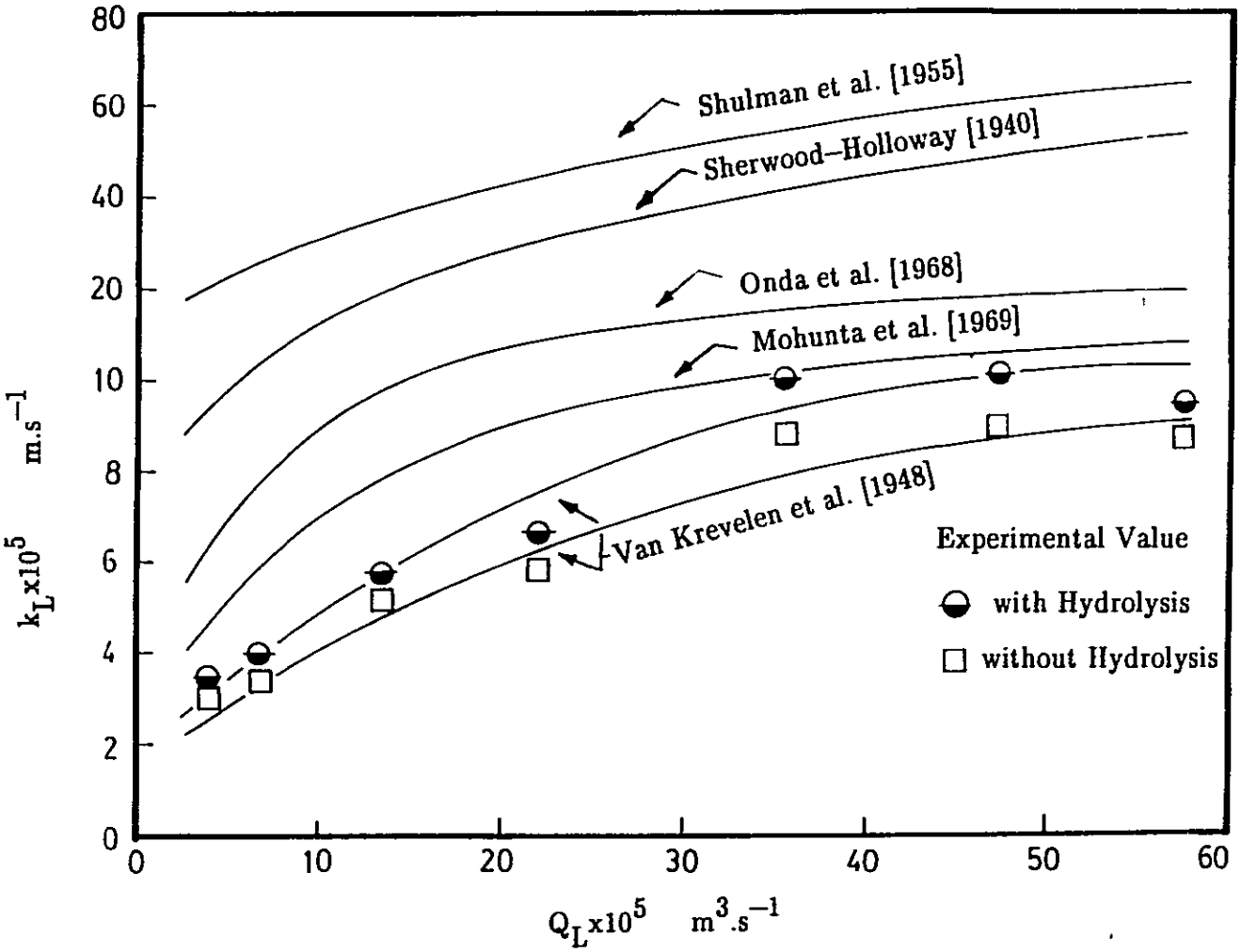

Figure D.2 k_L Values vs Liquid Flow Rate – SO_2/H_2O System; Operating Condition According to Whitney and Vivian [1949]; 8" Tower; 1" Ceramic Raschig Rings

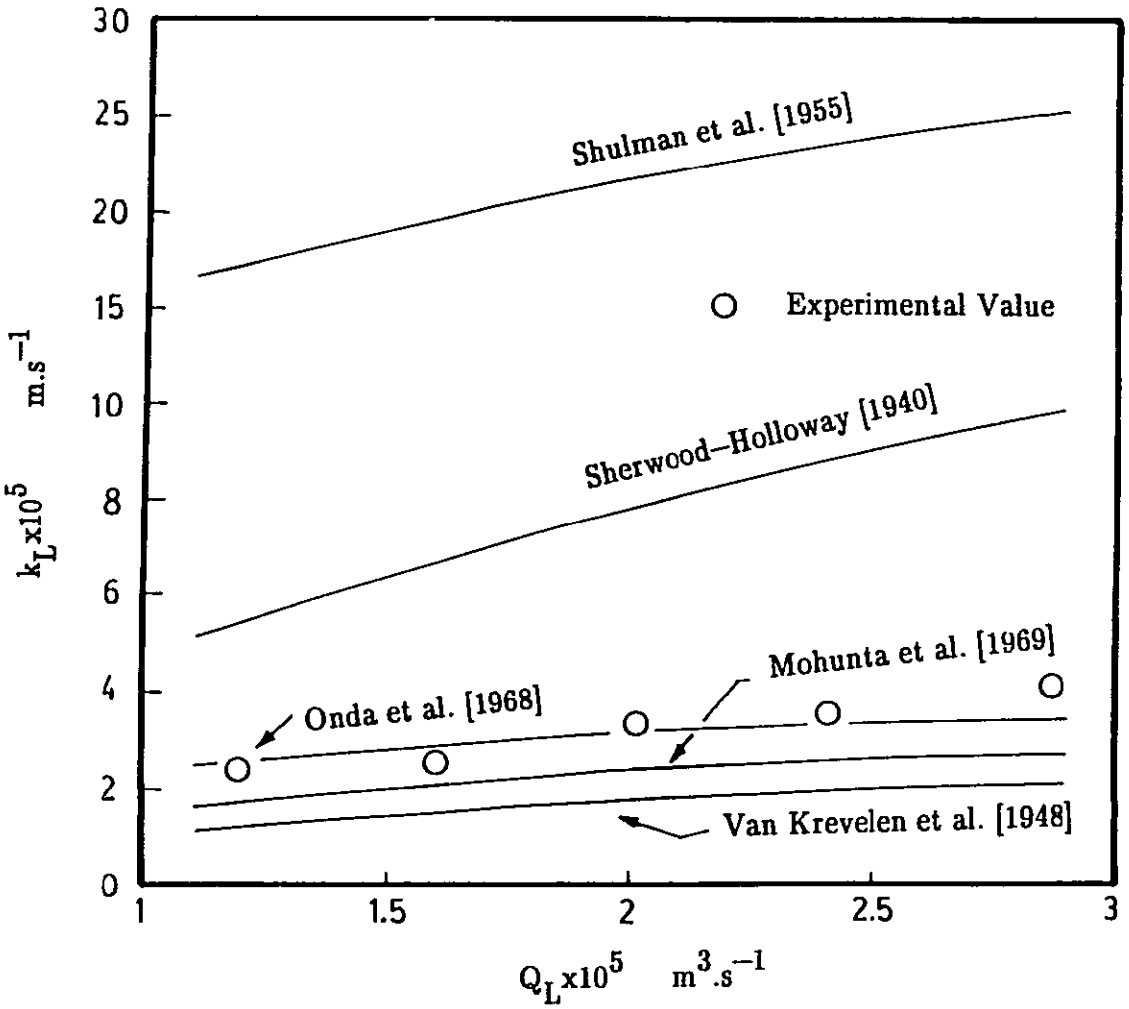

Figure D.3 k_L Values vs Liquid Flow Rate – Acetone/H_2O System; Operating Condition According to Hutchings et al. [1949]; 6" Tower; 3/8" Ceramic Raschig Rings

D.2 Gas and Liquid Phase Diffusivities

D.2.1 Gas Phase Diffusivity

As suggested by Reid et al. (1977), the equation proposed by Fuller–Schetter appears to be slightly more reliable than the Chapman–Enskog equation (Bird et al. 1960). The predicted values generally agree with experimental data to within 5 to 10 percent. Therefore, gas–phase diffusivities were estimated from the Fuller–Schetter equation (Bird et al. 1960) when experimental values were not available. The literature and estimated values are given Table D.4.

The Fuller–Schetter equation has the form:

$$D_{AB} = \frac{10^{-3} T^{1.75} [(M_A + M_B)/M_A M_B]^{\frac{1}{2}}}{P[\ (\Sigma v)_A^{\frac{1}{3}} + (\Sigma v)_B^{\frac{1}{3}}\ ]^2} \qquad \text{.....(D.4)}$$

where

D_{AB} = diffusivity of component A in B, $cm^2 s^{-1}$

Table D.4 Literature and Estimated Values of Gas Phase Diffusivities – 25°C

Diffusing Species A	Diffusivity in Air $D_{AG} \times 10^5$ $[m^2.s^{-1}]$	Reference
NO	2.30*	Reid et al. (1977)
NO_2	1.40	Chambers–Sherwood (1937)
N_2O_3	1.10*	Reid et al.(1977)
N_2O_4	0.98	Chambers–Sherwood (1937)
HNO_2	1.40	Chambers–Sherwood (1937)
SO_2	1.26*	Reid et al.(1977)

* estimated value for this study using Fuller–Schetter equation (Reid et al. 1977).

T	=	absolute temperature, K
M_A;M_B	=	molecular weight of component A and B, g.g–mole^{-1}
P	=	pressure of the system, atm
ΣV	=	atomic diffusion volume, cm^3.g–atom^{-1}

D.2.2 Liquid Phase Diffusivities

D.2.2.1 Liquid Phase Diffusivities in Water

Summaries of the liquid phase diffusivities of SO_2 and NO in water are given in Tables D.5 and D.6. There is a strong consensus in the literature on the values derived by various researchers. Roberts and Friedlander (1980) recommended a value of 1.60×10^{-9} $m^2 s^{-1}$ for SO_2 in water. Strictly speaking, his value and those listed in Table D.5 are valid either for dissolved SO_2 in excess of 0.02 mole.L^{-2} or when hydrolysis of the absorbed SO_2 is negligible. Therefore, the value recommended by Roberts and Friedlander (1980) is obviously inappropriate under the typical flue gas concentration levels where the absorbed SO_2 is anticipated to be largely hydrolysed to produce the species HSO_3^- and SO_3^{2-}.

Table D.5 **Literature Values for the Liquid Phase Diffusivity of SO_2 in Water -- 25 ^oC**

$D_{SO_2,w} \times 10^9$ $[m^2.S^{-1}]$	Reference
1.753	Laohavichitra et al. (1982)
1.760	Hikita et al (1978)
1.280	Eriksen (1969)
1.600	Kaji et al.(1985)
1.640	Rocheile et al. (1977)

Table D.6 **Literature Values for the Liquid Phase Diffusivity of NO in Water – 25 ^{o}C**

$D_{NO,W} \times 10^{9}$ $[m^{2} \cdot s^{-1}]$	Reference
2.26	Boslo et al.(1952)
2.53	Sada et al.(1978)
2.50	Takeuchi et al.(1977)
2.54*	Wilke – Chang (1955)

* Based on Wise and Houghton (1968) data and interpolated by the Wilke and Chang equation to account for the temperature and viscosity effects of water.

According to the works of Leaist (1983,1984), at concentrations below about 0.02 mole.L^{-1}, extensive hydrolysis occurs. As a result, there is a sharp increase in the rate of diffusion of the sulphur dioxide component. Therefore, the effective liquid phase diffusivity of SO_2 in water, which accounts for SO_2, HSO_3^- and SO_3^{2-} diffusion, is taken to be 2.13×10^{-9} $m^2 \cdot S^{-1}$ at 25 ^oC (Leaist, 1984). This value is reasonable according to the degree of hydrolysis (>90%) of $SO_{2(l)}$ under the present experimental conditions.

Other liquid phase diffusivity values can be estimated from the Wilke and Chang equation (1955) when experimental values are not available. The recommended and estimated liquid phase diffusivities in water are given in Table D.7.

The Wilke–Chang equation takes the form:

$$D_{AB} = \frac{7.4 \times 10^{-8} T \, [XM_B]^{0.5}}{\mu_B \, V_{mA}^{0.6}} \qquad \text{.....(D.5)}$$

Table D.7 **Recommended and Estimated Values of Liquid Phase Diffusivities – 25 ^{o}C**

Diffusing Species	Diffusivity in water $D_{AL} \times 10^{-9}$ $[m^{2} \cdot s^{-1}]$	Reference
NO	2.53	Sada et al.(1978)
NO_2	1.43*	Wilke–Chang (1955)
N_2O_3	1.76*	Wilke–Chang (1955)
N_2O_4	1.40	Andrew and Hanson (1961)
HNO_2	2.35*	Wilke–Chang (1955)
SO_2	2.13	Leaist (1984)

* estimated value for this study

where

D_{AB} = diffusivity of solute A in solvent B, $cm^2.s^{-1}$

T = absolute temperature, K

X = association factor of solvent B, dimensionless

X = 2.60 for water

X = 1.90 for methanol

X = 1.50 for ethanol

M_B = molecular weight of solvent B, $g.g\text{–}mole^{-1}$

μ_B = viscosity of solvent B, cp

V_{mA} = molal volume of solute A, $cm^3.g\text{–}mole^{-1}$

D.2.2.2 Liquid Phase Diffusivities in Electrolyte Solutions

The liquid phase diffusivity of nitric oxide, $D_{NO,l}$, in mixed sodium chlorite solution was estimated from the equation proposed by Joosten and Danckwerts (1972), in the form of:

$$\frac{D_{NO,l}}{D_{NO,water}} = \frac{D_{N_2O,l}}{D_{N_2O,water}} \qquad \text{.....(D.6)}$$

The recommended value of $D_{NO,water}$ is 2.53×10^{-5} $cm^2.S^{-1}$ at 25 ^oC. The diffusivities of nitrous oxide ($D_{N_2O,l}$) in mixed salt solutions is given in Table D.8, whereas the value for $D_{N_2O,water}$ are 1.92×10^{-5} $cm^2.s^{-1}$ at 25 ^oC (Joosten and Danckwerts, 1972).

The liquid phase diffusivity of sulphur dioxide, $D_{SO_2,l}$ in aqueous sodium chlorite solutions is available in the literature (Wise and Houghton, 1968), ($D_{SO_2,l} = 1.90 \times 10^{-5}$ $cm^2.s^{-1}$ at 25 ^oC).

D.3 Solubilities of Gases in Aqueous Electrolyte Solutions

According to Sada et al.(1978), the interfacial concentrations of sulphur dioxide or nitric oxide ($C_J^* = C_{SO_2}^*, C_{NO}^*$) in mixed aqueous solutions of sodium hydroxide and sodium chlorite can be estimated from the correlation of

Table D.8 **Diffusivities of Nitrous Oxide in Aqueous Mixed Solutions of $NaClO_2$ and NaOH Derived from Physical Absorption Data with a Laminar Liquid–Jet at 1 atm. and 25 ^{o}C (Wise and Houghton, 1968)**

Sodium Chlorite Concentration	Sodium Hydroxide Concentration	Diffusivity of Nitrous Oxide
[M]	[M]	$[cm^2.s^{-1}]x10^5$
0.00	0.00	1.66
0.25	0.10	1.62
0.50	0.10	1.60
1.00	0.10	1.57
1.50	0.10	1.52
2.00	0.10	1.46
1.00	0.20	1.58
1.00	0.50	1.23
1.00	0.70	0.948

gas solubility in mixed electrolyte solutions (Onda et al. 1970) expressed by:

$$\log_{10}\left[\frac{C_J^*}{C_{J,\,water}^*}\right] = -\left[K_{B_1} I_{B_1} + K_{B_2} I_{B_2}\right] \qquad \text{.....(D.7)}$$

where K_{B_1} and K_{B_2} are the salting–out parameters for the electrolyte B_1 ($NaClO_2$) and B_2 (NaOH) respectively. The magnitude of a salting–out parameter depends on the ion and gas present and is given by:

$$K = [\, X_g + X_a + X_c \,] \qquad \text{.....(D.8)}$$

The values of X for various species are listed in Table D.9. The symbols I_{B_1} and I_{B_2} represent the ionic strengths of sodium chlorite ($NaClO_2$) and sodium hydroxide (NaOH) respectively according to:

$$I = \frac{1}{2} \sum C_i \psi_i^2 \qquad \text{.....(D.9)}$$

where C_i represents the concentration of ions of valency ψ_i.

Table D.9 **Values of X for Various Species (Sada et al.,1978; Onda et al., 1970; Sada and Kumazawa, 1978)**

Species	X_g	X_a $m^3.[kg.ion]^{-1}$	X_c
NO (25 °C)	–0.1825	–	–
SO_2 (25 °C)	–0.3145	–	–
OH^-	–	0.3875	–
ClO_2^-	–	0.3497	–
Na^+	–	–	–0.0183

The interfacial concentration of sulphur dioxide in water, $C^{*}_{SO_2,water}$, in equilibrium with a gas of presure $P^{*}_{SO_2}$, is estimated from Henry's law constant for nonionized sulphur dioxide which can be determined according to:

$$H_{SO_2} = \exp\left[\frac{2851.1}{T} - 9.3795\right] \qquad .....(D.10)$$

where H_{SO_2} is the Henry's law constant in $gmol.bar^{-1}.L^{-1}$ and T is the temperature in K. On this basis the concentration of nonionized sulphur dioxide in pure water can be obtained from:

$$C^{*}_{SO_2,water} = P_{SO_2} H_{SO_2} \qquad .....(D.11)$$

where P_{SO_2} is the partial pressure of SO_2 in the gas phase.

The interfacial concentration of nitric oxide, $C^{*}_{NO,water}$, is estimated from:

$$C^{*}_{NO,water} = P_{NO}H_{NO} \qquad .....(D.12)$$

where H_{NO} is given in the literature (Sada et al. 1978) as $1.92x10^{-6}$ g–mole.cm^{-3}.atm^{-1} at 25 ^{o}C

D.4 Wetted and Effective Areas For Absorption

Packing surface area is known to play an important role in gas–liquid operations. A number of correlations have been proposed to account for this transport phenomenon variable. The complex fluid dynamics over irrigated packing in packed towers are discussed in terms of wetted or effective areas. The review of nine pertinent correlations is provided in Table D.10.

An evaluation of these correlations is given in Figure D.4. It appears that values predicted from the equations of Onda et al. (1967) and Puranik–Vogelpohl (1974) agree very well with the values reported by Danckwerts (1970).

Table D.10 Summary of Correlations on Wetted and Effective Areas

Investigator	Packing Material	Tower Diameter
Semmelbauer (1967)	Raschig Rings	–

Correlation:

$$\frac{a_e}{a_t} = C\left[\frac{L}{a_t \mu_L}\right]^{0.455}\left[\frac{\rho_L g}{a_L^2 \sigma}\right]^{0.5}$$

Raschig Rings C = 0.057784

Berl Saddles C = 0.0717545

Accuracy: Not reported

Range of Variables in the Correlation:

Not reported

Table D.10 Summary of Correlations on Wetted and Effective Areas (continued)

Investigator	Packing Material	Tower Diameter
Onda, Takeuchi and Koyama (19670)	1/2",1" Spheres 8 mm Raschig Rings 1/2",1",1.5",2" Berl Saddles	6 – 50 cm

Correlation:

$$\frac{a_w}{a_t} = 1 - \exp\left[-1.45(\mathrm{Re})^{0.1}(\mathrm{Fr})^{-0.05}(\mathrm{We})^{0.2}\left(\frac{\sigma_c}{\sigma}\right)^{0.75}\right]$$

where

$$\mathrm{Re} = \frac{L}{a_t \mu_L}$$

$$\mathrm{Fr} = \frac{a_t L^2}{\rho_L^2 g}$$

$$\mathrm{We} = \frac{L^2}{a_t \rho_L \sigma}$$

Accuracy: $\pm$ 20%

Table D.10 Summary of Correlations on Wetted and Effective Areas (continued)

Range of Variables in the Correlation:

$0.04 < Re < 500$

$1.2x10^{-8} < We < 1.8x10^{-2}$

$2.5x10^{-9} < Fr < 1.8x10^{-2}$

$0.3 < \frac{\sigma_c}{\sigma} < 2.0$

Remarks: Liquids tested included water and glycerol. The predicted values for Pall Rings are about 15% lower than the observed values (Danckwerts, 1970).

Table D.10 Summary of Correlations on Wetted and Effective Areas (continued)

Investigator	Packing Material	Tower Diameter
Mohunta, Vaidyanathan and Laddha (1969)	3/8",1/2",3/4" Raschig Rings	3",4"

Correlation:

$$\frac{a_I}{a_t} = 0.175 \left[\frac{L}{a_t \mu_L} \right]^{\frac{1}{3}}$$

Accuracy: Not reported

Range of Variables in the Correlation:

$80 < L < 31000$ lbs.h^{-1}.ft^{-2}

$0.73 < \mu_L < 1.48$ cp

Table D.10 Summary of Correlations on Wetted and Effective Areas (continued)

Investigator	Packing Material	Tower Diameter
Jackson and Marchello (1970)	Not reported	–

Correlation:

. at low Reynolds Number:

$$\frac{a_e}{a_w} = \frac{C_4 \; (N_{Re})^{1.55} \; [\frac{N_{We}}{N_{Fr}}]^{0.5} \; (\frac{\rho_L a_t}{L})^{0.5}}{1 - \exp\{-1.45 (\frac{\sigma_c}{\sigma})^{0.75} \; (N_{Re})^{0.1} \; [\frac{N_{We}^{0.2}}{N_{Fr}^{0.05}}]\}}$$

C_4 = constant for packing: 0.00608 for Raschig Rings
0.00755 for Berl Saddles

. at high Reynolds Number:

$$\frac{a_e}{a_w} = C_4 [\frac{\rho_L a_t}{L}] (Re)^{1.455} (\frac{N_{We}}{N_{Fr}})^{0.5}$$

Accuracy: Not reported

Table D.10 Summary of Correlations on Wetted and Effective Areas (continued)

Investigator	Packing Material	Tower Diameter
Puranik and Vogelpohl (1974)	Not reported	–

Correlation:

$$\frac{a_p}{a_t} = \frac{a_v}{a_t} = \frac{a_w}{a_t} = \frac{a_{ac}}{a_t} = \left(\frac{a_{ap}}{a_t} + \frac{a_{st}}{a_t}\right)$$

$$\frac{a_p}{a_t} = 1.045(\mathrm{Re})^{0.041}(\mathrm{We})^{0.133}\left(\frac{\sigma}{\sigma_c}\right)^{-0.182}$$

$$\frac{a_{st}}{a_t} = 0.229 - 0.091 \ln\left[\frac{\mathrm{We}}{\mathrm{Fr}}\right]$$

Accuracy: $\pm$ 20%

Table D.10 Summary of Correlations on Wetted and Effective Areas (continued)

Range of Variables in the Correlation:

$0.08 < \frac{a_p}{a_t} < 0.8$; $0.025 < L < 1.2$ $g.s^{-1}.cm^{-2}$

$0.5 < \mu_L < 13$ cp; $25 < \sigma < 75$ $dynes.cm^{-1}$

$0.8 < \rho_L < 1.9$ $g.cm^{-3}$; $10 < d < 37.5$ mm

$0.4 < We/Fr < 14$; $2.1x10^{-6} < We < 1.2x10^{-2}$

$0.5 < Re < 85$; $7.7x10^{-7} < Fr < 4.7x10^{-3}$

$0.3 < \sigma/\sigma_c < 1.05$

Remarks: This is a generalized correlation for predicting the effective interfacial area for

- . absorption without chemical reaction (a_{ap})
- . absorption with chemical reaction (a_{ac})
- . vaporization (a_v)
- . wetted surface area (a_w)
- . static surface area (a_{st})

Table D.10 Summary of Correlations on Wetted and Effective Areas (continued)

Investigator	Packing Material	Tower Diameter
Joshi, Mahajani and Juvekar (1985)	Raschig Rings Pall Rings	–

Correlation:

Raschig Rings (Ceramic)

$$a_e = \frac{8.0\ v_L^{0.403}}{\epsilon^3 d^{1.015}}$$

Pall Rings (Stainless steel)

$$a_e = \frac{28.4\ v_L^{0.5}}{\epsilon^3 d^{1.07}}$$

where

ϵ = porosity or void fraction, dimensionless

Accuracy: Not reported

Table D.10 Summary of Correlations on Wetted and Effective Areas (continued)

Range of Variables in the Correlation:

Raschig Rings

$6 < d < 89$ mm

$0 < v_L < 15$ mm.s^{-1}

Pall Rings

$12 < d < 89$ mm

$0 < v_L < 10$ mm.s^{-1}

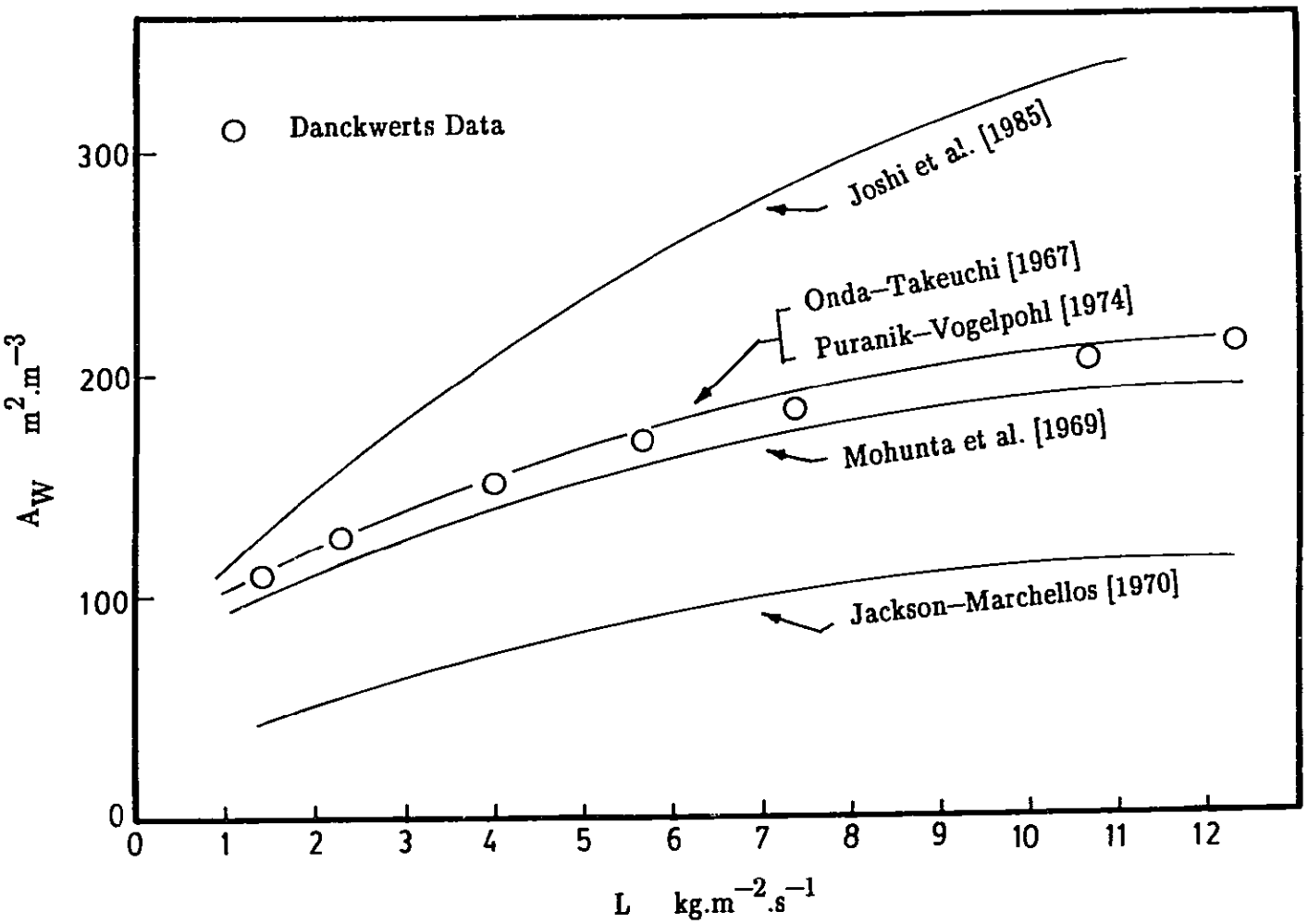

Figure D.4 Wetted Areas vs Liquid Mass Flow Rate
– $G = 7.4x10^{-2}$ $kg.m^{-2}.s^{-2}$

It has been shown that values predicted from the Puranik–Vogelpohl equation (1974) agree with all previous published experimental values to within 12.5 percent, whereas Onda's correlation (1967) is good to only $\pm$ 20 per cent. On the basis of this information, the Puranik–Vogelpohl equation was adopted for the present work.

The Puranik–Vogelpohl correlation (1974) has the form:

$$\frac{a_w}{a_t} = 1.045 \left[\frac{L}{a_t \mu_L}\right]^{0.041} \left[\frac{L^2}{\rho_L \sigma a_t}\right]^{0.133} \left[\frac{\sigma}{\sigma_c}\right]^{-0.182} \qquad .....(D.13)$$

where

a_w = wetted surface area per unit column volume, $m^2.m^{-3}$

L = superficial liquid mass flow rate, $kg.m^{-2}.s^{-1}$

σ = surface tension of the liquid, $N.m^{-1}$

σ_c = critical surface tension of the liquid for a particular material, $N.m^{-1}$

Values of σ/σ_c are available in the literature (Onda et al.,1967; Shulman et al., 1955).

D.5 Liquid Holdups

The effects of liquid holdups on effective interfacial areas and mass transfer rates have been studied extensively by Shulman et al. (1963; 1971). The total liquid holdup, as defined by Shulman et al. (1955), is the total liquid in the packing under operating conditions. It is expressed by:

$$h_t = h_s + h_d \qquad \text{.....(D.14)}$$

where h_s is the static holdup defined as liquid being trapped in the interstices of the packings and, h_d is the dynamic holdup or operating holdup of liquid which flows over the packing surface. These quantities have been measured experimentally by Shulman et al. (1955), Otake and Okada (1953), and De Waal and Van Mameren (1965). Static holdup has been shown to be constant (Shulman et al., 1955) for most common packings such as Raschig Rings and Berl Saddles. It has also been shown to be independent of liquid flow rate. On

the basis of the experimental values given by Otake–Okada (1953) and Shulman et al. (1955), a value of 0.04 $m^3.m^{-3}$ for h_s is recommended for this work. This value checked closely with that of Otake and Okada (1953), Van Swaaij et al. (1969) and Shulman et al.(1955) as shown in Table D.11.

Operating holdups (dynamic) were shown to vary with liquid flow rate. Therefore, values of h_d, other than those measured at the given liquid flow rate, can be estimated from the generalized correlation given by Otake and Okada (1953) in the form of:

$$h_d = 1.295 \left[\frac{dL}{\mu_L}\right]^{0.676} \left[\frac{d^3 g \rho_L^2}{\mu_L^2}\right] (a_t d) \qquad .....(D.15)$$

where

h_d = dynamic holdup, $m^3.m^{-3}$

d = nominal particle diameter, m

L = superficial mass liquid flow rate, $kg.m^{-2}.s^{-1}$

μ_L = dynamic liquid viscosity, $kg.m^{-1}.s^{-1}$

Table D.11 Static Liquid Holdups

h_s $[m^3.m^{-3}]$	Remark	Reference
0.036	1"Raschig Rings	Shulman et al.(1955)
0.039	10 mm Raschig Rings	Otake–Okada (1953)
0.029	graphical correlation	Sicardi and Baldi (1976) estimated
0.040	graphical correlation with Eotvos number ($\rho_L g d^2/\sigma_L$) $\epsilon = 0.902$ (ϵ is the porosity for 5/8" Pall rings)	Van Swaaij et al. (1969)
h_d $[m^3.m^{-3}]$		
$2.7x10^{-2}$		Otake–Okada (1953)
$2.8x10^{-2}$		Mohunta et al. (1969)

g = gravitational accelation, $m.s^{-2}$

ρ_L = liquid density, $kg.m^{-3}$

a_t = total surface area of packing, $m^2.m^{-3}$

This correlation is valid for packings wettable by water and other liquids. Agreement with experimental values is found to be within 20 percent. However, non–wettable packings have lower holdups than predicted by this equation.

VITA

Mr. Kam Foon Chan was born in the People's Republic of China on November 12, 1955. He left China at an early age for Hong Kong where he received his secondary school education. He was admitted to the University of Windsor where he received his B.A.Sc.(Hon.) in 1979 and M.A.Sc. in Chemical Engineering in 1983.

Currently, Mr. Chan is employed as a project engineer at Gore & Storrie Ltd., an engineering consulting firm in Toronto, Ontario. Mr. Chan is responsible for the design of air pollution control systems for sewage sludge incinerators and selection of the most appropriate continuous emission monitoring system for the Toronto Waste water Treatment Plant. He is also involved in the expansion of the Lakeview Waste Water Pollution Control Plant in Mississauga, Ontario.

Mr. Chan is a member of the Air and Waste Water Management Association and the Association of Professional Engineer of Ontario (APEO). His areas of interest include: gas–liquid mass transfer, gas–solid adsorption, particulate removal, flue gas kinetic reactions, absorption modelling and computer simulation.